Dissertation zur Erlangung des Doktorgrades

der Fakultät für Chemie und Pharmazie

der Ludwig-Maximilians-Universität München

Regulation of the Cytosolic Stress Response: Identification of Positive and Negative Modulators by a Genome-Wide RNA Interference Screen

---

vorgelegt von

Christian Frank Löw

aus Rotenburg, Deutschland

2014

Erklärung

Diese Dissertation wurde im Sinne von § 7 der Promotionsordnung vom 28. November 2011 von Herrn Prof. F. Ulrich Hartl betreut.

Eidesstattliche Versicherung

Diese Dissertation wurde eigenständig und ohne unerlaubte Hilfe erarbeitet.

München, am 27.01.2014

Dissertation eingereicht am 27.01.2014

1. Gutachter Prof. Dr. F. Ulrich Hartl

2. Gutachter PD Dr. Dietmar E. Martin

Mündliche Prüfung am 18.03.2014

Acknowledgement

I want to thank Prof. Dr. F. Ulrich Hartl for the opportunity to conduct my PhD research in his department at the Max Planck Institute of Biochemistry (MPIB). This work has benefited greatly from numerous valuable discussions, his intellectual support and scientific enthusiasm. I also would like to thank Dr. Manajit Hayer-Hartl for her constant advice and suggestions, especially during the publication process of our paper.

I also want to thank my supervisor, Dr. Swasti Raychaudhuri, for all the things I have learned from him over the last years and for the correction of this thesis. I am very grateful to have met him and that we can share so many unforgettable moments inside and outside of the lab.

I am also very grateful to all collaborators within and outside the department. I sincerely acknowledge Dr. Roman Körner for his mass spectrometry expertise and Dr. Stefan Pinkert for his assistance during the bioinformatic analysis of the interaction networks. I also would like to thank Prof. Dr. Frank Buchholz and his group for providing us with the esiRNA library.

I also want to thank all other members of Ulrich´s group for creating such a nice environment and all the things we have experienced in the last years. Thank you to Evelyn Frey-Royston, Darija Pompino, Silke Leuze-Bütün, and Andrea Obermayr-Rauter for their administrative support as well as Verena Marcus, Nadine Wischnewski, Ana Jungclaus, Romy Lange, Elisabeth Schreil, Emmanuel Burghardt, Albert Ries, Peter Nagy, Andreas Scaia, and Bernd Grampp for their invaluable technical support.

I also would like to thank PD Dr. Dietmar E. Martin for being the co-referee of this thesis and of course the other members of my PhD committee: Prof. Dr. Walter Neupert, Prof. Dr. Dieter Edbauer, Prof. Dr. Roland Beckmann, and Prof. Dr. Karl-Peter Hopfner.

Sigrun Polier I want to thank for correcting this thesis and her continuous support and love.

Mein herzlichster Dank gilt natürlich auch meinen Eltern Cornelia und Wilfried Löw sowie meinem Bruder Marc für ihren Rückhalt und ihre uneingeschränkte Unterstützung in allen Lebenslagen. Ihnen möchte ich diese Arbeit widmen.

Table of Contents

1 Summary

The cytosolic stress response, also known as the heat-shock response (HSR), is one of the major defense mechanisms activated by cells to maintain the integrity of the cellular proteome under proteotoxic environmental conditions. It is characterized by the increased synthesis of heat-shock proteins (Hsps), mainly molecular chaperones and proteases which prevent the aggregation of misfolded proteins and mediate their refolding or degradation. It is generally accepted that the induction of the HSR is coordinated by the heat-shock transcription factor 1 (HSF1). However, many mechanistic aspects of the HSF1 regulation remain unclear.

In the present study, a genome-wide RNA interference screen was combined with an extensive biochemical analysis and quantitative proteomics to better understand the regulation of the HSR upon thermal stress. In the screening experiments novel positive and negative modulators of the stress response were identified, including proteins involved in chromatin remodeling, transcription, mRNA splicing, DNA damage repair, and proteolytic degradation. The diversity of the identified regulators suggests that induction and attenuation of the HSR integrate signals from different cellular pathways and are rather multi-factorial processes than single gene/protein events. The modulator proteins are localized in multiple cellular compartments with the majority having their primary location in the nucleus. A protein-protein interaction analysis revealed a HSR regulatory network, with chromatin modifiers and nuclear protein quality control components occupying hub positions. These observations are supported by quantitative proteomics experiments, which showed specific stress-induced reorganizations of the nuclear proteome, including the transient accumulation of chaperones and proteasomal subunits.

The histone acetyltransferase EP300 was shown to specifically control the cellular level of HSF1 by stabilizing it against proteasomal turnover under normal conditions. Moreover, the ubiquitin-proteasome system (UPS) was found to participate in the attenuation of the HSR by degrading stress-activated, hyperphosphorylated HSF1. Since HSF1 competes with stress-denatured proteins for access to the proteasome, the extent of cellular protein damage modulates the rate of HSR attenuation.

In addition to thermal stress, various other proteotoxic stresses are known to induce the HSR such as the proteasome inhibitor MG132 and the triterpenoid celastrol, which activates HSF1 by an unknown mechanism. Therefore, the networks regulating HSF1 activation upon thermal stress, proteasome inhibition and celastrol treatment were compared in this study. Whereas there is a large overlap between the sets of regulatory factors activated

after heat stress and proteasomal impairment, HSF1 activation after celastrol treatment seems to bypass the HSR regulatory network to a large extent. Nevertheless, comparison of the regulatory networks under different proteotoxic conditions revealed a set of HSR core components, including factors involved in chromatin remodeling, DNA damage repair, RNA transport, transcription, and ion transport. The various cellular functions and localizations of these core components reinforce the multifaceted nature of the HSR regulation.

The results obtained in this study can help to identify potential targets for the pharmacologic manipulation of the HSR in the treatment of aggregate deposition diseases and cancer.

2 Introduction

In order to survive and reproduce, living organisms need to adapt to their specific habitat, in which they have to cope with a variety of adverse environmental conditions, which challenge the integrity of the cellular proteome. Protein homeostasis (proteostasis) – a balanced state of all protein components – is a prerequisite for cellular health and survival. A complex quality control network has evolved in cells and organisms to maintain proteostasis in the face of acute and chronic proteotoxicity. Imbalances in proteostasis result in the activation of universal and highly conserved stress response pathways; including the cytosolic stress response, leading to the transient expression of heat-shock proteins (Hsps), mainly molecular chaperones and proteases (Anckar and Sistonen 2011, Gidalevitz *et al.* 2011, Neef *et al.* 2011). Whereas chaperones either prevent the aggregation of misfolded proteins or assist in their refolding, proteases mediate their degradation, finally restoring proteostasis (Frydman 2001, Hartl *et al.* 2011).

2.1 Proteostasis

Proteostasis refers to the global control of protein biogenesis, folding, trafficking, aggregation, disaggregation, and degradation. Despite all environmental and intrinsic challenges, proteostasis ensures successful development and aging of cells or organisms by minimizing homeostasis perturbations that might cause disease. The proteostasis network maintains the cellular proteome in a stable and functional state and governs the "life of proteins" from birth to death (Balch *et al.* 2008).

The integrated network achieving proteostasis (Figure 2-1) comprises several hundreds of proteins, including molecular chaperones and their respective co-chaperones (see chapter 2.2.3), the ubiquitin-proteasome system (UPS), and the autophagy machinery (see chapter 2.3). While chaperones assist in the *de novo* folding, refolding, or disaggregation of proteins, the proteasomal and autophagic systems contribute to the proteolytic degradation of irreversibly misfolded proteins (Balch *et al.* 2008, Powers *et al.* 2009, Hartl *et al.* 2011). The capacity of the proteostasis network is adjusted by multiple interconnected stress-inducible signaling pathways, including the cytosolic stress response (Westerheide and Morimoto 2005), the unfolded protein response (UPR) of the endoplasmic reticulum (Ron and Walter 2007, Buchberger *et al.* 2010), and the mitochondrial UPR (Ryan and Hoogenraad 2007,

Haynes and Ron 2010). Furthermore, signaling pathways coupling ribosome biogenesis to the translational capacity are integrated (Hartl *et al.* 2011). These signaling pathways and their interconnection are discussed in chapter 2.4. Persistent imbalances in proteostasis have been linked with numerous pathological conditions, including neurodegeneration, cancer, type-2 diabetes, and cardiovascular diseases. It has been suggested that the manifestation of many of these diseases is related to an age-dependent decline of the cellular proteostasis capacity (Morimoto 2008, Powers *et al.* 2009, Ben-Zvi *et al.* 2009, David *et al.* 2010, Gupta *et al.* 2011).

2.2 Protein folding

Proteins are the most abundant, versatile, and conformationally complex biological marcomolecules and have important functions in virtually all biological processes. Protein biosynthesis takes place at the ribosomes, where linear chains up to several thousand amino acids are produced. For protein functionality these chains need to adopt their 'native conformations' – a few closely related specific three-dimensional structures (Bartlett and Radford 2009).

2.2.1 Folding versus aggregation

One main challenge in protein folding is the requirement of a stable, well defined native state on the one hand while still retaining conformational flexibility necessary for protein function on the other hand. Consequently, most native proteins show only marginal thermodynamic stabilization compared to their unfolded states under physiological conditions (Pace *et al.* 1981, DePristo *et al.* 2005). Other proteins inherently lack any three-dimensional structure and need to assemble with binding partners or ligands to acquire stability (Demchenko 2001, Park and Marqusee 2005, Dunker *et al.* 2008). Besides this, targeting of a protein to a specific subcellular compartment may enhance protein stability (Deshaies *et al.* 1988).

Pioneering work in the field of protein folding revealed that the primary sequence of a polypeptide chain contains all information necessary to specify its three-dimensional structure (Anfinsen 1973). Due to its high degrees of freedom and the astronomical number of possible conformations an unfolded polypeptide chain can adopt, the folding by a random sampling of all possibilities would occur on a biological unrealistic time scale (Levinthal 1968). However, the cooperation of many weak and non-covalent interactions between different amino acid

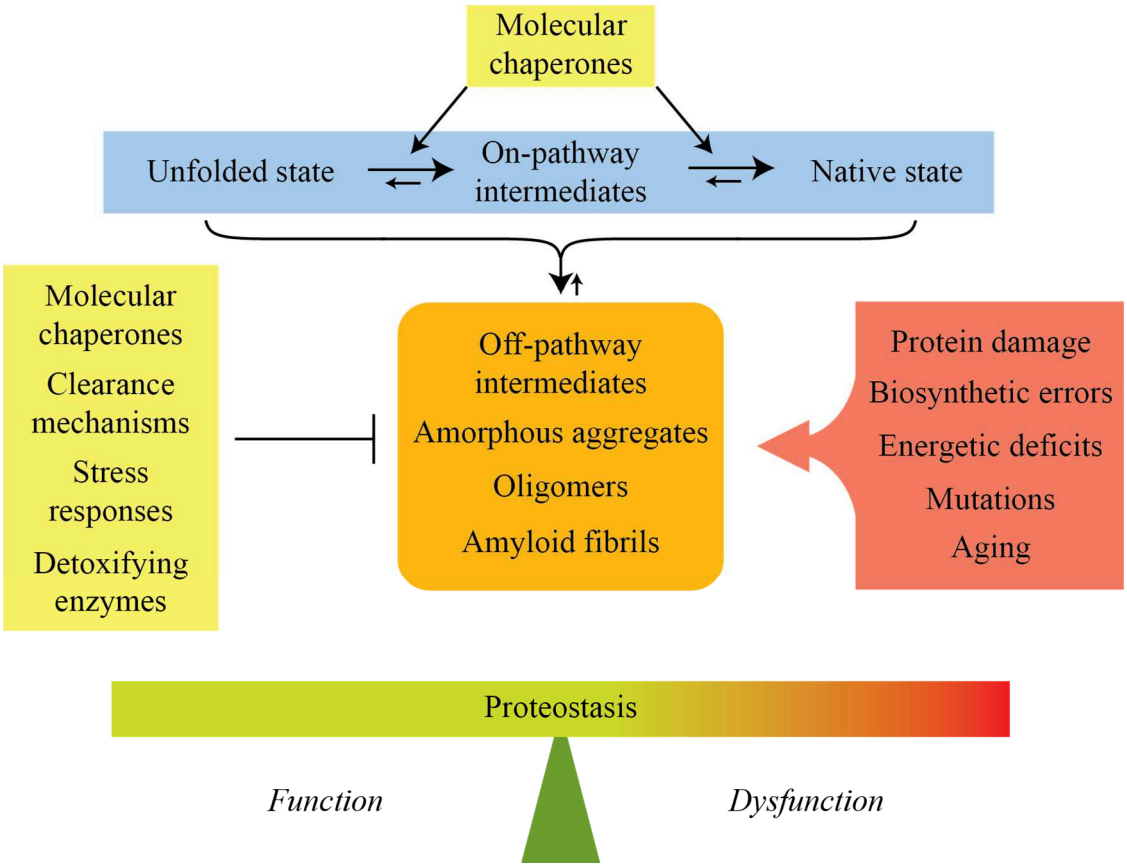

Figure 2-1: Protein homeostasis (proteostasis) network.
Cells integrate different components of the proteostasis network such as molecular chaperones and protein degradation machineries to maintain the cellular proteome in a functional and stable state. Whereas chaperones assist in the *de novo* folding of proteins and remodeling of misfolded proteins, proteases mediate their degradation. This enables cells to resist multiple intrinsic and extrinsic forces challenging proteome stability. Imbalances in proteostasis are associated with numerous pathological conditions such as neurodegeneration and cancer (adapted from Gidalevitz *et al.* 2011).

residues confines the accessible conformational space, thereby reducing the number of possible intermediates and transition states. In aqueous solution the main driving force for protein folding is the sequestration of non-polar residues in a hydrophobic core and the exposition of charged or polar amino acid side chains on the solvent-facing protein surface. In the current understanding, each protein explores a unique funnel-shaped potential energy landscape (Figure 2-2) during its folding process in which the number of accessible configurations decreases alongside with the energy (Wolynes *et al.* 1995, Dill and Chan 1997). Although the energy landscape may be rugged, with some local, non-native energy minima, in which partially folded intermediates may become kinetically trapped, the funnel-shaped energy surface suggests a deep energy minimum for the native state.

The folding of small single domain proteins (less than 100 amino acids) occurs on a sub-second time scale and can be best described by the nucleation condensation model, in which the secondary and tertiary structures form upon a general collapse around a diffuse

nucleus. In this two-state mechanism, only two species are populated - the unfolded and the native state. The energy landscape is relatively smooth without any substantial kinetic traps (Kim and Baldwin 1982, Ptitsyn 1998, Jackson 1998, Fersht 2000, Daggett and Fersht 2003). For proteins larger than 100 amino acids (~90% of all cellular proteins), it is assumed that folding occurs via the transient population of folding intermediates, which emerge from a rapid hydrophobic collapse of the polypeptide chain into a compact globular, non-native conformation (Brockwell and Radford 2007, Bartlett and Radford 2009). These molten globule states can either represent on-pathway folding intermediates towards the native state or kinetically stable but misfolded species which populate local, non-native energy minima in the rugged folding energy landscape (Figure 2-2) (Ptitsyn *et al.* 1990, Onuchic and Wolynes 2004, Jahn and Radford 2005, Lindberg and Oliveberg 2007, Vabulas *et al.* 2010). An increasing complexity in the domain structure of the protein results in a higher tendency to form misfolded intermediates (Netzer and Hartl 1997, Wright *et al.* 2005).

Proteins with non-native conformation are prone to aggregation due to the exposition of hydrophobic amino acid residues or even of unstructured regions of the polypeptide backbone (Eichner *et al.* 2011). A high concentration of non-native protein species further increases the likelihood of intermolecular interactions leading to protein aggregation. Hydrophobic forces drive the formation of amorphous aggregates which lack long-range order and that finally restructure and assemble in definite fibrillar amyloids (Figure 2-2). The amorphous, less ordered, soluble oligomeric intermediates are thought to serve as aggregation nuclei. These intermediate states are highly toxic for eukaryotic cells (Haass and Selkoe 2007) and are supposed to play important roles in neurodegenerative disorders and other pathological conditions (Chiti and Dobson 2006). It was shown that the toxicity of the transition states correlates with the exposure of hydrophobic surfaces (Bolognesi *et al.* 2010). These surfaces interfere deleteriously with other proteins and membranes, thereby promoting aberrant protein interactions and deregulation of the cellular stress response (Olzscha *et al.* 2011). The reorganization of the amorphous aggregates into insoluble fibrillar amyloids may present a cellular protection mechanism. The amyloids are characterized by a well-defined cross-β structure, in which β-strands run perpendicular to the long axis of the fibril (Sunde and Blake 1997, Tycko 2004). Under denaturing conditions or when the native state is destabilized (low pH, high temperature or amino acid substitutions), many proteins become capable of forming these thermodynamically very stable fibrils. Although the insoluble fibrils share a common structure, the soluble precursor proteins do not have any sequence similarity

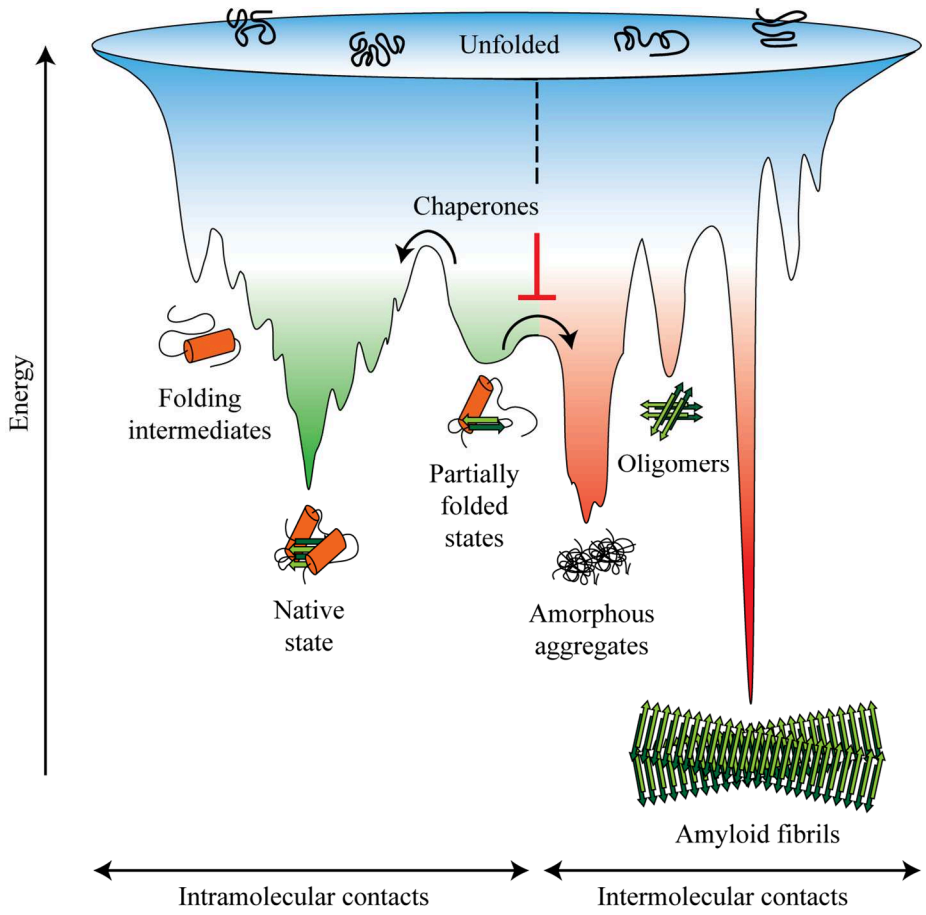

Figure 2-2: Free energy landscape of protein folding and aggregation.
Scheme of the multiple conformations explored by polypeptide chains as they move along the funnel-shaped energy surface towards their native state via intramolecular (green) contacts. Molecular chaperones may assist kinetically trapped folding intermediates or partially folded states to cross free energy barriers to reach their native conformation (Lin *et al.* 2008, Sharma *et al.* 2008, Chakraborty *et al.* 2010). The formation of amorphous aggregates, toxic oligomers, and highly ordered amyloid fibrils (red) is due to intermolecular contacts between intermediates that accumulate during the folding process or upon destabilization of the native state. Chaperones normally prevent these interactions (adapted from Hartl *et al.* 2011).

and are structurally very diverse, suggesting that formation of amyloids is an inherent property of the polypeptide chain (Dobson 2003).

2.2.2 Protein folding *in vivo* and the concept of molecular chaperones

Not only *in vitro* but also *in vivo*, the aggregation propensity of polypeptide chains is influenced by their local concentration. Compared to *in vitro* folding and refolding in dilute solutions, the folding in the cellular environment is challenged by the high concentration of proteins, nucleic acids and other macromolecules (up to 300-400 g/l). The so-called macromolecular crowding or, more precisely, the excluded volume effect refers to the fact that a significant proportion of the cell interior is occupied by macromolecules and, therefore,

unavailable to other molecules. The increased effective protein concentration enhances non-native intra- and intermolecular contacts resulting in an increased probability of misfolding and aggregation (Zimmerman and Trach 1991, Ellis 2001, Hartl and Hayer-Hartl 2002, Ellis and Minton 2006). Additionally, the translation of proteins at polyribosomes increases the probability of aggregation due to a high local concentration of nascent chains. Since the dimensions of the ribosomal exit tunnel do not allow folding beyond the formation of α-helical elements (Woolhead *et al.* 2004, Lu and Deutsch 2005), the entire sequence of a protein or at least a protein domain (on average 50-300 amino acids) has to emerge from the ribosome for its folding. In eukaryotes, the increased average protein length and reduced translation speed are further challenges for proper protein folding because protein synthesis takes longer than in prokaryotes leading to a prolonged exposure of nascent chains in partially folded, aggregation-sensitive states (Vabulas *et al.* 2010).

In living organisms, aggregation is minimized by different means. First, polypeptide sequences that favor folding over aggregation were selected by evolutionary pressure, resulting in a significantly reduced aggregation propensity of protein coding sequences as compared to random polypeptide sequences (Dobson 2004, Jahn and Radford 2008). Secondly, organisms try to create an environment supporting protein folding by the tight regulation of internal parameters, such as pH or temperature. Furthermore, cells invest in a complex proteostasis network consisting of molecular chaperones, for *de novo* folding or refolding, and proteolytic systems like the ubiquitin-proteasome system or the autophagy machinery, assisting in degradation and removal of terminally misfolded proteins (Balch *et al.* 2008, Glickman and Ciechanover 2002, Hartl and Hayer-Hartl 2002). The individual components of the network will be described in the following chapters.

2.2.3 Major chaperone classes

A molecular chaperone is defined as a protein that interacts with, stabilizes or helps another protein to acquire its functionally active state, without being part of the final structure. Molecular chaperones are of major importance in a multitude of cellular processes. They are involved in *de novo* folding of proteins, refolding of stress-denatured proteins, and disaggregation of at least some forms of aggregates. Moreover, they can contribute to the assembly of oligomeric complexes, assist in protein trafficking, and proteolytic degradation (Ellis and Hemmingsen 1989, Gething and Sambrook 1992, Parsell *et al.* 1994, Hartl and Hayer-Hartl 2009). Although different classes of structurally unrelated chaperones are known, chaperones are generally referred to as stress or heat-shock proteins (Hsps), because their

expression is increased under conditions of conformational stress. In general, chaperones increase the efficiency of the folding process rather indirectly by blocking competing reactions such as aggregation. They do not contribute any conformational information to the folding process and in most cases do not accelerate individual folding steps. An acceleration of protein folding can be promoted by proteins which contain either peptidyl-prolyl isomerase activity, increasing the rate of cis-trans isomerizations, or protein disulfide isomerase activity, playing important roles in the formation and reorganization of disulfide bonds (Fischer and Bang 1985, Wilkinson and Gilbert 2004, Appenzeller-Herzog and Ellgaard 2008). According to the molecular weight, chaperones are organized in five protein families: the small heat-shock proteins (sHsps), which lack any ATPase activity, and the ATPases Hsp100, Hsp90, Hsp70, and the chaperonins (Hsp60s). Chaperones, which are broadly involved in *de novo* folding and refolding (e.g. Hsp70s, Hsp90, and Hsp60s), reversibly bind to exposed hydrophobic sequences and promote folding through ATP-regulated binding and release cycles (Schiene and Fischer 2000, Dobson 2003, Vabulas *et al.* 2010, Hartl *et al.* 2011).

In all three kingdoms of life, the different classes of molecular chaperones form an interconnected network following the same principles of organization (Figure 2-3). As the growing polypeptide emerges from the ribosome, it is bound by ribosome-associated chaperones resulting in the stabilization of the nascent chain and the initialization of the folding process. If *de novo* folding intermediates require additional assistance, they are passed on to the downstream machinery such as the cytosolic Hsp70/40 and the Hsp60 protein families which complete the folding process. In the following sections the main classes of molecular chaperones will be discussed.

2.2.3.1 Ribosome-associated Chaperones

In eukaryotes, the folding of a polypeptide can occur co-translationally. However, since incomplete nascent chains are unable to adopt stable conformations, folding can only start when at least the polypeptide making up a protein subdomain has been synthesized (Cabrita *et al.* 2009, Eichmann *et al.* 2010). Due to the relatively slow translation speed (4-20 amino acids s^{-1}) growing nascent chains are exposed in a partially folded, aggregation-sensitive state during their synthesis. To guide initial folding events and protect growing polypeptides from misfolding and aggregation, some chaperones directly bind to the large ribosomal subunit in close proximity to the protein exit site. Whereas *de novo* folding in bacteria is supported by a chaperone called trigger factor (TF), eukaryotic cells possess two kinds of ribosome-associated systems, the ribosome-associated complex (RAC) and the nascent polypeptide-associated complex (NAC). In *Saccharomyces cerevisiae*, RAC is formed by the Hsp70

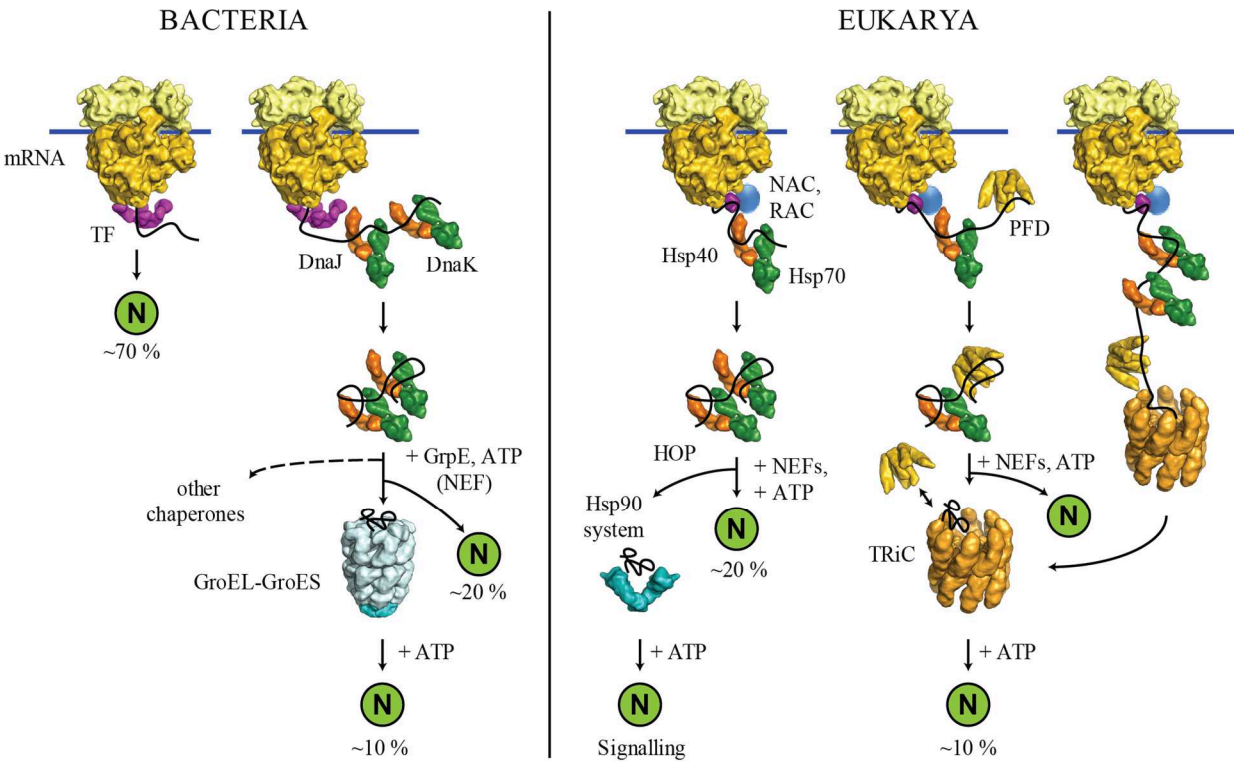

Figure 2-3: Pro- and eukaryotic cytosolic chaperone pathways.
In bacteria (left panel), the majority of nascent chains (~70%) rapidly adopt their native conformation without any further chaperone assistance after interaction with trigger factor (TF). Larger proteins are subsequently bound by the bacterial Hsp70 machinery (DnaK/DnaJ/GrpE) and fold upon ATP-dependent cycles of binding and release. Around 10% of the polypeptides need to be transferred to the chaperonin system GroEL-GroES for proper folding. Dashed arrows indicate that the pathway is not well established. In eukaryotes (right panel), the ribosome bound nascent chain-associated complex (NAC) generally interact with emerging polypeptides and the majority of proteins folds without further assistance. Around 20% of the synthesized chains are folded after interaction with the ribosome-associated complex (RAC) and the Hsp70/40 machinery. The Hsp-organizing protein (HOP) transfers a subset of these proteins to the downstream Hsp90 system for folding. About 10% of the polypeptide chains are passed on to chaperonin TRiC in an Hsp70 and prefoldin (PFD) dependent process. PFD is known to interact with certain TRiC substrates, including actin and tubulin (adapted from Hartl *et al.* 2011).

homologs Ssb1/2p, Ssz1p, and the Hsp40 chaperone zuotin. Mammalian RAC (mRAC) consists of the zuotin-like Mpp11 and the Ssz1p homolog Hsp70L1 but lacks a Ssb-like protein (Hundley *et al.* 2005, Otto *et al.* 2005, Preissler and Deuerling 2012). While NAC forms a homodimer in archaea, the eukaryotic heterodimer is highly conserved from yeast to humans (Pech *et al.* 2010).

Among the ribosome-associated chaperones, TF is best studied. The 48 kDa eubacterial protein consists of an N-terminal ribosome-binding domain, a peptidyl-prolyl cis-trans isomerase (PPI) domain, and a C-terminal domain, necessary and sufficient for its chaperone activity (Merz *et al.* 2006). According to the crystal structure, the carboxy-terminal domain is positioned in the center of the molecule (Ferbitz *et al.* 2004). With its two protruding arms, the C-terminal domain is the major binding region for hydrophobic

elements. The amino-terminal domain mediates the binding of TF to the ribosomal protein L23. (Kramer *et al.* 2002, Kaiser *et al.* 2006, Merz *et al.* 2006, Lakshmipathy *et al.* 2007). Whereas ribosome binding induces conformational changes in TF that are a prerequisite for the capturing of emerging polypeptides, the hydrophobicity of the nascent chain determines the dwell time of TF on the ribosome (Baram *et al.* 2005, Schlunzen *et al.* 2005, Kaiser *et al.* 2006). After the chain is released from the ribosome, the TF-nascent chain complex dissociates independently of ATP (Hesterkamp *et al.* 1996). The nascent chain is either folded without further assistance or transferred to downstream chaperoning systems such as the bacterial Hsp70 system DnaK/DnaJ/GrpE. TF does not actively assist protein folding by ATP-driven cycles of nascent chain binding and release but functions rather indirectly by shielding hydrophobic stretches, thereby preventing misfolding and aggregation (Young *et al.* 2004).

2.2.3.2 The Hsp70 system

Hsp70s, the most versatile class of chaperones, are key components of the chaperone network and are expressed in eubacteria, eukaryotes, some archaea, as well as in eukaryotic organelles like mitochondria and the endoplasmic reticulum (Hartl and Hayer-Hartl 2002). Members of this family actively participate in polypeptide folding through ATP-dependent cycles of protein binding and release. Two different forms of Hsp70 molecules exist in the cytosol of higher eukaryotes: constitutively expressed Hsp70s (Hsc70) and stress-inducible ones (Hsp70, Chang *et al.* 2007). Hsp70s function together with co-chaperones of the Hsp40 family and various nucleotide exchange factors (NEFs) that regulate the ATP-dependent reaction cycle (Hartl *et al.* 2011). All Hsp70s share a similar domain architecture, consisting of an N-terminal ATPase and a C-terminal substrate binding domain, which is composed of an α-helical lid segment and a β-sandwich domain (Zhu *et al.* 1996).

During the reaction cycle, an unfolded or partially folded substrate protein is delivered to ATP-bound Hsp70 by one of the numerous Hsp40 cofactors (Langer *et al.* 1992, Kampinga and Craig 2010). The β-sandwich domain of Hsp70 specifically binds to hydrophobic seven-residue segments which occur on average every 50-100 residues in proteins (Rudiger *et al.* 1997). The Hsp40 molecule stimulates ATP hydrolysis by Hsp70, thus leading to lid closure and stable peptide binding. NEF binding catalyzes ADP dissociation and subsequent binding of ATP results in lid opening and substrate release, thereby completing the reaction cycle.

The exact mechanism by which Hsp70 mediates protein folding and prevents aggregation is not clear yet (Mayer and Bukau 2005). According to the kinetic partitioning model, Hsp70 binding shields hydrophobic segments in substrate proteins, thereby hindering misfolding and aggregation. Upon release, fast-folding molecules or domains adopt their

native conformation by burying hydrophobic residues, whereas slower folding molecules will rebind to Hsp70. (Re)binding of substrates to Hsp70 may also help remodeling of kinetically trapped folding intermediates by overcoming free energy barriers of the folding process (Sharma *et al.* 2010). Proteins that are unable to fold after Hsp70 cycling may be transferred to further downstream chaperone systems, such as the chaperonins or Hsp90 (Langer *et al.* 1992, Kerner *et al.* 2005).

With its well-established role in *de novo* protein folding Hsp70 represents a key component of the proteostasis network. *Drosophila* studies revealed that increased Hsp70 levels can prevent toxic protein aggregation (Auluck *et al.* 2002) Moreover, interaction of Hsp70 with CHIP (Carboxyl-terminus of Hsc70 Interacting Protein), an U-box containing ubiquitin ligase, targets misfolded proteins to the proteasome, thus linking chaperone function with the proteolytic degradation of misfolded proteins (Ballinger *et al.* 1999, Luders *et al.* 2000, Petrucelli *et al.* 2004, Arndt *et al.* 2010).

2.2.3.3 The chaperonins

The chaperonins are a conserved class of large double-ring complexes with a molecular mass of approximately 800 kDa. They can be divided into two different subgroups. Group I chaperonins, also known as Hsp60s, are present in bacteria (GroEL) as well as in organelles of endosymbiotic origin – chloroplasts and mitochondria. They are built of two homoheptameric rings and functionally cooperate with their Hsp10 cofactors (bacterial GroES), which serve as a seven-membered detachable lid for the cavity, thereby creating a folding cage for encapsulated polypeptide substrates. The group II chaperonins in archaea (thermosome) and the eukaryotic cytosol (TRiC/CCT) are composed of octa- or nonameric rings formed by up to eight different subunits. In contrast to group I chaperonins, members of the second group possess a built-in lid and function independently of GroES-like co-chaperones. Likewise Hsp70s, substrate binding and release of chaperonins is regulated by ATP. However, the mechanism by which these two classes of chaperones promote protein folding differ essentially. In general, chaperonins assist folding of non-native substrates by (i) protein encapsulation and isolation to prevent aggregation, and by (ii) restriction of the conformational space (confinement) to avoid the formation of kinetically trapped intermediates. Although it was shown that chaperonins function as passive aggregation-prevention devices (Brinker *et al.* 2001, Apetri and Horwich 2008), other studies imply that protein encapsulation can substantially accelerate protein folding (Brinker *et al.* 2001, Tang *et al.* 2006, Chakraborty *et al.* 2010).

Among the different chaperonins from all kingdoms of life, the bacterial group I GroEL-GroES system is best studied. The reaction cycle generally follows a postitive intra- but a negative inter-ring allostery (Horovitz 2005). The characteristic GroEL double-ring is formed of fourteen identical 57 kDa subunits, each consisting of an equatorial ATPase domain, an intermediate hinge domain, and an apical substrate-binding domain. The interaction with substrate proteins (up to 60 kDa in size) is mediated by hydrophobic amino acid residues in the apical domain (Hartl and Hayer-Hartl 2002). The ATP-regulated binding of the homoheptameric GroES ring encapsulates the substrate and induces an extensive conformational change in GroEL resulting in the formation of a highly hydrophilic cage with a net-negatively-charged inner wall (Xu *et al.* 1997, Horwich and Fenton 2009). During the time of ATP hydrolysis (10-15 s) in the GroES-bound GroEL heptamer, the so-called *cis*-ring, the protein is free to fold. After ATP binding to the opposite ring, the *trans*-ring, and GroES dissociation from the *cis*-ring, the protein substrate leaves the cavity. Substrates that have not reached their final conformation yet may rebind to GroEL for additional folding cycles.

2.2.3.4 The Hsp90 system

Hsp90 is a highly abundant molecular chaperone found in the cytoplasm, ER and mitochondria of all branches of eukaryotes as well as eubacteria (Young *et al.* 2004, Chen *et al.* 2006). It functions downstream of the Hsp70 system in the stabilization and final structural maturation of many signal-transducing molecules such as regulatory kinases and transcription factors including steroid hormone receptors. The Hsp90 client proteins participate in cell-cycle progression, protein trafficking and secretion, telomere maintenance, tumorigenesis, and targeted protein degradation – thereby establishing the role of Hsp90 as a hub in protein homeostasis (Pearl and Prodromou 2006, Taipale *et al.* 2010, Hartl *et al.* 2011). Furthermore, Hsp90 is thought to be important during developmental processes and in evolution. Under normal conditions, Hsp90 is thought to buffer the phenotypic manifestation of genetic variation. However, when the buffering capacity of Hsp90 is environmentally challenged, new traits might appear in some individuals (Rutherford and Lindquist 1998, Taipale *et al.* 2010). In addition, a new role for Hsp90 in chromatin remodeling has emerged in recent years. In *Drosophila* it has been shown that Hsp90 and several co-chaperones are involved in stress-induced chromatin inactivation (Ruden and Lu 2008).

Hsp90 functions as a dimer with each monomer consisting of an N-terminal ATPase domain (ND), a middle domain for client binding (MD) and a C-terminal homo-dimerization domain (CD). As for many other chaperones, the Hsp90 reaction cycle is ATP-dependent. ATP binding induces closure of the so-called ATP lid in the NDs, domain dimerization, and

formation of a closed Hsp90 conformation (molecular clamp) in which the individual monomers are twisted around each other. After ATP hydrolysis, the N-terminal domains dissociate (open state) and another cycle can be initiated (Pearl and Prodromou 2006, Wandinger *et al.* 2008). Client protein loading and the Hsp90 reaction cycle are regulated by various cofactors, of which tetratricopeptide repeat (TPR) domain containing proteins represent a major group. For example, the Hsp-organizing protein (HOP) bridges Hsp70 and Hsp90 chaperones, thereby providing a physical link for substrate transfer from the Hsp70 complex to Hsp90. HOP also inhibits the N-terminal dimerization and thus ATP hydrolysis. Other well-known cofactors of Hsp90 are CDC37, AHA1, p23, and CHIP. Whereas the co-chaperone CDC37 inhibits the ATPase activity of Hsp90, AHA1 functions as an activator. p23 is known to stabilize the dimerized form of Hsp90 (Jackson 2013). Similar to its interactions with Hsp70, CHIP can bind the C-terminal domain of Hsp90 and causes the targeting of at least some proteins for proteasomal degradation (Ballinger *et al.* 1999, Xu *et al.* 2002, McClellan *et al.* 2005). Despite all research on Hsp90, little is known about the molecular basis for client recognition and the mechanism by which Hsp90 mediates conformational changes in client proteins (Wandinger *et al.* 2008, Taipale *et al.* 2010).

2.2.3.5 Hsp100 chaperones and small heat-shock proteins

Hsp100 chaperones are members of the AAA+ ATPase superfamily (ATPases associated with various cellular activities). Their unfoldase activity is strictly dependent on the AAA domain, which binds and hydrolyses ATP. Furthermore, the AAA domain mediates the oligomerization to barrel shaped hexameric rings with a central pore. By association with either a peptidase or a chaperone system, Hsp100 chaperones contribute to the degradation or refolding of misfolded proteins, respectively. The prokaryotic Hsp100/Clp family has been studied best. Proteins tagged for degradation are recognized by AAA+ proteins (e.g. ClpA) that cooperate with the ClpP peptidase via a conserved P-element. Conserved aromatic residues at the central pore of the AAA+ proteins bind and release the substrate in a nucleotide dependent manner, thereby generating a mechanical force and threading the substrate into the proteolytic chamber of the protease. In contrast to ClpA, AAA+ proteins that do not contain the conserved P-element (e.g. ClpB) do not associate with peptidases such as ClpP but rather with other chaperones (e.g. Hsp70/DnaK) to resolubilize aggregated proteins. In this bi-chaperone disaggregation system Hsp70 controls the interaction of misfolded substrates with ClpB. The ATP-driven threading activity of the AAA+ protein is thought to loosen single unfolded polypeptide chains from the aggregate. After translocation,

the polypeptide is likely to be transferred to the Hsp70 system for proper folding (Liberek *et al.* 2008, Mogk *et al.* 2008, Haslberger *et al.* 2008, Zolkiewski *et al.* 2012).

Small heat-shock proteins (sHsps) are a ubiquitous and conserved but rather heterogeneous family of ATP-independent chaperones with strong anti-aggregation properties. Their molecular weight ranges from 15 to 30 kDa. They display chaperone function *in vitro* and have been shown to exert cytoprotective functions under conditions of oxidative stress. Furthermore, they interfere with apoptotic proteins and are involved in cytoskeletal organization. sHsps form dynamic oligomeric structures ranging from 12 up to 50 individual subunits. A temperature dependent activation of oligomeric sHsps results in their binding to partially unfolded protein intermediates. Co-aggregation of destabilized proteins with sHsps increases the efficiency of resolubilization and refolding by the Hsp100/Hsp70 system (Liberek *et al.* 2008). The 10 human sHsps (HSPB1-HSPB10) share a highly conserved amino acid sequence of 80-90 residues at their C-termini, the so-called α-crystallin domain. Interestingly, sHsps show a highly tissue-specific expression pattern. (Jakob *et al.* 1993, Haslbeck 2002, Brownell *et al.* 2012, Garrido *et al.* 2012).

2.3 Protein degradation systems

Besides the sophisticated cellular chaperone network, proteolytic systems such as the ubiquitin-proteasome system or autophagy machinery (Figure 2-4 and Figure 2-5) are key components of the proteostasis network and are responsible for the degradation of either terminally misfolded or short-lived and regulatory proteins. Whereas the UPS is mainly involved in the degradation of short-lived proteins, the autophagic pathway is responsible for the degradation of long-lived polypeptides, protein aggregates and cytoplasmic organelles (Rubinsztein 2006).

2.3.1 The ubiquitin-proteasome system

In eukaryotes, the UPS is one of the critical components in maintaining the cellular protein homeostasis. Furthermore, it plays an important role in a large variety of other processes which include cell cycle regulation, differentiation and development, DNA repair, the modulation of nuclear hormone receptors, and the regulation of the immune and inflammatory response (Ciechanover *et al.* 2000, Nawaz and O'Malley 2004). The UPS represents a highly specific and tightly regulated pathway of intracellular protein degradation. In general, the

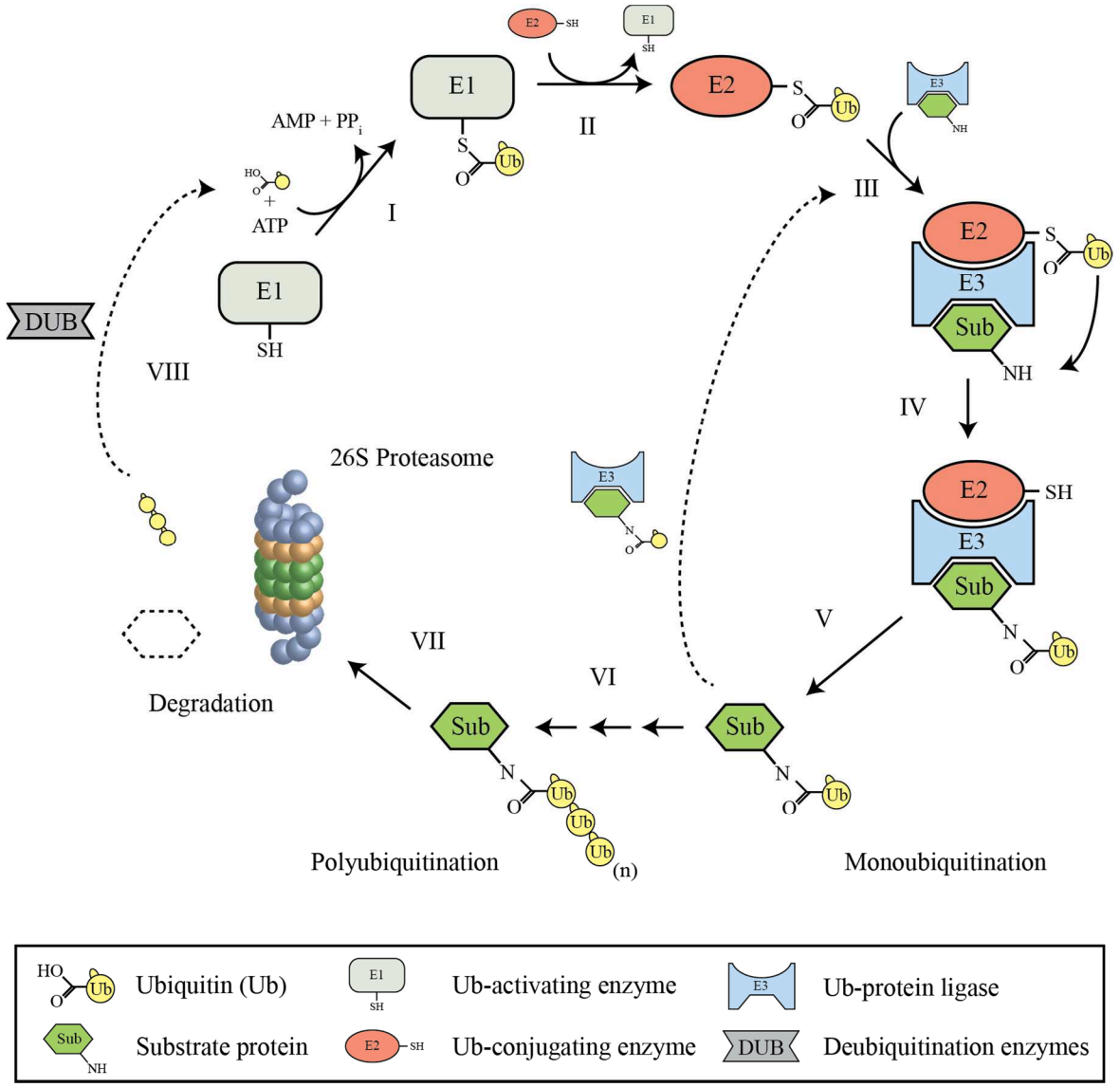

Figure 2-4: The ubiquitin-proteasome pathway (UPS).
The degradation of a target protein by the UPS involves its tagging with multiple ubiquitin molecules and the successive proteolysis via the 26S proteasome. The ubiquitin moiety (Ub) is activated in an ATP-dependent reaction and forms a high-energy thiol ester with the E1 Ub-activating enzyme (I). After transfer to the E2 Ub-conjugating enzyme (II), Ub is covalently bound to a lysine residue in the target protein. This process is ameliorated by specific E3 Ub-protein ligases which bridge the E2 enzymes with the UPS substrates (III-V). Monoubiquitination is known to be involved in the regulation of many cellular processes such as endocytosis, DNA repair and transcriptional regulation. The re-entering of a monoubiquitinated substrate at step III results in its polyubiquitination (VI) and the subsequent degradation by the 26S proteasome (VII). Specialized deubiquitinating enzymes (DUBs) assist in the recycling of the Ub moieties (VIII).

degradation of a protein by the UPS involves two consecutive steps: (i) covalent modification of substrate proteins with multiple ubiquitin molecules and (ii) degradation of the tagged proteins by the 26S proteasome (Ciechanover *et al.* 2000, Glickman and Ciechanover 2002).

2.3.1.1 Ubiquitin and the ubiquitin conjugating machinery

Ubiquitin is a highly conserved regulatory polypeptide consisting of 76 amino acids. It has been found in almost all tissues of eukaryotic cells but is absent in eubacteria and archaea. In mammals, ubiquitin is encoded by four different genes. It is either expressed as a single copy fused to the ribosomal proteins S27a and L40 or as a polyubiquitin precursor molecule encoded by *ubb* and *ubc* (Kimura and Tanaka 2010).

Ubiquitination is a reversible and highly versatile post-translational modification of cellular proteins, in which the C-terminal glycine residue of ubiquitin (G76) is conjugated via its carboxyl group to the ε-amino group of an internal lysine residue in the substrate protein. The conjugation of ubiquitin to the N-terminal α-amino group of a protein or to other amino acids such as threonine, cysteine, or serine has also been reported but rarely occurs (Hershko *et al.* 1984, Glickman and Ciechanover 2002, Cadwell and Coscoy 2005, Wang *et al.* 2007). The ubiquitination of a substrate protein is a multi-step process which involves numerous enzymes (Figure 2-4). The first step, ubiquitin activation, is an ATP-driven process in which the ubiquitin moiety forms a high-energy thiol ester bond with the active site cysteine residue of the ubiquitin-activating enzyme E1. A ubiquitin-conjugation enzyme (UBC), E2, then transfers the activated ubiquitin via another high-energy thiol ester bond to the target protein, which is recognized by a member of the E3 ubiquitin-protein ligase family. Moreover, it has been shown that efficient polyubiquitination may require an additional conjugation factor termed E4 polyubiquitin ligase (Hershko *et al.* 1983, Koegl *et al.* 1999, Glickman and Ciechanover 2002, Chitra *et al.* 2012). The human genome encodes two E1 enzymes, 30-40 UBCs and more than 600 ubiquitin-protein ligases (Komander 2009). The latter ones can be further divided into three different groups. While RING finger E3 ligases catalyze a direct conjugation of ubiquitin to the substrate protein, HECT domain-containing E3 ligases transfer the ubiquitin moiety via a third high-energy thiol ester intermediate between ubiquitin and the E3 ligase itself. Members of the third group, the U-box proteins, perform polyubiquitination. They contain a conserved 70 amino acid domain, the so-called U-box, which mediates the interaction with ubiquitin-conjugated substrates. Some U-box proteins have been shown to function as E4 polyubiquitin ligases (Koegl *et al.* 1999, Hatakeyama *et al.* 2001, Hatakeyama *et al.* 2004).

Several forms of ubiquitination can be distinguished. Whereas the attachment of one ubiquitin molecule, monoubiquitination, is known to be involved in cellular processes such as endocystosis, histone regulation, DNA repair, transcriptional regulation, and general protein localization, the attachment of several ubiquitin polypeptides, polyubiquitination, primarily

targets a protein for proteasomal degradation (Schnell and Hicke 2003, Mukhopadhyay and Riezman 2007, Woelk *et al.* 2007). Polyubiquitination is achieved by the successive addition of further ubiquitin molecules to one of the seven internal lysine residues of the previously added ubiquitin (Glickman and Ciechanover 2002). As all lysine residues were shown to be ubiquitinated *in vivo*, a great variety of ubiquitin-dependent modifications exist. The two best-studied examples are the linkage of multiple ubiquitin moieties to lysine residue 48 and 63. While polyubiquitination at lysine residue 48 targets a substrate protein for proteasomal degradation (Hershko and Ciechanover 1998), the modification at residue 63 generates a non-proteolytic signal comparable to monoubiquitination. Furthermore, polyubiquitination at lysine 63 plays a major role in autophagy (Tan *et al.* 2008, Komander 2009). For details see chapter 2.3.2.

2.3.1.2 Ubiquitin-like proteins

Besides ubiquitin, several other proteins are known to be conjugated to polypeptides as post-translational modifications. The family of ubiquitin-like proteins (UBLs) contains a growing number of molecules such as small ubiquitin-like modifier (SUMO), neuronal-precursor-cell-expressed developmentally downregulated protein-8 (NEDD8), human leukocyte antigen F-associated (FAT10), autophagy-related gene 8 (ATG8, also known as LC3), and ATG12 as well as ubiquitin-like protein-5 (UBL5). Although they show only modest sequence similarity to ubiquitin, they are structurally closely related. The enzymatic cascade that conjugates UBLs to their substrates is comparable to the ubiquitin machinery, involving activation, conjugation and ligation of the different UBLs. Substrates modified by UBLs are generally not targeted for proteasomal degradation, but rather regulate a diverse set of cellular processes including transcription and translation, nuclear transport, DNA repair, and autophagy (Welchman *et al.* 2005, van der Veen and Ploegh 2012). However, conjugation of FAT10 has been shown to promote proteasomal degradation (Hipp *et al.* 2005).

2.3.1.3 The 26S proteasome and proteasomal degradation

Proteasomes are large, multi-subunit proteases found in all eukaryotes and archaea as well as in some bacteria. They play a major role in cellular protein turnover. The process of proteasomal degradation includes recognition, unfolding, and degradation of specifically tagged proteins into small peptides. Whereas eukaryotic and archaeal proteasomes share a common structure, the 20S core particle, bacteria express a much simpler homolog, the so-called heat-shock locus V (Glickman and Ciechanover 2002, Maupin-Furlow *et al.* 2000, Valas and Bourne 2008).

The structure of the eukaryotic proteasome holoenzyme (26S proteasome) can be divided in two subcomplexes: one catalytically active 20S core particle (CP) and two identical 19S regulatory particles (RPs). The 20S core particle is composed of four stacked rings that form a barrel-shaped structure. The two outer rings contain seven highly homologous α-subunits each, the two inner rings consist of similarly conserved β-subunits, leading to the overall $\alpha_7\beta_7\beta_7\alpha_7$ structure of the CP. Three of the seven β-subunits, namely subunits 1, 2, and 5, display threonine peptidase active sites with caspase-like, trypsin-like, and chymotrypsin-like activity, respectively. The combination of these different activities enables the proteasome to cleave substrate peptide bonds behind any amino acid, generating short peptides with a median length of seven to nine amino acids. To protect cellular proteins from non-specific degradation, the catalytic sites face the inside of the cavity and can only be accessed through a narrow gate at the end of the barrel which is formed by the N-termini of the α-subunits (Dick *et al.* 1998, Kisselev *et al.* 1999, Groll *et al.* 2000, Orlowski and Wilk 2000, Bedford *et al.* 2010). The access to the proteolytic chamber is tightly controlled by the 19S regulatory particle, which generally sits on both sides of the CP and is involved in substrate recognition, unfolding, and translocation. The structure of the RP reveals two distinct multi-subunit subcomplexes, called base and lid. The base is formed of six homologous AAA+-ATPase subunits (Rpt1-6) and four non-ATPase subunits, Rpn1, Rpn2, Rpn10, and Rpn13. The latter two function as ubiquitin receptors with at least four K48-linked ubiquitin moieties being necessary for efficient substrate recognition. Following the initial recognition, interactions of substrate proteins with the remaining base subunits are likely to occur. The ATPase activity of the Rpt subunits couples ATP hydrolysis with the unfolding of substrate proteins and their threading into the catalytic cavity. Furthermore, the direct interaction of the ATPase subunits with the α-rings mediates the opening of the CP gate. The lid of the regulatory particle is composed of eight non-ATPase subunits and exhibits deubiquitination activity via Rpn11. The recovery of the ubiquitin moieties is further assisted by specialized deubiquitinating enzymes (DUBs) (Lupas *et al.* 1997, Wilkinson 1997, Glickman *et al.* 1998, Thrower *et al.* 2000, Verma *et al.* 2002, Smith *et al.* 2007, Bedford *et al.* 2010, Sakata *et al.* 2012).

Although the most prominent role of the proteasome is the degradation of polyubiquitinated protein substrates, there is a growing list of molecules which undergo ubiquitin-independent proteolysis. The best-studied examples are the proteasomal activation of the transcription factor NF-κB, the “default” degradation of proteins with inherently unstructured regions, and proteolysis of the enzyme ornithine decarboxylase (ODC). For the

cell cycle regulator p53 a ubiquitin-dependent as well as a ubiquitin-independent degradation mechanism is known (Rape and Jentsch 2002, Zhang *et al.* 2003, Asher and Shaul 2005, Asher *et al.* 2006). The same holds true for the hypoxia-inducible factor 1 α (HIF1α), a stress-responsive transcription factor regulating the cellular response to hypoxia. The primary degradation mechanism of HIF1α involves its hydroxylation, subsequent polyubiquitination by VHL (von Hippel-Lindau) and degradation via the 26S proteasome. However, histone deacetylase inhibitors have been shown to mediate HIF1α degradation in a ubiquitin-independent way (Kong *et al.* 2006, Geng *et al.* 2012).

2.3.2 Autophagy

The autophagic pathway is a basic and highly conserved mechanism for the bulk degradation of cytoplasmic components and organelles by the lysosomal machinery and plays an important role in the cellular adaptation to changing environmental conditions. Three forms of autophagy have been described, which differ in the mechanism by which the substrates enter the degradation pathway: macroautophagy, microautophagy, and chaperone-mediated autophagy (CMA, Figure 2-5). While macroautophagy involves the formation of double-membrane-bound structures known as autophagosomes, cellular components are directly incorporated into lysosomes during microautophagy and CMA (Yorimitsu and Klionsky 2005, Rubinsztein 2006, Cheung and Ip 2009, Shaid *et al.* 2013).

Among the different types, macroautophagy is best studied and likely to be responsible for the majority of autophagy-related degradation (Mortimore and Poso 1987). In the initial step, cytoplasmic organelles and proteins are surrounded by lunate double-membrane structures, the phagophores, which then subsequently close to fully sequester the cytosolic content, forming so-called autophagosomes. Recent data suggest that the endoplasmic reticulum (ER), the Golgi complex, and endosomes are potential sources for membrane generation (Tooze and Yoshimori 2010). Afterwards, autophagosomes undergo a stepwise maturation resulting in their fusion with lysosomes and the formation of autolysosomes. Finally, the cytoplasmic content is degraded by acidic lysosomal hydrolases. Overall, the biogenesis of the autolysosome is regulated by approximately 30 autophagy-related genes (ATG), among which several UBLs are found. Autophagic cargos can either be sequestered by bulk engulfment or by a process termed selective autophagy, in which the inward facing membrane of the phagophore/autophagosome is lined with specific autophagy receptors facilitating a highly selective degradation of large protein aggregates and cellular

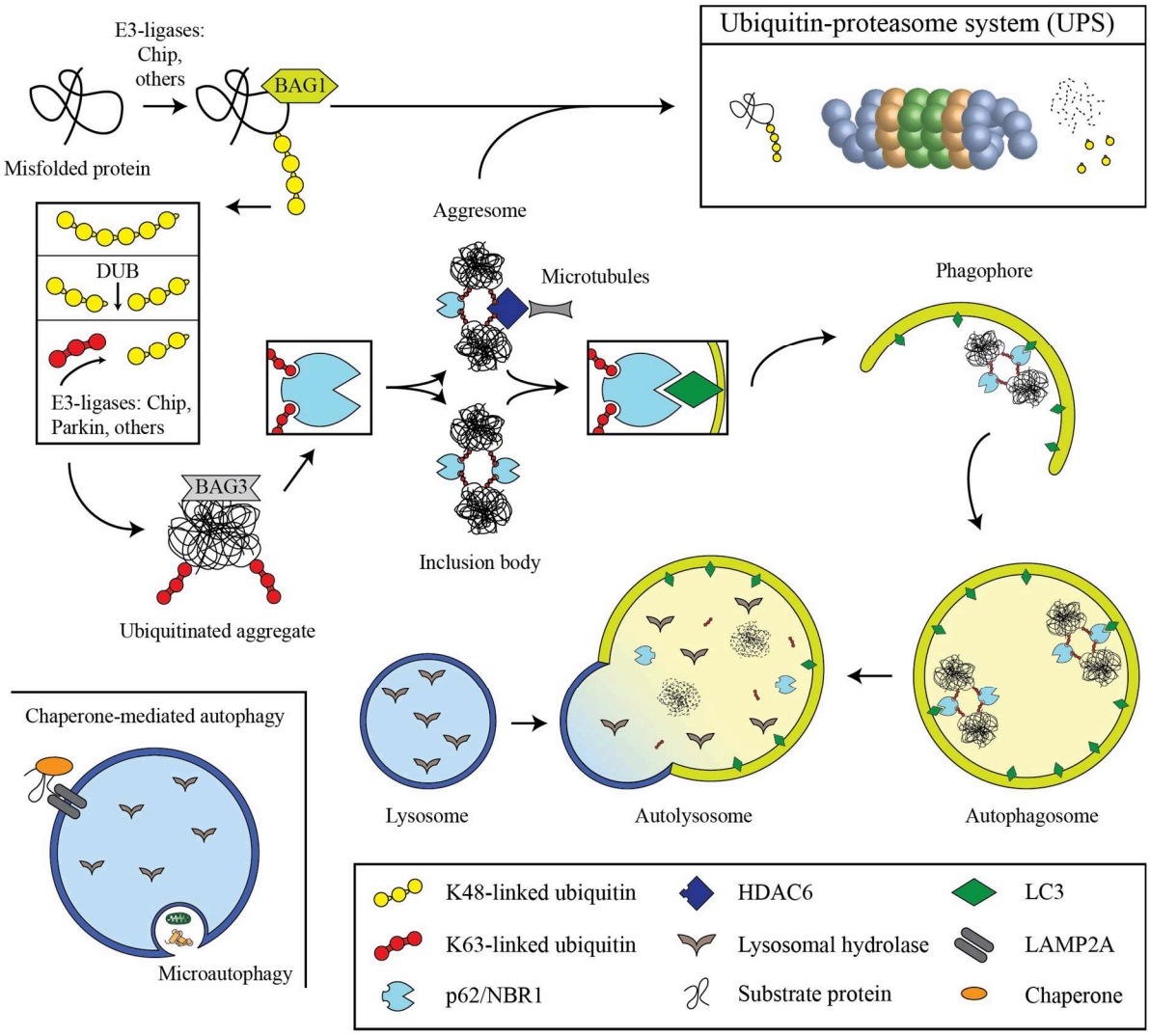

Figure 2-5: The autophagy system.
Different forms of ubiquitin conjugation and the interaction of misfolded proteins with the co-chaperones Bag1 (BCL-associated athanogene 1) or Bag3 link between proteasomal and autophagic degradation. K48-linked ubiquitin molecules and interaction with Bag1 generally target proteins for degradation by the proteasome. Under certain conditions (e.g. proteotoxic stress) the remodeling of polyubiquitin chains by DUBs and E3 ligases like CHIP or Parkin lead to the formation of K63-linked ubiquitin chains. Recognition of these chains by the ubiquitin-binding domains of p62/NBR1 or HDAC6 and interaction with Bag3 either induce the formation of inclusion bodies or directly target aggregated proteins to the aggresome. Aggresomes are intracellular deposits of misfolded proteins and can be degraded via the proteasome as well as autophagy. For autophagic degradation, p62/NBR1 interact with the selective autophagy marker LC3 (light chain 3), thereby targeting protein aggregates to the emerging semicircle-shaped double-membrane-bound phagophores. After subsequent membrane closure the so-called autophagosomes fuse with lysosomes leading to the degradation of aggregates in autolysosomes. This process is known as selective autophagy or macroautophagy. During microautophagy misfolded proteins or cellular organelles are directly incorporated into lysosomes. The chaperone-mediated autophagy (CMA) involves the recognition of misfolded proteins by chaperone complexes, binding to the specific receptor LAMP2A (lysosome-associated membrane protein 2A), and translocation into the lysosome (adapted from Cheung and Ip 2009 and Shaid *et al.* 2013).

organelles. (Mizushima *et al.* 2002, Kang *et al.* 2011, Mizushima *et al.* 2011, van der Veen and Ploegh 2012, Shaid *et al.* 2013).

In principal, microautophagy resembles macroautophagy in the direct sequestration of cytosolic contents, but cargos are directly incorporated into lysosomes instead of autophagosomes (Cheung and Ip 2009). The third autophagic pathway, the CMA, differs from the former two in several aspects. CMA substrates are predominantly soluble cytosolic proteins carrying a common KFERQ-like targeting motif which is recognized by the HSC70 chaperone complex. After binding to a specific receptor, the lysosome-associated membrane protein 2A (LAMP2A), substrates are directly translocated into the lysosome for degradation (Massey *et al.* 2006**,** Rubinsztein 2006).

2.3.3 Interconnection between protein degradation pathways

The UPS and the autophagy machinery are two complementary and distinct cellular degradation systems. However, a growing body of evidence suggests that there are several molecular links between the two pathways. While a proteins half-life is determined by the N-end rule and the possible occurrence of a PEST-degradation signal, its ubiquitination pattern determines if it is targeted for proteasomal or autophagic degradation. It has been shown that CHIP, a U-box containing ubiquitin-ligating enzyme, which targets a broad range of proteins for proteasomal degradation, is also able to promote the formation of K63-linked polyubiquitin chains, thus enabling degradation by the autophagic machinery. Similar observations have been made for other ubiquitin-ligation enzymes like Parkin, leading to the conclusion that there is a group of dual-function E3 ligases targeting proteins either for proteasomal or autophagic clearance mechanisms (Zhang *et al.* 2005, Olzmann *et al.* 2007, Shaid *et al.* 2013).

Additionally, the relative activity of the two degradation systems partly influences the way of substrate protein degradation. It has been shown that autophagy is induced upon UPS impairment and that a microtubule-associated deacetylase, HDAC6, is an essential molecular link in this compensatory reaction (Varshavsky 1997, Johnston *et al.* 1998, Iwata *et al.* 2005, Pandey *et al.* 2007, Komander 2009). Furthermore, activation of the autophagic machinery can protect cells from death induced by proteasomal inhibitors (Kawaguchi *et al.* 2011, Benbrook and Long 2012). On the other hand, inhibition of autophagy leads to an increase in levels of proteasome substrates (Korolchuk *et al.* 2009).

The protein levels of the co-chaperones Bag1 (BCL-2-associated athanogene 1) and Bag3 provide another regulatory intersection of these two degradative pathways. Whereas Bag1, highly expressed in young cells, promotes protein degradation by the proteasomal machinery, the increased Bag3 level in aged cells leads to a more intensive usage of the

macroautophagic system for turnover of polyubiquitinated proteins. Furthermore, it has been demonstrated that the Bag3-associated increase in autophagy is dependent on the ubiquitin-binding protein p62/SQSTM1. Together with NBR1 (neighbor of breast cancer), p62 binds K63-ubiquitinated protein aggregates and targets them to the emerging phagophore through an interaction with the autophagy specific light chain 3 (LC3) modifier, thereby acting as a selective autophagy receptor (Pankiv *et al.* 2007, Gamerdinger *et al.* 2009, Kirkin *et al.* 2009).

2.4 Stress-responsive pathways in proteostasis

Under normal conditions, the proteostasis network, composed of molecular chaperones as well as the proteolytic degradation machinery, is able to ensure the stability and functionality of the cellular proteome (see chapters 2.2.3 and 2.3). However, only limited information is available regarding the percentage of chaperones actually engaged in protein maintenance and it remains to be elucidated if cells possess a reserve chaperoning capacity (Morimoto 2008). An excess folding capacity could buffer unexpected changes in the protein flux but would require a reservoir of freely available chaperones, thereby representing a waste of cellular resources. It is more likely that the proteostasis capacity of a cell is titrated closely to the folding requirements at a given time. A prerequisite for this are highly robust stress-inducible pathways that respond rapidly to any imbalances in proteostasis by mounting an appropriate protective cellular response (Morimoto 2008, Gidalevitz *et al.* 2011). These defense mechanisms include general protection pathways like the cytosolic stress response as well as organelle-specific stress responses such as the unfolded protein response of the ER or the mitochondria and the nuclear DNA damage response (Zhou and Elledge 2000, Westerheide and Morimoto 2005, Ron and Walter 2007, Buchberger *et al.* 2010, Ryan and Hoogenraad 2007, Haynes and Ron 2010).

2.4.1 Challengers of proteostasis

All cells and tissues are constantly challenged by numerous adverse environmental or intrinsic conditions that might lead to an imbalance in proteostasis. These stress-inducing signals include a wide range of acute and chronic perturbations of the physiological state and can be grouped into four categories: environmental stress, pathophysiological stress, protein conformational diseases as well as cell growth and development (Morimoto 1998, Morimoto 2008). The first group, environmental stress, mainly includes classical physical stressors such

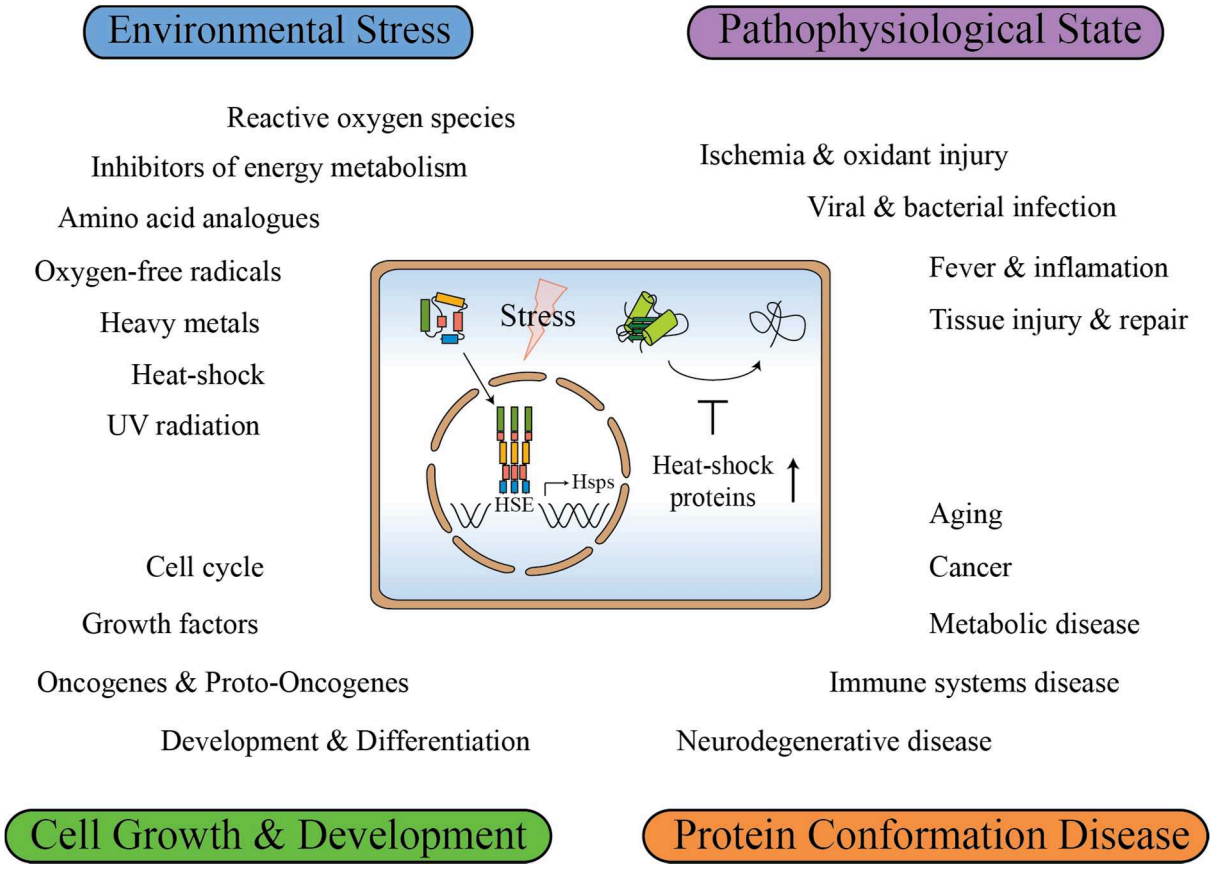

Figure 2-6: Inducers of the cytosolic stress response.
Stress inducing conditions can be grouped into four major categories: Three classes of environmental and physiological stresses (environmental stress, pathophysiological state, protein conformation disease) and a fourth class that summarizes intrinsic stimuli during cell growth and development. All conditions are known to result in an increased expression of Hsps in response to the stress-dependent activation of heat-shock transcription factor 1 (HSF1) and its binding to specific heat-shock elements (HSE) in the promotor regions of the Hsps (adapted from Morimoto 2008).

as elevated temperature, oxidative stress, heavy metal ions, UV radiation, and the incorporation of amino acid analogues. Group two refers to the changes of the physiological state due to fever, inflammation, various infections, and tissue injuries. The protein conformational disease category summarizes the more chronic insults like cancer, neurodegenerative diseases, and aging. For the latter two the accumulation of misfolded proteins is a constant challenge to the proteostasis system. Moreover, cell growth and development represent intrinsic challenges for the cellular homeostasis (Figure 2-6). To restore the balance, all stress-inducing signals mentioned above result in the activation of heat-shock transcription factor 1 (HSF1) and consequently in an increased expression of heat-shock genes including molecular chaperones and other components of the protein quality control machinery. The inability to restore proteostasis might lead to disease and even cell death (Morimoto 1998, Hartl *et al.* 2011).

2.4.2 The cytosolic stress response

Cultured cells as well as whole organisms respond to conditions of proteotoxic stress with the activation of a universal and highly conserved pathway, the cytosolic stress response. This cytoprotective mechanism, also known as the heat-shock response (HSR), results in the transient expression of Hsps to ensure stress adaptation, recovery, and survival (Lindquist 1986, Wu 1995, Morimoto 1998, Anckar and Sistonen 2011). The gene induction occurs nearly instantaneously and is proportional to the intensity, duration, and type of stress (Abravaya *et al.* 1991, Gasch *et al.* 2000, Hahn *et al.* 2004). Although the magnitude of the HSR is mainly regulated at the transcriptional level, other post-transcriptional regulatory mechanisms such as stress-induced changes in mRNA stability or alterations in the translation efficiency are known (Banerji *et al.* 1984, Theodorakis and Morimoto 1987). While the HSR in isolated cells is triggered by protein damage in each cell individually, in metazoans, the HSR is also subject to cell non-autonomous signaling by mechanisms of endocrine communication between different tissues and organs (Prahlad *et al.* 2008, Gidalevitz *et al.* 2011, van Oosten-Hawle *et al.* 2013).

Commonly, the cytosolic stress response is stimulated by heat stress (Tissieres *et al.* 1974, Lewis *et al.* 1975, Spradling *et al.* 1977). Remarkably, a few degrees temperature increase is sufficient for dramatic changes in key cellular structures and activities, apparently due to the metastable nature of many proteins in the physiological temperature range (Figure 2-7). Beyond the (partial) unfolding of individual proteins, mild heat stress already leads to the reorganization of the actin cytoskeleton into stress fibers. Severe heat stress results in a broad collapse of the cytoskeletal network including intermediate and actin-containing filaments as well as microtubules. However, the temperature-induced changes may vary with cell type and organism. Furthermore, rod-shaped structures of densely packed actin filaments are formed in the nucleus (Welch and Suhan 1985, Rivera *et al.* 2004). Intracellular transport processes are disrupted, organelles such as mitochondria lose their correct subcellular localization, and the Golgi complex as well as the ER undergo fragmentation. A reduced number of mitochondria and the uncoupling of the oxidative phosphorylation result in a strong decline in the cellular ATP level (Welch and Suhan 1985, Patriarca and Maresca 1990, Richter *et al.* 2010).

The enhanced expression of Hsps is accompanied by a significant decrease in transcript levels of constitutively expressed genes and a global decrease in translation (Murray *et al.* 2004). The chromatin in the nucleus condenses and the nucleoli disperse (Nickells *et al.* 1988). Non-translating mRNAs and translation initiation factors are stored in cytoplasmic

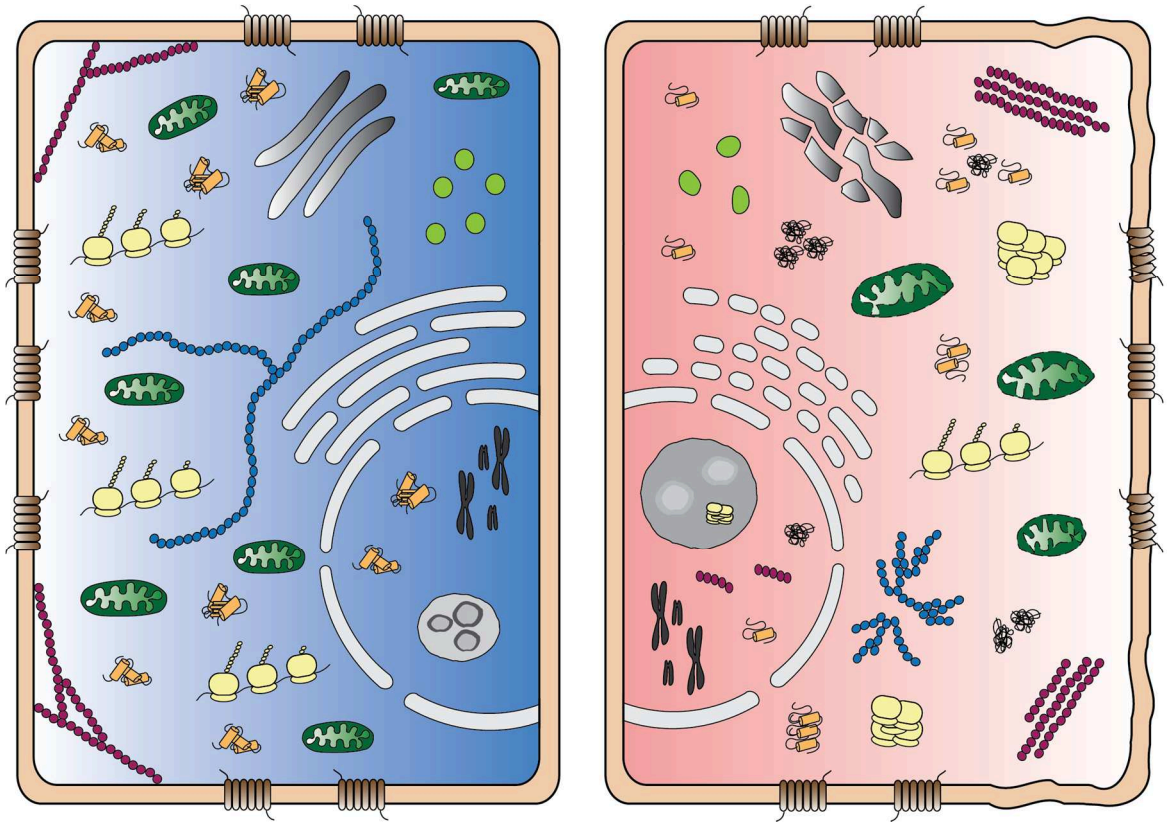

Figure 2-7: Cell physiological changes induced by thermal stress.
Eukaryotic cells grown at physiological temperature (left) and after exposure to heat stress (right) are compared. Temperature increase does not only result in the unfolding and aggregation of individual proteins but also leads to the reorganization of actin filaments into stress fibers (purple) and the collapse of intermediate filaments (blue). The ER (light grey) and the Golgi complex (white-grey gradient) undergo fragmentation. The number of lysosomes (light green) and mitochondria (green) decrease. The nucleoli (grey) swell and deposits of incorrectly processed ribosomal RNAs and aggregated ribosomal proteins become visible. The global decrease in translation is accompanied by the formation of cytoplasmic stress granules (yellow). Temperature-dependent changes in the membrane morphology (brown) lead to increased membrane fluidity as well as permeability. In summary, the different effects result in a transient cell cycle arrest and stop of proliferation (adapted from Richter *et al.* 2010).

stress granules (Nover *et al.* 1989, Buchan and Parker 2009). Moreover, heat-shock leads to an arrest in ribosome biogenesis due to changes in the organization and composition of the nucleoli. They swell and deposits of incorrectly processed ribosomal RNAs and aggregated ribosomal proteins become visible (Welch and Suhan 1986, Boulon *et al.* 2010). Stress-induced changes in the membrane morphology including an altered protein to lipid ratio as well as a general increase in membrane fluidity are also observed after thermal insults. As a consequence of the increased membrane permeability, the cytosolic pH drops and the ion homeostasis is disturbed (Kruuv *et al.* 1983, Balogh *et al.* 2005, Vigh *et al.* 2007, Richter *et al.* 2010).

Induction of the HSR is mediated by heat-shock transcription factors (HSFs). Whereas invertebrates such as yeast, *Caenorhabditis elegans,* and *Drosophila melanogaster* possess

only one HSF, four distinct but related HSFs have been found in vertebrates, HSF1-4, with HSF1 being the master regulator of the cytosolic stress response (Pirkkala *et al.* 2001, Trinklein *et al.* 2004, Anckar and Sistonen 2011). HSR induction is abolished in HSF1-deficient cells or organism and cannot be rescued by the other HSFs. After a short description of HSF2-4, the current knowledge regarding HSF1 will be discussed in greater detail.

Upon proteasomal inhibition, simultaneous activation of HSF1 and HSF2 as well as formation of DNA-binding-competent HSF1/HSF2 heterotrimers have been described, suggesting a modulatory role of HSF2 in the expression of selected heat-shock genes. (Mathew *et al.* 1998, Pirkkala *et al.* 2000, Loison *et al.* 2006, Ostling *et al.* 2007). An HSF1-dependent DNA binding of HSF1/HSF2 heterotrimers is also known to be involved in the regulation of satellite III DNA transcription in nuclear stress bodies, although the function of this process remains to be elucidated (Sandqvist *et al.* 2009, Vabulas *et al.* 2010). Furthermore, HSF2 is associated with the development of the brain and reproductive organs (Kallio *et al.* 2002, Wang *et al.* 2004, Chang *et al.* 2006). Recently, HSF3, which is mainly present in avian species, has been shown to activate the transcription of non-classical Hsps in mouse fibroblasts (Fujimoto *et al.* 2010). HSF4 plays a role in the development and maintenance of lens cells and mutations are associated with cataract formation (Bu *et al.* 2002, Fujimoto *et al.* 2004).

Because of its conserved role in the transcriptional activation of the cytosolic stress response, HSF1 represents the best-studied member of the HSF family. It is constitutively expressed in almost all cell types and tissues (Anckar and Sistonen 2011). The HSF1-mediated stress-inducible synthesis of Hsps is required for thermotolerance acquisition and protection against heat-inducible apoptosis (McMillan *et al.* 1998). Furthermore, HSF1 is involved in protecting cells from various pathophysiological conditions including neurodegeneration and other degenerative diseases (Fujimoto *et al.* 2005, Cohen *et al.* 2006, Tanaka *et al.* 2007), lifespan extension in *C. elegans* (Hsu *et al.* 2003) as well as development and maintenance of neuronal tissues (Santos and Saraiva 2004, Homma *et al.* 2007). Besides promoting Hsp gene expression, HSF1 drives transcriptional programs to support malignant transformation, cancer cell survival, and proliferation (Mendillo *et al.* 2012). It has been shown that HSF1-deficient cells are highly resistant to tumorigenesis driven by mutations of the RAS oncogene or the tumor suppressor p53 (Dai *et al.* 2007).

HSF1 is a ~60 kDa protein consisting of an N-terminal DNA-binding domain (DBD), a bipartite heptad repeat oligomerization domain, a regulatory domain (RD), and a C-terminal

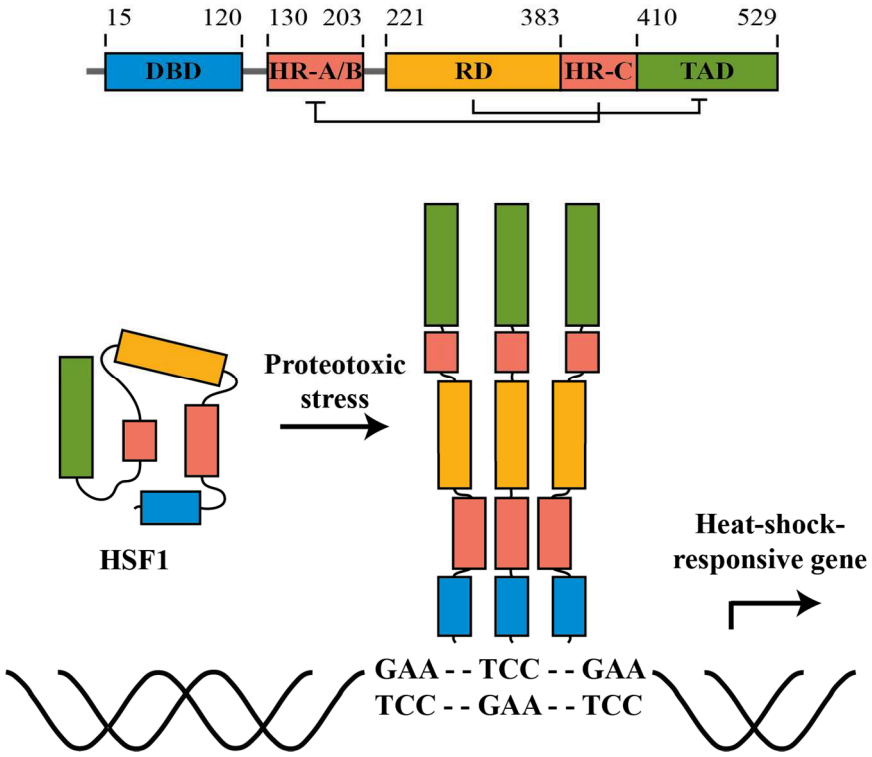

Figure 2-8: Domain structure of human HSF1.
The human HSF1 consists of an N-terminal DNA-binding domain (DBD), three hydrophobic heptad repeat domains (HR-A/B/C), a regulatory domain (RD), and a C-terminal transactivation domain (TAD). Intermolecular contacts between the oligomerization domains HR-A/B result in the trimerization of HSF1 and are negatively regulated by intramolecular contacts between HR-A/B and HR-C. The RD exerts negative control over the trans-activating capacity of HSF1. Under conditions of proteotoxic stress, HSF1 trimerizes, accumulates in the nucleus, is post-translationally modified, and drives the transcription of heat-shock-responsive genes by binding to inverted nGAAn repeats in the promotor regions of target genes (adapted from Anckar and Sistonen 2011).

trans-activation domain (TAD) (Figure 2-8). The helix-turn-helix motif containing DBD is the best-conserved region within the HSF family and represents the only functional domain for which structural data are available (Littlefield and Nelson 1999, Anckar and Sistonen 2011). The oligomerization domain (HR-A/B) can be further divided into two subdomains, each containing an amphiphilic helix with the hydrophobic heptad repeats HR-A and HR-B. Interactions between the HR-A/B domains result in the formation of a triple-stranded coiled-coil structure, thereby regulating HSF1 trimerization. A third hydrophobic heptad repeat domain, HR-C, is located between the RD and the TAD and is thought to avoid spontaneous trimerization of HSF1 by folding back to the HR-A/B domain, thus keeping HSF1 in an inactive state (Peteranderl and Nelson 1992, Peteranderl *et al.* 1999). Oligomerization of HSF1 and its subsequent binding to extended repeats of the nGAAn consensus sequence in the promotor regions of target genes, the so-called heat-shock elements (HSEs), are induced by proteotoxic stress. Although monomeric HSF1 has been shown to interact with HSEs as

well, trimerization increases its DNA-binding affinity by several orders of magnitude. The RD, which is located between the heptad repeat domains HR-A/B and HR-C, is proposed to exert negative control over the TAD in the absence of protein damage. The RD was shown to be target of multiple post-translational modifications, including phosphorylation, sumoylation, and acetylation, all modulating the transcriptional activity of HSF1. The TAD is located at the very C-terminus of HSF1 and is involved in both transcriptional initiation and elongation (Anckar and Sistonen 2011).

Stress-dependent transcriptional regulation by HSF1 is a multi-step process that is only partially understood. Under basal conditions, inactive HSF1 monomers are predominately located in the nucleus due to a potent bipartite nuclear localization signal, but HSF1 shuttling between the nucleus and cytosol has been reported. Thermal stress results in the inactivation of HSF1 export leading to its further nuclear accumulation (Mercier *et al.* 1999, Vujanac *et al.* 2005, Anckar and Sistonen 2011). Although the exact mechanism underlying HSF1 activation remains unclear, different models have been proposed (Figure 2-9). According to the chaperone displacement theory, the repressed monomeric state of HSF1 is thought to be stabilized by transient interactions with chaperones including Hsp90, Hsp70, and their cofactors (Abravaya *et al.* 1992, Shi *et al.* 1998, Zou *et al.* 1998). Phosphorylation at serine residues 303 and 307 further contributes to HSF1 repression (Neef *et al.* 2011). In response to proteotoxic stress, HSF1 is thought to get displaced from Hsp90 and other co-chaperones, which bind to misfolded proteins instead (Anckar and Sistonen 2011). Free HSF1 trimerizes and acquires HSE-binding competence (Pelham 1982). In contrast to Hsp90, Hsp70 and Hsp40 can remain associated with HSF1 even under stress conditions (Abravaya *et al.* 1992). To become trans-activation competent, HSF1 requires extensive post-translational modification (PTM). Trimer formation is accompanied by phosphorylation of multiple serine residues, mainly localized in the regulatory domain. However, the functional significance of most of these phosphorylation events is still unclear (Anckar and Sistonen 2011, Neef *et al.* 2011). PTM are also known to be involved in the repression of HSF1-dependent trans-activation. Sumoylation at lysine residue 298, for example, follows phosphorylation of serine 303 and has an inhibitory effect on HSF1 (Hietakangas *et al.* 2003). Acetylation of the DBD at lysine 80 has been reported to reduce the dwell time of HSF1 on DNA and mediates HSR attenuation. In turn, deacetylation of HSF1 by the deacetylase sirtuin 1 (SIRT1) results in a prolonged binding to HSEs (Westerheide *et al.* 2009). Once activated, HSF1 drives the expression of Hsps, which assist in reducing the cellular load of misfolded proteins either by refolding or degradation. When proteotoxicity is

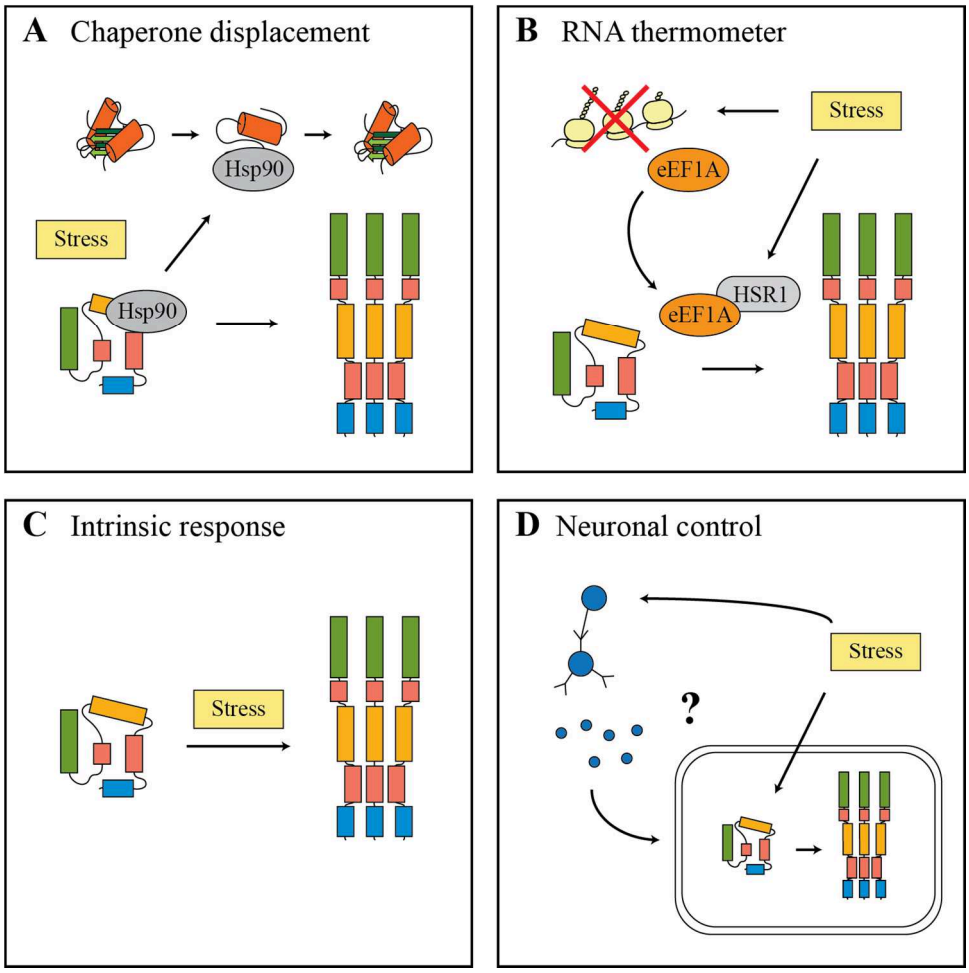

Figure 2-9: Proposed activation mechanisms for HSF1.
(A) In the chaperone displacement model, a transient interaction of monomeric HSF1 with chaperone complexes, predominantly Hsp90, represses its activity. Proteotoxic conditions lead to the accumulation of non-native proteins which displace HSF1 from the chaperones. HSF1 is free to trimerize and drives the transcription of heat-shock-responsive genes. (B) According to the RNA thermometer theory, a complex of the heat-sensing RNA molecule HSR-1 and the translation elongation factor eEF1A stimulates HSF1 activity. (C) The intrinsic response model proposes a built-in ability of HSF1 to directly sense various kinds of stresses. *In vitro* studies revealed that HSF1 trimerizes upon exposure to such proteotoxic conditions. (D) In the nematode *Caenorhabditis elegans*, an additional level of cell non-autonomous HSR regulation was shown. Animals deficient in the thermosensory AFD neurons fail to induce the HSR in somatic cells. The mechanism of how AFD neurons influence somatic HSF1 activity is far from being understood (adapted from Anckar and Sistonen 2011).

overcome, cells are left with an increased pool of freely available chaperones. Rebinding of these chaperones to HSF1 is thought to result in the attenuation of the HSR.

Although the existence of an inhibitory HSF1/multichaperone complex is well established, the high molar excess of intracellular chaperones over HSF1 complicates a fine-tuned regulation of HSF1 and is unlikely to be the only regulatory mechanism (Shamovsky and Nudler 2008). Several other models for HSF1 regulation have been proposed (Figure 2-9). The RNA thermometer model postulates the participation of a ribonuleoprotein complex

consisting of the heat-sensing RNA HSR-1 (heat-shock RNA-1) and the translation elongation factor eEF1A in the regulation of HSF1 activity. As eEF1A is also known to be involved in the organization of the cytoskeleton, the general shutdown of protein biogenesis and the collapse of the cytoskeleton are linked to HSF1 activation (Shamovsky *et al.* 2006, Shamovsky and Nudler 2008, Anckar and Sistonen 2011). Furthermore, HSF1 possesses an intrinsic ability to directly sense different forms of proteotoxic conditions including increased calcium concentrations, thermal and oxidative stress. Purified HSF1 has been shown to undergo trimerization upon exposure to such conditions (Mosser *et al.* 1990, Goodson and Sarge 1995, Zhong *et al.* 1998). Additionally, a cell non-autonomous HSF1 regulation has been described in the nematode *C. elegans*. Thermosensory AFD neurons and their successional postsynaptic cells influence the HSR in somatic cells and regulate the temperature-dependent behavior of the worm. Although it was shown that HSF1 appears to be a downstream target of these neurons, the mechanistic details of this process remain to be uncovered (Prahlad *et al.* 2008, Anckar and Sistonen 2011).

2.4.3 Organelle-specific stress response pathways

As discussed in chapter 2.4.1, proteotoxic conditions lead to the activation of the HSR, the main stress response of the cytosol. In eukaryotic cells, individual compartments vary in their susceptibility to protein damage. Cells have developed compartment-specific protein quality control strategies to counteract the accumulation of non-native proteins. In the following sections, the unfolded protein responses of the ER and mitochondria will be discussed (Figure 2-10).

The ER is the organelle in which proteins are folded and post-translationally modified before they are secreted, integrated into membranes, or delivered to other compartments of the endomembrane system. The ER exerts major quality control function for almost all signaling proteins involved in the communication of cells with their environment. Whereas properly folded proteins advance from the ER, misassembled proteins are targeted for proteasomal degradation in a process called ER-associated degradation (ERAD). Proteotoxic conditions, which disturb ER homeostasis and lead to an increased load of misfolded proteins, trigger conserved stress-signaling pathways commonly known as the unfolded protein response (UPR). Activation of the UPR results in the upregulation of ER chaperones, expansion of the ER membrane system, pausing of translation, and an increased degradation of misfolded proteins. If cells fail to re-establish ER homeostasis, they undergo apoptosis (Ron and Walter 2007, Walter and Ron 2011, Kourtis and Tavernarakis 2011). The UPR is mediated by three

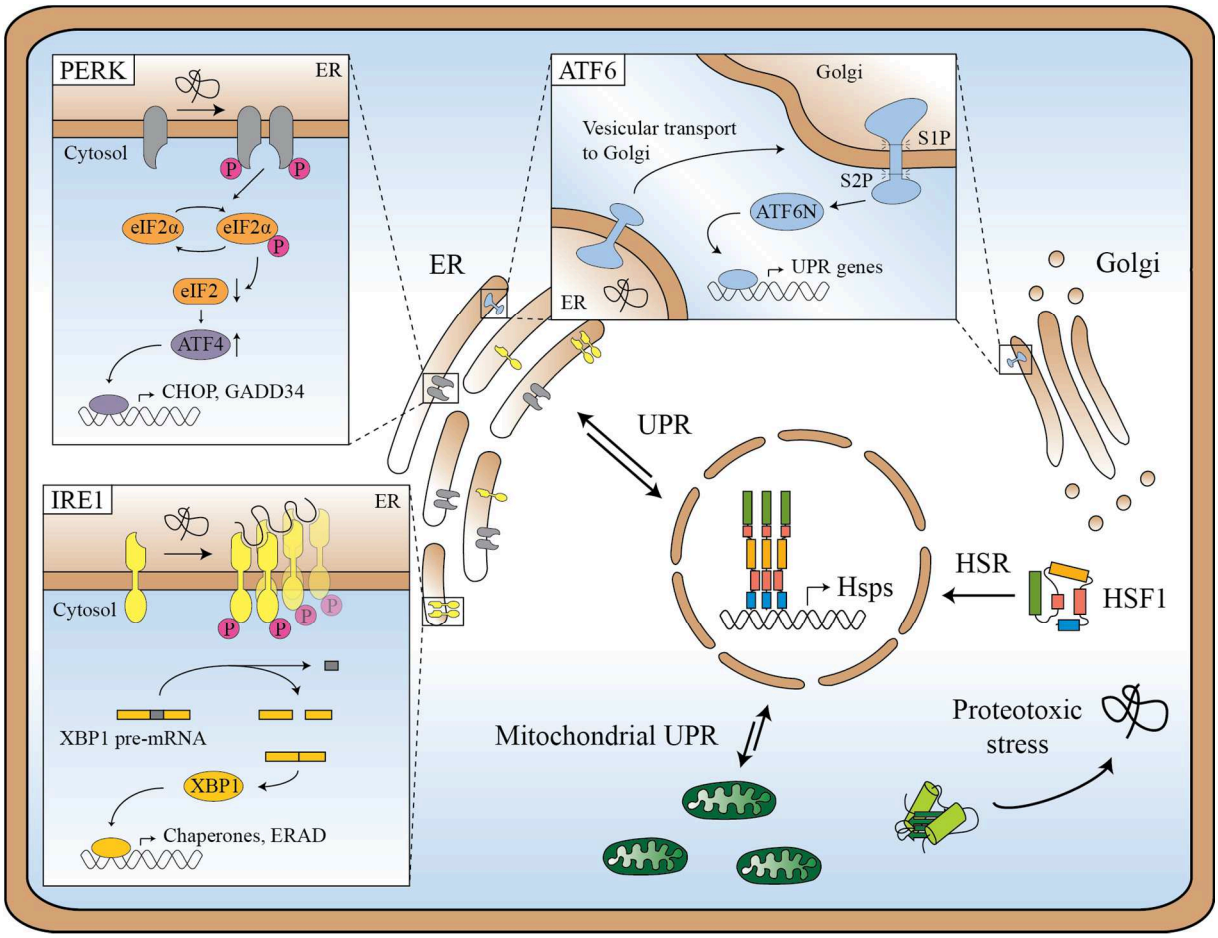

Figure 2-10: General and organelle-specific stress responses.
Exposure of the cell to proteotoxic stress and the subsequent accumulation of misfolded and aggregated protein species lead to the induction of general as well as organelle-specific stress response pathways. The activation of the cytosolic HSR involves the oligomerization and translocation of HSF1 to the nucleus, where it drives the transcription of Hsps. Stressful conditions in the ER result in the activation the UPR. The protein folding conditions in the organelle are monitored by three families of signal transducers, namely PERK, ATF6, and IRE1. Activation of each receptor leads to the production of transcription factors that drive the expression of UPR target genes. IRE1 and PERK also reduce the load of proteins entering the ER by the degradation of ER bound mRNAs or inhibition of general translation, respectively. Mitochondrial stress induces an organelle-specific UPR leading to an increased expression of the mitochondrial quality control machinery (adapted from Walter and Ron 2011).

classes of transmembrane sensors, each representing an individual branch of the response: inositol requiring enzyme 1 (IRE1), PKR-like ER kinase (PERK), and the activating transcription factor 6 (ATF6) (Figure 2-10). Similar to the inactivation of HSF1 through interaction with Hsp90, the transmembrane receptors are repressed through the binding to the ER Hsp70 chaperone BiP/GRP78 (Ig-binding protein/glucose-regulated protein 78). The accumulation of un- and misfolded proteins leads to the displacement of BiP/GRP78 from the receptors and their subsequent activation (Zhang and Kaufman 2006). While IRE1 is the most conserved branch of the UPR and the only one in lower eukaryotes, metazoans have additionally developed the PERK and ATF6 branches (Walter and Ron 2011).

ATF6 is a transcription factor initially localized in the ER membrane. After the accumulation of misfolded proteins, ATF6 is activated and translocates to the Golgi apparatus, where two proteases, S1P and S2P, cleave its luminal and cytosolic domains from the transmembrane part (Figure 2-10). The 50 kDa cytosolic N-terminal fragment, ATF6N, enters the nucleus and drives the transcription of UPR target genes, including BiP and the ER Hsp90 GRP94 (Yoshida *et al.* 1998, Haze *et al.* 1999, Ye *et al.* 2000).

The second branch of the UPR is controlled by the ER-resident transmembrane kinase PERK. Upon activation, PERK oligomerizes, undergoes auto-phosphorylation, and phosphorylates the α-subunit of translation initiation factor 2, eIF2 (Figure 2-10). This phosphorylation inactivates eIF2 and inhibits translation in response to ER stress. The overall decrease in translation reduces the ER protein folding load (Harding *et al.* 1999). Furthermore, the reduced eIF2 activity results in the preferred translation of a specific subset of mRNAs carrying particular motifs in their 5'-untranslated regions (5'-UTR) such as upstream open reading frames (uORF) and internal ribosomal entry sites (IRES, Dang Do *et al.* 2009). The transcription factor ATF4 is one of them and in turn drives the transcription of CHOP and GADD34. Whereas CHOP controls the transcription of genes involved in apoptosis, GADD34 is part of a protein phosphatase complex regulating the dephosphorylation of eIF2α. Thus, GADD34 participates in a negative feedback loop which restores translation (Novoa *et al.* 2001, Walter and Ron 2011).

The third branch of the UPR is regulated by the bifunctional transmembrane kinase/endoribonuclease IRE1. Oligomerization and auto-phosphorylation of IRE1 lead to the activation of its ribonuclease activity. Active IRE1 splices the pre-mRNA coding for the UPR-specific transcription factor XBP1, which enhances the expression of ER chaperones and ERAD components. Furthermore, IRE1 is involved in a process called RIDD (regulated IRE1-dependent decay) to degrade ER-bound mRNAs and reduce the ER protein folding load (Yoshida *et al.* 2001, Lee *et al.* 2003, Hollien and Weissman 2006, Walter and Ron 2011).

The mitochondrial UPR represents another example for an organelle-specific stress-responsive pathway and results in an increased resistance to oxidative damage. It activates the transcription of nuclear-encoded mitochondrial quality control genes in response to perturbations of the protein homeostasis within the organelle. In eukaryotes, mitochondria are involved in many important processes including the regulation of apoptosis. Therefore, the mitochondrial matrix contains its own protein quality control machinery consisting of molecular chaperones as well as proteases, including chaperonin 60 (Cpn60/Hsp60), chaperonin 10 (Cpn10/Hsp10), mtHsp70, mtGrpE, mtDnaJ, and the mitochondrial ClpP

protease. These proteins ensure the maintenance of the mitochondrial proteome by assisting in the import, refolding, aggregation prevention, and degradation of proteins encoded by the nuclear genome and mitochondrial DNA (mtDNA). The upregulation of the mitochondrial stress response machinery involves the transcription factors CHOP and C/EBPβ (Zhao *et al.* 2002, Haynes and Ron 2010, Kourtis and Tavernarakis 2011). Interestingly, CHOP activation results in the upregulation of different target genes in ER and mitochondrial UPR and further research will be needed to identify factors providing specificity to the two responses (Kourtis and Tavernarakis 2011).

2.5 Integration of the proteostasis network and its relation to aging and disease

As previously discussed, cells and organisms invest in a complex network to maintain protein homeostasis. The individual modules of this proteostasis network do not function in an isolated manner but are rather interconnected via multiple hubs coordinating the various components (Hartl *et al.* 2011, Kourtis and Tavernarakis 2011).

The conserved serine/threonine kinase target of rapamycin (TOR) represents one of these intersections and is part of a signaling pathway linking cellular growth, metabolism, and translation control with environmental cues (Gingras *et al.* 2004, Wullschleger *et al.* 2006). The mammalian target of rapamycin complex 1 (mTORC1) was shown to stimulate cell growth by enhancing translation through the phosphorylation of ribosomal protein S6 kinase (S6K) and the eukaryotic initiation factor 4E (eIF-4E). mTORC1 also inhibits autophagy when nutrients are plentiful and is involved in the regulation of ribosome biogenesis by promoting pre-rRNA synthesis (Mayer and Grummt 2006, Chan 2009, Boulon *et al.* 2010). Moreover, mTORC1 is able to sense the chaperone availability in cells, thereby linking protein quality and protein quantity control (Qian *et al.* 2010). Recently, it has been shown that mTORC1 also plays a role in the regulation of the HSR by direct phosphorylation of HSF1 on serine 326, a key residue for its transcriptional activation (Chou *et al.* 2012). Furthermore, mTOR is involved in the progression of neurodegenerative diseases, as its inhibition induces autophagy and reduces toxic effects of polyglutamine expansions in fly and mouse models of Huntington's disease (Ravikumar *et al.* 2004).

Sirtuins, a family of highly conserved NAD^+-dependent protein deacetylases, also play a major role in the regulation of the proteostasis network. Initially discovered in yeast, they

were identified to mediate chromatin silencing. Sir2, the best-studied member of the sirtuins, has been shown to promote longevity in yeast, nematodes, and flies through caloric restriction, thus linking the metabolic status of a cell to aging (Rine and Herskowitz 1987, Kaeberlein *et al.* 1999, Rogina and Helfand 2004). The sirtuin-mediated lifespan increase of *C. elegans* has been shown to be dependent on a member of the forkhead transcription factor (FOXO) family, DAF-16 (Lin *et al.* 1997, Brunet *et al.* 2004). However, the role of sirtuins in the life span regulation of worms and flies is controversial and still a matter of debate (Burnett *et al.* 2011). The mammalian genome encodes seven sirtuins with SIRT1 being the ortholog of yeast Sir2. There is a growing body of evidence that SIRT1 directly couples the cellular energy metabolism to the chromatin structure and the regulation of gene expression by deacetylation of histones and several transcription factors (Li 2013). Some of these transcription factors are key players in cellular stress-responsive pathways. For example, SIRT1-mediated deacetylation of HSF1 prolongs its binding to the HSEs in the promotor regions of target genes, thus establishing a role for SIRT1 in protein homeostasis and the HSR. (Westerheide *et al.* 2009). Moreover, SIRT1 is known to regulate the activity of FOXO3. Mammalian FOXO transcription factors mediate the cellular response to oxidative stress and are involved in further biological processes such as aging. Sirtuins also play a role in the onset of neurodegenerative diseases. Whereas a decreased sirtuin level in *C. elegans* accelerates the age-dependent aggregation of α-synuclein, flies and mice show the opposing effects, namely that a reduced sirtuin activity promotes survival of neuronal cells in a Huntingtin's disease model and delays the onset of prion disease, respectively (Chen *et al.* 2008, Pallos *et al.* 2008, van Ham *et al.* 2008). Activation of sirtuins leads to the clearance of toxic oligomeric intermediates by the cellular protein degradation machinery as it has been shown that sirtuins promote the degradation of the amyloidogenic Aβ peptide via the UPS and autophagy (Marambaud *et al.* 2005, Lee *et al.* 2008).

The insulin/insulin-like growth factor 1 (IGF-1) pathway represents another hub in the proteostasis network. It connects the regulation of stress resistance with the aging process (Douglas and Dillin 2010). The *C. elegans* tyrosine kinase DAF-2, a homolog of the mammalian insulin/IGF-1 receptor, is activated by the binding of insulin-like molecules and initializes a signaling cascade including the phosphatidylinositol-3 kinase AGE-1, which ultimately results in the repression of the forkhead transcription factor DAF-16 (Dorman *et al.* 1995, Lin *et al.* 1997, Rincon *et al.* 2005). Any changes in the insulin/IGF-1 pathway leading to the derepression of DAF-16 such as mutations of *daf-2* or *age-1* increase the stress resistance of *C. elegans* and extend its life span (Cohen *et al.* 2006). Furthermore, it has been

shown that the life-prolonging function of the nematode HSF1 is also controlled by the insulin/IGF-1 pathway (Kenyon *et al.* 1993, Morimoto 2008). Together with DAF-16, HSF1 drives the expression of specific stress-responsive target genes, including sHsps, which promote longevity (Hsu *et al.* 2003). Modifications of the insulin/IGF-1 pathway have also been demonstrated to be involved in the onset of neurodegenerative diseases since reduced signaling causes a dramatic delay of toxicity associated with polyglutamine expansions as well as amyloidogenic Aβ-peptides (Morley *et al.* 2002, Cohen *et al.* 2006). Taken together, these data suggest that the insulin/IGF-1 signaling pathway plays a key role in life-span determination and amelioration of aggregation-associated proteotoxicity by regulating HSF1, DAF-16, and the subsequent expression of molecular chaperones and other anti-aging genes (Cohen *et al.* 2006).

The protein degradation machinery is another key determinant in maintaining the cellular protein homeostasis. The clearance of terminally misfolded proteins is tightly regulated and dysregulation is related to the pathogenesis of several human diseases including Parkinson's, Alzheimer's, Huntington's, and Prion diseases as well as amyotrophic lateral sclerosis and breast cancer (Ciechanover and Brundin 2003, Ohta and Fukuda 2004, Cheung and Ip 2009). However, only limited information is available concerning the linkage of the impaired proteolytic machinery with the pathogenesis of these diseases. It remains to be seen if the reduced degradation capacity is the primary cause or the secondary consequence of disease progression (Ciechanover and Brundin 2003). For example, it has been shown that the expression of aggregation-prone proteins causes an almost complete inhibition of the UPS by protein aggregates (Bence *et al.* 2001). Inhibition of the proteasome represents a major challenge of the proteostasis network which leads to the accumulation of ubiquitinated proteins and an increased expression of Hsps in an HSF1-dependent manner (Pirkkala *et al.* 2000). It is likely that HSF1 plays an additional role in degradation of ubiquitinated proteins as HSF1-deficient mice show a reduced ability to degrade ubiquitinated proteins and accumulate polyglutamine aggregates in a Huntington's model (Homma *et al.* 2007). Moreover, recent findings suggest a role of HSF1 in the negative regulation of autophagy (Dokladny *et al.* 2013).

The aging process represents a major challenge for cellular proteostasis and can generally be explained with a decline of the cellular quality control mechanisms and decreased capacity of the protein degradation machinery. Aging cells and organisms show an increased expression level of Hsps even in the absence of environmental challenges suggesting that aging is an intrinsic stress signal (Kourtis and Tavernarakis 2011). Although

an age-dependent decline in proteasomal degradation has been shown by several groups, the ubiquitination machinery is not affected to the same extent (Conconi *et al.* 1996, Shibatani *et al.* 1996, Ponnappan *et al.* 1999, Carrard *et al.* 2002). The reduced degradation capacity can be explained with a decrease in the expression of proteasomal subunits during aging and increasing oxidative stress that further enhances dysfunction of the proteasome (Bulteau *et al.* 2002, Carrard *et al.* 2002). The important role of protein degradation systems in the complex proteostasis network is further demonstrated by the fact that reduced degradation is accompanied by the activation of the HSR and the UPR of the endoplasmic reticulum (Kisselev and Goldberg 2001, Kourtis and Tavernarakis 2011).

2.6 Aim of the study

When facing proteotoxic environmental conditions, cells and organisms respond with the activation of the HSR to ensure stress adaptation, recovery, and survival. The HSF1-dependent transient expression of stress proteins, predominantly molecular chaperones, is a key feature of this cytoprotective mechanism. Although the function of HSF1 as the master regulator of the HSR is well established and has been described in cell culture models as well as at the organismal level, the understanding of how proteotoxic stimuli are sensed by cells and organisms and how this results in the activation of HSF1 is far from complete. The question if different stresses are detected by distinct molecular sensors or if there is a common basis for stress recognition also remains to be solved (Anckar and Sistonen 2011). Furthermore, it has been shown that the HSR plays an important role in the aging process as well as in the progression of several human pathologies including neurodegenerative disorders and cancer. Whereas an (age-dependent) decline in the cellular proteostasis capacity leads to aberrant protein folding and aggregation, tumor cells generally express increased levels of chaperones compared to untransformed cells due to their higher dependence on chaperones (Dai *et al.* 2007, Ben-Zvi *et al.* 2009, Powers *et al.* 2009, Neef *et al.* 2011).

The goal of the present study was to elucidate the mechanisms underlying the stress-dependent activation of HSF1 and to define the cellular networks that regulate the HSR. Understanding the activation of the HSR is medically relevant as it counteracts the accumulation of disease associated protein aggregates. This knowledge would open the possibility to pharmacologically modulate the HSR, thereby boosting cellular proteostasis and offering a possible strategy to mitigate various degenerative conditions associated with

neurodegeneration and the aging process. On the other hand, inhibition of the HSR is considered beneficial in cancer and may lead to the development of new therapeutic anti-cancer strategies.

3 Material and methods

3.1 Chemicals and biochemicals

Biochrom AG (Berlin, Germany):

- Dulbecco's MEM (w 3.7 g/l $NaHCO_3$, w 4.5 g/l D-Glucose)

BioMol (Hamburg, Germany):

- MG132
- Withaferin A

Biozym Scientific GmbH (Hessisch Oldendorf, Germany):

- Agarose

Cambridge Isotope Laboratories (Tewksbury, USA):

- Arginine-13C6
- Arginine-13C6,15N4
- Lysine-13C6,15N2
- Lysine-4,4,5,5-d4

Dako (Glostrup, Denmark):

- Fluorescent Mounting Medium

Difco (Heidelberg, Germany):

- Bacto Tryptone
- Bacto Yeast Extract

Enzo® Life Sciences (Lörrach, Germany):

- 17-AAG
- 17-DMAG

Gibco (Paisley, UK):

- 0.05% Trypsin-EDTA
- L-Glutamine 200 mM (100x)
- Opti-MEM® I Reduced Serum Medium
- PBS pH 7.2
- Penicillin-streptomycin (10.000 units/ml Pen, 10.000 µg/ml Strep)

Invitrogen (Karlsruhe, Germany):

- Blasticidin S HCl
- Colloidal blue
- DAPI
- LDS sample buffer
- Lipofectamine
- Lipofectamine Plus Reagent
- Lipofectamine RNAiMAX
- NuPAGE 4-12% Bis-Tris gradient gel
- SYBR® Safe DNA gel stain

Life Technologies (Paisley, UK):

- Dynabeads His-tag isolation and pull-down beads

Merck (Darmstadt, Germany):

- 3-Methyladenine
- Celastrol, *Celastrus scandens*
- DCIC
- Disodium EDTA
- EDTA (Titriplex III)
- InSolution^{TM} Epoxomicin, Synthetic
- Lactacystin, Synthetic
- Magnesium chloride
- Magnesium sulfate
- Paraformaldehyde
- Tween 20

Metabion (Martinsried, Germany):

- dNTP Set 100 mM

Millipore (Schwalbach, Germany):

- Luminata Classico Western HRP substrate

New England BioLabs® (Frankfurt am Main, Germany):

- BSA
- NEBuffer 4

PerkinElmer (Waltham, USA):

- EasyTag™ L-[35S]-methionine

Pierce Biotechnology (Bonn, Germany):

- EGS

PAA (Cölbe, Germany):

- G418 sulfate
- Customized DMEM for SILAC
- Dialyzed FCS for SILAC

Roche Applied Science (Basel, Switzerland):

- Nonidet P-40 (NP40)
- Protease inhibitor cocktail tablets, complete-Mini, EDTA-free

Roth (Karlsruhe, Germany):

- Agar-Agar
- Ampicillin
- Calcium chloride
- Glucose
- Glycine
- HEPES
- Imidazole

Saliter (Obergünzburg, Germany):

- Milk powder

Serva (Heidelberg, Germany):

- Acrylamide
- Coomassie Blue R250
- SDS

Sigma (Steinheim, Germany):

- Ammonium persulfate
- Arachidonic acid
- Arginine
- Boric acid
- Cycloheximide
- DMSO
- Kanamycin
- Lysine
- MOPS
- MTT
- Potassium phosphate monobasic
- Puromycin dihydrochloride from *Streptomyces alboniger*
- Rubidium chloride
- Sodium deoxycholate
- TEMED
- Trizma® base
- β-Mercaptoethanol

USB (Cambridge, USA):

- Sodium phosphate, dibasic

VWR (Darmstadt, Germany):

- Glycerol
- Guanidinium hydrochloride

- Manganese(II) chloride
- Potassium chloride
- Potassium acetate
- Sodium chloride
- Sodium hydroxide

3.2 Antibodies

Abcam (Cambridge, UK):

- Mouse anti-EP300, dilution 1:1000
- Rabbit anti-lamin B1, dilution 1:400 for microscopy, 1:1000 for WB
- Rat anti-HSF1, dilution 1:2000 for WB

Cell signaling (Danvers, USA):

- Rabbit anti-HSF1, dilution 1:500 for microscopy

Dianova (Hamburg, Germany):

- Cy3^{TM}-conjugated AffiniPure goat anti-rabbit IgG, dilution 1:200

Millipore (Schwalbach, Germany):

- Mouse anti-GAPDH, dilution 1:3000
- Mouse anti-Renilla luciferase, dilution 1:1000

Promega (Mannheim, Germany):

- Goat anti-firefly luciferase, dilution 1:2000

Sigma (Steinheim, Germany):

- Anti-Goat IgG (whole molecule)-Peroxidase antibody, dilution 1:4000
- Anti-Mouse IgG (whole molecule)-Peroxidase antibody, dilution 1:4000
- Anti-Rat IgG (whole molecule)-Peroxidase antibody, dilution 1:4000
- Mouse anti-α-tubulin, dilution 1:200 for microscopy, 1:1000 for WB

3.3 Media and buffers

3.3.1 Media

Bacterial media were prepared with deionized water (electrical resistance 18.2 MΩ·cm) and autoclaved after preparation.

LB medium:
10 g/l Bacto Tryptone
5 g/l Bacto Yeast Extract
10 g/l NaCl

Solid LB medium:
10 g/l Bacto Tryptone
5 g/l Bacto Yeast Extract
10 g/l NaCl
15 g/l Agar-Agar

100 µg/ml Ampicillin or 50 µg/ml Kanamycin added for antibiotics selection

SOB medium:
20 g/l Bacto Tryptone
5 g/l Bacto Yeast Extract
10 mM NaCl
2.5 mM KCl
10 mM $MgCl_2$
10 mM $MgSO_4$

SOC medium: SOB medium with 20 mM glucose

3.3.2 Buffers and standard solutions

Buffers were prepared with deionized water (electrical resistance 18.2 MΩ·cm).

Antibiotic solutions (1000x):
100 mg/ml Ampicillin
50 mg/ml Kanamycin

Blocking buffer:	5% (w/v) Milk powder in TBST
Coomassie destaining solution:	10% (v/v) Ethanol 10% (v/v) Acetic acid
Coomassie staining solution:	0.1% (w/v) Serva Coomassie Blue R250 40% (v/v) Ethanol 10% (v/v) Acetic acid
HSF1 cross-linking buffer:	50 mM HEPES pH 7.8 150 mM NaCl 1% (v/v) NP-40 0.25% Sodium deoxycholate 1 mM EDTA 1 tablet protease inhibitor cocktail per 10 ml (Roche)
His-Ubi pull-down lysis buffer:	6 M Guanidinium-HCl 0.1 M HEPES 5 mM Imidazole pH adjusted to 7.4
His-Ubi pull-down wash buffer:	300 mM NaCl 50 mM Tris-HCl 20 mM Imidazole 1% (v/v) NP-40 pH adjusted to 7.6

PBS (10x):	1.37 M NaCl
	27 mM KCl
	100 mM Na_2HPO_4
	18 mM KH_2PO_4
	pH adjusted to 7.4
RF1:	100 mM $RbCl_2$
	50 mM $MnCl_2$
	30 mM Potassium acetate
	10 mM $CaCl_2$
	15% (w/v) Glycerol
	pH adjusted to 5.8 with 0.2 M acetic acid
RF2:	10 mM $RbCl_2$
	10 mM MOPS
	75 mM $CaCl_2$
	15% (w/v) Glycerol
	pH adjusted to 6.8 with 1 M NaOH
RIPA lysis buffer:	50 mM Tris-HCl, pH 7.8
	150 mM NaCl
	1% (v/v) NP-40
	0.25% Sodium deoxycholate
	1 mM EDTA
	1 tablet protease inhibitor cocktail per 10 ml (Roche)
SDS-loading buffer:	62.5 mM Tris-HCl, pH 6.8
	10% (v/v) Glycerol
	2% (w/v) SDS
	5% (v/v) β-mercaptoehanol
	0.2 % (w/v) bromphenolblue

SDS-running buffer (5x):
125 mM Tris-HCl
960 mM Glycine
0.5% (w/v) SDS

Stripping buffer:
2% (w/v) SDS
62.5 mM Tris-HCl, pH 6.8
100 mM β-mercaptoehanol

TBE (5x):
0.89 M Tris-HCl
0.89 M Boric acid
20 mM Na_2EDTA

TBS (10x):
100 mM Tris-HCl, pH 7.5
1.54 M NaCl

TBST:
10 mM Tris-HCl, pH 7.5
0.154 M NaCl
0.1% (v/v) Tween 20

Towbin Buffer:
25 mM Tris
192 mM Glycine
1.25 mM SDS
20% (v/v) Methanol

3.4 Materials and instruments

Applied Biosystems (Paisley, UK):

- Gene Amp PCR System 2400

BD BioCoatTM Cellware (San Jose, USA):

- Poly-L-lysine 12 mm coverslips

BD Falcon (San Jose, USA):

- 100 mm tissue culture dish
- 6-well plates
- 12-well plates
- 48-well plates
- 96-well plates

Beckman Coulter GmbH (Krefeld, Germany):

- Centrifuge GS-6R
- DU640 UV/VIS Spectrophotometer

Biometra (Göttingen, Germany):

- T3 Thermocycler

Bio-Rad (München, Germany):

- Mini Protean® Tetra Cell (SDS gel)
- Mini ProteanTM II (WB)
- Mini Trans-Blot® Module
- Power supply Power Pac Basic 300

Biotek (Bad Friedrichshall, Germany):

- Microplate reader Synergy HT

Costar (Tewksbury, USA):

- 24-well plates
- Stripette (5 ml, 10 ml, 25 ml)

Dr. Maisch GmbH (Ammerbuch-Entringen, Germany):

- Reprosil-Pur C18-AQ

Drummond Scientific (Broomall, USA):

- Pipet-Aid XP

EG&G Berthold (Bad Wildbad, Germany):

- Luminometer Lumat LB9507

Eppendorf (Hamburg, Germany):

- Centrifuge 5415C, 5415R
- Thermomixer comfort
- Pipettes
- 1.5 ml tubes
- 2 ml tubes
- Tips

Fisher Scientific (Schwerte, Germany):

- Accumet Basic pH meter

Forma Scientific (Waltham, USA):

- CO_2 Water Jacketed Incubator

Fuji/Raytest (Straubenhardt, Germany):

- Fuji LAS3000
- Gel imaging software AIDA (version 4.15.025)

Greiner (Frickenhausen, Germany):

- 550 ml tissue culture flask
- Cryo.sTM freezing tube

Heidolph (Schwabach, Germany):

- Heatable magnetic stirrer
- Shaker Duomax 1030

Heraeus Instruments (Hanau, Germany):

- Cell culture hood
- Microbiological Incubator Function Line B12

Invitrogen (Karlsruhe, Germany):

- Safe Imager™ 2.0 Blue Light Transilluminator

Josef Peske GmbH & Co KG (Karlsruhe, Germany):

- 1.5 ml tubes
- 2 ml tubes

LG (Seoul, South Korea):

- Microwave Wavedom

Melter Toledo (Gießen, Germany):

- Balances (AB265-S, FACT)

Millipore (Schwalbach, Germany):

- Millex-SV syringe filter unit, 0.22 µm
- Millipore Milli Q Plus PF water purification system
- Scepter™ Handheld Automated Cell Counter
- Scepter™ Sensors 60 µm

MWG Biotech AG (Göttingen, Germany):

- Gel documentation system

Nalgene (Steinheim, Germany):

- Cryo 1°C Freezing Container

Nunc (Roskilde, Denmark):

- Aluminium Seal Tape for 96-well plates

Qiagen (Hilden, Germany):

- QIAshredder columns

Sarstedt (Nümbrecht, Germany):

- 15 ml tubes
- 50 ml tubes

- Filter tips
- Pipettes
- Serological pipette, 1 ml
- Tube, 5ml, 75x12 mm

Schott (Mainz, Germany):

- Laboratory glass ware

Scientific Industries (Bohemia, USA):

- Vortex-Genie® 2

Sorensen™ BioScience, Inc. (Salt Lake City, USA):

- Safe Seal Microcentrifuge Tubes (0.65 ml, 1.7 ml)

Störktronic (Stuttgart, Germany):

- Heating block

Thermo Scientific (Waltham, USA):

- LTQ-Orbitrap mass spectrometer
- Microscopy slides
- Nanodrop 1000 Spectrophotometer
- Orbital shaker

Waters (Milford, USA):

- nanoACQUITY HPLC system

Whatman™ (Dassel, Germany):

- Nitrocellulose membrane
- Chromatography Paper 3MM Chr

Zeiss (Jena, Germany):

- Axiovert 200M fluorescence microscope

3.5 Marker, kits, and enzymes

3.5.1 Marker and loading dyes

Fermentas (St. Leon-Rot, Germany):

- 6x DNA Loading Dye
- GeneRulerTM 100bp DNA Ladder
- GeneRulerTM 1kb DNA Ladder
- PageRulerTM Prestained Protein Ladder

3.5.2 Kits

Bio-Rad (München, Germany):

- iScript™ cDNA Synthesis Kit

Pierce Biotechnology (Bonn, Germany):

- NE-PER® Nuclear and Cytoplasmic Extraction Reagents

Promega (Mannheim, Germany):

- Dual-GloTM Luciferase Assay System
- Luciferase Assay System
- Proteasome-Glo™ Chymotrypsin-Like Assay
- PureYield™ Plasmid Midiprep System
- Renilla Luciferase Assay System
- Wizard® Plus SV Miniprep DNA Purifiaction System
- Wizard® SV Gel and PCR Clean Up-System

Qiagen (Hilden, Germany):

- EndoFree® Plasmid Maxi Kit
- RNeasy Mini Kit

3.5.3 Enzymes

New England BioLabs® (Frankfurt am Main, Germany):

- ApaI

- CIP
- FseI
- SmaI
- T4 DNA ligase
- XhoI

Promega (Mannheim, Germany):

- Pfu DNA Polymerase

3.6 Strains and vectors

3.6.1 Bacterial strains

Invitrogen (Karlsruhe, Germany):

- *E. coli* DH5α

3.6.2 Vectors

Invitrogen (Karlsruhe, Germany):

- pUB/Bsd

Promega (Mannheim, Germany):

- pCI-neo
- phRL-TK

3.7 Molecular biological methods

3.7.1 DNA analytical methods

3.7.1.1 DNA quantification

DNA concentrations were determined by UV spectroscopy using the NanoDrop 1000. DNA solutions were measured directly and DNA-free water served as a reference. The absorbance ratio

260/280 nm for pure DNA should be approximately 1.85. Deviations from this value indicate quality deficiencies caused by impurities such as RNA or protein.

3.7.1.2 Agarose gel electrophoresis

Agarose gel electrophoresis was used to separate DNA fragments according to their molecular weight (Helling *et al.* 1974). Agarose was melted by heating and gels ranging from a concentration of 0.8 to 2% (w/v) were prepared in 1x TBE buffer supplemented with 1:5000 SYBR® Safe DNA gel stain. Before electrophoresis, 6x loading dye was added to the samples. Gels were run at a constant voltage of 120 V for 15 to 20 min in 1x TBE. The DNA was visualized using Safe Imager™ 2.0 Blue Light Transilluminator and a gel documentation system.

3.7.1.3 DNA sequencing

Sequencing of nucleic acids was performed by the Core Facility of the MPI for Biochemistry in Martinsried. 300 ng plasmid DNA was mixed with 5 pmol sequencing primer (primers are listed in Table 3-1) and 2.5 µl of a pre-mixed PCR solution in a final volume of 10 µl. The chromatograms were analyzed using the program Chromas (Technelysium Pty Ltd, C. McCarthy, Griffith University, Australia) and comparative sequence alignment was performed with the MultAlin analysis program (Corpet, 1988; http://bioinfo.genopole-toulouse.prd.fr/multalin/multalin.html).

Table 3-1: Sequencing primers.

Primer	Sequence
CMV-forward	5'-CGCAAATGGGCGGTAGGCGTG-3'
T7-forward	5'-TAATACGACTCAGTATAGGG-3'
pUB-forward	5'-GAGCCTATGGAAAAACGCCAG-3'
pCI-neo-forward	5'-GCACCTATTGGTCTTACTG-3'

3.7.2 Purification of plasmid DNA and DNA fragments

Anion-exchange-based chromatography methods were used for purification of plasmid DNA from *E. coli* cultures or DNA fragments after gel electrophoresis. For isolation of plasmid DNA the Wizard® *Plus* SV Miniprep DNA Purification System, the PureYield™ Plasmid Midiprep System and the EndoFree® Plasmid Maxi Kit were used according to the manufacturer's protocol, respectively. Isolation of DNA fragments after PCR or digestion was performed by using Wizard® SV Gel and PCR Clean Up-System according to the manufacturer's recommendations.

3.7.3 Generation of expression constructs

To generate the CMV-Rluc construct, the *Renilla luciferase* gene was PCR-amplified out of the phRL-TK vector and subcloned into the pCI-neo vector using SmaI and XhoI restriction enzymes. To generate the construct HSPA1A-Fluc, the HSF1-dependent *HSPA1A* promoter followed by the *Fluc* gene was amplified from plasmid HSP70-Luc (a kind gift from Dr. H Wagner) and cloned into the pUB/Bsd vector using ApaI and FseI restriction enzymes. Generation of the CMV-Fluc and FlucDM-GFP expression constructs was previously described (Gupta *et al.* 2011). pCMV-HSF1-Flag (plasmid 1932) and pCl-His-hUbi (plasmid 31815) were procured from Addgene (Knauf *et al.* 1996, Young *et al.* 2011).

3.7.4 Polymerase chain reaction

The polymerase chain reaction (PCR) was utilized to amplify DNA (Mullis *et al.* 1986).

3.7.4.1 PCR for cloning

For amplification of the *Rluc* gene and *HSPA1A-Fluc* from vector DNA, the *Pfu* polymerase was used. The compositions of the PCR mixtures can be found in Table 3-2, the cycling conditions are summarized in Table 3-3. The primers are listed in Table 3-4. The PCR products were separated by 0.8% agarose gel electrophoresis for 20 min at 120 V, excised, and purified (see 3.7.2).

Table 3-2: PCR mixture.

Solution components	Volume	Final concentration
Pfu 10x Rxn. Buffer (w/20 mM $MgSO_4$)	2.5 µl	1x
Pfu DNA Polymerase	0.5 µl	
Primers (10 µM)	1 µl each	0.4 µM each
dNTPs (5 mM each)	1 µl	100 µM each
Template DNA (200 ng/µl)	1µl	
ddH_2O	18 µl	
Total volume	25 µl	

Table 3-3: Thermal cycling conditions.

	Step	Purpose	Temperature	Duration
	1	Initial denaturation	95°C	5 min
35 cycles	2	Cycle denaturation	95°C	45 s
	3	Primer annealing	55°C	45 s
	4	Primer elongation	72°C	2 min
	5	Final extension	72°C	20 min
	6	Cooling	4°C	∞

Table 3-4: Cloning primers.

Primer	Sequence	T_m
CMV-Rluc-forward	5'-ACGCCTCGAGATGGCTTCCAAGGTGTACGA-3'	75°C
CMV-Rluc-reverse	5'-ACGCCCCGGGTTACTGCTCGTTCTTCAGCACG-3'	79°C
HSPA1A-Fluc-forward	5'-ACGCGGGCCCTGGAGAGTTCTGAGCAGG-3'	78°C
HSPA1A-Fluc-reverse	5'-ACGCGGCCGGCCTTACAATTTGGACTTTCC-3'	75°C

3.7.4.2 Reverse transcriptase-PCR

The expression levels of endogenous transcripts were accessed by semiquantitative reverse transcriptase-PCR (RT-PCR) (Marone *et al.* 2001). HeLa cells were transfected with esiRNA in 6- or 12-well format as described in chapter 3.9.2.3. 72 h later, total RNA was prepared using RNeasy® Mini Kit according to the manufacturer's protocol. Briefly, the cells were washed twice with PBS, trypsinized and pelleted at 14,000 rpm. The pellet was disrupted by adding 350 µl RLT buffer. The lysate was transferred directly into a QIAshredder spin column placed in 2 ml collection tube and centrifuged for 2 min at 14,000 rpm. 350 µl of 70% ethanol were added to the homogenized lysate, mixed, transferred to an RNeasy spin column, and centrifuged for 15 s at 14,000 rpm. The column was washed once with 700 µl RW1 buffer, twice with 500 µl RPE buffer and each time centrifuged for 15 s at 14,000 rpm. After the last washing step, the column was transferred to a new 2 ml collection tube and centrifuged again for 1 min at 14,000 rpm. Total RNA was eluted from the column by adding 30 µl of RNase-free water and centrifugation for 1 min at 14,000 rpm. RNA was stored at -80°C. RNA concentration was measured with a Nanodrop 1000 spectrophotometer. For cDNA synthesis, the iScript^{TM} cDNA Synthesis Kit was used according to the manufacturer's

protocol. 500 ng total RNA were mixed with 4 µl 5x iScript reaction mix and 1 µl iScript reverse transcriptase and nuclease-free water was added to a final volume of 20 µl. The complete reaction mix was incubated for 5 min at 25°C followed by 30 min at 42°C. The reverse transcriptase was inactivated at 85°C for 5 min. The polymerase chain reaction was performed using *Pfu* DNA polymerase. PCR mixtures and thermal cycling conditions are summarized in Table 3-5 and Table 3-6. Primers are listed in Table 3-7 (Westerheide *et al.* 2009). PCR products were analyzed by 2% agarose gel electrophoresis (15 min at a constant voltage of 120 V).

Table 3-5: RT-PCR mixture.

Solution components	Volume	Final concentration
Pfu 10x Rxn. Buffer (w/20mM $MgSO_4$)	2.5 µl	1x
Pfu DNA Polymerase	0.5 µl	
Forward primer (10µM)	1 µl	0.4 µM
Reverse Primer (10µM)	1 µl	0.4 µM
dNTPs (5mM each)	1 µl	50 µM each
cDNA	2µl	
ddH_2O	17 µl	
Total volume	25 µl	

Table 3-6: Thermal cycling conditions RT-PCR.

	Step	Purpose	Temperature		Duration
			Fluc, GAPDH, HSPA1A, Rluc	HSF1	
	1	Initial denaturation	94°C	94°C	3 min
25-30 cycles	2	Cycle denaturation	94°C	94°C	30 s
	3	Primer annealing	55°C	61°C	30 s
	4	Primer elongation	72°C	72°C	30 s
	5	Cooling	4°C	4°C	∞

Table 3-7: RT-PCR primers.

Primer	Sequence	T_m
Fluc-forward	5'-TTGTTTCCAAAAAGGGGTTG-3'	55°C
Fluc-reverse	5'-CATCGACTGAAATCCCTGGT-3'	59°C
GAPDH-forward	5'-CCACTCCTCCACCTTTGAC-3'	59°C
GAPDH-reverse	5'-ACCCTGTTGCTGTAGCCA-3'	56°C
HSF1-forward	5'-CCTGATGCTGAACGACAGTG-3'	65°C
HSF1-reverse	5'-GTAGAGGCTGGAGCTGCTGT-3'	63°C
HSPA1A-forward	5'-AGAGCCGAGCCGACAGAG-3'	61°C
HSPA1A-reverse	5'-CACCTTGCCGTGTTGGAA-3'	56°C
Rluc-forward	5'-CCTGATCAAGAGCGAAGAGG-3'	61°C
Rluc-reverse	5'-GTAGGCAGCGAACTCCTCAG-3'	63°C

3.7.5 Restriction endonuclease digestion and DNA ligation

pCI-neo vector (1.5 µg) and *Rluc* insert were sequentially digested using the restriction enzymes SmaI and XhoI. First, vector and insert were digested with SmaI at 25°C for 2 h, then XhoI was added, and mixtures were kept at 37°C for 2 h. pUB/Bsd vector (1.5 µg) and the *HSPA1A-Fluc* insert were digested first with ApaI for 2 h at 25°C, followed by 2 h FseI digestion at 37°C. All digestions were performed with 1 µl of each enzyme in NEBuffer 4 supplemented with 0.1 mg/ml BSA. Digestion products were separated by agarose gel electrophoresis and purified (see 3.7.1.2 and 3.7.2).

For ligation, a three-fold molar excess of the insert was mixed with the corresponding vector and 300 U of T4 DNA ligase in a final volume of 15 µl. Ligation mixtures were incubated at 16°C for 1 h followed by heat deactivation of the ligase at 65°C for 10 min. Complete mixtures were used for transformation into DH5α cells.

3.7.6 Preparation and transformation of competent *E. coli* DH5α cells

To prepare chemically competent *E. coli* DH5α cells (Hanahan 1983), 10 ml SOB were inoculated with one bacterial colony and grown at 30°C over night. The next day, 50 ml of fresh SOB medium were inoculated with 0.5 ml of the pre-culture and grown at 30°C to an OD_{550} of 0.48. Next, cells were cooled on ice for 15 min, pelleted at 4°C (2500 rpm for 15 min) using a Beckman GS-6R, and resuspended in 16 ml of pre-chilled buffer RF1. Then, the cells were incubated on ice for 15 min, centrifuged again, and resuspended in 4 ml of buffer RF2. After 15 min on ice, 50 µl aliquots of the cells were transferred to pre-chilled 1.5 ml tubes and stored at -80°C.

Transformation of chemically competent *E. coli* cells was either performed with 15 µl ligation mixture or 100 ng plasmid DNA. Cells were thawed on ice and the DNA was added. After 20 min incubation on ice, the mixture was heat-shocked at 42°C for 90 s and chilled on ice for 5 min. Then, 1 ml of SOC medium was added and cells were incubated in a shaker for 1 h at 37°C and 300 rpm. 200 µl of the mixture were plated on selective LB agar plates and incubated over night at 37°C.

3.8 Protein biochemical methods

3.8.1 Protein quantification

Protein concentrations of the RIPA soluble lysate as well as the nuclear and cytoplasmic extracts were measured colorimetrically using the Bio-Rad protein assay reagent according to the manufacturer's recommendations (Bradford 1976). 5µl of a 1:9 dilution of the protein extracts were mixed with 795 µl ddH_20 and 200 µl Bradford solution. The mixture was mixed briefly and the absorption was measured at 595 nm using a spectrophotometer (Beckman).

3.8.2 Preparation of cell extracts

To prepare whole cell extracts for western blotting, cells were washed with PBS, trypsinized and pelleted at 5,000 g for 1 min at RT. The pellet was washed twice with PBS and boiled in SDS sample buffer at 95°C for 1 h. To prepare soluble cell fractions, cells were trypsinized and washed twice with PBS. Cells were then pelleted, resuspended in RIPA lysis buffer (Ong and Mann 2006) and mixed at regular intervals while incubating for 40 min on ice. After that, the crude cell lysate was centrifuged at 16,000 g for 30 min at 4°C. The supernatant fraction was used for analysis.

3.8.3 SDS-PAGE

For cell extract analysis, samples were separated by discontinuous Tris-glycine sodium dodecylsulfate polyacrylamide gel electrophoresis (SDS-PAGE) according to their electrophoretic mobility (Laemmli 1970). The compositions of the resolving and stacking gels are shown in Table 3-8.

Table 3-8: Compositions of resolving and stacking gels.

Solution components	10% resolving gel	12% resolving gel	5% stacking gel
H_2O	5.9 ml	4.9 ml	5.5 ml
30% Acrylamide/ 0.8% bis-acrylamide	5 ml	6 ml	1.3 ml
1.5 M Tris (pH 8.8)	3.8 ml	3.8 ml	-
0.5 M Tris (pH 6.8)	-	-	1 ml
10% SDS	150 µl	150 µl	80 µl
10% APS	150 µl	150 µl	80 µl
TEMED	6 µl	6 µl	8 µl

Directly after casting, the resolving gel was covered with a layer of isopropanol. Before loading, the samples were boiled in SDS loading buffer for 10 min at 95°C and spun briefly for 5 s at 14,000 rpm. Electrophoresis was performed at a constant voltage of 150 V in SDS-running buffer using Mini Protean® Tetra Cell.

3.8.4 Western blotting

For western blotting (Towbin *et al.* 1979), protein extracts were separated by SDS-PAGE and transferred to a nitrocellulose membrane by tank blotting. Wet transfer was performed in Towbin buffer at a constant current of 300 mA for 90 min using Mini Protean^{TM} II and Mini Trans-Blot Module. The membrane was blocked in 5% milk powder in TBST for 1 h at room temperature. Incubation with the primary antibody (dilutions see chapter 3.2) was performed over-night at 4°C. Afterwards, blots were washed three times in TBST for 5 min each and incubated with a horseradish peroxidase-conjugated (HRP) secondary antibody (dilutions see chapter 3.2) for 2 h at room temperature. For immunodetection, the membranes were covered with the Luminata Classico Western HRP substrate. Signals were detected and documented with the densitometry system Fuji-LAS3000. If needed, membranes were stripped at 70°C for 40 min, followed by a second round of antibody detection.

3.9 Cell biological methods

3.9.1 Basic cell culture techniques

3.9.1.1 Culturing, passaging, and counting of mammalian cells

HeLa and HEK293T cells were maintained in Dulbecco's Modified Eagle's Medium (DMEM) supplemented with 10% fetal bovine serum (FBS), 1% penicillin-streptomycin and 1% L-glutamine at 37°C in an atmosphere of 5% CO_2. Experiments were performed in 96-, 48-, 24-, 12-, or 6-well format. To avoid senescence, cells were subcultured before reaching 100% confluence. Adherent HeLa cultures and semi-adherent HEK293T lines needed to be detached by using 0.05% trypsin-EDTA. Cells were rinsed once in PBS, trypsinized and taken up in culture medium. For maintenance, cells were seeded in a ratio 1:10 or cultured in multi-well tissue culture plates for experiments. The cell number was determined by either using a Neubauer counting chamber or with the Scepter™ Handheld Automated Cell Counter.

3.9.1.2 Cryopreservation of cells

HeLa and HEK293T cells were grown to a confluence of 80-90%, washed once with PBS, trypsinized and taken up in culture medium. Cells were pelleted for 5 min at 1000 rpm using a Beckman GS-6R centrifuge. The supernatant was removed and the pellet was resuspended in culture medium supplemented with additional 10% DMSO and 30% FBS to minimize cell damage (Morris 1995). 1.5 ml of the cell solution was transferred to a sterile freezing tube, stored in a cryo freezing container at -80°C for 24 h, and subsequently transferred to liquid nitrogen (Mazur 1984).

3.9.2 Manipulation of cultured cells

3.9.2.1 Transient transfection of mammalian cells

Transfection of HeLa and HEK293T cells was performed with Lipofectamine and PLUS reagent according to the manufacturer's protocol. DNA and PLUS reagent were mixed in Opti-MEM and incubated for 15 min at room temperature. In between, Lipofectamine was diluted in Opti-MEM. After incubation, the pre-complex DNA was combined with the Lipofectamine mixture and incubated for further 15 min at room temperature. The growth medium of the cells was replaced by Opti-MEM, the transfection mix was added, and incubated for 3 h in a CO_2 incubator at 37°C. Finally, antibiotic-free DMEM was added and

cells were grown over-night. The amounts of plasmid DNA, Lipofectamine, PLUS reagent, Opti-MEM, and growth medium used for the different culture vessels are summarized in Table 3-9.

Table 3-9: Composition of transfection mixtures.

Culture vessel	DNA	Dilution Medium (Opti-MEM)	Lipofectamine (in µl Opti-MEM)	PLUS reagent (in µl Opti-MEM)	Vol. of plating medium (DMEM)	Number of cells
100 mm	3 µg	2 ml	12 µl (250)	8 µl (250)	5 ml	$1.5x10^6$
6-well	1.5 µg	1 ml	6 µl (250)	3 µl (250)	2 ml	$4x10^5$
12-well	1 µg	1 ml	4 µl (150)	2 µl (150)	1 ml	$2x10^5$

3.9.2.2 Generation of stably transfected cell lines

To generate the luciferase reporter cell line (iFluc-Rluc), HeLa cells were transfected with HSPA1A-Fluc and CMV-Rluc constructs using Lipofectamine and PLUS reagent. One day after transfection, 10,000 cells were seeded in a 100 mm dish and selected with 5 µg/ml Blasticidin S HCl and 400 µg/ml G-418 sulfate. Culture medium was replaced every 3 days. Colonies that formed after 2-3 weeks were separated inside a cell culture hood using an inverted microscope and a 200 µl pipette. Each colony was transferred to a single well of a 96-well plate and grown further. Subsequently, the colonies were transferred into 48- and 24-well plates, ultimately into 100 mm dishes. After having a sufficient number of cells, individual colonies were tested for their luciferase expression. The same protocol was followed to generate HEK293T cells stably expressing FlucDM-GFP. After transfection, the cells were selected with 500 µg/ml G-418 sulfate.

3.9.2.3 Reverse esiRNA transfection

Reverse esiRNA transfections were performed with Lipofectamine RNAiMAX according to the manufacturer's protocol. EsiRNA was diluted in Opti-MEM (in the experimental culture vessel), mixed with Lipofectamine RNAiMAX, and incubate for 20 min at room temperature. In between, the cells were trypsinized, resuspended in antibiotic-free DMEM, and added to the RNAi-Lipofectamine duplex. After rocking the culture vessels back and forth, the cells were incubated in a CO_2 incubator for 48-72 h. The amounts of esiRNA, Lipofectamine, Opti-MEM, and growth medium used for the different culture vessels are summarized in Table 3-10.

Table 3-10: Composition of reverse esiRNA transfection mixtures.

Culture vessel	Dilution Medium (Opti-MEM)	esiRNA	Lipofectamine RNAiMAX	Plating medium (DMEM)	Number of cells
384-well	20 µl	15 ng	0.1 µl	50 µl	3000
96-well	25 µl	30 ng	0.3 µl	75 µl	7500
12-well	200 µl	300 ng	2 µl	1 ml	50000
6-well	500 µl	750 ng	5 µl	2.5 ml	175000
100 mm	2 ml	1750 ng	25 µl	8 ml	750000

3.9.3 Cell biological assays

3.9.3.1 Cell viability assay

Cell viability was measured using the MTT (3-(4,5-dimethylthiazol-2-yl)-2,5-diphenyltetrazolium bromide) assay (Mosmann 1983). The yellow MTT is reduced to purple formazan via NAD(P)H-dependent oxidoreductase enzymes in living cells and can thus be used to quantify cell viability. One day prior to the experiment, 15,000 HeLa cells were cultured in 96-well format. The next day, cells were heat-stressed at 43°C or treated with 5 µM celastrol or MG132 for 8 h. 20 µl of a 5 mg/ml MTT solution in PBS were added to each well, followed by incubation at 37°C for 3 h. The growth medium was removed and the formazan crystals were dissolved in 200 µl DMSO. Absorbance at 550 nm was measured using the BIOTEK Synergy HT plate reader. All measurements were normalized to DMSO-treated control cells.

3.9.3.2 Measuring luciferase activities

Luciferase activities were measured using the Dual-Glo™ Luciferase Assay System according to the manufacturer's protocol. To assay Fluc activity in 96-well format, 50 µl of Dual-Glo™ Luciferase Reagent were added to each well. After 10 min of incubation in the dark, Fluc luminescence was recorded using a Lumat luminometer (acquisition time 2 s). Then 50 µl Dual-Glo™ Stop & Glo® Reagent diluted 1:100 in Dual-Glo™ Stop & Glo® buffer were added to each well and after 10 min of incubation in the dark, Rluc luminescence was measured. For analysis, Fluc:Rluc ratios were calculated.

3.9.3.3 Refolding of Fluc and Rluc

To assay the refolding kinetics of Fluc and Rluc, HeLa cells were transfected with CMV-Fluc or CMV-Rluc constructs in 100 mm dish format. 24 h later, 150,000 cells were seeded into each well of a 24-well plate. Next day, the growth medium was replaced by DMEM containing 5 mM CHX 20 min before starting the assay. For luciferase unfolding, cells were heat-stressed for 30 min at 45°C. Transfer to 37°C allowed refolding. Cell lysates were prepared in 100 µl RIPA buffer at different time points and Fluc and Rluc activities were measured using Luciferase Assay System and Renilla Luciferase Assay System. 10 µl of RIPA soluble lysate were mixed with an equal volume of the respective assay buffer and luminescence was recorded. The remaining cell lysate was centrifuged at 14,000 rpm for 30 min at 4°C and luciferase protein level was determined from the supernatant fraction by western blotting with anti-Fluc and anti-Rluc antibodies, respectively. Band intensities were quantified by densitometry using AIDA. To determine specific luciferase activities, luciferase luminescence values were divided by band intensities.

3.9.3.4 His-ubiquitin pull-down assay

Cells (two 6-wells/pull-down) were transfected with FLAG-HSF1 and/or His-ubiquitin and heat-stressed for 2 h at 43°C in presence of 5 µM MG132, followed by recovery for 2 h at 37°C. Cells were washed with ice-cold PBS, trypsinized, pelleted at 14,000 rpm, and lysed in 1 ml pull-down lysis buffer. Dynabeads His-tag isolation and pull-down beads were equilibrated with pull-down lysis buffer, 50 µl were added to each cell lysate, and incubated at room temperature for 15 min on a rotating wheel. Magnetic beads were collected using Dynal Magnetic Particle Concentrator, washed twice with 400 µl pull-down lysis buffer and four times with 400 µl pull-down wash buffer. Elution was performed by boiling the beads in 40 µl 2x SDS-PAGE loading buffer supplemented with 300 mM imidazole for 15 min. Samples were separated on a NuPAGE 4-12% Bis-Tris gel and HSF1 was visualized by western blotting.

3.9.3.5 HSF1 cross-linking

Cells were lysed in cross-linking buffer. 100 µg of HeLa cell extract were cross-linked with 1 mM ethylene-glycol-bis(succinimidyl succinate) (EGS) by incubation for 30 min at room temperature. Cross-linking reactions were quenched by addition of 75 mM glycine and analyzed on NuPAGE 4-12% Bis-Tris gel. Cross-linked HSF1 products were visualized by western blot analysis.

3.9.3.6 Radioactive protein labeling

HeLa cells were transfected in 12-well format. 48 h later, cells were washed first with PBS, then with pre-warmed FCS-free, methionine-reduced DMEM (DMEM minus). Labeling was initiated by adding 50 µCi/ml ^{35}S-Met (EasyTag™ L-[35S]-methionine) in DMEM minus. 15 min later, labeling was stopped by discarding the radioactive medium and applying cold PBS. The cells were lysed in SDS-PAGE loading buffer, boiled for 15 min and separated on a NuPAGE 4-12% Bis-Tris gel followed by Coomassie blue staining and autoradiography.

3.9.3.7 Formation of nuclear stress bodies

HeLa cells were transfected with esiRNA in 12-well format (chapter 3.9.2.3) and grown on poly-L-lysine-coated cover slips. 71 h after transfection, the cells were heat-stressed for 1 h at 43°C and fixed with 4% paraformaldehyde for 15 min at room temperature. Cells were rinsed three times in PBS for 5 min each, covered with ice-cold methanol, incubated for 10 min at -20°C and rinsed in PBS for 5 min again. Unspecific antibody binding was blocked by incubating the cells for 60 min in 5% milk powder dissolved in PBS. Primary antibody incubation with rabbit-α-HSF1 antibody (dilution 1:500 in PBS) was performed at 4°C over-night. The next day, cells were washed three times in PBS for 5 min each and incubated at room temperature with a secondary goat-α-rabbit-cy3 antibody (dilution 1:200 in PBS) for 2 h in the dark. Then, cells were rinsed in PBS for 5 min and the DNA was stained for 1 min using 500 nM DAPI. Cover slips were rinsed five times in PBS and mounted on microscopy slides. Fluorescence microscopy is described in chapter 3.9.3.9. For analysis, cells showing the formation of nuclear stress bodies were counted and normalized to the total number of cells.

3.9.3.8 FlucDM-GFP aggregation assay

HEK293T cells stably expressing the proteostasis sensor protein FlucDM-GFP were transfected with esiRNA in 12-well format (chapter 3.9.2.3) and grown on poly-L-lysine coated cover slips. 70 h after transfection, the cells were heat-stressed for 2 h at 43°C and fixed with 4% paraformaldehyde for 15 min at room temperature. Washing, blocking, DAPI staining, and mounting were performed as described in chapter 3.9.3.7. GFP fluorescence was recorded (see chapter 3.9.3.9) and cells showing the formation of green fluorescent foci were counted and normalized to the total number of cells.

3.9.3.9 Fluorescence microscopy

Fluorescence imaging was performed on a Zeiss Axiovert 200M fluorescence microscope equipped with a Zeiss Axiocam HRM camera. The following filter sets were used to capture the images: for DAPI, filter set 1 (beam splitter FT395, excitation filter BP365/12, emission filter LP397); for GFP, filter set 38 (beam splitter FT580, excitation filter BP470/40, emission filter BP525/50); and for cy3, filter set15 (beam splitter FT495, excitation filter BP546/12, emission filter LP590). Images were taken using Axiovision Rel 4.7 software. Size, brightness, and contrast of the images were adjusted by Adobe Photoshop CS3.

3.9.3.10 Proteasome activity assay

The chymotrypsin-like activity of the proteasome was measured using the Proteasome-Glo™ Chymotrypsin-Like Assay kit according to the manufacturer's protocol. Nuclear, cytoplasmic, and RIPA soluble cell extracts were prepared from control and heat-stressed cells (with and without recovery) as described in chapter 3.11.1 and 3.8.2. 20 µg of protein extracts were mixed with 40 µl Proteasome-Glo™ reagent, incubated for 15 min at room temperature, and luminescence was recorded.

3.10 Genome-scale esiRNA screen

The genome-scale esiRNA screen was performed at the High-Throughput Technology Development Studio (TDS) of the Max Planck Institute of Molecular Cell Biology and Genetics (Pfotenhauerstr. 108, 01307 Dresden).

3.10.1 Genome-scale esiRNA screening protocol

The esiRNA library was designed and synthesized as described previously (Kittler *et al.* 2005, Kittler *et al.* 2007). For cell-based screening, 15 ng esiRNA in 5 µl nuclease-free water were mixed with 5 µl Opti-MEM containing 0.1 µl Lipofectamine RNAiMAX in 384-well format (Eppendorf) using an automated pipetting system (TeMo equipped with a 384-well head, Tecan). After incubating for 20 min at room temperature, 3000 iFluc-Rluc cells in 40 µl DMEM were added to the RNAi-Lipofectamine duplex using a WellMate dispensing system (Matrix) and incubated at 37°C in a 5% CO_2 incubator. 66 h after transfection, cells were exposed to HS by placing them in a CO_2 incubator for 2 h at 43°C, followed by a recovery period of 4 h at 37°C. Afterwards the medium was aspirated to a final volume of 20 µl (Tecan

384Powerwasher) followed by addition of 20 µl of Dual-Glo™ Luciferase Reagent to each well (WellMate). After incubation for 10 min in the dark, Fluc activities were measured with a 384-well plate luminometer (Envision, Perkin Elmer). Following the initial measurement, 20 µl of Dual-Glo™ Stop & Glo® reagent diluted 1:100 (v/v) in Dual-Glo™ Stop & Glo® buffer were added to each well. After 10 min of incubation in the dark, Rluc activities were measured.

3.10.2 Computational and bioinformatic analysis

To generate protein interaction networks, the Uniprot ID mapping service was used to translate the ENSEMBL gene identifiers of the found HSR modulators to reviewed UniProtKB Accessions. Interaction data were downloaded from BioGRID database, release: 3.1.90 (Stark *et al.* 2011) and networks were prepared using Cytoscape version 3.0.1. 100,000 random protein networks were used to calculate network statistics. The "One Sample t-test" was performed in R to calculate the randomness of the network (http://www.R-project.org/). All p-values are $< 2.2e^{-16}$. Statistics were calculated with the help of Dr. S. Pinkert (MPI of Biochemistry, Martinsried).

3.11 Mass spectrometry (MS)

3.11.1 SILAC medium and sample preparation

Arginine- and lysine-free DMEM was supplemented with 10% dialyzed FCS, 100 IU/ml penicillin G, 100 µg/ml streptomycin sulfate, 2 mM L-glutamine, and non-essential amino acid cocktail. To prepare light (L), medium (M), and heavy (H) media for SILAC labeling of cells, the following amino acids were added: for L, Arg0 and Lys0 (arginine and lysine); for M, Arg6 and Lys4 (arginine-13C6 and lysine-4,4,5,5-d4); for H, Arg10 and Lys8 (arginine-13C6,15N4 and lysine-13C6,15N2).

10^6 SILAC-labeled HeLa cells were treated as indicated in the figure (Figure 4-18), trypsinized, and harvested in PBS. Cells were counted, equal numbers of L-, M-, and H-labeled cells were mixed, and protein extracts were prepared.

Nuclear and cytoplasmic extracts were prepared using the NE-PER Nuclear and Cytoplasmic Extraction Kit following the manufacturer's instructions. Briefly, $2x10^6$ cells were suspended in 200 µl of ice-cold CER I, mixed for 15 s, and incubated on ice for 10 min. After the addition of 11 µl of ice-cold CER II, tubes were mixed for 5 s, and incubated on ice

for 1 min. Subsequently, tubes were mixed and centrifuged at 16,000 g for 5 min at 4°C. The supernatant fractions contained the cytoplasmic proteins. Pellets were washed twice with cold PBS, resuspended in 100 µl ice-cold NER, and incubated on ice for 40 min with mixing intervals of 10 min. Tubes were centrifuged at 16,000 g for 10 min at 4°C. The supernatant fractions, containing the nuclear proteins, were transferred to pre-chilled tubes.

3.11.2 SDS-PAGE

Prior to SDS-PAGE, samples were mixed with 10% (v/v) LDS sample buffer and 2% β-mercaptoethanol. After heating at 70°C for 10 min, samples were separated on NuPAGE 4-12% Bis-Tris gels. Gels were fixed and stained with Colloidal blue. Preparation of gel slices, reduction, alkylation, and in-gel protein digestion were carried out as described by Shevchenko (Shevchenko *et al.* 1996). Finally, peptides were desalted, filtered, and enriched according to Rappsilber (Rappsilber *et al.* 2003).

3.11.3 LC-MS/MS

Peptides eluted from desalting tips were dissolved in 5% (v/v) formic acid, followed by 5 min of sonication. Samples were analyzed on a nanoACQUITY HPLC system (Waters) coupled to a LTQ-Orbitrap mass spectrometer (Thermo). Peptides were separated on home-made spray-columns (ID 75 µm, 20 cm long, 8 µm tip opening) packed with 1.9 µm C18 particles using a stepwise 150 min gradient between buffer A (0.2% formic acid in water) and buffer B (0.2% formic acid in acetonitrile). Samples were loaded onto the column with the nanoACQUITY autosampler at a flow rate of 0.5 µl/min. No trap column was used. The HPLC flow rate was set to 0.2 µl per min during analysis. MS/MS analysis was performed with standard settings using cycles of 1 high resolution (60000 FWHM) MS scan followed by eight MS/MS scans of the eight most intense ions with charge states of 2 or higher.

3.11.3.1 Analysis of MS data

MaxQuant (version 1.1.1.36) was used for protein identification and SILAC-based quantitation. Default settings were used, except that the “keep low-scoring versions of identified peptides” option was disabled to increase the confidence of quantitation. The human sequences of UNIPROT (version 2011-02-14) were used as database for protein identification. MaxQuant used a decoy version of the specified UNIPROT database to adjust the false discovery rates for proteins and peptides below 1%.

Proteins with normalized ratios > 1.657584 or < 0.625 (1/1.6) in at least two out of three independent replicate experiments were considered as enriched or depleted, respectively. The probability of incorrect assignment of a protein as being enriched or depleted was determined to be smaller than 1% in control experiments (data not shown). In these control experiments, equal amounts of H- and L-labeled cells were mixed after HS, lysed and analyzed as described. The number of proteins with normalized ratios > 1.657584 or < 0.625 (1/1.6) in at least two out of three replicates was determined to be smaller than 1%. Due to limitation of the biochemical separation protocol, mitochondrial proteins contaminated the nuclear proteome (Boisvert *et al.* 2010). These contaminant mitochondrial proteins were removed from the list before bioinformatic analysis of nuclear proteins.

4 Results

4.1 Generation and validation of luciferase reporter cell line

In order to conduct a genome-scale RNAi screen for modulators of the HSR, a HeLa reporter cell line (iFluc-Rluc) was generated stably expressing firefly luciferase (Fluc) under the control of the human *HSPA1A (hsp70.1)* promoter (Figure 4-1A). Under conditions of proteotoxic stress, HSF1 binds to this promotor and induces Fluc expression (Williams *et al.* 1989, Westerheide *et al.* 2004, Calamini *et al.* 2012). Any change in the stress-induced Fluc expression upon down-regulation of a particular gene can be explained either by an alteration in HSF1-mediated transcription or by a non-specific effect (e.g. cell death). To address this problem, a second construct, coding for the unrelated luciferase protein from *Renilla reniformis* (Rluc) under the control of the *CMV* promoter, was stably introduced into the reporter cell line (Figure 4-1A). CMV is an HSF1-independent and constitutive promoter, resulting in stable Rluc expression under normal as well as stress conditions (Figure 4-1B). Rluc differs from Fluc in terms of substrate and reaction mechanism and can therefore be assayed orthogonally (Figure 4-1A), providing a measure for cell viability. Rluc activity was used to normalize the activity of Fluc to identify only HSF1 specific events. Fluc expression was expected to be low under normal conditions and to be strongly increased relative to Rluc upon exposure to stress (Figure 4-1A). The down-regulation of potential positive or negative HSR modulators was supposed to inhibit or enhance the expression of Fluc, respectively.

The iFluc-Rluc cell line was extensively tested in terms of optimal stress-induced reporter expression and reproducibility with different physical and small molecule activators of the HSR (Figure 4-1B and Figure 4-2). The validation experiments revealed that heat stress (HS) at 43°C for 2 h followed by a 2-4 h recovery period at 37°C resulted in a high and reproducible Fluc expression and a strong increase in the Fluc:Rluc activity ratio (up to 50-fold). Longer exposure to elevated temperatures caused substantial cell death and a reduced Fluc:Rluc ratio (Figure 4-1C). Both luciferase reporters are thermo-labile enzymes and are known to be deactivated by thermal stress (Liu *et al.* 1997, Baggett *et al.* 2004, Gupta *et al.* 2011). Heat shock at 45°C resulted in the rapid loss of their enzymatic activities which were retrieved with similar kinetics upon shift to normal growth temperature (Figure 4-1D). This result excludes any influence of the luciferase refolding kinetics on the proper estimation of

their relative expression. Amongst the selection of pharmacologically active small molecule modulators of the HSR, which have been described in the literature and were tested in the iFluc-Rluc cell line, only the proteasome inhibitor MG132 and celastrol, a modifier of reactive thiol groups, lead to a ~ 20-fold increase of the Fluc:Rluc ratio. Treatment of the

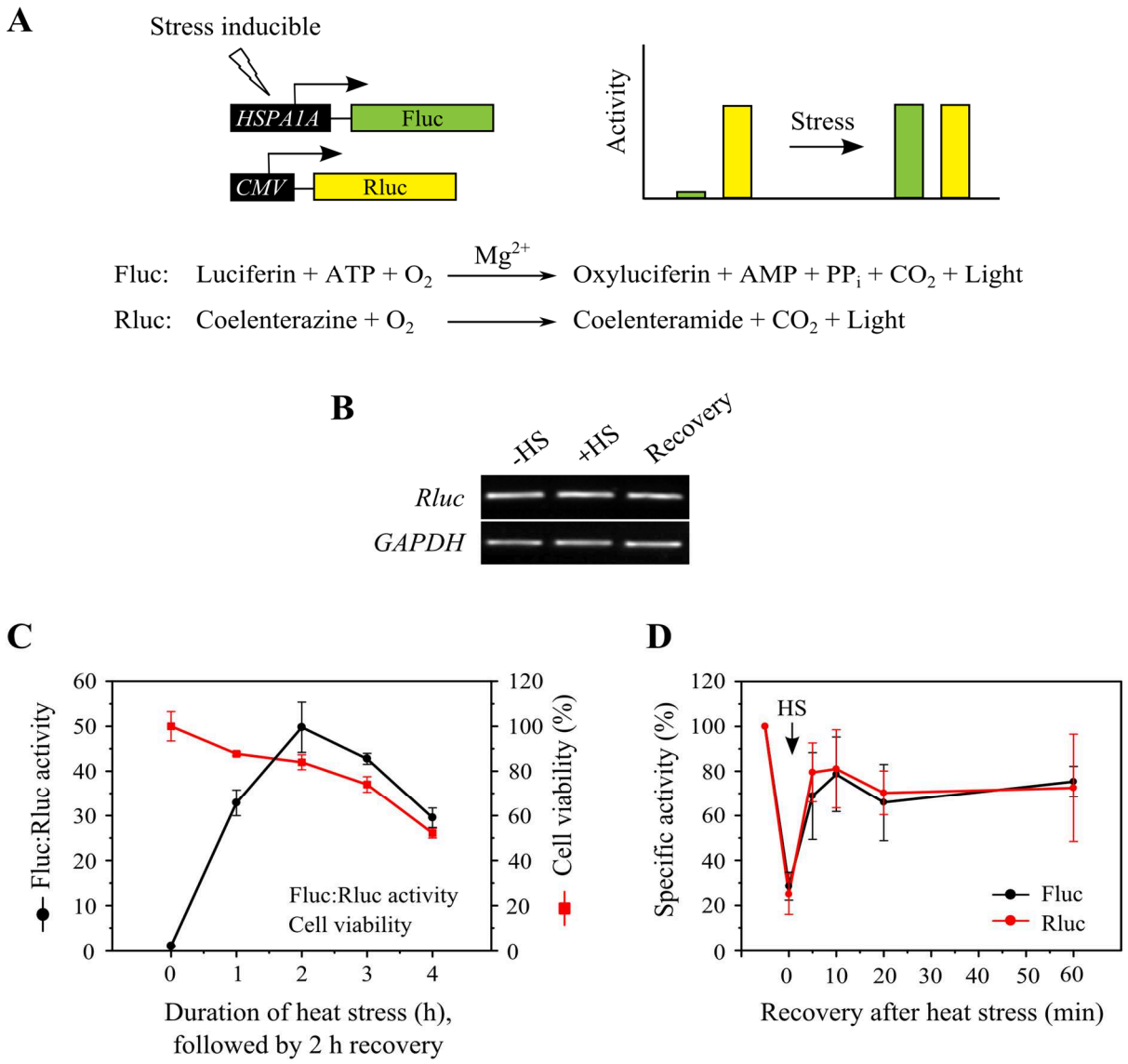

Figure 4-1: Design and characterization of iFluc-Rluc cell line.
(A) Scheme of the reporter constructs and bioluminescent reactions. Left: *HSPA1A*-Fluc and *CMV*-Rluc construct. Right: Expected reporter activities with and without stress. Bottom: Bioluminescent reactions catalyzed by Fluc and Rluc. (B) *Rluc* and *GAPDH* mRNA levels in the iFluc-Rluc cell line after heat-shock and recovery. Cells were heat-stressed for 2 h at 43°C (+HS) followed by recovery at 37°C for 2h (Recovery) or kept at 37°C throughout the experiment (-HS). Total RNA was prepared and *Rluc* and *GAPDH* mRNA levels were estimated by RT-PCR. (C) Time course of Fluc:Rluc activity ratio (black) and cell viability (red) in the iFluc-Rluc cell line after thermal stress. Cells were heat-stressed at 43°C for the indicated time spans. Reporter activities and cell viability were measured after a 2 h recovery period at 37°C. Standard deviations were derived from at least three independent experiments (D) Refolding kinetics of Fluc and Rluc in HeLa cells. Cells were transfected with *CMV*-Fluc and *CMV*-Rluc constructs. 24 h after transfection, cells were heat-stressed at 45°C for 30 min and recovered at 37°C. Specific luciferase activities were measured at the indicated time points after heat stress. Standard deviations were derived from at least three independent experiments.

iFluc-Rluc cells with 17-DMAG (17-Dimethylaminoethylamino-17-demethoxy-geldanamycin), Arachidonate, DCIC (3,4-Dichloroisocoumarin), Lactacystin, Puromycin (Westerheide and Morimoto 2005), and Withaferin A (Kaileh *et al.* 2007) failed to induce Fluc expression (Figure 4-2).

As a "proof-of-principle" experiment and to demonstrate the HSF1-dependence of Fluc expression, iFluc-Rluc cells were transfected with an endoribonuclease-prepared short interfering RNA (esiRNA) (Kittler *et al.* 2005) targeting HSF1, with control esiRNA targeting EGFP, or were treated with transfection reagent only (Figure 4-3A). 68 h after the transfection, cells were either exposed to thermal stress at 43°C, followed by a 2 h recovery period at 37°C (+HS), or maintained at 37°C throughout the experiment (-HS). The increased Fluc:Rluc activity ratio after heat stress reflects that HSR induction is neither affected by treatment with transfection reagent only nor by transfection with control esiRNA. Down-

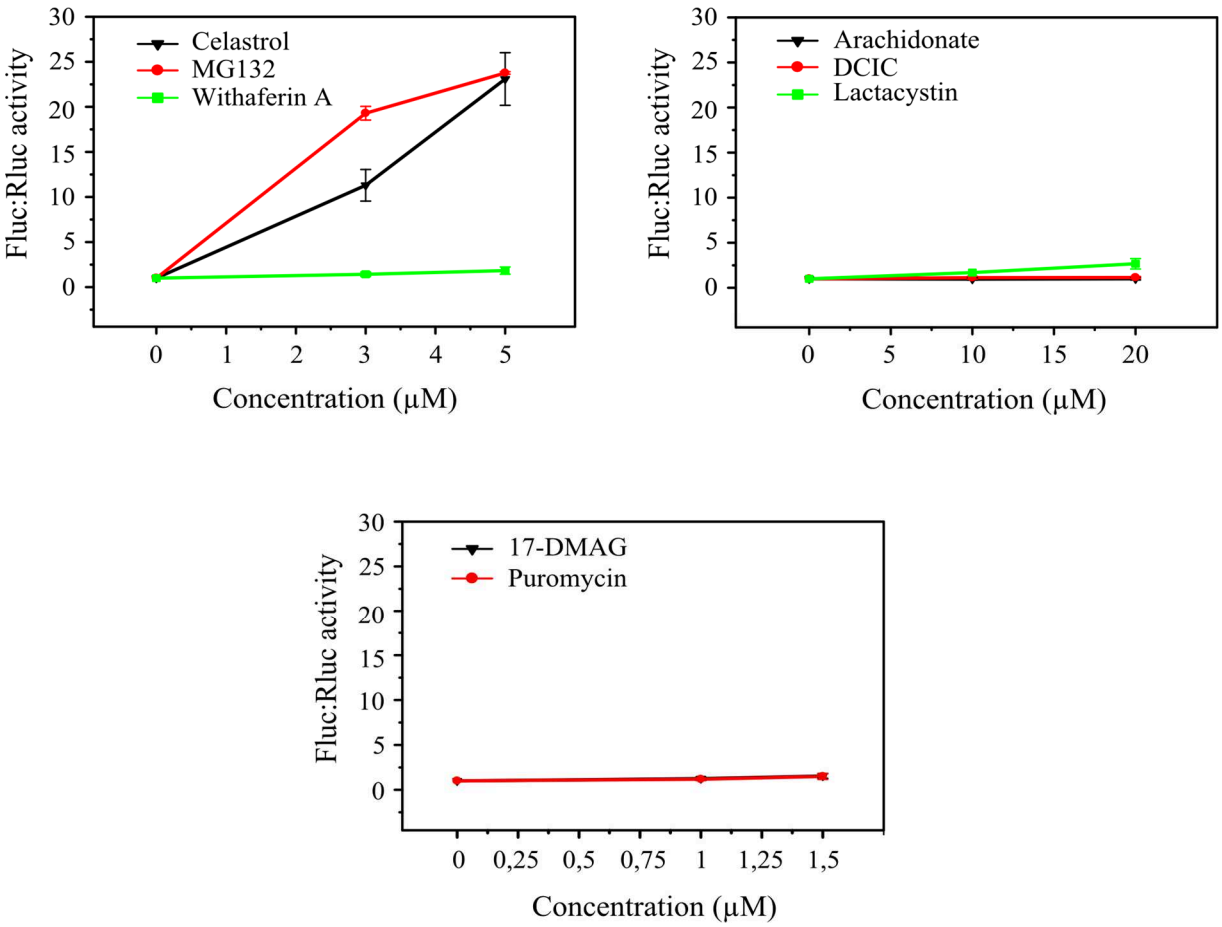

Figure 4-2: Validation of screening condition.
Fluc:Rluc activity ratios in the iFluc-Rluc cell line after exposure to different stress inducers. Cells were treated with Celastrol, MG132, Withaferin A, Arachidonate, DCIC (3,4-Dichloro-isocoumarin), Lactacystin, 17-DMAG (17-Dimethylaminoethylamino-17-demethoxygeldanamycin), and Puromycin at the indicated concentrations for 8 h. Standard deviations were derived from at least three independent experiments.

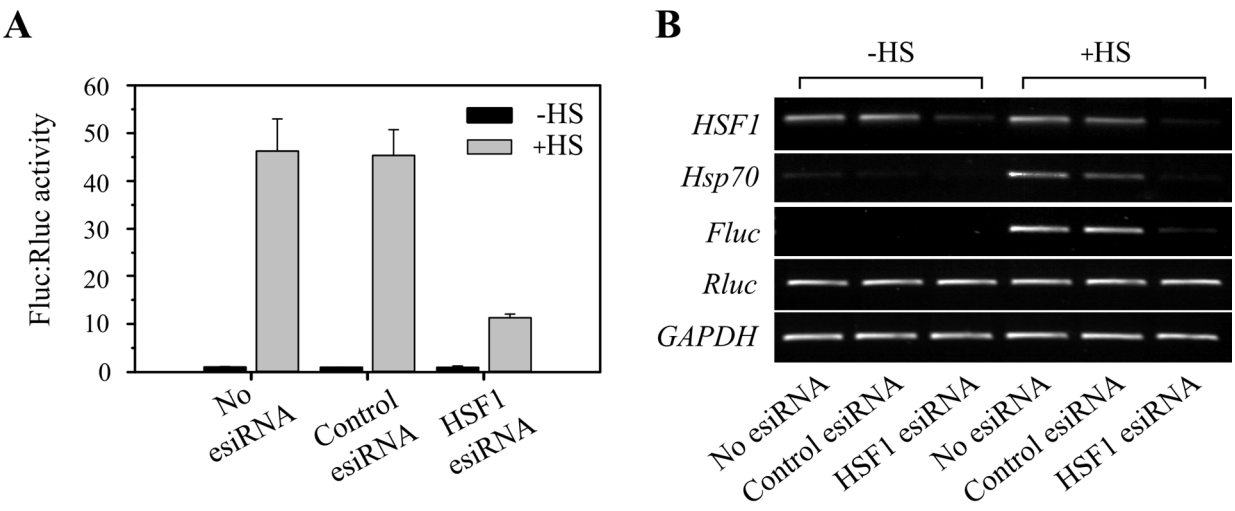

Figure 4-3: Establishment of screening principle.
(A) Fluc:Rluc activity ratios after esiRNA treatment in the iFluc-Rluc cell line. Cells were transfected with esiRNA targeting HSF1, control esiRNA targeting EGFP, or just treated with transfection reagent (no esiRNA). After 68 h, cells were heat-stressed for 2 h at 43°C followed by recovery at 37°C for 2 h (+HS). Non-stressed control cells were kept at 37°C (-HS). Standard deviations were derived from at least three independent experiments. (B) mRNA levels of *HSF1*, *Hsp70*, *Fluc*, *Rluc*, and *GAPDH* after esiRNA treatment of iFluc-Rluc cells. Cells were transfected similarly as described in (A). After 70 h, cells were exposed to HS for 2 hr at 43°C (+HS) or maintained at 37°C (-HS). mRNA levels were estimated by RT-PCR.

regulation of HSF1, on the other hand, strongly inhibited the induction of the stress response. The results were confirmed at mRNA level (Figure 4-3B). While control treatment of iFluc-Rluc cells did not interfere with the stress-dependent increase in *Fluc* mRNA level, down-regulation of HSF1 inhibited the induction of *Fluc*. A similar effect was observed for *Hsp70*, an endogenous target of HSF1. *Rluc* mRNA levels were neither affected by thermal stress nor by HSF1 down-regulation. Furthermore, the reduced *HSF1* mRNA level upon down-regulation clearly demonstrates the efficiency of the used esiRNA.

4.2 Genome-scale RNAi screen for modulators of the heat-shock response

The primary RNAi screen was performed in technical duplicate in a 384-well plate format. Individual primary esiRNAs targeting over 15,000 human genes were transfected in the iFluc-Rluc cell line and the Fluc:Rluc activity ratios were used as read-out (Figure 4-4A and B). Design and synthesis of the esiRNA library have been previously described (Kittler *et al.* 2005, Kittler *et al.* 2007) and a detailed screening protocol can be found in chapter 3.10.

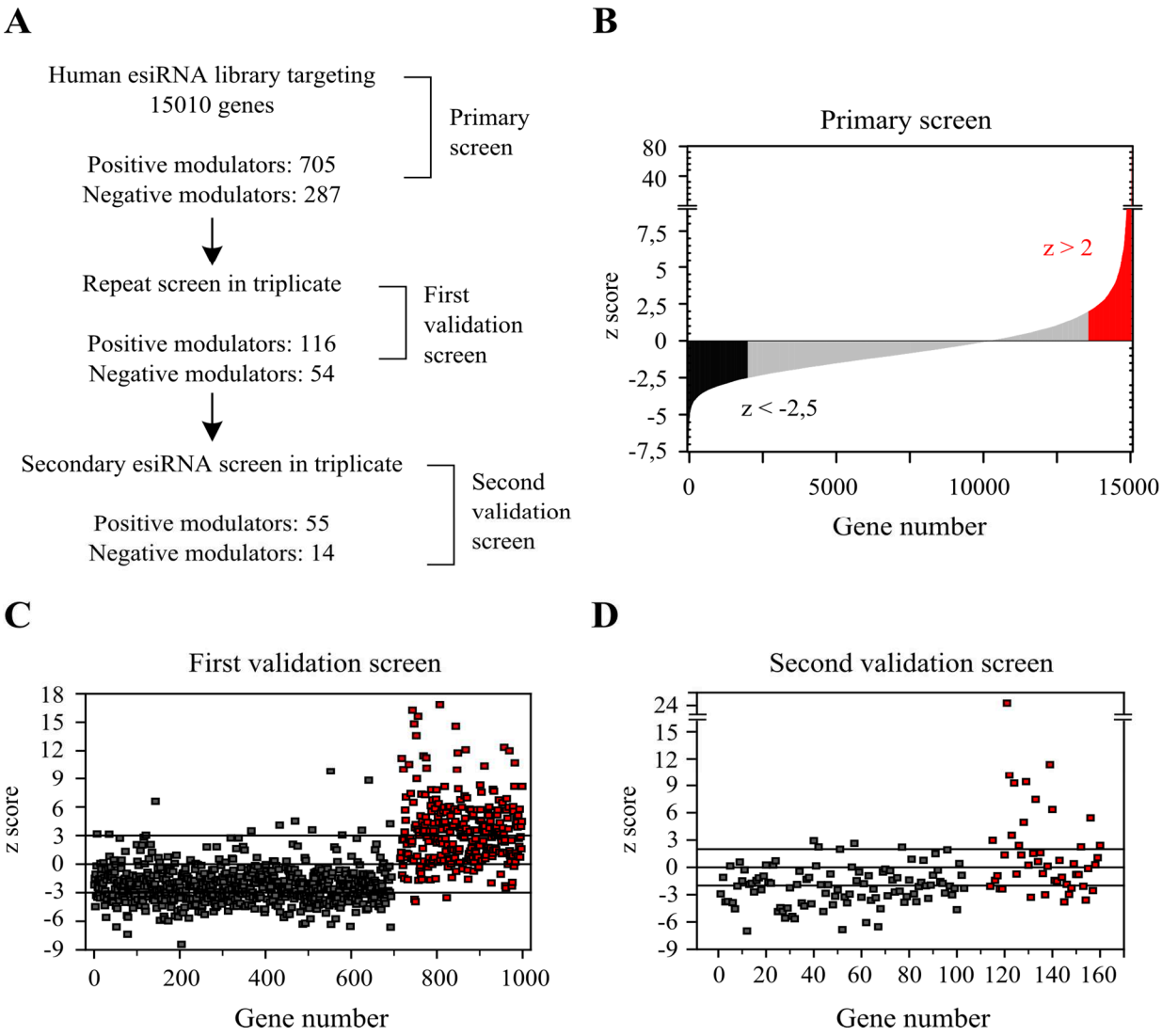

Figure 4-4: Summary of genome-scale RNAi screening.
(A) Flowchart describing different steps of the screen. The numbers of positive and negative modulators found at every step are indicated. (B) Z score distribution of the primary screening results. Z scores > 2 and < -2.5 are shown in red and black, respectively. (C and D) Z score distributions from the first and second validation screens. Positive and negative modulators are shown in black and red, respectively.

For normalization purposes and the verification of the transfection efficiency, several controls were included on each plate. Four wells were transfected with non-specific esiRNA targeting EGFP (negative control) and three wells with HSF1 esiRNA (positive control), respectively. Z scores, representing the deviation of individual Fluc:Rluc activity ratios from the mean of the negative control wells in units of standard deviation, were calculated for each down-regulation (Boutros *et al.* 2004, Malo *et al.* 2006). To allow a uniform analysis of results from separate plates and to analyze them in a cooperative way, the mean z score of positive control wells on every plate was set to a fixed value (-6). Consequently, z scores of experimental wells were normalized with respect to the positive control on the same plate. Henceforward, the normalized z scores of all plates were analyzed together. The primary

screen results were analyzed by following a low stringency protocol in order to minimize the chances of excluding false-negatives. But at the same time, this protocol increased the possibility of including false-positives. A gene was considered as a potential positive modulator of the HSR in case the normalized z scores were smaller than -2.5 for each of the respective duplicates. In case the two particular z scores showed values greater than +2, the respective gene was scored as a negative modulator of HSR. A distribution plot summarizing the results of the primary screen is shown in Figure 4-4B. The stringency of the results was increased considering Rluc activity values from each well as an indicator of overall cellular health. Results were not included in the further evaluation process, in case the mean Rluc activity ratio of experimental to control wells fell out of the range of 0.75-1.25. The mean Fluc activity ratio of experimental to control wells was an additional criterion for consideration as a modulator of the HSR. It was set to be below 0.8 for a positive HSR modulator and above 1.2 for a negative modulator, respectively. These selection criteria allowed the identification of 705 positive modulators of the HSR, for which the Fluc:Rluc activity ratio was significantly reduced upon down-regulation. Down-regulation of 287 genes enhanced the Fluc:Rluc activity ratio significantly, suggesting a potential role as negative modulators of the HSR (Figure 4-4A and B).

To identify the strongest modulators of the HSR, the primary screen was repeated for this set of candidates using the same esiRNAs but more stringent criteria. The reliability of the results was increased by the performance of three independent experiments. For technical reasons, down-regulation of 10 positive and 2 negative modulators from the primary candidate list could not be repeated. To nominate the strongest candidates for further validation, a high stringency protocol was followed only considering genes whose down-regulations resulted in z scores smaller than -3 or greater than +3 in all three biological replicates. Thereby, the number of validated positive and negative HSR modulators could be reduced to 116 and 54, respectively (Figure 4-4A and C).

For the next round of validation, a secondary set of esiRNAs was prepared, targeting an independent region of the same transcript. In total, 151 (104 positive and 47 negative modulators) were tested in triplicate during the secondary validation screen. For 19 genes no high-quality secondary esiRNA could be designed. With selection criteria of z scores smaller than -2 or greater than +2 in two out of three experiments, the results for 55 positive and 14 negative modulators were confirmed (Figure 4-4A and D; Table 7-1 and Table 7-2).

4.3 Biochemical validation of Hsp70 mRNA level after thermal stress

In order to validate whether the positive modulators identified in the screen are implicated in endogenous HSR, RT-PCR experiments were performed for a representative set of

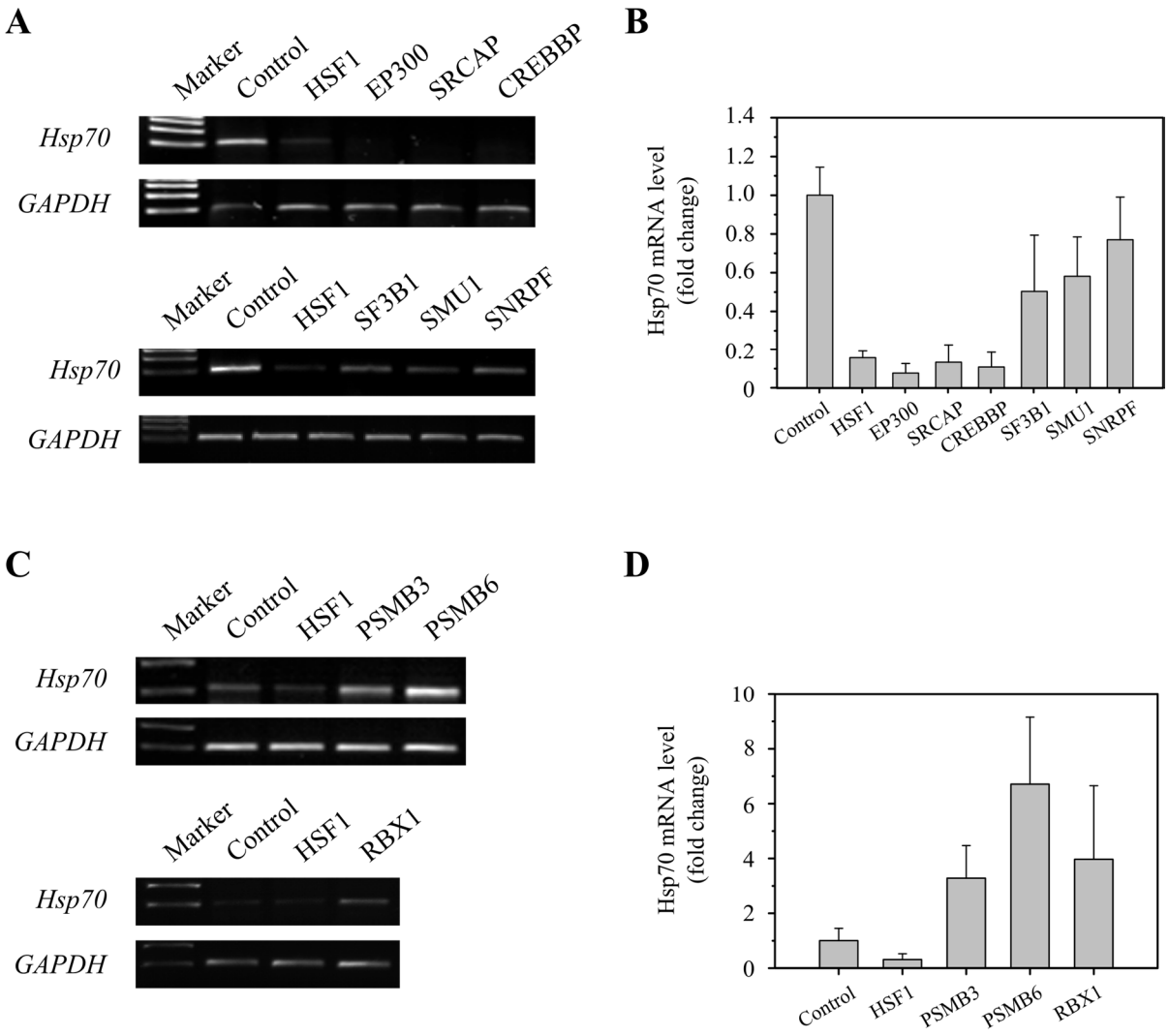

Figure 4-5: *Hsp70* mRNA levels in HeLa cells with down-regulation of different HSR modulators.
(A) HeLa cells were transfected with esiRNA targeting positive HSR modulators. 70 h after transfection, cells were heat-stressed for 2 h at 43°C and total RNA was prepared. *Hsp70* and *GAPDH* mRNA levels were estimated by RT-PCR. (B) Quantification of (A). *Hsp70* mRNA levels were estimated using AIDA, normalized to corresponding *GAPDH* mRNA levels and plotted. Standard deviations from at least three independent experiments are shown. (C) HeLa cells were transfected with esiRNA targeting negative HSR modulators. 66 h after transfection cells were heat-stressed for 2 h at 43°C followed by recovery for 4 h at 37°C and total RNA was prepared. *Hsp70* and *GAPDH* mRNA levels were estimated by RT-PCR. (D) Quantification of (C). *Hsp70* mRNA levels were estimated using AIDA, normalized to corresponding *GAPDH* mRNA levels and plotted. Standard deviations from at least three independent experiments are shown.

modulators to confirm that down-regulation of the particular genes interfered with the induction of endogenous *Hsp70* mRNA transcription upon HS. Indeed, when cells were thermally stressed, the Hsp70 mRNA level was reduced for several positive modulator down-regulations (Figure 4-5A and B; Table 7-1). The validation of the several chromatin modifiers was of special interest, because the screening experiment was performed in a stable cell line with the reporter genes being integrated into "unknown" regions of the chromosomes. Thus, the chromatin modifiers identified could be merely specific for reporter expression and do not represent a universal requirement for HSR induction. However, the induction of endogenous *Hsp70* mRNA level was decreased upon down-regulation of EP300, SRCAP, and CREBBP, establishing their role in the HSR regulation (Figure 4-5A).

A reduction of the *Hsp70* mRNA level could not be confirmed for all positive modulators tested, including the small ribosomal subunit protein RPS25 as well as several subunits of the cytosolic chaperonin TRiC/CCT (Figure 4-6; Table 7-1). Since the folding of Fluc is dependent on chaperones such as Hsp70, Hsp90, and TRiC/CCT (Schroder *et al.* 1993, Frydman *et al.* 1994) down-regulation of the corresponding genes may have interfered with Fluc maturation rather than induction of the HSR. Furthermore, the Hsp70-Hsp90 organizing protein Hop (STIP1) and CCT6A were also shown not to be involved in regulation of the HSR (data not shown). The genes, whose down-regulation failed to reduce *Hsp70* mRNA level in RT-PCR validation, were removed from the list of HSR modulators.

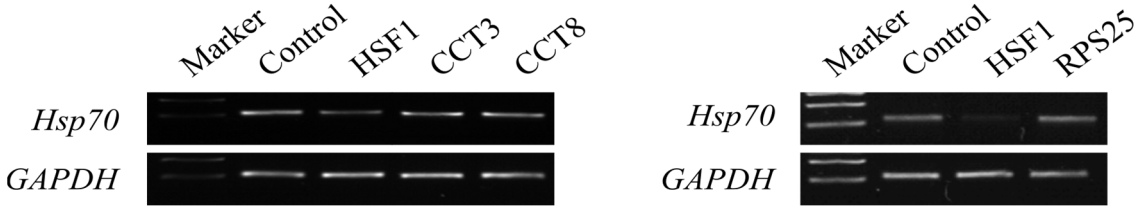

Figure 4-6: *Hsp70* mRNA levels in HeLa cells with down-regulation of positive modulators of Fluc activity that do not interfere with HSR induction.
HeLa cells were transfected with esiRNA targeting different modulators categorized as positive HSR modulators according to the esiRNA screen. 70 h after transfection, cells were heat-stressed for 2 h at 43°C and total RNA was prepared. *Hsp70* and *GAPDH* mRNA levels were estimated by RT-PCR.

In contrast to the reduced *Hsp70* mRNA level observed immediately upon HS after down-regulation of positive HSR modulators (Figure 4-5A and B; Table 7-1), down-regulation of negative HSR modulators generally did not increase the level of *Hsp70* mRNA but rather delayed the return to the normal *Hsp70* mRNA level during stress recovery (Figure 4-5C and D; Table 7-2).

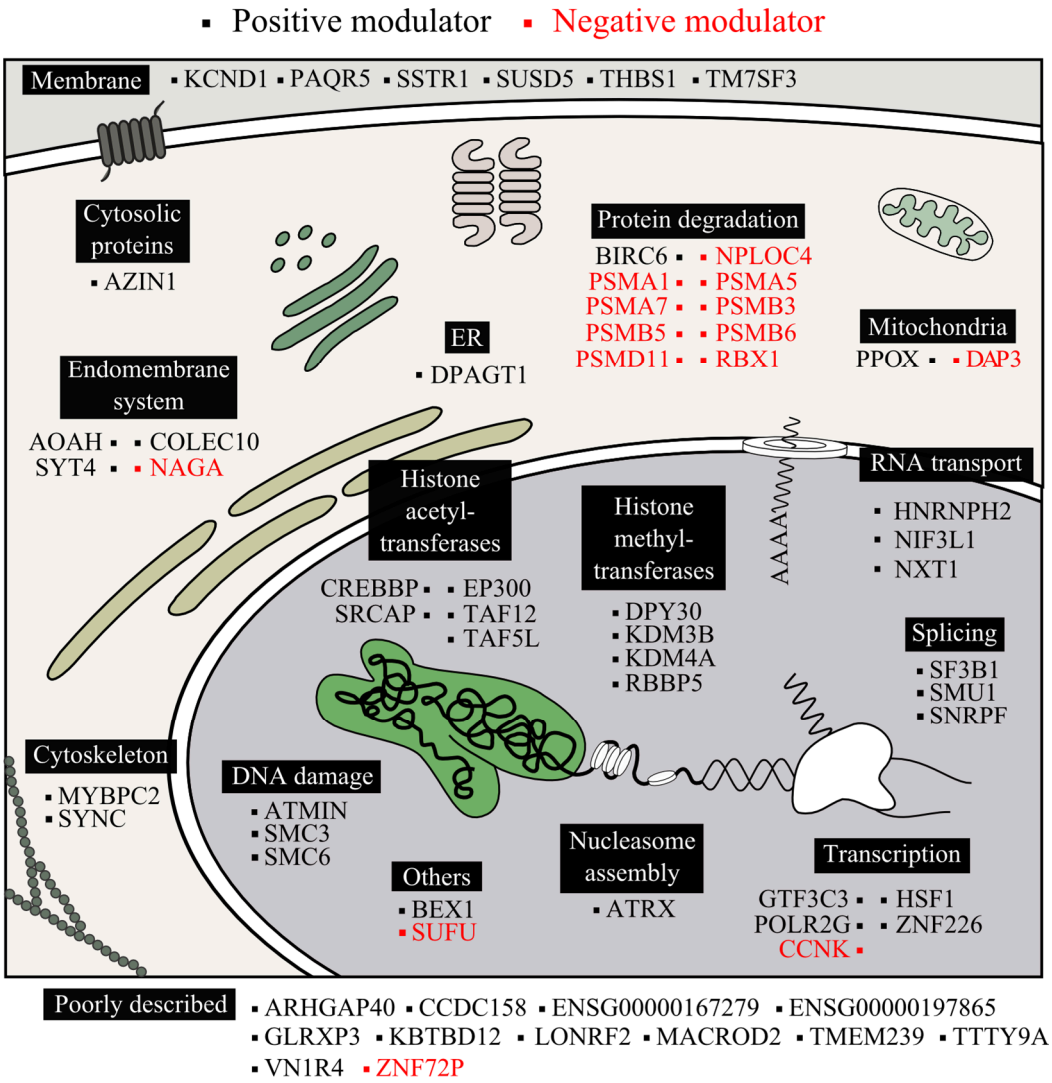

Figure 4-7: Primary localization of the HSR modulators.
The HSR modulators are grouped according to their primary cellular localization and function. Positive modulators are shown in black, negative modulators in red. Genes whose down-regulation failed to reduce the induction of the endogenous *Hsp70* mRNA level after thermal stress as evaluated by RT-PCR are excluded (layout adapted from Olzscha *et al.* 2011).

After these validation experiments, the number of positive modulators was reduced to 50 and the number of negative modulators remained unchanged (Table 7-1 and Table 7-2).

4.4 Overview of the screening results and functional validation

The primary localization of the modulator proteins, as found in the HPRD (Prasad *et al.* 2009) database and by literature research, revealed that the regulation of the HSR relies on the integration of signals generated in several cellular processes and compartments (Figure 4-7).

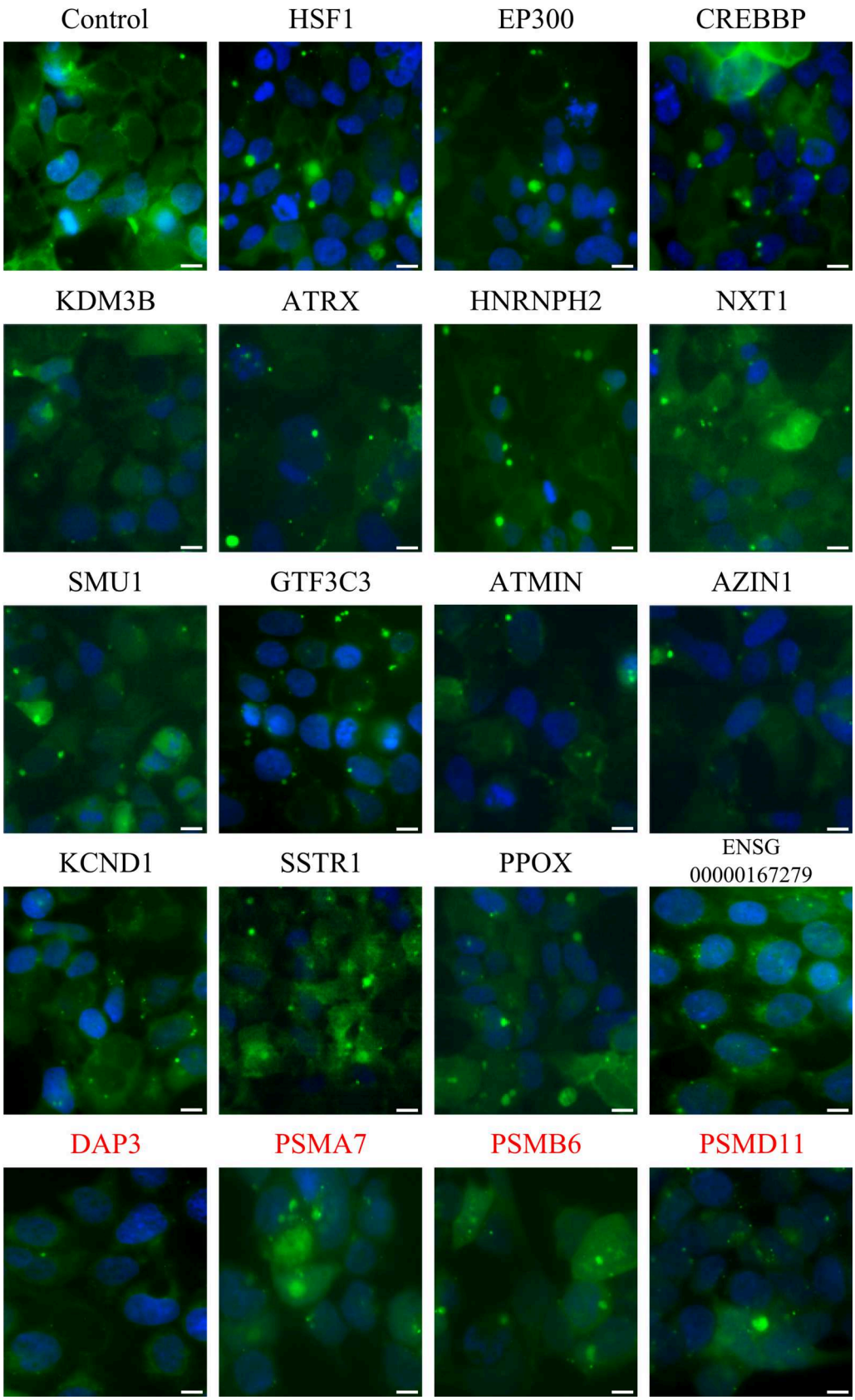

Figure 4-8: FlucDM-GFP aggregation propensity upon HSR modulator down-regulation.
HEK293T cells stably expressing FlucDM-GFP were transfected with control esiRNA targeting Rluc or esiRNAs targeting different HSR modulators. 70 h after transfection, cells were heat-stressed at 43°C for 2 h, fixed and micrographed. Representative images indicating FlucDM-GFP (green) and DAPI (blue) are shown. Scale bar: 10 µm.

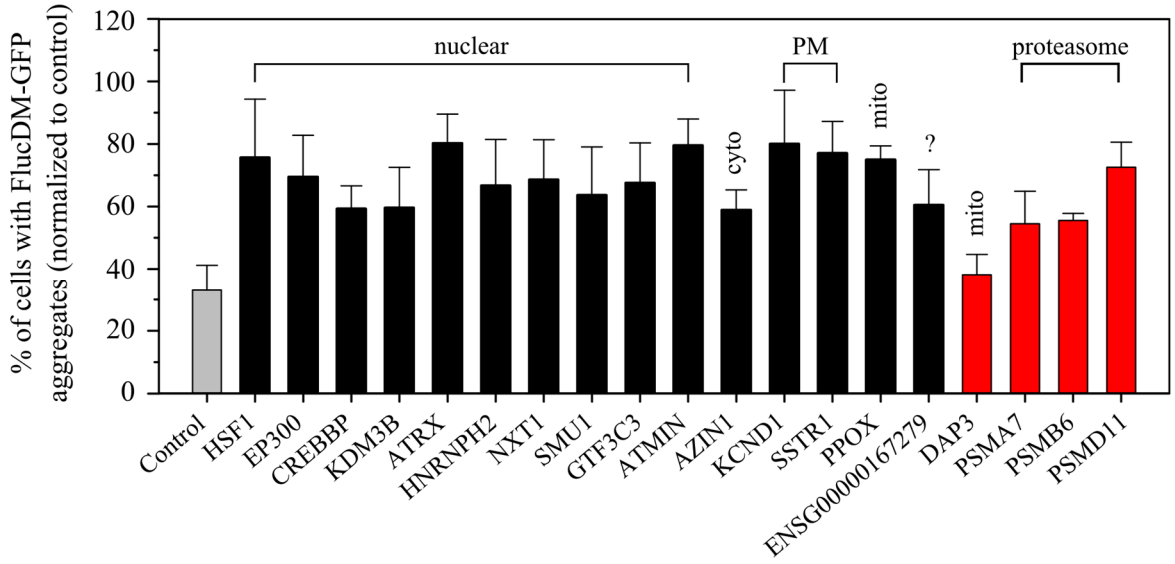

Figure 4-9: FlucDM-GFP aggregation propensity upon HSR modulator down-regulation.
Quantification of FlucDM-GFP aggregate formation. For each down-regulation, the percentage of cells with FlucDM-GFP aggregates was determined and plotted. Positive modulators are shown in black, negative modulators in red, control is shown in grey. Standard deviations for counting from at least three different fields of view are indicated.

Approximately 40% of the HSR modulators (24 positive and 2 negative modulators) are primarily localized in the nucleus, including proteins involved in chromatin remodeling, transcription, mRNA splicing, and DNA damage repair. 18 modulators (~ 30% of total) are cytosolic (or cytosolic and nuclear), including several proteasome subunits identified as negative modulators. Furthermore, several modulators are also localized in the plasma membrane and in organelles such as mitochondria, ER, and lysosomes. 12 proteins (11 positive and 1 negative HSR modulator) are poorly described. Sequence analysis of these proteins by WoLF PSORT (Horton *et al.* 2007) revealed that LONRF2 and MACROD2 might be nuclear and TTTY9A as well as ENSG00000197865 extracellular proteins. According to TMHMM, a membrane protein topology prediction method (Krogh *et al.* 2001), ENSG00000197865, TMEM239, TTTY9A, and VN1R4 contain predicted transmembrane segments.

4.4.1 Influence of HSR modulators on cellular proteostasis

An alteration in HSR induction is expected to influence cellular proteostasis under stress conditions. To explore their functional significance in proteostasis maintenance, several HSR modulators from each functional category were down-regulated in a HEK293T cell line stably expressing the proteostasis sensor protein FlucDM-GFP (Gupta *et al.* 2011). The Fluc reporter protein is destabilized by the introduction of two mutations, which render the protein

aggregation-sensitive. When thermally stressed for 2 h at 43°C, approximately 30% of the cell population formed visible FlucDM-GFP aggregates. Down-regulation of the positive HSR modulators strongly increased the formation of FlucDM-GFP aggregates, indicating a reduced Hsp expression during stress and a compromised proteostasis (Figure 4-8 and Figure 4-9). In contrast, down-regulation of the negative modulator DAP3 did not result in increased aggregation, suggesting that the enhanced stress response observed under these conditions is functionally relevant. Down-regulation of the proteasome components PSMA7, PSMB6, and PSMD11 did not suppress FlucDM-GFP aggregation, confirming that proteasome inhibition results in an increased formation of reporter inclusions (Gupta *et al.* 2011). In addition, these observations in HEK293T cells confirmed that the HSR modulators found in the screen were not only specific for HeLa cells.

4.4.2 Influence of HSR modulators on formation of nuclear stress bodies

Activation of the HSR results in the formation of nuclear stress bodies (nSB), which represent transcription sites of non-coding satellite-III RNA. During stress, HSF1 rapidly localizes to these dynamic structures by binding to pericentric tandem repeats of satellite III sequences. nSB are found in human and primate cells, but are absent in rodent cells. Their functional significance is unknown. However, since non-coding RNAs play important roles in heterochromatin assembly, nSB may be sites for specific chromatin remodeling processes during stress (Jolly *et al.* 1997, Jolly and Lakhotia 2006, Biamonti and Vourc'h 2010). The satellite-III transcripts are known to recruit splicing and other pre-mRNA processing factors to nSB suggesting a role in RNA maturation (Denegri *et al.* 2001, Metz *et al.* 2004). Recently, it was also shown that the formation of nSB may represent an evolutionary aspect of HSF1 regulation *in vivo* (Morton and Lamitina 2013).

To check, whether the identified HSR modulators influence the formation of nSB, a representative set was down-regulated and the percentage of cells showing nSB formation after thermal stress was determined. Surprisingly, most down-regulations had no influence on percentage of cells containing nSB. This may indicate that these HSR modulators are not required for nSB formation. However, the down-regulation of the acetyltransferase EP300, the splicing factor SF3B1, and the transcription factor GTF3C3, all identified as positive modulators in the screen, caused a significant reduction in the percentage of cells with nSB (Figure 4-10 and Figure 4-11A). The reduced nSB formation upon SF3B1 down-regulation may be consistent with a regulatory relationship between the movement of splicing machinery to nSB and HSF1 activation. Interestingly, down-regulation of the proteasome components

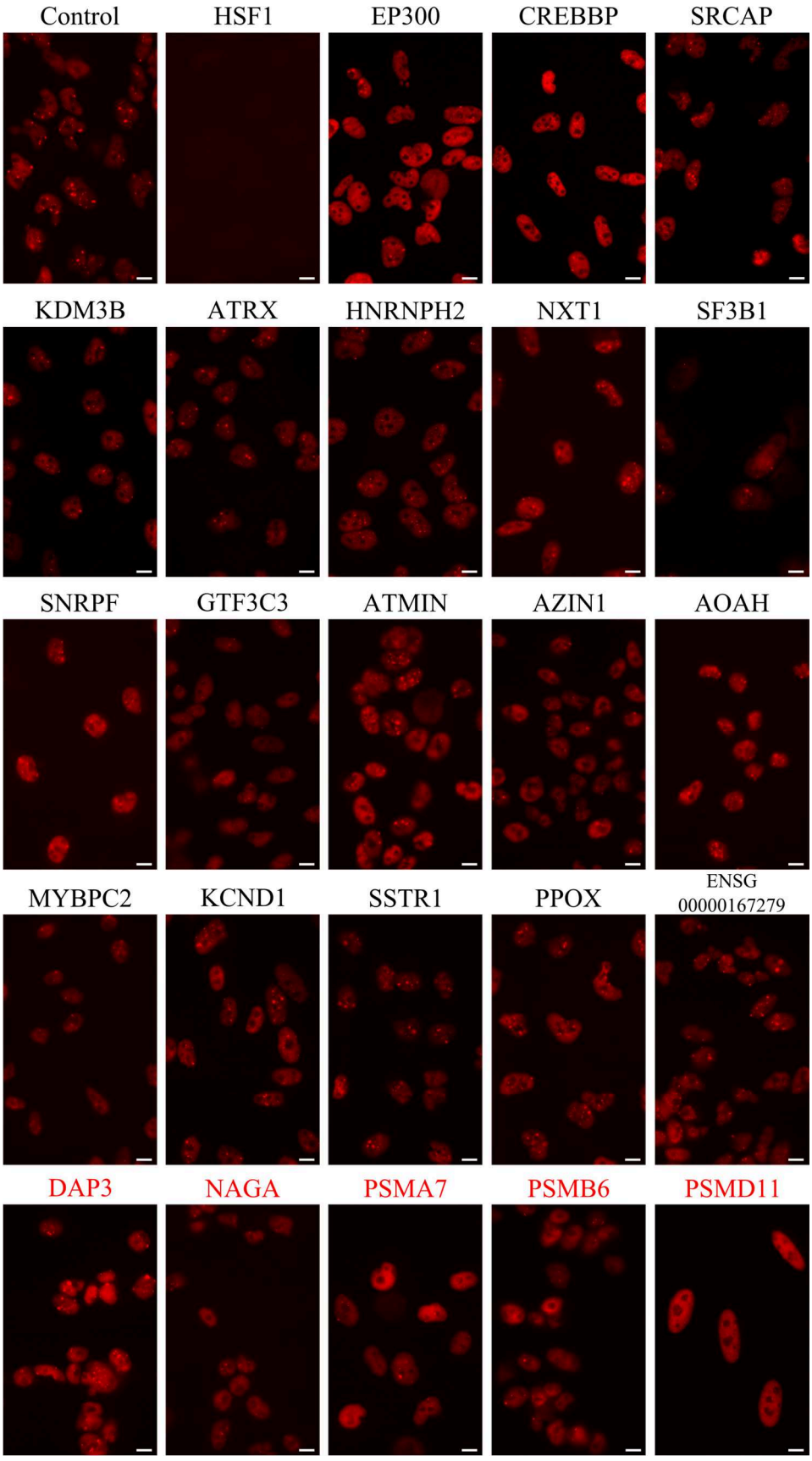

Figure 4-10: nSB formation upon HSR modulator down-regulation.
HeLa cells were transfected with control esiRNA targeting Rluc or esiRNAs targeting different HSR modulators. 71 h after transfection, cells were heat-stressed at 43°C for 1 h, fixed, stained with rabbit anti-HSF1 antibody, and micrographed. Representative images indicating HSF1 in red are shown. Scale bar: 10 µm.

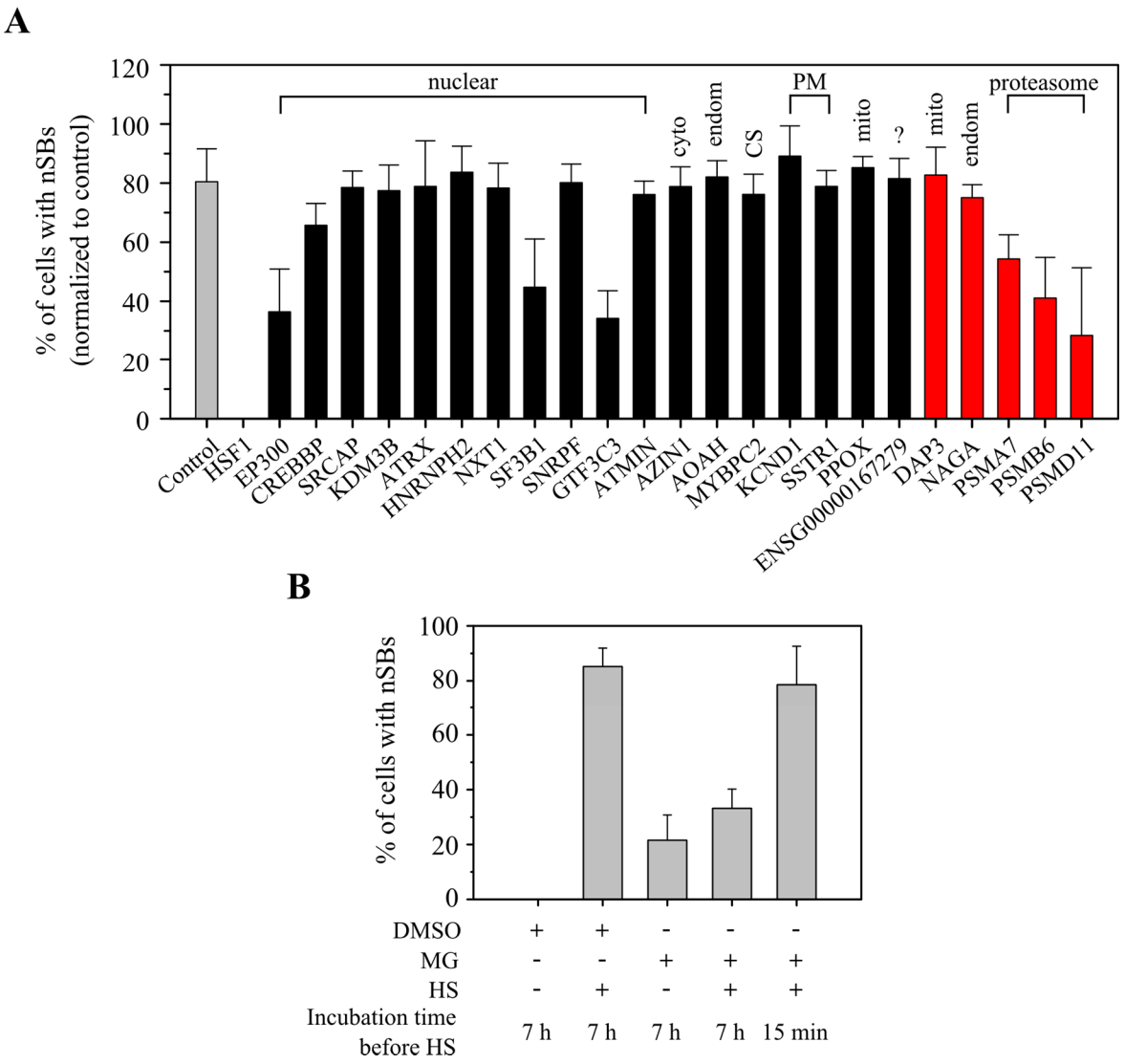

Figure 4-11: nSB formation upon HSR modulator down-regulation and proteasome impairment.
(A) Formation of nuclear stress bodies (nSB) in HSR modulator down-regulated cells upon heat stress. Quantification of nSB formation. For each down-regulation, the percentage of cells with nSB was determined and plotted. Averages and standard deviations are derived from counting of at least three different fields of view. (B) nSB formation upon MG132 treatment. HeLa cells were treated with 5 µM MG132 for the indicated time spans and heat-stressed at 43°C for 1 h. Cells were fixed, stained with rabbit anti-HSF1 antibody, and the percentage of cells with nSB was determined. Standard deviations from at least three independent experiments are shown.

PSMA7, PSMB6, and PSMD11 but not other negative HSR modulators (DAP3 and NAGA7), also reduced the accumulation of HSF1 in nSB. Instead, HSF1 was diffusely distributed in the nucleus, possibly excluded only from the nucleoli (Figure 4-10 and Figure 4-11A). Reduced nSB formation was also observed upon proteasome inhibition with MG132 for 7 hours prior to heat-shock, but not when treatment began 15 min before thermal stress (Figure 4-11B). These results suggest that changes in the nuclear environment due to long-term proteasome inhibition interfere with nSB formation. The dependence of HSF1 recruitment to nSB on

proteasome function was surprising as proteasome impairment enhanced the HSR (Figure 4-7).

In summary, these results suggest that nSB formation and HSR induction differ mechanistically and nSB may rather have a role in buffering the magnitude of the response.

4.5 Positive modulators of the HSR

4.5.1 Regulation of the HSR by multiple nuclear proteins

Most of the identified positive HSR modulators are localized in the nucleus, including five histone acetyltransferases, four histone methyltransferases/demethylases and one nucleosome assembly factor. This finding underscores the importance of chromatin landscape reorganization during HSR regulation (Figure 4-5 and Figure 4-7; Table 7-1; Petesch and Lis 2008). EP300 and the closely related CREB-binding protein (CREBBP) are transcriptional co-activators and histone acetyltransferases that couple chromatin remodeling to transcription factor recognition. The Snf2-related CREBBP activator protein (SRCAP) has acetyltransferase as well as ATP-dependent helicase activity and is known to interact with CREBBP and EP300 (Johnston *et al.* 1999). DPY30 is a subunit of a methyltransferase complex with lysine 4 methylation activity on histone H3, resulting in transcriptional activation (Takahashi *et al.* 2011). It functionally interacts with the retinoblastoma binding protein, RBBP5 (Cho *et al.* 2007). The trimethylation-specific histone demethylase KDM4A is associated with transcriptional repression and specifically demethylates lysine 9 and 36 on H3, but not lysine 4. A loss of KDM4A activity results in the down-regulation of the longevity-associated Hsp22 in *Drosophila* (Lorbeck *et al.* 2010). KDM3B has also been shown to demethylate lysine residue 9 on histone H3 (Kim *et al.* 2012).

The three modulators involved in DNA repair include ATMIN as well as the ATPases SMC3 and SMC6 (structural maintenance of chromosomes). ATMIN is a regulator of the phosphatidylinositol kinase-related cell cycle check point kinase ATM (Ataxia teleangiectasia mutated), which is activated in response to DNA double strand breaks to halt cell cycle progression and promote DNA repair. Complex formation of ATMIN and ATM is required for ATM signaling in response to chromatin remodeling and oxidative stress (Kanu and Behrens 2007, Kanu *et al.* 2010). SMC3 and SMC6 are involved in DNA repair and chromosomal organization (Carter and Sjogren 2012, Sun *et al.* 2013).

Three core components of the mRNA splicing machinery were among the identified positive HSR modulators. This finding is surprising, scince splicing is generally inhibited during thermal stress (Biamonti and Caceres 2009). Notably, a few specific pre-mRNAs undergo maturation during HS and the identified splicing proteins might participate in such specific splicing events (Ninomiya *et al.* 2011). However, down-regulation of SF3B1, SMU1, and SNRPF lowered the mRNA as well as the protein level of HSF1 (Figure 4-12), thereby explaining the reduced HSF1 reporter activity in the screen.

The identified RNA transport proteins are likely to be required for the transport of newly synthesized mRNAs from the nucleus to the cytoplasm under stress conditions. The NTF2-like export factor 1 (NXT1) is known to mediate the transport of *Hsp70* mRNA as a heterodimeric complex with NXF1 (Katahira 2009), down-regulation of which was toxic and therefore excluded from the screening analysis. The identification of NXT1 suggests that this protein may not be specific for *Hsp70* mRNA but is more generally involved in nuclear export of nascent mRNAs upon heat stress.

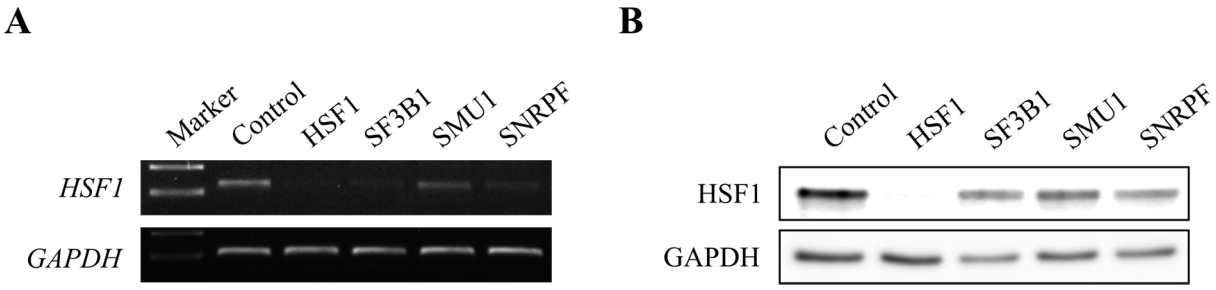

Figure 4-12: *HSF1* mRNA and protein levels in HeLa cells with down-regulation of splicing factors.
(A) HeLa cells were transfected with esiRNA targeting a set of three splicing factors identified as positive HSR modulators in the screen. Total RNA was prepared 72 h after transfection and *HSF1* and *GAPDH* mRNA levels were estimated by RT-PCR. (B) Cells were treated similarly as described in (A) and HSF1 as well as GAPDH protein levels of the whole cell extracts were determined by western blotting.

4.5.2 HSR modulators in the cytosol and organelles

The positive modulators in the cytoplasm include AZIN1, SYNC, and MYBPC2 and connect the HSR to polyamine synthesis and the cytoskeleton (Figure 4-7). AZIN1 is an inhibitor of the ornithine decarboxylase (ODC) antizyme. The latter destabilizes ODC and mediates its degradation at high polyamine levels. ODC itself catalyzes the rate-limiting step in the polyamine biosynthesis. Thus, down-regulation of AZIN1 is expected to enhance ODC degradation (Kramer *et al.* 2001). Interestingly, down-regulation of ODC antizyme caused a strong increase in the Fluc:Rluc ratio upon heat stress, but was not considered as a negative HSR modulator in the screen due to the increase in the absolute Rluc activity. Syncoilin

(SYNC) is a member of the intermediate filament family and connects the cytoskeleton to the extracellular matrix via interaction with the dystrophin-associated protein complex. Loss of SYNC activity might disrupt the intermediate filament network (Poon *et al.* 2002). The second cytoskeleton HSR modulator, the myosin binding protein MYBPC2, plays a structural role and is of particular importance in the striatal muscle (Weber *et al.* 1993).

The screen also identified several positive HSR modulators localized within subcellular compartments such as mitochondria, ER, and other endomembrane systems. The mitochondrial enzyme protoporphyrinogen oxidase (PPOX) catalyzes a critical oxidation step in the heme biosynthesis. Therefore it might contribute to cellular protection under condition of oxidative stress caused by ROS (Shinjyo and Kita 2007). Furthermore, mitochondrial oxidative stress has been shown to induce the HSR (Barrett *et al.* 2004).

4.5.3 Role of the cell membrane in stress sensing

The identification of several multi-pass membrane proteins as positive HSR modulators strongly suggests a role of the cell membrane in HSR regulation. The putative cell surface receptors PAQR5, SSTR1, and TM7SF3 function as G-protein coupled receptors (GPCRs) and may be involved in stress sensing and intercellular communication. SSTR1 is one of the five receptors for the paracrine peptide hormone somatostatin. Interestingly, ligand-independent activation of GPCRs upon membrane fluidization has been reported (Chachisvilis *et al.* 2006). This is consistent with the finding that membrane hyperfluidization stress induces the HSR (Balogh *et al.* 2005). Moreover, the potassium channel KCND1 was found among the HSR regulator proteins in the membrane. This confirms the role of membrane potassium channels in the HSR (Saad and Hahn 1992). A role of the membrane in the HSR is further supported by the identification of thrombospondin 1 (THBS1) as a positive modulator. THBS1 is an adhesive glycoprotein that mediates intercellular and cell to matrix interactions. It belongs to the family of thrombospondins (TPSs), which are known to regulate tissue genesis and remodeling.

4.6 Negative modulators of the HSR

Most of the identified negative HSR modulators are components of the UPS including six subunits of the 20S proteasome core complex, one subunit of the 19S regulatory particle, PSMD11, as well as two other UPS components, RBX1 and NPLOC4 (Figure 4-7). In

general, down-regulation of negative modulators did not increase the level of *Hsp70* mRNA observed immediately upon HS but rather delayed the return to normal mRNA levels during recovery at 37°C (Figure 4-5; Table 7-2). Proteasomes are large, multi-subunit proteases, mainly involved in protein turnover and are localized in the cytoplasm and the nucleus (Glickman and Ciechanover 2002). The role of the proteasome in the regulation of the HSR will be discussed in chapter 4.10. The ring-box protein RBX1 is an E3 ubiquitin protein ligase known to interact with cullin proteins, the largest family of E3 ubiquitin ligases. Together, these proteins play an important role in ubiquitination processes necessary for cell cycle progression (Wei and Sun 2010).

Mitochondrial proapoptotic death-associated protein 3 (DAP3) is a subunit of the mitochondrial ribosome. It is known to interact with Hsp90 and its identification as a negative HSR modulator suggests a regulatory interplay between mitochondrial and cytosolic proteostasis machineries (Hulkko *et al.* 2000). The lysosomal enzyme N-acetyl galactosaminidase (NAGA) is involved in the cleavage of glycosphingolipids and glyco-peptide conjugates. Its identification as a negative modulator may point to a link between the clearance of membrane components with attenuation of the HSR. Notably, glycosphingolipids occur only in the outer leaflet of the cell membrane where they may participate in sensing thermal stress (Dickson *et al.* 1997). The nuclear cyclin K (CCNK) plays a role in regulating the cell cycle or apoptosis (Mori *et al.* 2002). Through their activation of cyclin-dependent kinases (CDK) and the subsequent phosphorylation of the C-terminal domain (CTD) of the large subunit of RNA polymerase II, cyclins may also participate in transcriptional regulation (Baek *et al.* 2007).

4.7 Nuclear protein network regulating the HSR

To analyze the interactions of the HSR modulators and their interconnections, the BioGRID interaction database was used (Stark *et al.* 2011). 59 of the 64 identified modulators have valid UniProt accession numbers and were included in the analysis, in which only experimentally determined physical interactions were considered. The analysis revealed a network including 30 positive and 13 negative HSR modulators that interact with each other either directly or via other proteins (Figure 4-13; Table 7-3). 31 of these modulators are either localized exclusively in the nucleus (24 proteins) or shuttle between the nucleus and cytoplasm (7 proteins). The number of proteins connected in this network (449) is

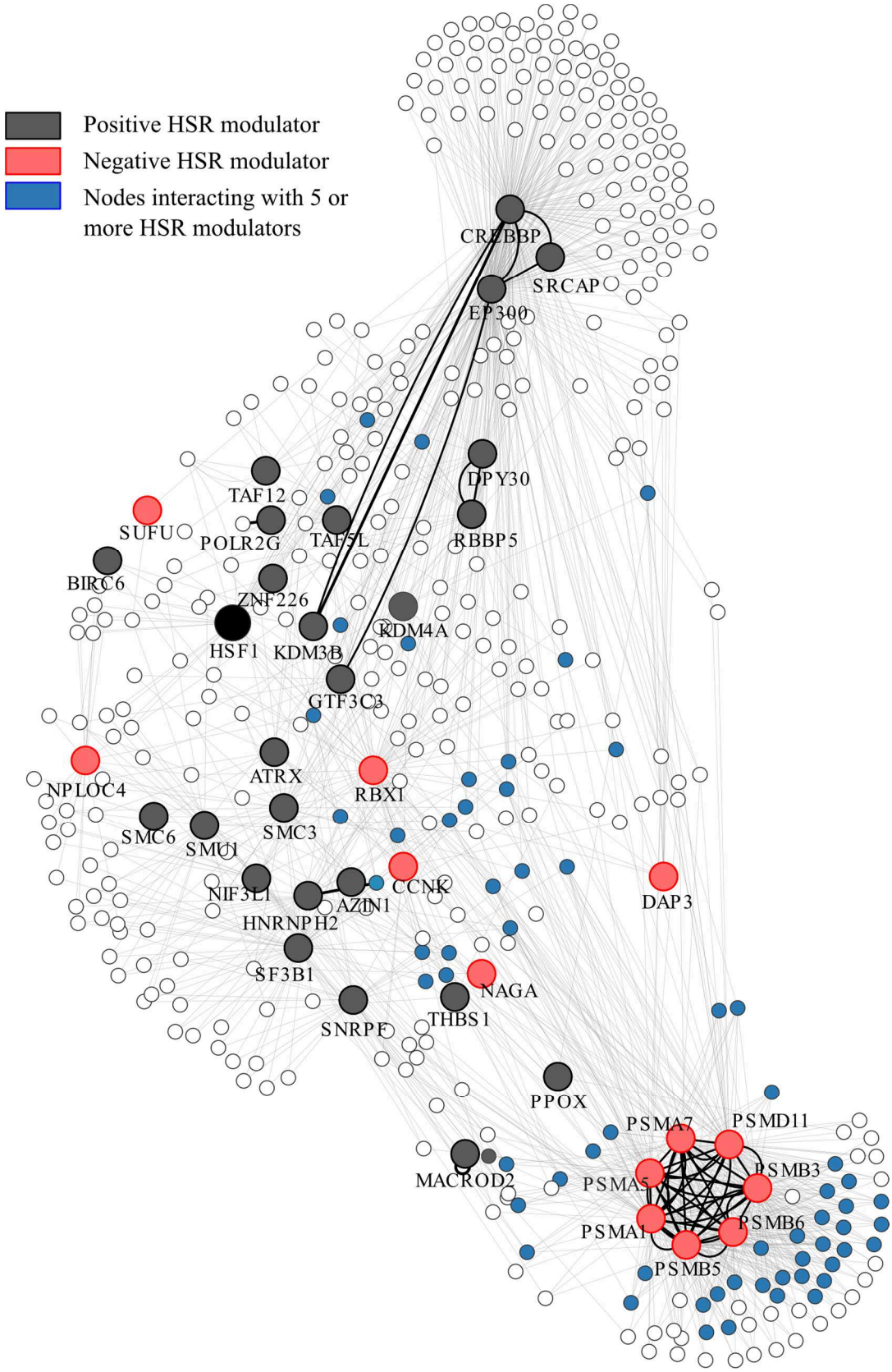

Figure 4-13: Network of HSR modulators.
Largest connected component analysis of physical interactions between the HSR modulators based on interactions retrieved from the BioGRID database. Ubiquitin (UBC, P0CG48) with all its interactions was deleted from the network for clarity. Bold black lines indicate direct interactions between the HSR modulators identified in the screen. See also Table 7-3.

significantly greater than observed on average with randomly chosen proteins (80; $p < 2.2 \times 10^{-16}$, statistics were calculated with the help of Dr. S. Pinkert).

A central element of the HSR modulator network is formed by chromatin modifying factors. For example, the EP300/CREBBP histone acetyltransferase complex is found to interact directly with SRCAP (Snf2-related CREBBP activator protein) and via 15 different proteins with HSF1 (Figure 4-13; Table 7-3), most of which function as transcriptional co-activators and histone deacetylases. Moreover, HSF1 interacts to two further histone acetyltransferases, TAF12 and TAF5L, via TAF9 and TBP. Since TAF12 and TAF5L are subunits of the PCAF histone acetylase complex, this further supports the notion that HSF1 cooperates closely with chromatin modifiers. The DPY30-RBBP5 complex (see chapter 4.5.1) interacts via other proteins with EP300/CREBBP as well as with the E3 ubiquitin protein ligase RBX1, a negative HSR modulator. Via several other proteins, RBX1 is connected to EP300/CREBBP and the proteasome network (Figure 4-13; Table 7-3), suggesting a possible functional link between chromatin modification and protein degradation upon heat stress. Interestingly, RBX1 is also connected to HSF1 via BTRC, HSPA1A, HSPA8, and PLK1. The SUMO proteins SUMO1 and SUMO2 connect HSF1 with the splicing factor SF3B1, a positive HSR modulator found in the screen. SF3B1 is connected via 13 proteins with SNRPF, another splicing protein and positive HSR modulator. Moreover, SF3B1 indirectly interacts with the chromatin modifying factors EP300/CREBBP and ATRX as well as with different proteasome subunits (Table 7-3). The positive HSR modulator ATRX is connected to HSF1 via SUMO2 and DAXX.

Interestingly, 63 proteins of the HSR network (marked in blue in Figure 4-13; Table 7-3) interact directly with at least five of the identified HSR modulators, but were not found in the screen. Their functional analysis confirms that survival during stress relies on a complex interplay of cellular key processes, including chromatin modification, splicing, apoptosis, cell communication, and the UPS. Most of the processes in which the HSR modulators and their interactors participate are nuclear and either linked with EP300/CREBBP or the UPS (Figure 4-13), suggesting important roles of these complexes in HSR regulation.

4.8 Specific role of EP300 in HSF1 regulation

One central hub of the HSR modulator interaction network is formed by the chromatin modifying histone acetylase complex EP300/CREBBP (Figure 4-13). Interestingly,

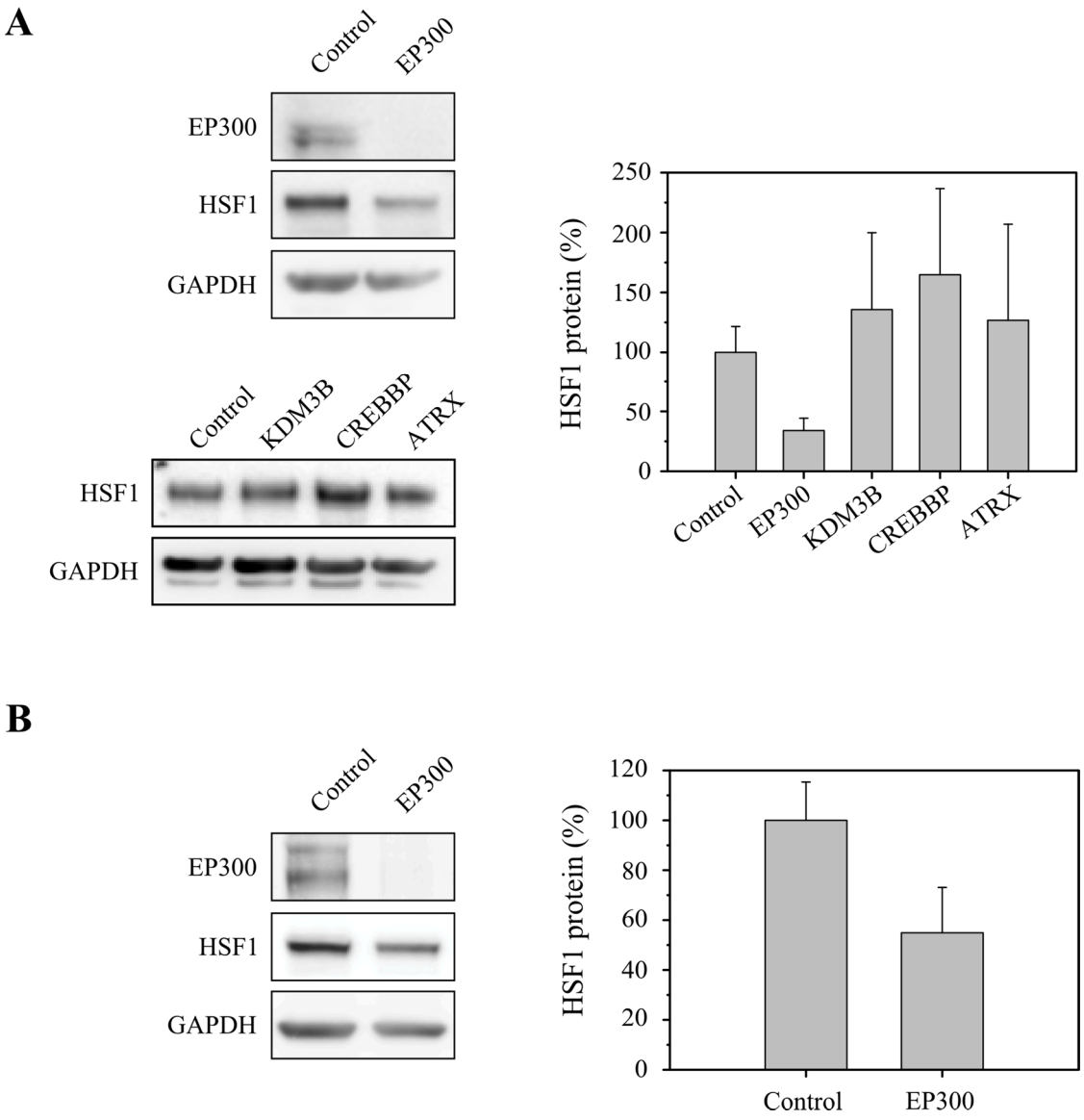

Figure 4-14: Chromatin modifiers and their influence on the steady state level of HSF1.
(A) HSF1 protein level in HeLa cells upon down-regulation of chromatin modifiers. Left: HeLa cells were transfected with control esiRNA targeting EGFP or esiRNAs targeting different chromatin modifiers. After 48 h, whole cell extracts were prepared and endogenous HSF1 and GAPDH levels were detected by western blotting. Efficiency of EP300 down-regulation was also determined by western blotting. Right: Quantification of HSF1 level. HSF1 protein levels were estimated by densitometry using AIDA, normalized to the corresponding GAPDH levels, and plotted. Standard deviations are derived from at least three independent experiments. (B) HSF1 protein level in EP300 down-regulated HEK293T cells. Left: HEK293T cells were transfected with control esiRNA targeting EGFP or esiRNA targeting EP300. After 48 h, whole cell extracts were prepared and endogenous EP300, HSF1, and GAPDH levels were detected by western blotting. Right: Quantification of HSF1 level. HSF1 protein levels were estimated by densitometry using AIDA, normalized to corresponding GAPDH levels, and plotted. Standard deviations from at least three independent experiments are shown.

overexpression of EP300 has been reported to result in the acetylation of nine lysine residues of exogenously expressed HSF1. Subsequent deacetylation of HSF1 by SIRT1 has been

shown to prolong the dwell time of HSF1 on heat shock elements, thereby decelerating the attenuation of the HSR (Westerheide *et al.* 2009, Raynes *et al.* 2013).

Accordingly, down-regulation of EP300 would be expected to increase the magnitude of the HSR by reducing HSF1 acetylation and thus delaying attenuation. However, EP300 and several other histone acetyltransferases were surprisingly identified as positive HSR modulators in the screen. This suggests a more complex role of these factors in HSR regulation.

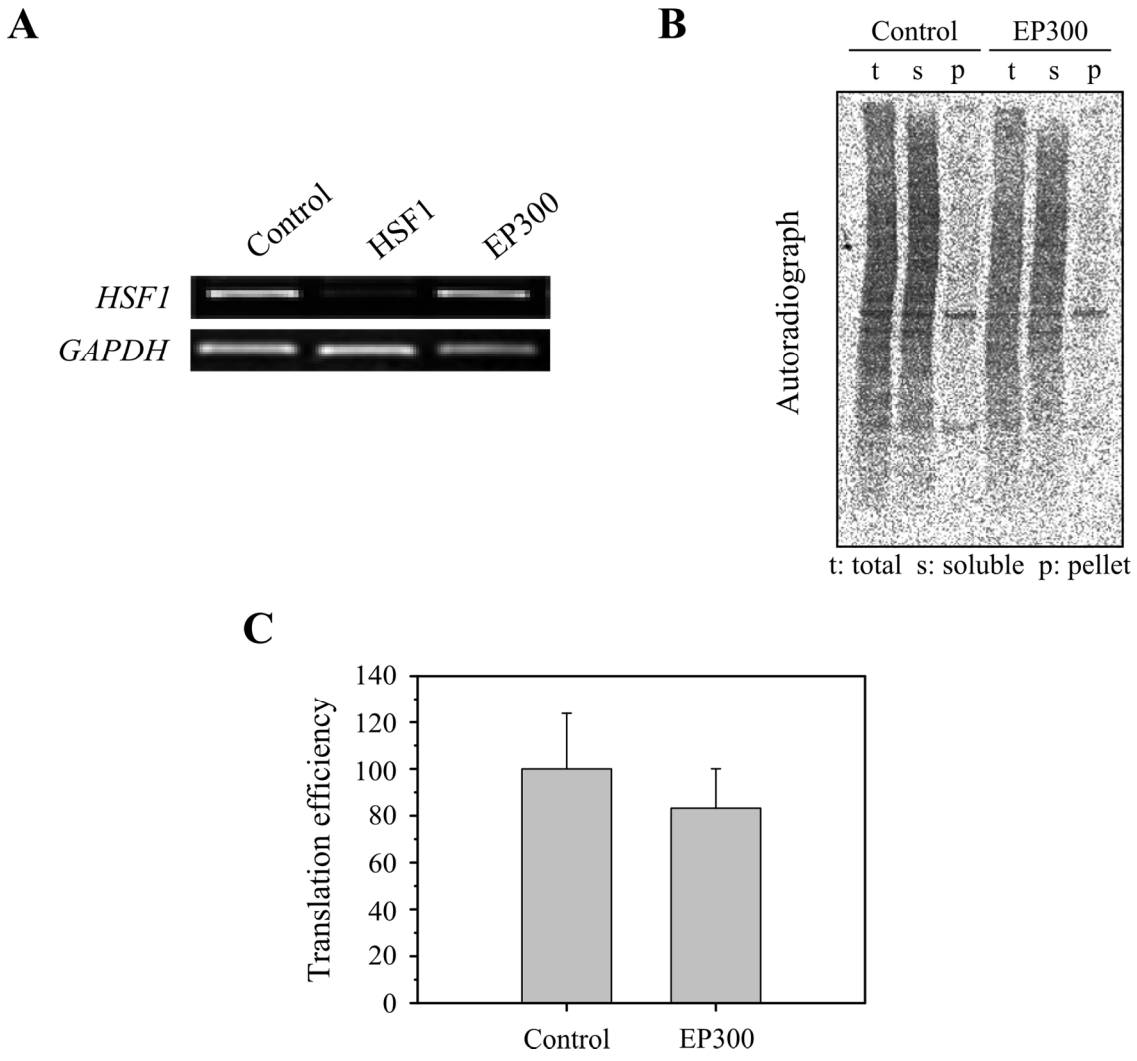

Figure 4-15: Effects of EP300 down-regulation on HSF1 transcription and overall translation.
(A) *HSF1* mRNA level after EP300 down-regulation. HeLa cells were transfected with esiRNA targeting EGFP, HSF1, or EP300 and total RNA was prepared 48 h later. *HSF1* and *GAPDH* mRNA levels were determined by RT-PCR. (B) Overall translation efficiency in EP300 down-regulated cells. HeLa cells were transfected with esiRNA targeting EGFP or EP300 and nascent peptides were labeled with ^{35}S-Met after 48 h. Cells were divided and whole cell extract (total), RIPA soluble (soluble), and RIPA insoluble (pellet) fractions were prepared. Equal amounts of cell extract from control and EP300 down-regulated cells were separated by SDS-PAGE and radiographed. (C) Quantification of overall translation efficiency in whole cell extracts from (B) using AIDA. Standard deviations from at least three independent experiments are shown.

To explore the effect of EP300 on HSF1, first, the down-regulation efficiency of EP300 was checked. Western blot experiments confrimed a reduction of the EP300 level by ~ 95% (Figure 4-14A). Strikingly, the HSF1 steady-state level was reduced in the same cells by almost 70% (Figure 4-14A). The effect on the level of HSF1 was specific for EP300 as it was not observed upon down-regulation of several other positive HSR modulators, including the closely related histone acetylase CREBBP, the histone demethylase KDM3B, or the nucleosome assembly factor ATRX (Figure 4-14A). Down-regulation of EP300 in HEK293T confirmed the results for HeLa cells. The levels of EP300 and HSF1 were reduced by 95% and 40%, respectively (Figure 4-14B).

Since EP300 is a chromatin modifying histone acetyltransferase, the observed effect could be due to a reduced *HSF1* transcript level. However, no change in the *HSF1* mRNA level was detected in RT-PCR experiments (Figure 4-15A). Overall translation efficiency was

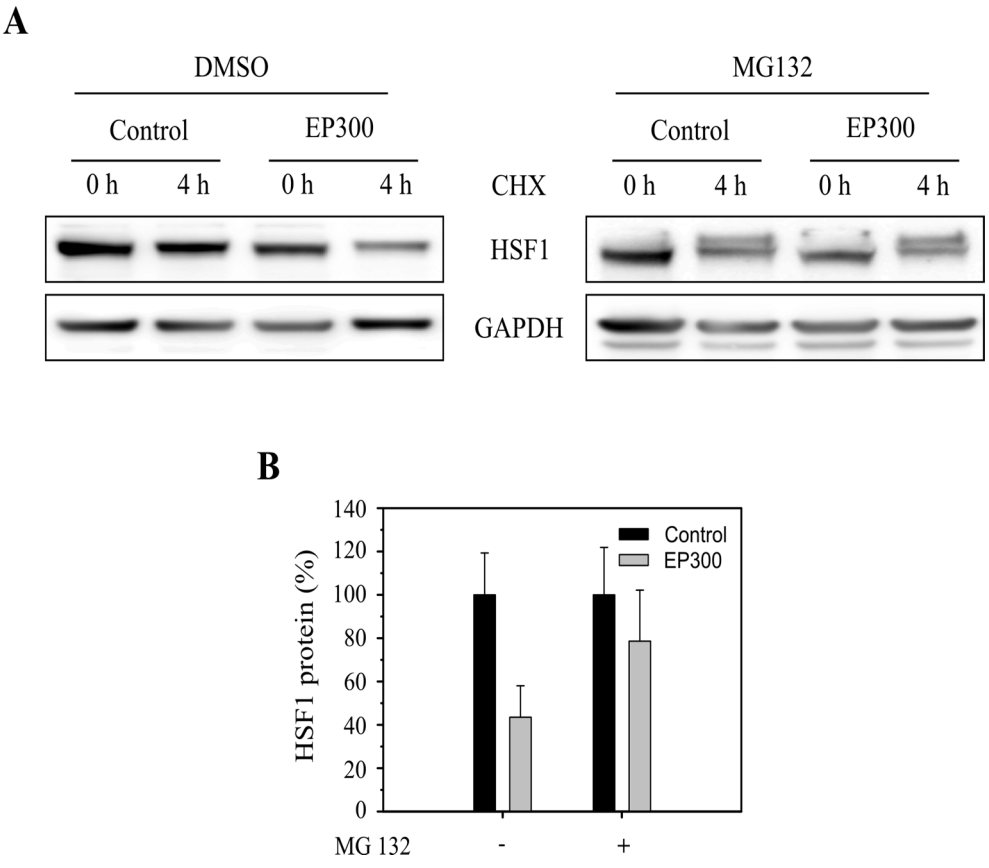

Figure 4-16: Effects of EP300 down-regulation on HSF1 degradation.
(A) Down-regulation of EP300 results in degradation of HSF1 in HEK293T cells. HEK293T cells were transfected with control esiRNA targeting EGFP or esiRNA targeting EP300. After 48 h, cells were treated with 5 mM CHX for 4h with or without MG132 (5 µM) and whole cell lysates were prepared. After separation by SDS-PAGE, HSF1, and GAPDH protein levels were detected by western blotting. (B) Quantification of HSF1 level. HSF1 protein levels were estimated by densitometry using AIDA, normalized to the corresponding GAPDH levels, and plotted. Standard deviations from at least three independent experiments are shown.

also not effected by down-regulation of EP300 as shown by labeling nascent peptides with ^{35}S-methionine in a pulse chase experiment (Figures 15B and C). These findings suggest an either direct or indirect role of EP300 in the regulation of HSF1 protein turnover. Indeed, a cycloheximide (CHX) chase experiment revealed rapid degradation of endogenous HSF1 in HEK293T cells upon EP300 down-regulation (Figure 4-16A and B). Proteasome inhibition by

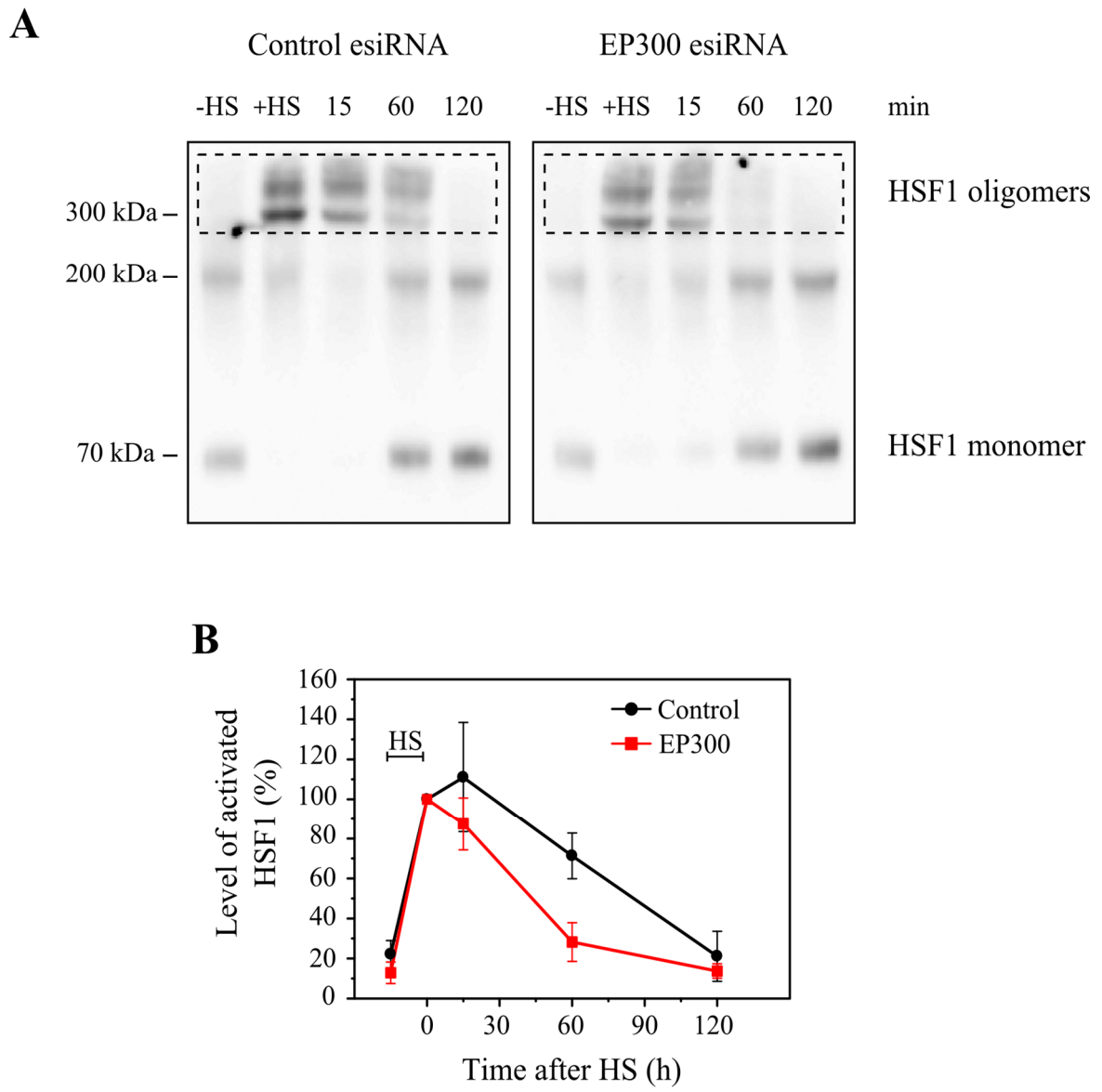

Figure 4-17: Implication of EP300 down-regulation on stress-activated HSF1.
(A) High molecular weight oligomer of HSF1 formed during HS is destabilized upon EP300 down-regulation. HeLa cells were transfected with control esiRNA targeting EGFP (left) or esiRNA targeting EP300 (right). After 48 h, cells were heat-stressed at 43°C for 2 h followed by recovery at 37°C for the times indicated. RIPA soluble fractions were prepared and 100 µg of cell extract in cross-linking buffer was treated with 1 mM EGS for 30 min at room temperature. Cross-linking was stopped by addition of 3 mM glycine. Cross-linked samples were separated by SDS-PAGE and blotted with anti-HSF1 antibody. (B) Quantification of cross-linked HSF1 oligomers at ~ 300 kDa (dashed rectangle) (Sarge *et al.* 1993) using AIDA. Amounts present immediately after HS were set to 100%. Standard deviations represent are derived from at least 3 three independent experiments

MG132 stabilized HSF1, indicating a role of the proteasome in HSF1 turnover. The HSF1 double band after 4 h MG132 treatment is due to stress-induced hyper-phosphorylation of HSF1and will be further discussed in chapter 4.10.

Down-regulation of EP300 may affect the stability of HSF1 in many ways. However, it is most likely that the stability is affected either directly due to loss of HSF1 acetylation or indirectly due to a reduced accessibility of chromatin for HSF1 binding caused by a decreased histone acetylation in the absence of EP300. Trimerization of HSF1 upon HS is a prerequisite for chromatin binding and HSF1 transcriptional activity (Anckar and Sistonen 2011). Formation of HSF1 oligomers can be visualized by SDS-PAGE after chemical cross-linking with EGS (Sarge *et al.* 1993). Treatment of HeLa cell extract with 1 mM EGS resulted in HSF1 bands at ~ 70 kDa and ~ 200 kDa, representing the monomer and possibly a dimer (Figure 4-17A). In cells treated with control esiRNA, HSF1 complexes migrating at ~ 300 kDa, consistent with trimers or tetramers, accumulated upon HS and then decayed during recovery over a period of 1-2 h (Figure 4-17A left panel and B). The HS-induced oligomer formation was also observed upon EP300 down-regulation but showed a substantially faster decay during recovery from HS, indicating a destabilization of the active form of HSF1 upon EP300 down-regulation (Figure 4-17A right panel and Figure 4-16B). Taken together, these results suggest that EP300 might be an important regulator of the *in vivo* stability of HSF1, both of the steady state and the transcriptionally active state.

4.9 Reorganization of the nuclear proteome during heat stress

Several nuclear proteins and the proteasome complex were identified as potent modulators of the HSR in the screen. Since these proteins regulate the HSR via chromatin remodeling, RNA metabolism and splicing, mRNA transport, transcription as well as protein degradation, a re-arrangement of the nuclear proteome during heat stress seems likely. Hence, quantitative proteomics experiments with SILAC (stable isotope labeling by amino acids in cell culture; Ong and Mann 2006) were performed to analyze the changes in the nuclear proteome immediately after HS as well as after recovery and to better understand the link between UPS and the nuclear HSR network.

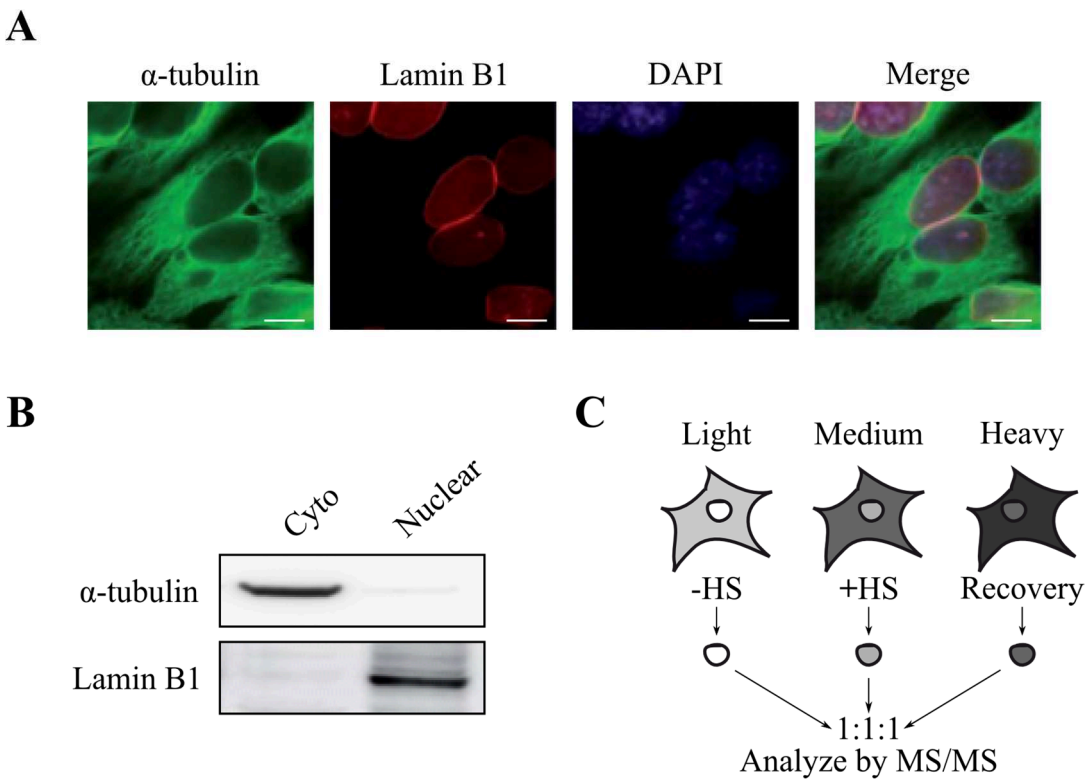

Figure 4-18: Separation of cytoplasmic and nuclear protein fraction, SILAC scheme.
(A) HeLa cells were grown on coverslips, fixed, and stained with anti-α-tubulin (green, cytoplasmic marker) and anti-lamin B1 (red, nuclear marker) antibodies. DNA was stained with DAPI (blue). Representative images are shown. Scale bar: 10 µm. (B) Cytoplasmic and nuclear extract HeLa cell extracts were prepared and equal amounts (50 µg) were separated by SDS-PAGE. Western blotting was performed using antibodies recognizing α-tubulin and lamin B1. (C) Experimental scheme of SILAC experiments performed to identify the reorganization of the nuclear proteome during thermal stress (+HS, 43°C for 2 h) and recovery (Recovery, 43°C for 2 h followed by 2 h at 37°C) compared to control cells (-HS, 37°C). HeLa cells were cultured in light (Arg0, Lys0), medium (Arg6, Lys4) as well as heavy (Arg10, Lys8) medium and treated as indicated in the figure. Equal numbers of cells were mixed, nuclear extract was prepared, and analyzed by LC-MS/MS.

Nuclear and cytoplasmic protein extracts of HeLa cells were prepared and checked for their purity (Figure 4-18A and B). While microscopy experiments confirmed the expected localization of the cytoplasmic marker protein α-tubulin and the nuclear marker lamin B1 (Figure 4-18A), proper separation of the cytoplasmic and the nuclear fraction was proven by western blot analysis (Figure 4-18). For SILAC experiments, cells were labeled with three different pairs of arginine and lysine amino acid isotopes and grown at 37°C, heat-stressed for 2 h at 43°C, or heat-stressed for 2 h followed by a 2 h recovery period at 37°C (Figure 4-18C).

Approximately 4000 proteins could be quantified in the nuclear extracts, including 36 proteins identified as HSR modulators (Figure 4-7) and 212 additional proteins identified as components of the nuclear HSR network (Figure 4-13; Table 7-3). Immediately after thermal stress, a highly specific set of 32 proteins was significantly enriched in the nucleus (Figure

4-19; Table 7-4). These proteins include several HSR modulators such as HSF1, PSMA1, PSMB3, PSMB5, and PSMB6 as well as multiple chaperone or co-chaperone proteins and most of the remaining 20S proteasome subunits (chapter 4.7; Figure 4-19 and Figure 4-20C). Among the enriched chaperone components, two stress-inducible Hsp70s (HSPA1A, HSPA6; Pelham 1984) and the constitutively expressed Hsc70 (HSPA8) were found. Numerous Hsp70 co-chaperones (BAG5, DNAJA1, DNAJA4, DNAJB1, DNAJB4, DNAJC7, ST13, STIP1) were enriched as well (Figure 4-19; Table 7-4). Furthermore, ten subunits of the 20S proteasome core complex were significantly enriched in the nucleus after heat stress. Components of the 19S regulatory particle were also enriched, albeit to a lesser extent (Figure 4-19 and Figure 4-20A). A protein interaction analysis of the enriched proteins revealed a network, which connects the Hsp70 and Hsp90 chaperone systems with the proteasome (Figure 4-20B). This suggests a cooperation of these systems in the removal of heat-denatured proteins. The presence of RPS27A among the enriched proteins is of particular interest, because this protein is expressed as a fusion of ubiquitin at the N-terminus and ribosomal protein S27A at the C-terminus. This finding further emphasizes the importance of protein degradation in the nucleus after thermal stress.

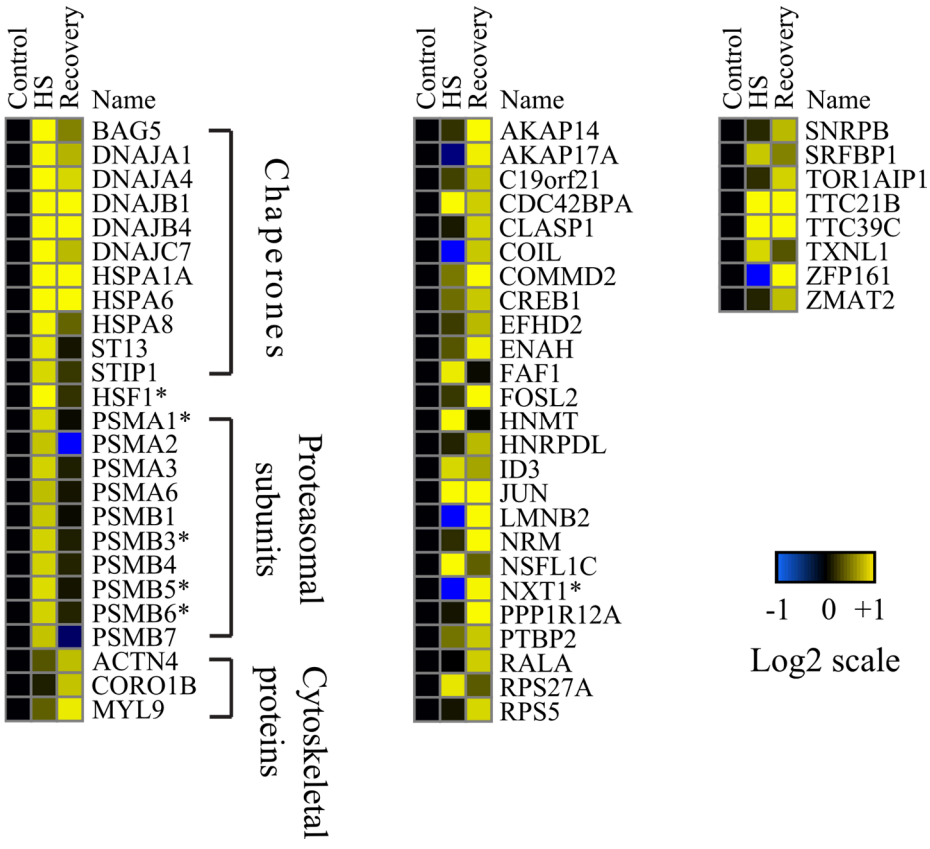

Figure 4-19: Nuclear proteome during HS and after recovery.
Heatmap showing the relative enrichment of proteins in the nucleus during HS and after recovery. Color scheme indicates fold enrichment. The asterisk marks HSR modulators identified in the screen.

As discussed above, the nuclear proteome was substantially enriched with proteins of the quality control machinery immediately after heat stress. However, this effect was partially reversed after two hours of recovery. 34 proteins showed a significant enrichment in the nucleus after recovery, but HSF1 and the subunits of the 20S core particle were no longer enriched (Figure 4-19; Table 7-5). In contrast, several chaperones and co-chaperones (HSPA1A, HSPA6, DNAJA4, DNAJB1, DNAJB4, and DNAJC7) remained enriched in the nucleus during the recovery period. In addition, a variety of factors involved in nuclear architecture (LMNB2), transcription (FOSL2, JUN), RNA transport (NXT1), and RNA splicing (SNRPB) were enriched in the nucleus during recovery. Notably, several enriched proteins contain disordered regions longer than 30 residues as predicted by DISOPRED (e.g. ACTN4, C19orf21, COIL, CORO1B, CREB1, EFHD2, ENAH, FOSL2, JUN, LMNB2, RALA, SNRPB, TOR1AIP1). Three regulatory components of the actin/myosin cytoskeletal machinery were found to be enriched during recovery: the actin binding proteins actinin 4 (ACTN4) and coronin 1B (CORO1B) as well as myosin regulatory light chain 9 (MYL9). This supports the notion that the actin/myosin machinery adopts nuclear roles in transcription and nuclear architecture and may thus be important for the reorganization of the nuclear morphology after stress (Bettinger *et al.* 2004). However, one cannot completely exclude the possibility that the identification of these three components in nuclear extracts is due to contamination, since the actin cytoskeleton is affected during heat-shock.

A large number of proteins (237) were found to be depleted from the nucleus after heat stress and the number increased to 358 upon two hours of recovery (Table 7-6 and Table 7-7). GO analysis by Ontologizer revealed that during heat stress mostly pre-ribosome proteins, ribonucleoprotein biogenesis factors, DNA damage-responsive proteins, and proteins involved in tRNA transcription were depleted. During recovery, tRNA transcription factors as well as proteins involved in nucleic acid metabolism made up a high percentage of the proteins depleted from the nucleus. We also found several HSR modulators (Figure 4-13) to be depleted in the nuclear proteome during and after stress. Thus, BIRC6 (protein degradation), the mitochondrial protein DAP3, GTF3C3 (tRNA transcription), HNRNPH2 (RNA metabolism), and KDM3B (histone methyltransferase) were depleted after two hours of thermal stress as well as after the recovery period (Figure 4-20C). These factors could possibly participate in the early phase of HSR induction but are no longer required during sustained stress and recovery and their removal from the nucleus might play a role in HSR attenuation. Whereas ATRX (nucleosome assembly) was merely depleted after heat stress, SMC6 (DNA repair) was only depleted during recovery (Figure 4-20C).

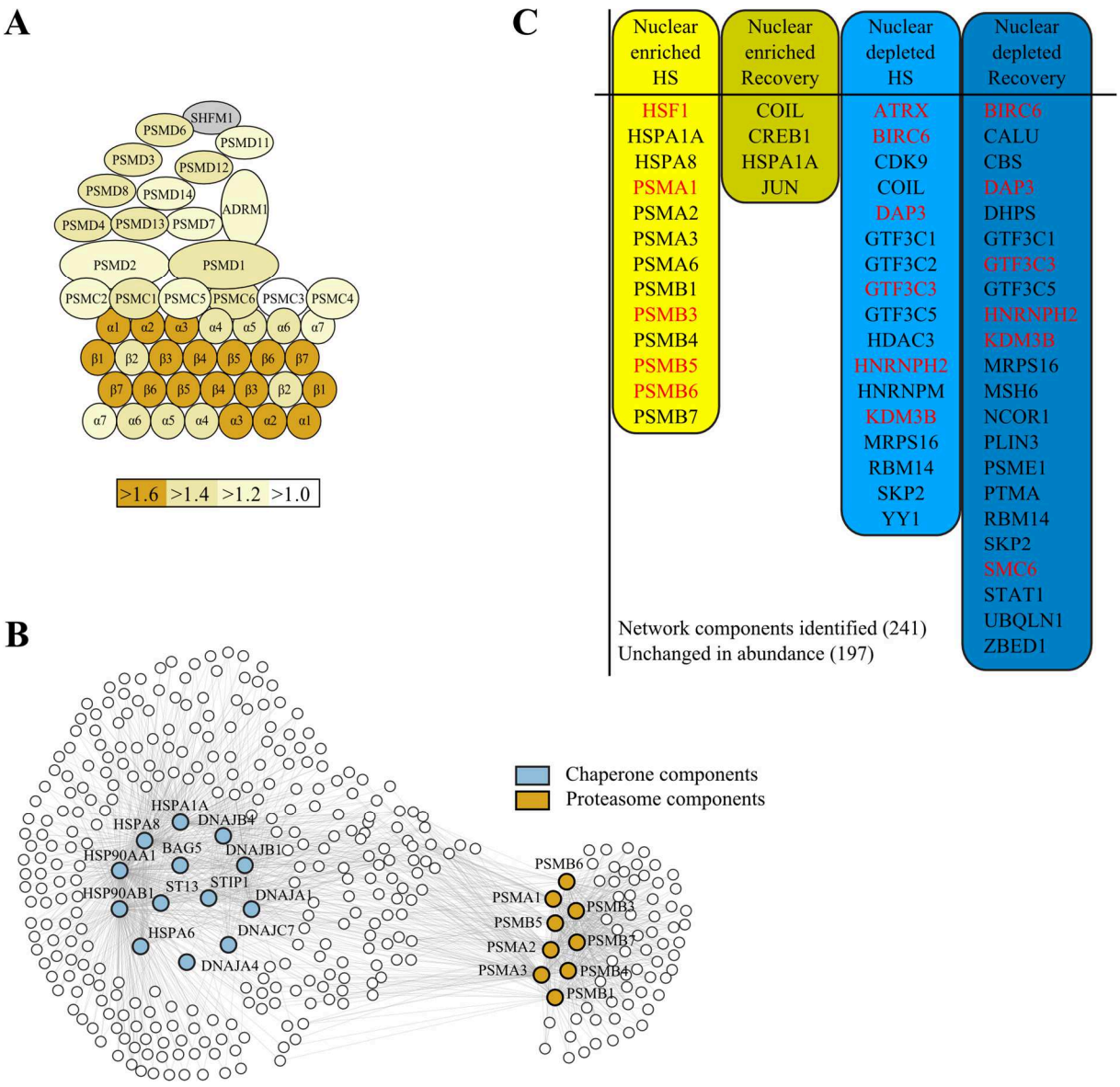

Figure 4-20: Proteasomal enrichment in the nucleus during heat stress and network analysis of nuclear proteome.
(A) Schematic representation of the proteasome illustrating the relative enrichment of individual subunits in the nucleus during HS as identified in the SILAC experiment. Color scheme indicates fold enrichment of the proteasomal subunits in the nucleus; grey: subunit not identified. (B) Interaction network of the nuclear enriched chaperones (blue) and proteasome components (dark yellow) during thermal stress. The network is created and analyzed as in Figure 4-13. One of the central nodes of the chaperone network, Hsp90 (HSP90AA1 and HSP90AB1), is also shown. (C) Changes in the abundance of components of the nuclear HSR regulatory network (Figure 4-13) during and after thermal stress. 44 out of 241 HSR network components identified in the nuclear extracts by proteomics changed in abundance during HS or recovery, or both. A protein was considered depleted when its abundance was reduced < 0.63-fold and enriched, when its abundance increased more than 1.6-fold compared to the nuclear fraction of control cells. Proteins shown in red font are HSR modulators identified in the esiRNA screen.

To confirm the SILAC results regarding the nuclear enrichment of the proteasome, biochemical validation experiments were performed. Western blot experiments with HeLa cells cultivated at 37°C showed that the proteasomal core complex subunits PSMA5, PSMA6,

and PSMB6 were mainly cytosolic, albeit a significant fraction was also present in the nucleus. Thermal stress resulted in a nuclear enrichment of these subunits (Figure 4-21A), which was reversed during recovery. To prove that the enrichment is of functional importance, proteasomal activity was determined for the cytoplasmic and the nuclear protein fractions as well as for the RIPA soluble lysate. These experiments revealed a significant increase in the proteasomal activity of the nuclear fraction directly after HS (Figure 4-21B).

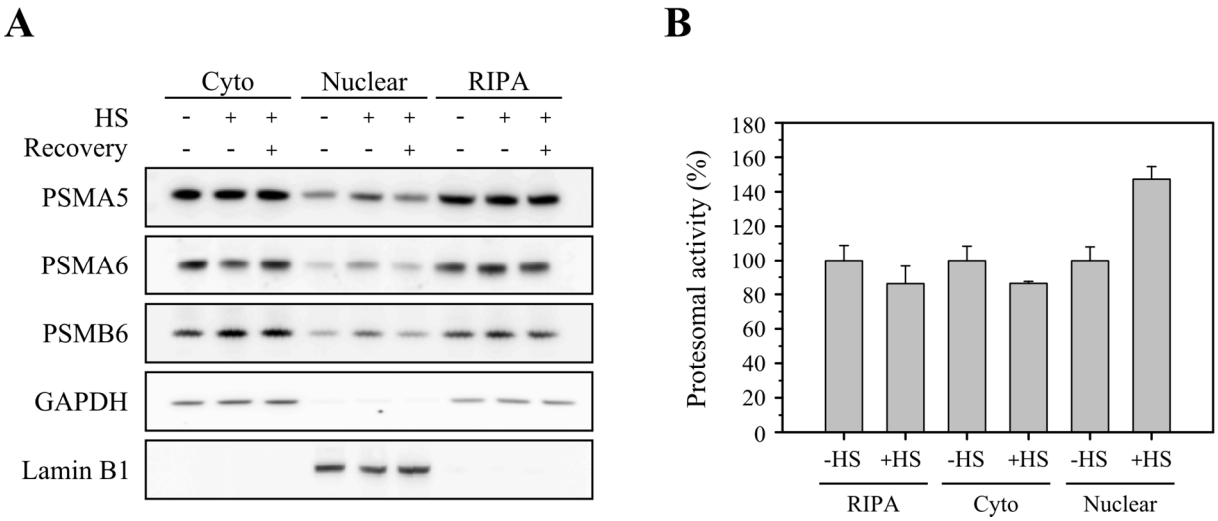

Figure 4-21: Biochemical and functional validation of proteasomal enrichment in the nucleus after thermal stress.
(A) Western blot experiments analyzing the localization of proteasomal subunits in control cells, heat-stressed cells and cells exposed to heat shock and subsequent recovery. HeLa cells were grown at 37°C and then treated as indicated (HS: 43°C for 2 h; Recovery: 43°C for 2 h followed by 2 h at 37°C). RIPA soluble, cytoplasmic and nuclear extracts were prepared. Equal protein amounts (50 µg) were separated by SDS-PAGE and PSMA5, PSMA6, PSMB6, GAPDH (cytoplasmic marker), and lamin B1 (nuclear marker) levels were determined by western blotting. (B) Proteolytic activity after HS. HeLa cells were heat-stressed for 2 h at 43°C (+HS) or kept at 37°C throughout the experiment (-HS). RIPA soluble, cytoplasmic, and nuclear extracts were prepared and equal protein amounts (20 µg) were assayed for their chymotrypsin-like proteolytic activity. Standard deviations of at least three independent experiments are shown.

Taken together, the results of the quantitative proteomics experiments and the biochemical validation indicate an extensive reorganization of the nuclear proteome upon heat stress and during recovery. Amongst other proteins, several HSR modulators are affected by this reorganization, with the proteasome being a particularly important example.

4.10 Role of the proteasome in attenuation of the HSR

Several proteasomal subunits were identified as negative modulators of the HSR in the screening experiments. Their individual down-regulation was found to strongly amplify the HSR when Fluc:RLuc activity ratios were measured four hours after thermal stress (Figure 4-22A). Moreover, the HSR was induced in iFluc-Rluc cells upon treatment with the proteasome inhibitor MG132 (Figure 4-2 and Figure 4-22A). The magnitude of this response was amplified approximately six-fold when the MG132 treated cells were additionally thermally stressed (Figure 4-22B).

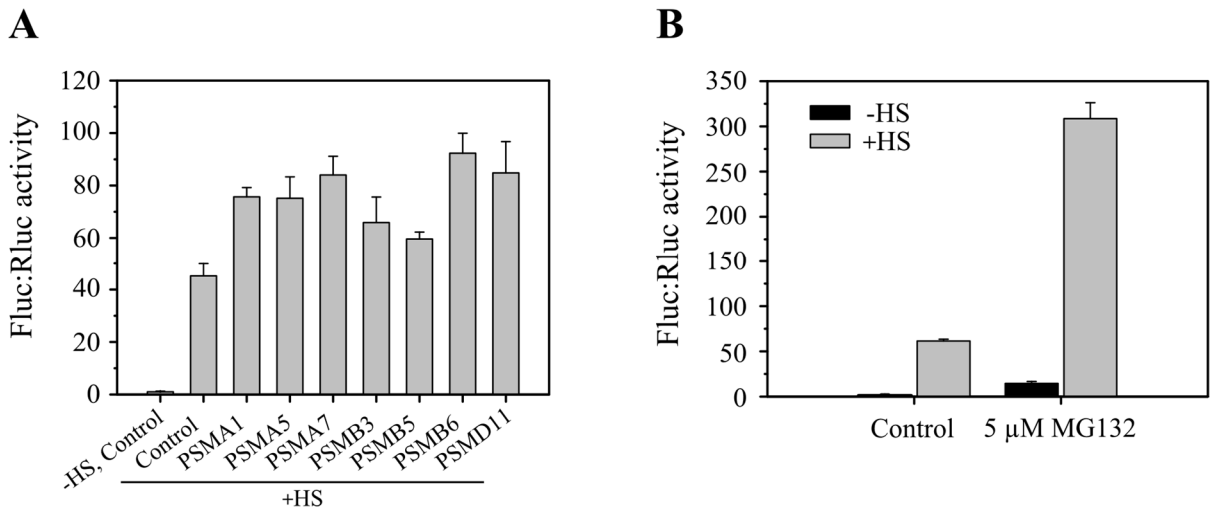

Figure 4-22: Proteasomal impairment in combination with thermal stress.
(A) Normalized Fluc:Rluc activity ratios from the second validation screen upon proteasomal subunit down-regulation. Standard deviations are derived from at least three independent experiments. (B) Induction of the HSR after thermal stress in combination with proteasome inhibition. iFluc-Rluc cells were treated with 0.1% DMSO (control) or 5 µM MG132. One hour after MG132 addition, cells were heat-stressed for 2 h at 43°C followed by a recovery of 2 h (+HS) or kept at 37°C throughout the experiment (-HS). Fluc and Rluc activities were measured and normalized Fluc:Rluc activity ratios were plotted. Standard deviations from at least three independent experiments are shown.

Down-regulation of proteasomal subunits has been previously reported to decrease protein degradation (Wang *et al.* 2009). Accordingly, down-regulation of PSMA7 was accompanied by a functionally relevant partial inhibition of proteasome activity, as judged by the accumulation of ubiquitin-GFP (GFPu), a reporter protein that is normally rapidly degraded by the proteasome (Bence *et al.* 2001). Total proteasome inhibition with MG132 resulted in an even stronger accumulation (Figure 4-23A and B). According to the results from the proteomics experiments described in chapter 4.9, the accumulation of proteasome complexes in the nucleus occurred transiently during HS and coincided with the accumulation

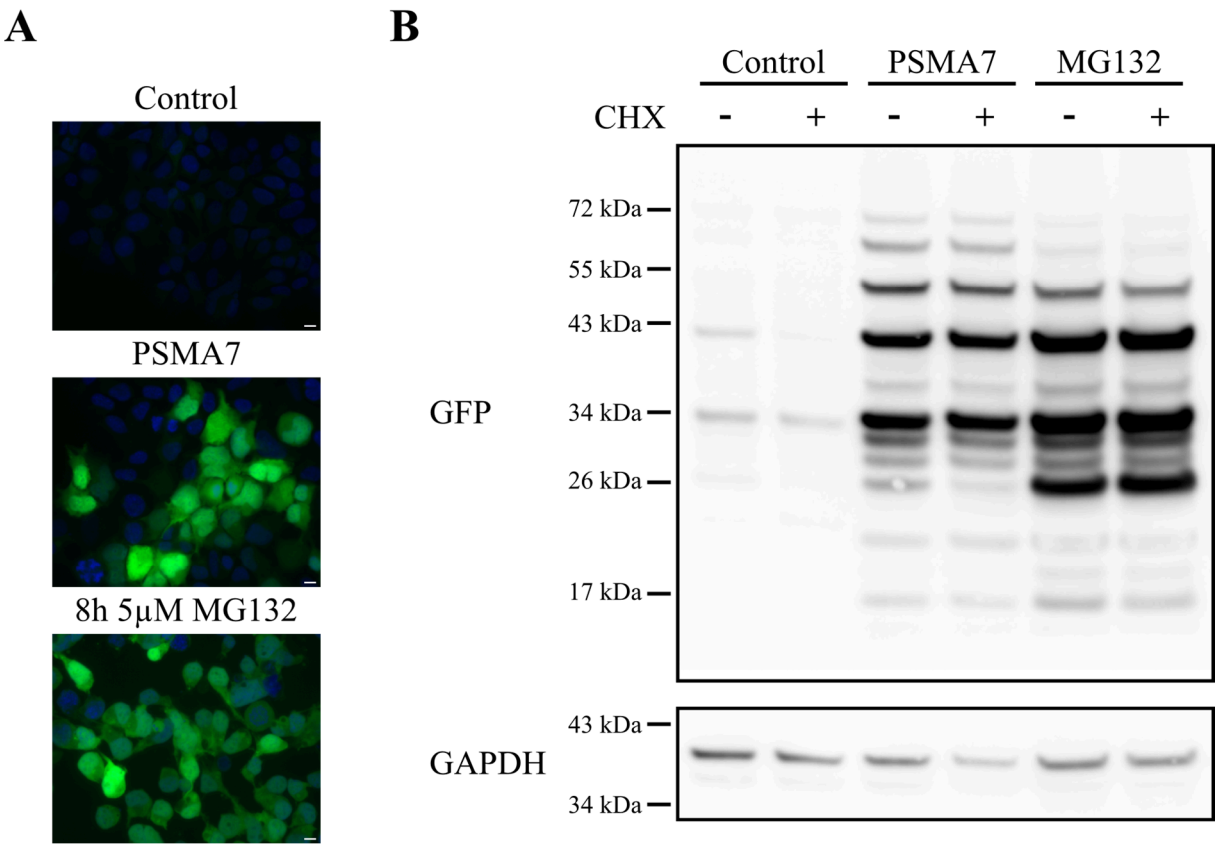

Figure 4-23: Protein degradation upon proteasomal impairment.
(A) Representative microscopy images of HEK293T cells stably expressing highly proteasome-dependent destabilized GFPu (GFP destabilized by the CL-1 degron). Cells were grown on coverslips and either transfected with control esiRNA targeting Rluc or PSMA7 esiRNA or were treated with 5 µM MG132 for 8 h. Green fluorescence indicates GFPu distribution. Scale bar: 10 µm. (B) Western blot showing CHX chase of GFPu. Cells were treated similarly as described in (A) and 5mM CHX was added to the cells as indicated in the figure. 60 min after CHX addition whole protein extract was prepared, separated by SDS-PAGE, and analyzed via western blotting.

of HSF1 (Figure 4-19). There are two possible explanations for the enhancement of the HSR upon proteasome inhibition. In a rather indirect mechanism, proteasomal impairment results in the accumulation of heat-denatured proteins, thereby increasing the strength of HSF1 activation and/or proteasome inhibition delays the deactivation of HSF1. The attenuation of the HSR was measured by time course experiments, in which *Hsp70* mRNA levels were determined by RT-PCR. Down-regulation of PSMA7 did not increase the peak level of *Hsp70* mRNA during HS, but rather delayed the return to normal Hsp70 mRNA levels by about four hours (Figure 4-24A and B). This suggests a role of the proteasome during the attenuation phase of the HSR. According to the current model of HSF1 regulation, proteasome inhibition in combination with thermal stress increases misfolding of proteins and induces dissociation of HSF1 from Hsp90 (Shi *et al.* 1998, Morimoto 2008). The load of misfolded proteins

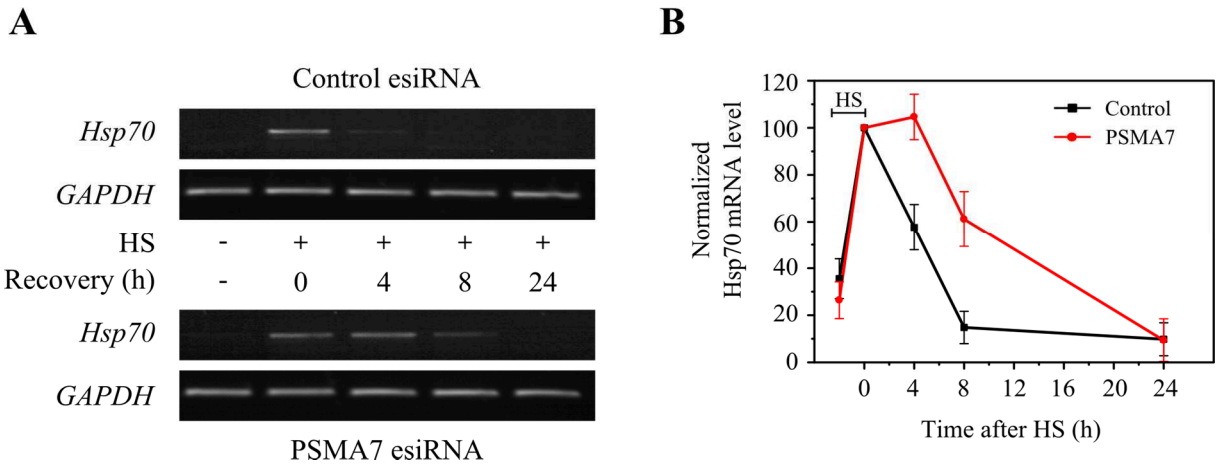

Figure 4-24: HSR attenuation after proteasomal subunit down-regulation.
(A) *Hsp70* mRNA level upon PSMA7 down-regulation. HeLa cells were transfected with esiRNAs targeting either EGFP (control) or PSMA7. 70 hours after transfection, cells were heat-stressed (HS) for 2 h at 43°C followed by a recovery period as indicated in the figure. Total RNA was prepared and *Hsp70* mRNA level was determined by RT-PCR. Representative agarose gel images are shown. (B) Quantification of (A). *Hsp70* mRNA levels were quantified from the band intensities using AIDA, normalized with *GAPDH* and plotted against time. Standard deviations from at least three independent experiments are shown.

increases chaperone occupancy, thereby delaying rebinding of HSF1 to chaperones and consequently HSF1 attenuation.

The delay in HSR attenuation upon proteasomal impairment could also be explained by a more direct role of the UPS in HSF1 deactivation or degradation. Little is known about the turnover of HSF1 from literature (Neef *et al.* 2011). However, Figure 4-16 already suggests a role of the proteasome in HSF1 turnover. To further validate the involvement of the UPS, CHX chase experiments were performed in the presence and absence of proteasome inhibitors. In HeLa cells, HSF1 was degraded with a half-time of approximately five hours in the absence of thermal stress and HSF1 was stabilized upon proteasome inhibition with MG132 or the more specific inhibitor epoxomicin (Figure 4-25A). Importantly, HS was found to accelerate the degradation of HSF1 approximately twice, resulting in a half-time of ~ 2.5 hours. Again, addition of MG132 or epoxomicin resulted in a stabilization of HSF1 (Figure 4-25A). To confirm the proteasome-dependent degradation of HSF1, the ubiquitination status of HSF1 was checked. Attempts to pull-down endogenous HSF1 with His-tagged ubiquitin failed, presumably due to the low amounts of endogenous HSF1 protein. However, in cells over-expressing His_6-tagged ubiquitin together with Flag-tagged HSF1, a ladder of polyubiquitylated HSF1 was detected upon thermal stress and proteasome inhibition (Figure 4-25B). Interestingly, overexpression of His_6-ubiquitin resulted in reduced cellular HSF1 levels, further supporting the notion of a UPS-regulated HSF1 degradation (Figure 4-25B).

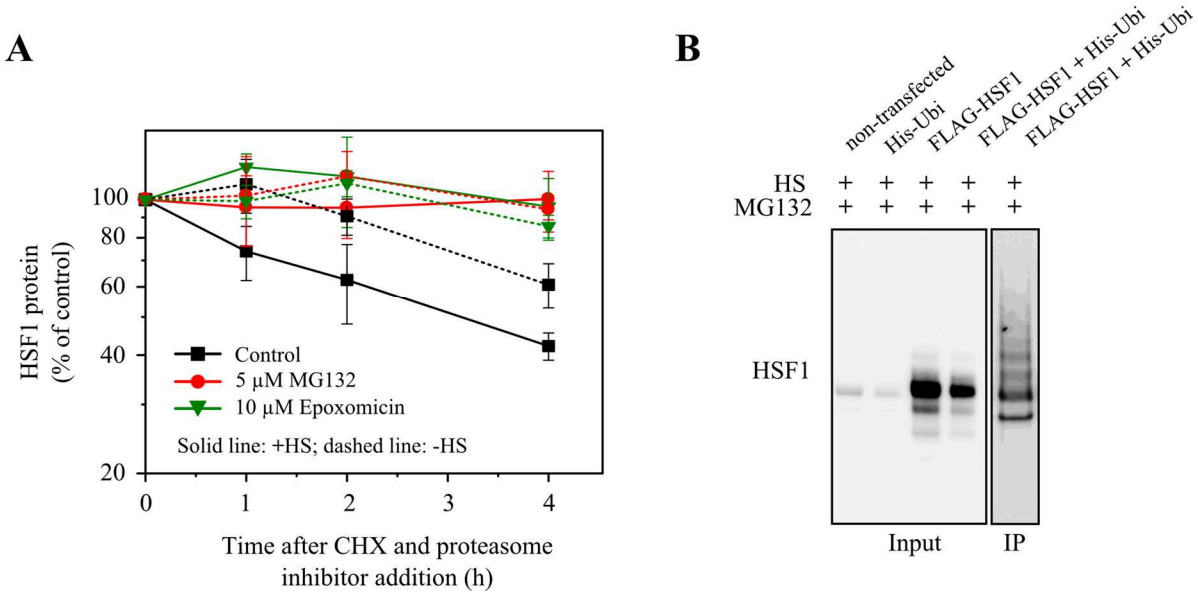

Figure 4-25: CHX chase and ubiquitination of HSF1.
(A) HSF1 protein level in CHX chase experiments in presence and absence of the proteasome inhibitors MG132 or epoxomicin; with (solid lines) or without (dashed lines) heat stress for 2 h at 43°C. 5 mM CHX and 0.1% DMSO, 5 µM MG132, or 10 µM epoxomicin were added to the HeLa cells immediately after thermal stress or to non-stressed cells. Whole cell extracts were prepared at the indicated time points, separated by SDS-PAGE, and analyzed by western blotting. HSF1 protein levels were quantified from band intensities using AIDA, normalized against corresponding GAPDH levels, and plotted against time. Standard deviations from at least three independent experiments are shown. (B) HeLa cells were transfected as described in the figure. 24 h later, 5 µM MG132 were added to the cell culture medium and cells were heat-stressed at 43°C for 2 h followed by 2 h recovery period at 37°C. Cells were lysed and His-ubiquitin pull-down was performed using Dynaloads His-Tag isolation beads. Input and IP samples were separated by SDS-PAGE and blotted with anti-HSF1 antibody.

Upon proteotoxic stress, HSF1 has been shown to undergo inducible phosphorylation necessary for its transcriptional activity. The phosphorylation leads to a slower migrating HSF1 band in SDS-PAGE (Holmberg *et al.* 2001). Accordingly, thermal stress resulted in an upshift of the HSF1 band by ~ 2 kDa (Figure 4-26A). CHX chase experiments revealed that upshifted (active) HSF1 was not dephosphorylated to the faster migrating band during recovery, but was degraded (Figure 4-26A left panel). Upshifted HSF1 was markedly stabilized by proteasome inhibition (Figure 4-26A right panel). Treatment with calf intestinal phosphatase confirmed that the upshift of HSF1 is at least partly due to phosphorylation, as dephosphorylation caused down-shift of HSF1, both of the transcriptionally active species and of the HSF1 species present before HS (Figure 4-26B).

.

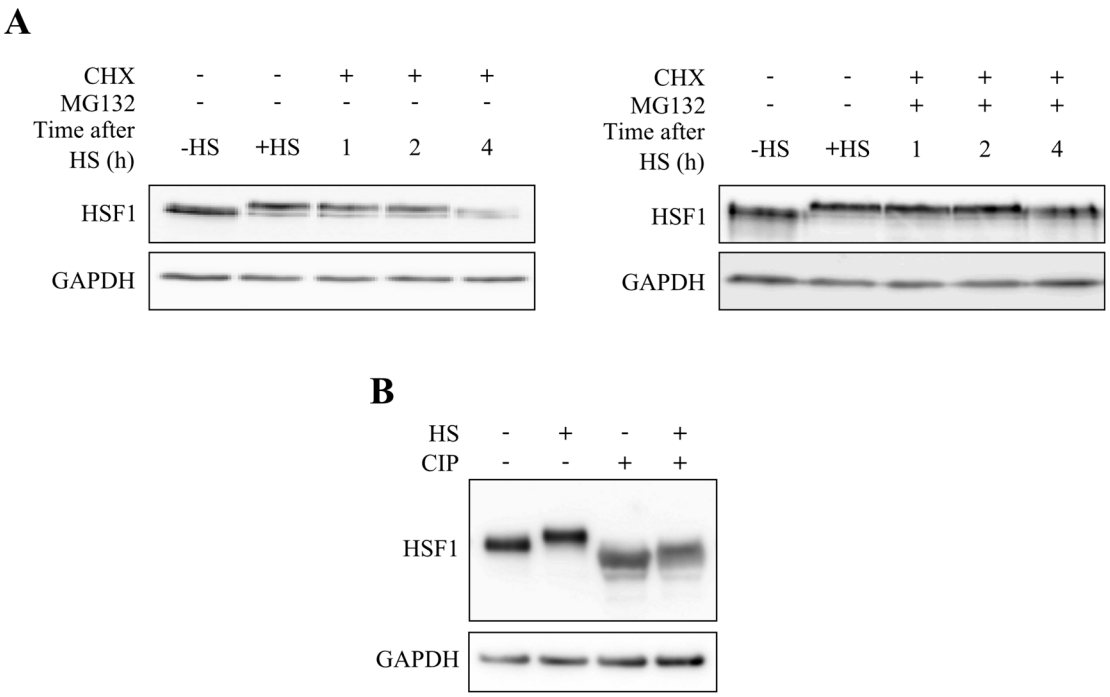

Figure 4-26: Stress-dependent upshift of HSF1.
(A) Representative western blots showing stress-activated HSF1 in CHX chase experiment. HeLa cells were heat-stressed for 2 h at 43°C and CHX chase was performed in presence and absence of MG132. 5 mM CHX and 0.1% DMSO (left) or 5 µM MG132 (right) were added to the cells immediately after thermal stress. Whole cell extracts were prepared at the indicated time points, separated by SDS-PAGE, and analyzed by western blotting using anti-HSF1 and anti-GAPDH antibodies. (B) Dephosphorylation of HSF1. 75 µg of RIPA soluble cell extract from heat-stressed (1 h at 43°C) and control HeLa cells were incubated with 20 U calf intestinal phosphatase (CIP) for 90 min at 37°C. The reaction was stopped by boiling in SDS loading buffer. Samples were separated by SDS-PAGE and blotted against HSF1.

Apart from proteasomal degradation, it might be conceivable that HSF1 is also degraded by another cellular proteolytic pathway, autophagy. To test this, CHX chase experiments were performed in the presence and absence of the autophagy inhibitor 3-methyladenine (3-MA). However, the addition of 3-MA did not slow down or inhibit the degradation of HSF1, but resulted in a slightly faster degradation in stressed as well as non-stressed cells (Figure 4-27).

To check whether degradation of active HSF1 requires the rebinding to chaperones such as Hsp90, CHX chase experiments were performed in the presence and absence of the Hsp90 inhibitor 17-AAG, which is known to cause dissociation of HSF1 from Hsp90 (Zou *et al.* 1998). Inhibition of Hsp90 immediately after HS had no significant effect on HSF1 turnover (Figure 4-28A), although 17-AAG treatment for two hours effectively induced the HSR as shown by an increase in the level of *Hsp70* mRNA (Figure 4-28B). This result suggests that rebinding to Hsp90 is not a prerequisite for the proteasomal removal of active HSF1.

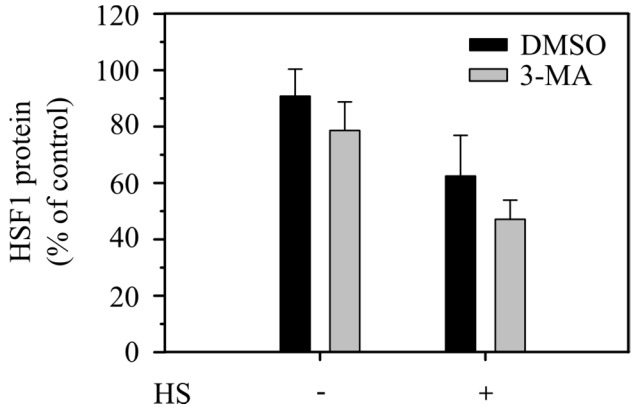

Figure 4-27: CHX chase of HSF1 upon autophagy inhibition.
HSF1 protein levels in stressed (43°C for 2 h) and non-stressed cells in presence and absence of the autophagy inhibitor 3-MA. 5 mM CHX and 0.1% DMSO or 10 mM 3-MA were added to HeLa cells immediately after thermal stress or to non-stressed cells. Whole cell extracts were prepared 2 h later, separated by SDS-PAGE, and analyzed by western blotting using anti-HSF1 and anti-GAPDH antibodies. HSF1 protein levels were quantified from band intensities using AIDA and normalized against corresponding GAPDH levels. HSF1 amounts of non-treated control cells before CHX addition were set to 100% (data not shown). Standard deviations from at least three independent experiments are shown.

Taken together, the results in this chapter show that stress-activated HSF1 in particular undergoes rapid proteasomal degradation during HSR attenuation with kinetics similar or faster than the decay of the HSR.

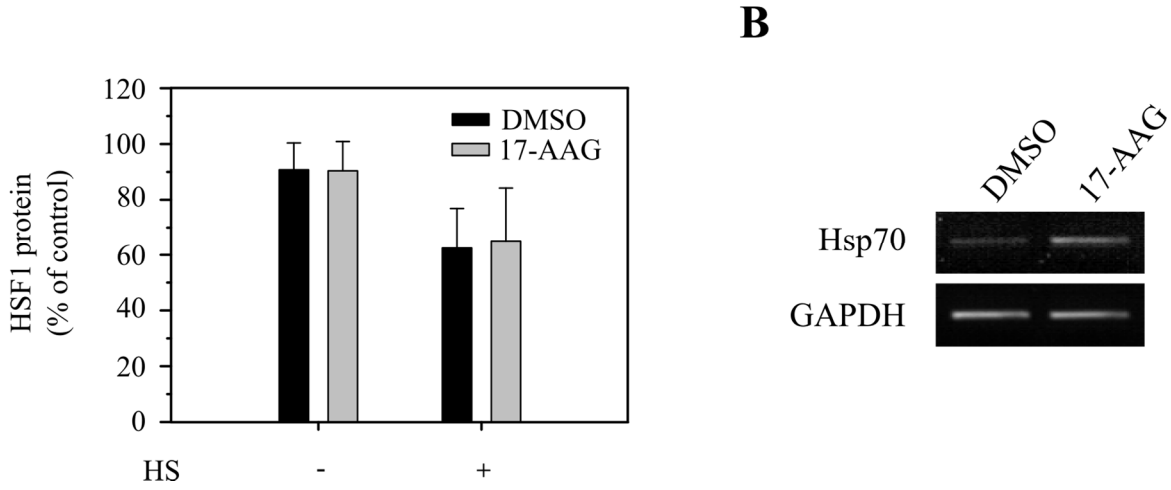

Figure 4-28: CHX chase of HSF1 upon Hsp90 inhibition.
(A) HSF1 protein levels in stressed (43°C for 2 h) and non-stressed cells in presence and absence of the Hsp90 inhibitor 17-AAG. 5 mM CHX and 0.1% DMSO or 5 µM 17-AAG were added to HeLa cells immediately after thermal stress or to non-stressed cells. Whole cell extracts were prepared 2 h later, separated by SDS-PAGE, and analyzed by western blotting using anti-HSF1 and anti-GAPDH antibodies. HSF1 protein levels were quantified from band intensities using AIDA and normalized against corresponding GAPDH levels. HSF1 amounts of non-treated control cells before CHX addition were set to 100% (data not shown). Standard deviations from at least three independent experiments are shown. (B) *Hsp70* mRNA level after 17-AAG treatment. HeLa cells were treated with 0.1% DMSO or 5 µM 17-AAG for 2 h, total RNA was prepared, and *Hsp70* mRNA level was determined by RT-PCR. A representative agarose gel image is shown.

4.11 HSR regulation after heat-shock and other stresses

In addition to heat stress, various other stresses are known to induce the HSR. However, only little information is available on HSR regulation under stress conditions other than

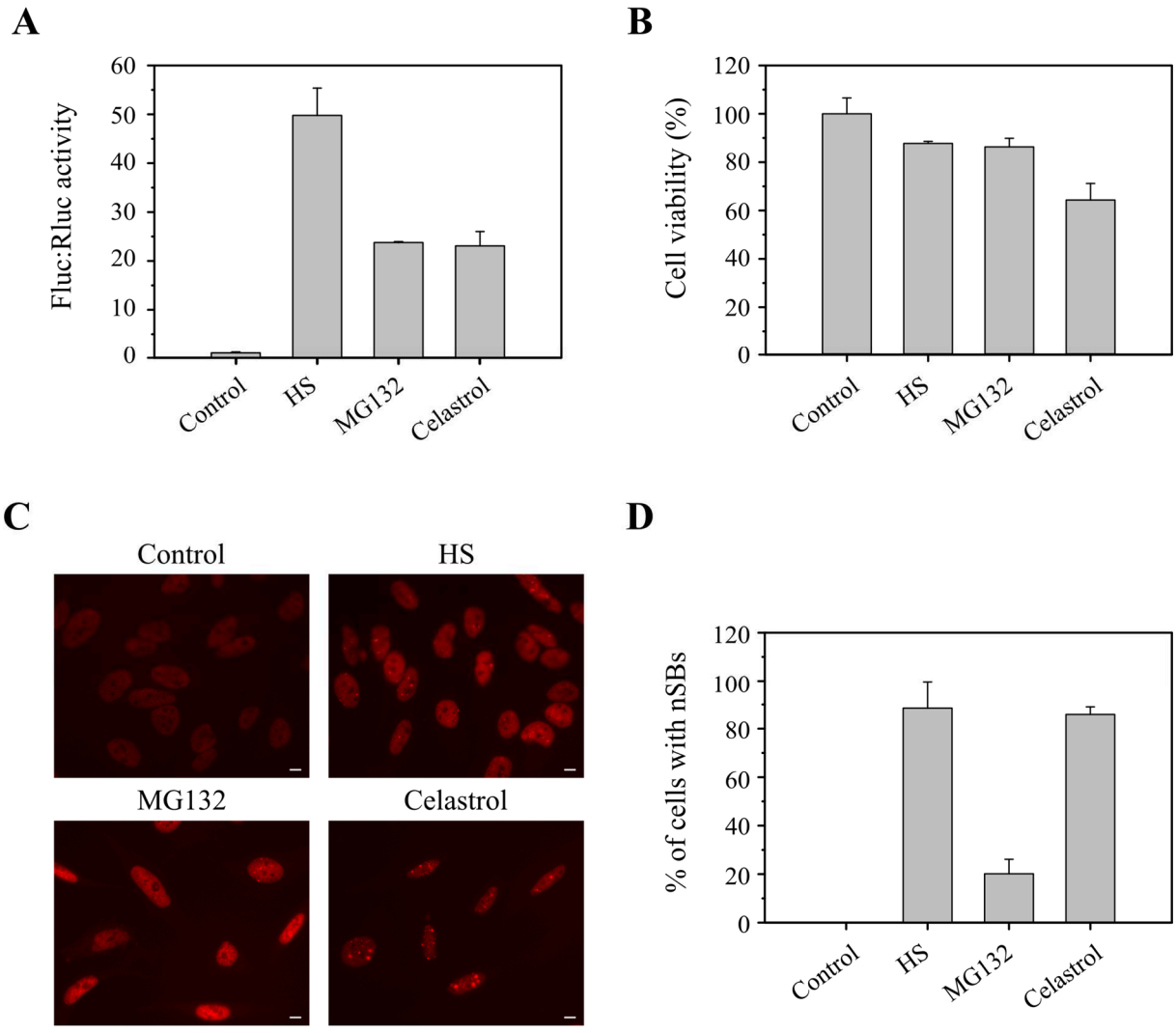

Figure 4-29: Comparison of the HSR induction by HS, MG132, and celastrol.
(A) Fluc:Rluc activity ratios in the iFluc-Rluc cell line after thermal stress (2 h at 43°C, 2 h at 37°C) or treatment with 5 µM MG132 or celastrol for 8 h, respectively. Fluc:Rluc activity ratios were normalized to DMSO treated control cells. Standard deviations were derived from at least three independent experiments. (B) Cell viability after different stresses. HeLa cells were either heat shocked for 2 h at 43°C followed by a recovery period of 2 h at 37°C or treated with 5 µM MG132 or celastrol for 8 h, respectively. Cell viability was normalized to DMSO treated control cells. Standard deviations were derived from at least three independent experiments. (C) Formation of nSB in HeLa cells after thermal stress (1 h at 43°C) or treatment with 5 µM MG132 or celastrol for 8 h, respectively. After the treatment, cells were fixed, stained with rabbit anti-HSF1 antibody, and micrographed. Representative images indicating HSF1 in red are shown. Scale bar: 10 µm. (D) Quantification of (C). The percentage of cells with nSB formation was determined and plotted. Averages and standard deviations of countings from at least three different experiments are shown.

hyperthermia (Anckar and Sistonen 2011). Since the nature of proteotoxicity might influence the mode of HSR regulation, the overlap of the regulatory networks involved in stress adaption upon thermal stress and other proteotoxic conditions was determined. The iFluc-Rluc cell line was well-responsive to the proteasome inhibitor MG132 and celastrol, a modifier of reactive thiol groups (Figure 4-2 and Figure 4-29A). However, compared to thermal stress, both agents activated the HSR more mildly as evidenced by the Fluc:Rluc activity (Figure 4-29A). MTT assays with HeLa cells revealed that treatment with the stressors also had a different effect on cell viability. Whereas thermal stress and treatment with MG132 only led to a slight reduction in cell viability, treatment with celastrol caused substantial toxicity (Figure 4-1 and Figure 4-29B). Furthermore, the stressors induced nSB formation to different extends. As already shown in Figure 4-11B, treatment with MG132 only led to nSB formation in approximately 20% of the cells. However, nSB were found in the vast majority of cells following thermal stress and treatment with celastrol (Figure 4-29C and D).

In summary, these results suggest differences in the cellular stress response dependent on the nature of proteotoxicity. Therefore, it is conceivable that the network participating in HSR regulation also varies with the stressor.

To test this hypothesis, the positive HSR modulators found in the screen were down-regulated in the iFluc-Rluc cell line. 64 h later, cells were treated with either 5 µM MG132 or celastrol for 8 h, respectively, and Fluc:Rluc activity ratios were determined. Notably, for approximately 90% of the modulators, down-regulation also inhibited HSR induction upon MG132 treatment (Figure 4-30A and B; Table 7-8). Only six HSR modulators (BEX1, ENSG00000197865, MYBPC2, SYT4, TMEM239, and VN1R4) were apparently not required for the HSR induction by proteasome inhibition (Table 7-8). BEX1 is an X-chromosomal gene and links neurotrophin signaling to the cell cycle, thereby connecting external signals to the cellular status (Vilar *et al.* 2006). SYT4 is present in the Golgi apparatus and may play a role in cellular plasticity during heat stress (Ibata *et al.* 2000). MYBPC2 is a cytoskeletal protein and TMEM239 as well as VN1R4 are putative transmembrane proteins which might be involved in sensing HS and transmitting the signal to HSF1. The large overlap between factors participating in HSR regulation upon thermal stress and MG132 treatment is particularly remarkable when one considers that induction by MG132 is much slower than that by HS (Figure 4-29A).

In contrast, down-regulation of only 46% of the positive modulators found in the screen affected HSR induction after celastrol treatment, indicating that celastrol can either

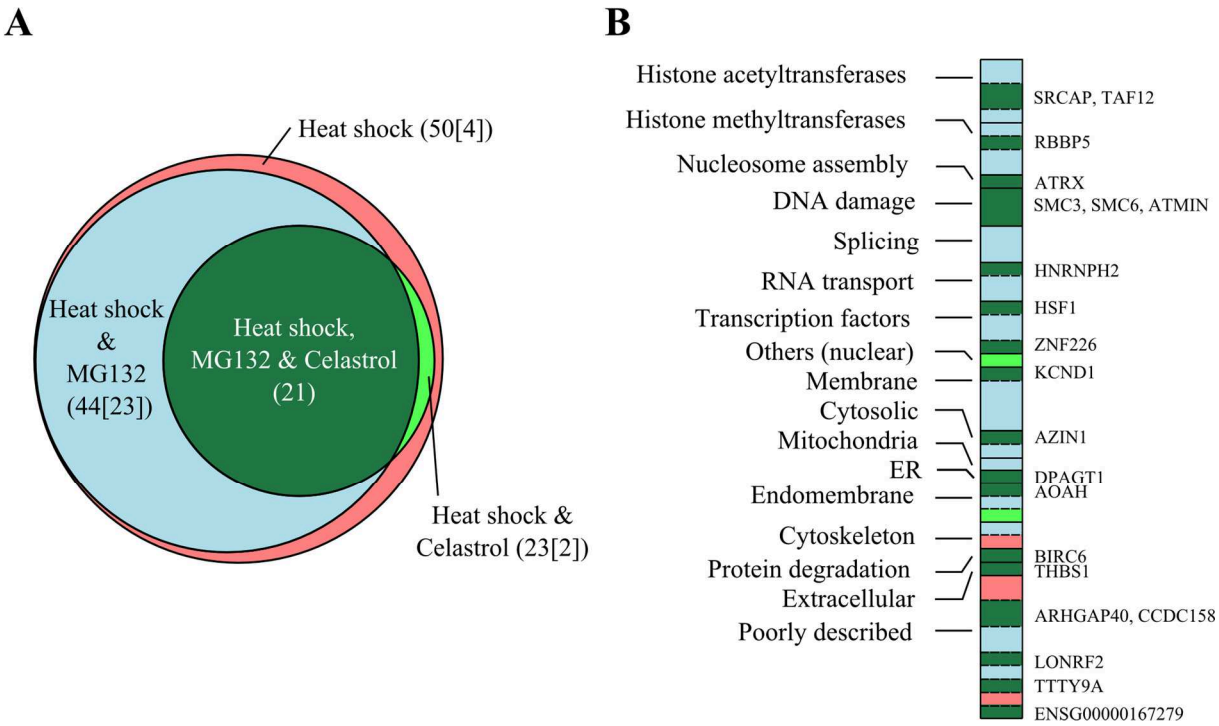

Figure 4-30: HSR modulators in MG132 and celastrol induced stress.
(A and B) Positive HSR modulators found in the screen were down-regulated in the iFluc-Rluc cell line in 96-well format by esiRNA transfection. 64 h after transfection, cells were treated for 8 h with 5 µM MG132 or 5 µM celastrol, luciferase reporter activities were measured, and Fluc:Rluc activity ratios were calculated. Experiments were repeated three times. Only gene down-regulations with similar phenotypes in two out of three experiments were considered. (A) Number of gene down-regulations reducing reporter activity after each treatment and their overlap are shown in a Venn diagram. First number is the sum of modulators in each group, the second number in brackets indicates the number of modulators unique to each group. Red color represents the group of modulators whose down-regulation only affects the HSR induction upon thermal stress, light blue represents the overlap between heat shock and MG132 induction, light green the overlap between heat stress and celastrol treatment, and dark green the overlap between all three stresses. (B) Summary of HSR-modulator distribution showing their differential inducibility and functional classes. Color code as in (A). Core components of the HSR, i.e. gene down-regulations affecting induction of the stress response by all three stresses, are labeled on the right-hand side.

bypass some HSR regulatory pathways or only activates specific HSR regulatory pathways. Specifically, down-regulation of most of the HSR modulators encoding transmembrane proteins, histone acetyl- and methyltranferases as well as proteins involved in RNA transport and transcription did not interfere with HSF1 activation (Figure 4-30B). For example, celastrol-dependent HSR induction no longer required CREBBP and EP300, two histone acetyltransferases, but was still dependent on SRCAP and TAF12, two other histone acetyltransferases. This indicates that even modulators belonging to the same group may work in different pathways to regulate HSR induction. Down-regulation of splicing factors in combination with celastrol treatment caused substantial cell death and the luciferase reporter activity could not be measured. Celastrol is suggested to modify reactive thiol groups (Trott *et*

al. 2008) and these groups are known to be involved in many enzymatic processes with various biological functions (Chapman *et al.* 1997, Klomsiri *et al.* 2011). Inactivation of these cysteine containing proteins is supposed to cause cellular toxicity. Indeed, celastrol treatment is more toxic as compared to thermal stress and proteasome impairment by MG132 (Figure 4-29B). As a result, sensing an emergency situation, cells might bypass several steps of the normal HSR activation.

The down-regulation of 21 positive modulators impaired the activation of the HSR under all three stress conditions tested. These include the histone actetyltransferases SRCAP and TAF12, the histone methyltransferase RBBP5, the nucleosome assembly factor ATRX, DNA damage repair proteins SMC3, SMC6 and ATMIN, RNA transport protein HNRNPH2, the transcription factors HSF1 and ZNF226, antizyme inhibitor AZIN1, the secretory proteins DPAGT1 and AOAH, UBCc (ubiquitin-conjugating enzyme E2, catalytic) domain containing protein BIRC6, glycoprotein THBS1, and 5 uncharacterized proteins (Figure 4-30B). The potassium channel KCND1 is the only membrane protein present in this set, indicating a possible importance of potassium transport in stress response signaling. All these factors form a core set of proteins required for regulation of the HSR.

5 Discussion

Health and survival of living organisms are dependent on the integrity of the cellular proteome. Thus, protein homeostasis or proteostasis is crucial for successful development, cellular health, and normal aging. The cellular network maintaining proteostasis comprises proteins which are involved in protein synthesis, folding, and trafficking as well as in the proteolytic degradation of irreversibly misfolded proteins. Persistent imbalances in proteostasis are associated with disease and even cell death. The capacities of the cellular quality control machinery under normal (non-stress) conditions are not sufficient to maintain proteostasis during proteotoxic insults. Thus, upon stress, multiple interconnected stress-inducible signaling pathways are induced, including the HSR. A key feature of this highly conserved cytoprotective mechanism is the increased synthesis of Hsps, which assist in the re-establishment of proteostasis. The transcriptional activation of the HSR is coordinated by HSF1. According to the current model of HSR regulation, the activity state of HSF1 is regulated by its binding to molecular chaperones including members of the Hsp70, Hsp40, and Hsp90 families. A key role in HSF1 activation is its displacement from Hsp90 by misfolded proteins, which accumulate upon stress. Furthermore, oligomerization and numerous post-translational modifications are a prerequisite for HSF1 to become trans-activation competent. Although the role of HSF1 in the regulation of the HSR is well established, many aspects of the mechanisms by which HSF1 is activated remain unclear.

In the present study, a systemic approach was taken to better understand the cellular events during thermal stress. In a genome-scale RNA interference screen in HeLa cells, novel protein modulators of the cytosolic HSR were identified. For several of those proteins additional HSR-unrelated functions had been described previously. The results strongly suggest that the HSR integrates signals from multiple cellular locations and processes to ensure proteostasis under stress conditions (Figure 4-7) and that its induction and attenuation is rather a multi-factorial process than a single gene/protein event. While most of the identified HSR modulators exert their functions in the nucleus, we also detected novel regulatory factors in the cytoplasm, endomembrane system, mitochondria, and plasma membrane (Figure 4-7). The nuclear machineries of chromatin modifiers and protein quality control were shown to play a central role in the regulation of the HSR. Importantly, we could show that HSF1 is degraded via the UPS. Thus, the proteasome is directly involved in the attenuation of the HSR. Interestingly, activated HSF1 is degraded more rapidly than inactive one. Unexpectedly, the histone acetyltransferase EP300 was found to regulate the magnitude

of the HSR by stabilizing HSF1 against proteasomal degradation. The special roles of EP300 and the UPS in HSR regulation will be discussed in greater detail in chapters 5.2 and 5.4.

5.1 Identification of novel HSR modulators

Our screen led to the identification of 50 positive and 14 negative HSR modulators, which form a highly interconnected network (Figure 4-13), demonstrating that stress response regulation relies on the integration of multiple intra- and extracellular signals. Approximately 40% of the identified regulatory proteins are primarily localized in the nucleus, strongly suggesting an important role of nuclear processes in HSR regulation (Figure 4-7). For example, three transcription factors (GTF3C3, POLR2G, ZNF226) were identified apart from HSF1. They positively modulate the HSR and may exert their functions in cooperation with HSF1. It is conceivable that these transcription factors are involved in the recruitment of HSF1 to HSEs, but also to transcription sites other than the classical heat shock promoters. This would be consistent with recent findings that HSF1 regulates HSE-independent transcriptional programs supporting cell survival and tumorigenesis (Mendillo *et al.* 2012, Santagata *et al.* 2013). Furthermore, we identified two novel nucleo-cytoplasmic transport proteins, HNRNPH2 and NIF3L1, which likely mediate mRNA export during HS along with the known factor NXT1. These components may cooperate with splicing factors which in addition to their splicing functions also participate in the proper translocation of mRNA (Hocine *et al.* 2010).

Moreover, several multi-spanning membrane proteins were identified as positive HSR modulators, including putative G-protein coupled cell surface receptors. This supports the notion that not only the heat-induced increase in membrane fluidity (Balogh *et al.* 2005) but also membrane proteins are involved in signaling cascades that participate in HSF1 activation. These membrane proteins may be involved in stress sensing and communicating the stress status between cells (Prahlad *et al.* 2008, van Oosten-Hawle *et al.* 2013). The identification of KCND1 as positive HSR modulator reconfirmed the importance of membrane potassium channels in HSR. The activation of these voltage-dependent channels may be an early event in HSR initiation (Saad and Hahn 1992).

Elevated temperatures are known to be associated with a change in mitochondrial morphology and localization (Collier *et al.* 1993, Funk *et al.* 1999). The resulting respiratory deficiencies as well as the generation of oxidative stress have been shown to result in an

increased expression of Hsps (Barrett *et al.* 2004, Kuzmin *et al.* 2004, Rikhvanov *et al.* 2005). The identified mitochondrial positive HSR modulator, PPOX, might contribute to cellular protection, since heme biosynthesis was suggested to be beneficial under condition of oxidative stress caused by ROS (Shinjyo and Kita 2007).

The absence of kinases and major chaperone components (e.g. Hsp70 or Hsp90) among the identified HSR modulators is notable. Phosphorylation of HSF1 is a prerequisite for its transcriptional activity and multiple kinases appear to be involved (Anckar and Sistonen 2011), suggesting a functional redundancy. Similarly, the participation of multiple chaperone systems in HSF1 regulation and the high abundance of these factors may have prevented the identification of these components as significant hits in the screen. The identification of three subunits of the cytosolic chaperonin TRiC/CCT and the Hsp70-Hsp90 organizing protein Hop is most likely due to the chaperone-dependent folding of the Fluc reporter protein, as their down-regulation did not prevent the increased transcription of *Hsp70* mRNA upon HS.

5.2 Role of EP300 in regulating the HSR

Major re-arrangements of the chromatin landscape in response to elevated temperatures have already been demonstrated in the early 1960s, when Ferruccio Ritossa published his observations on the heat-induced puffing pattern in the polytene chromosomes of *Drosophila* larvae (Ritossa 1962). During the following decades, the high transcriptional activity in these puffs could be correlated to the expression of heat-shock proteins (Tissieres *et al.* 1974, Lindquist 1986). Our screen revealed the participation of multiple chromatin modifiers, centering on the EP300/CREBBP histone acetyltransferase complex and the Snf2-related CREBBP activator protein, SRCAP, in the activation of HSF1. Two other positive HSR modulators, the histone methyltransferases RBPP5 and DPY30, are also connected to EP300/CREBBP (Figure 4-13). Taken together, the abundance of histone modifiers among the HSR modulators confirm the significance of chromatin remodeling to initiate HSR (Sullivan *et al.* 2001).

Importantly, overexpression of EP300 has been shown to acetylate nine lysine residues of HSF1 including K80 in the DNA binding domain and several other lysine residues close to and within the heptad repeat oligomerization domain. Deacetylation of HSF1 by SIRT1 prolongs the dwell time of HSF1 on heat shock elements (Westerheide *et al.* 2009, Raynes *et*

al. 2013). Surprisingly, we observed that the down-regulation of EP300 destabilizes HSF1 and induces its proteasomal degradation (Figure 4-14, Figure 4-16 and Figure 5-1 ① and ⑨). This effect is specific for EP300 and is not seen for down-regulations of the closely related acetyltransferase CREBBP or other chromatin modifiers (Figure 4-14). The destabilization of HSF1 in the absence of EP300 already occurs under normal growth conditions and is likely to be caused by reduced HSF1 acetylation at lysine residues other than K80 (data not shown; Figure 5-1 ① to ③). In this context it is notable that acetylation of lysine residues is known to interfere with ubiquitination and may also modulate conformational protein stability by removing positively charged residues (Caron *et al.* 2005). In addition to HSF1 acetyltransferase activity, EP300 also exerts histone acetyltransferase activity which may be necessary for altering the chromatin structure prior to transcription (Ogryzko *et al.* 1996). Therefore, it is conceivable that the down-regulation of EP300 can result in lower chromatin accessibility for HSF1. This may have an additional destabilizing effect on HSF1, particularly upon stress. Interestingly, HIF1α, the transcription factor regulating the cellular response to hypoxic conditions, was also shown to be destabilized in the absence of EP300. Moreover, EP300-mediated acetylation protected HIF1α against proteasomal degradation (Geng *et al.* 2012). Down-regulation of the deacetylase SIRT1 resulted in a reduced transcriptional activity of HIF1α due to hyper-acetylation (Laemmle *et al.* 2012).

Based on these findings, we propose a model for the regulation of HSR activation and attenuation, in which the increasing acetylation of HSF1 by EP300 functions as a timing mechanism (Figure 5-1). The initial acetylation of HSF1 by EP300 protects HSF1 against proteasomal degradation and together with other post-translational modifications, including phosphorylations and deacetylation of K80 (Westerheide *et al.* 2009), HSF1 becomes competent for DNA binding (Figure 5-1 ①). Once bound to chromatin, the number of acetylated lysine residues increases (Figure 5-1 ②). Eventually, acetylation of the regulatory lysine residues weakens DNA binding, thereby initiating HSR attenuation (Figure 5-1 ③ and ⑤). The cooperated deacetylation of HSF1 by SIRT1 serves as a fine-tuning mechanism in HSR regulation (Figure 5-1 ③ to ⑥).

5.3 Reorganization of the nuclear proteome during heat stress

The nuclear proteome is known to undergo substantial changes during various forms of stress, including a nuclear enrichment of the proteasome in response to DNA damage and glucose

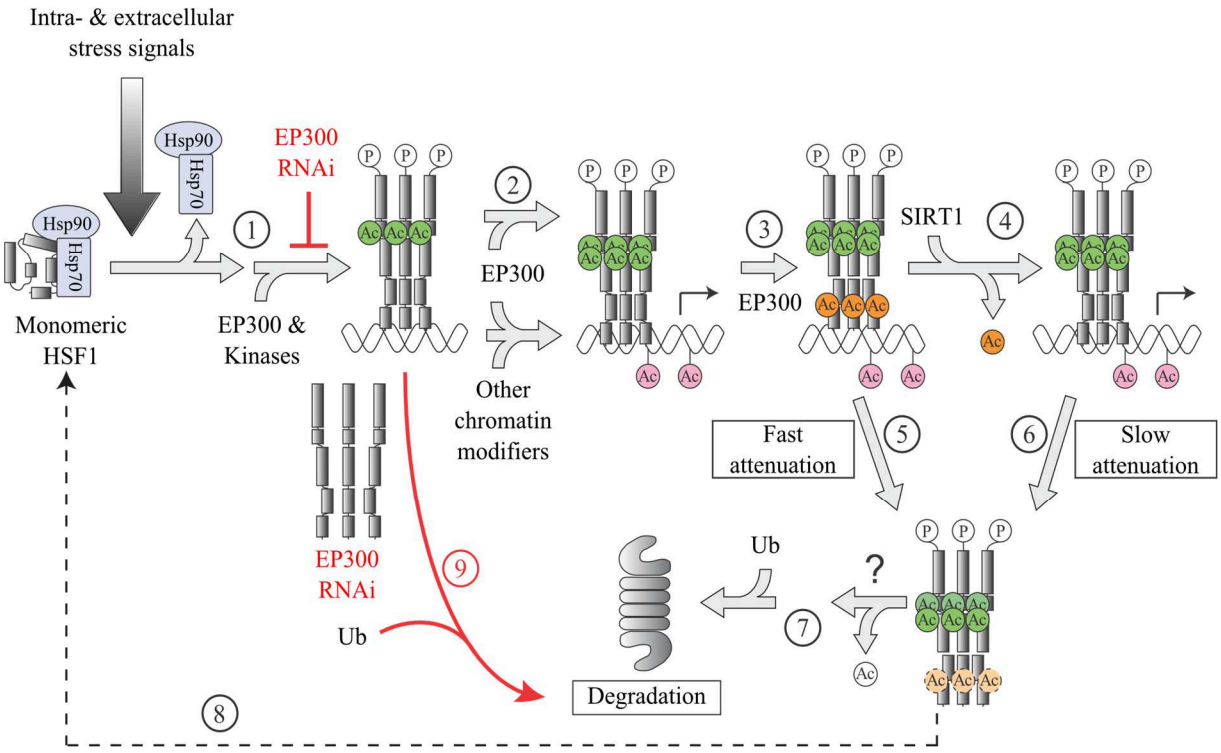

Figure 5-1: Model of nuclear pathways involved in HSR regulation.
The activation and attenuation of HSF1 requires the integration of intra- and extracellular stress signals. In the absence of stress, HSF1 is maintained in an inactive, monomeric state by the chaperones Hsp70/Hsp90 and is mainly localized in the nucleus and partially in the cytosol. HS and other protein conformational stresses result in the accumulation of misfolded proteins and the displacement of HSF1 from Hsp70/Hsp90. HSF1 oligomerizes, undergoes post-translational modifications (e.g. phosphorylation and acetylation), and triggers the HSR. Increasing acetylation of HSF1 by EP300 functions as a timer for the induction as well as attenuation of the HSR. This occurs in close cooperation with the deacetylase SIRT1. EP300 down-regulation results in destabilization of HSF1 and premature degradation by the proteasome. Activated HSF1 is normally degraded by the proteasome during the attenuation phase of the HSR. Ac, acetylation (green: stabilizing acetylation, orange: HSF1 inactivating acetylation); P, phosphorylation; Ub, ubiquitin. See Discussion for details of the proposed model.

starvation (Ogiso *et al.* 2002, Boisvert *et al.* 2010, Boulon *et al.* 2010). Furthermore, it was shown that thermal stress can induce proteasomal protein degradation (Medicherla and Goldberg 2008). The quantitative proteomics experiments (Figure 4-18 and Figure 4-19) performed in this study and further biochemical validation (Figure 4-21) revealed that the nuclear proteome becomes substantially enriched with proteins of the quality control machinery in response to thermal stress. These proteins include mainly subunits of the 26S proteasome, HSF1, and multiple chaperones and co-chaperones. This may reflect the attempt of the cell to prevent the accumulation of potentially dangerous destabilized proteins in the nucleus. The proteasome system is likely to cooperate in this process with multiple Hsp70 and Hsp40 chaperones, which is consistent with earlier observations that Hsp70 accumulates in the nucleus and nucleolus during HS (Pelham 1984). Remarkably, two stress inducible Hsp70s, the constitutively expressed Hsc70, and at least five different J-domain proteins

(Hsp40s) accumulate in the nuclear fraction upon HS, suggesting an important role of chaperones in the protein refolding, aggregation prevention, and proteasomal degradation. The presence of Hsp40s among the enriched proteins is consistent with recent findings that the yeast Hsp40, Sis1p, and its mammalian homolog DnaJB1 have a specific role in the degradation of misfolded proteins in the nucleus (Park *et al.* 2013).

5.4 Attenuation of the HSR by the proteasome

The inactivation of HSF1 is thought to be the result of its rebinding to Hsp90 as soon as sufficient free Hsp90 is available during stress recovery (Zou *et al.* 1998, Bharadwaj *et al.* 1999) (Figure 7, ⑧). However, direct evidence for this attractive model is limited. The finding that active, i.e. hyper-phosphorylated, HSF1 is degraded by the proteasome (Figure 4-25) suggests an alternative (or parallel) mechanism for attenuation of the HSR (Figure 5-1, ⑦). The Hsp90-independent degradation of active HSF1 (Figure 4-28) further supports this model. Moreover, the reduced half-life of transcriptionally competent HSF1 under conditions of proteotoxic stress compared to HSF1 in absence of thermal stress, implies that post-translational modifications associated with the activation of HSF1, such as phosphorylation and acetylation, control its proteasomal clearance. Accumulating stress-denatured proteins would generally compete with HSF1 for ubiquitination and subsequent proteasomal degradation. This would delay the clearance of HSF1, thereby slowing down the attenuation of the HSR until proteome balance has been restored. Thus, the degradation of active HSF1 by the proteasome would directly link the extent of protein damage to the quality control capacity required for the re-establishment of proteostasis. Whereas HSF1 rebinding to chaperones like Hsp70/90 may contribute to attenuation, it is also conceivable that these chaperones mainly interact with newly synthesized HSF1. This may support the folding of HSF1 to a state primed for activation under conditions of proteotoxic stress.

5.5 Comparing the regulatory networks of heat-shock and other proteotoxic stresses

Up to now, most of the published studies investigating the function of HSF1 used a temperature upshift to induce its transcriptional activity. However, it is conceivable that HSF1

activation may differ mechanistically in response to different proteotoxic stresses (Anckar and Sistonen 2011). To address this question we determined the overlap of the HSF1 regulatory networks upon thermal stress, proteasome inhibition, and treatment with celastrol, a modifier of reactive thiol groups. The comparison revealed a large overlap between the factors that regulate HSF1 activation upon thermal stress and proteasome inhibition. This may reflect an overlapping impact of the stresses on the cellular proteome. It was shown that the increased load of misfolded or aberrant proteins following heat stress can impair the UPS activity (Salomons *et al.* 2009), thereby mimicking proteasomal inhibition upon treatment with MG132. However, six HSR modulators were not required for the HSR induction by proteasomal impairment (Figure 4-30). Physical stress, such as heat-shock, is known to cause extensive cellular damage, particularly to membranous structures (Nickells *et al.* 1988). The heat-shock specific factors are mainly membrane-associated or play a role in cellular plasticity and as such, they might be involved in sensing cell morphological changes during thermal stress and transmitting the signal to HSF1.

Unexpectedly, only 46% of the positive HSR modulators were required for the activation of HSF1 by celastrol (Figure 4-30). After down-regulation of several histone acetyl- and methyltranferases, membrane proteins, RNA transport, and transcription factors, cells were still able to properly induce the HSR. Surprisingly, even the absence of EP300 with its direct regulatory effect on HSF1 stability did not interfere with HSR induction. This might be explained by the different nature of proteotoxicity. In contrast to the more general effects on the cellular proteome induced by heat stress or proteasome inhibition, celastrol effects specific processes by modifying reactive thiol groups of multiple enzymes (Chapman *et al.* 1997, Klomsiri *et al.* 2011). Loss of these enzymatic functions may explain the higher cellular toxicity of celastrol (Figure 4-29B). To cope with the resulting emergency situation, cells seem to bypass the HSR regulatory network to a large extent. The comparably low overlap of positive modulator proteins identified after thermal stress and celastrol treatment (Figure 4-30) strongly suggests a difference in HSR regulation dependent on the formal stress.

Apart from that, comparison of the overlap of the regulatory networks under different stress conditions enabled us to identify core components of the HSR (Figure 4-30). This core set comprises 21 proteins with various cellular functions and localizations, including factors involved in chromatin remodeling, DNA damage repair, RNA transport, transcription, and ion transport. Although the specific functions of these modulator proteins remain to be elucidated, it strengthens the hypothesis that the regulation of the HSR is a multi-factorial process.

5.6 Implications of the HSR in aging and disease

The cytosolic stress response ensures proteostasis under a variety of proteotoxic conditions and represents the primary defense of mammalian cells against the accumulation of potentially toxic protein species in the cytoplasm and nucleus. Imbalances in proteostasis are associated with numerous neurodegenerative diseases including Alzheimer's, Huntington's, and Parkinson's, all of which are characterized by the accumulation of specific proteins in inclusions or aggregates (Douglas and Dillin 2010). The manifestation of these late-onset diseases has been linked to an age-dependent, gradual decline of the cellular proteostasis capacity, which may be partly explained by an impaired ability of the cells to induce the HSR in response to the accumulation of aberrant proteins (Morimoto 2008, Powers *et al.* 2009, Ben-Zvi *et al.* 2009, David *et al.* 2010). Moreover, an age-related decrease in the transcriptional activity of HSF1 was shown in rat hepatocytes (Heydari *et al.* 2000). Considering the extensive participation of chromatin modifiers in regulating the HSR, age-related modifications of the chromatin structure may contribute to this decline (Dimauro and David 2009). Indeed, down-regulation of *cbp-1*, the *C. elegans* ortholog of EP300, blocks the lifespan extension normally afforded by calorie restriction (Zhang *et al.* 2009). The observation that the histone acetyltransferase activities of EP300 and CREBBP are high in the brain and liver of fetal and newborn mice and are attenuated in liver, muscle, and testes with age further emphasizes the role of chromatin modifiers as positive modulators of the HSR (Li *et al.* 2002). It is notable that stability of the transcription factor HIF1α, which is involved in lifespan extension of *C. elegans* and suppression of proteotoxicity (Mehta *et al.* 2009), is also controlled by EP300-mediated acetylation (see chapter 5.2).

While restoring the cellular proteostasis capacity by boosting the HSR is considered beneficial in delaying the manifestation of age-related degenerative diseases (Powers *et al.* 2009, Neef *et al.* 2011), an increased HSR activity is a major hallmark of cancer (Dai *et al.* 2007). The resulting higher level of Hsps has been implicated in several steps of tumorigenesis including the resistance to cell death, inhibition of replicative senescence, and the induction of angiogenesis (Ciocca *et al.* 2013). Although a potential drawback for the treatment of neurodegenerative diseases, the dependency of cancerous cells on the HSF1/Hsp system is already exploited for the development of anti-cancer drugs.

Understanding the molecular mechanisms of HSR induction and attenuation can help to identify potential targets for the pharmacologic manipulation of the stress response. In this study we identified several key molecular components involved in HSR regulation, which

may be beneficial for the future treatment of aggregate deposition diseases and cancer. Whereas the positive modulators may be explored as potential targets in correcting the overshooting stress response in cancer cells, the negative modulators offer opportunities to activate the HSR. This might mitigate various degenerative conditions associated with neurodegeneration and the aging process. However, the complexity of the integrated network regulating cellular proteostasis complicates the development of therapeutic strategies because manipulating one branch of the network may affect others. In this context, especially the identification of several proteins with unknown function as stress response modulators seems promising, as they might specifically participate in HSR regulation without contributing to other important cellular processes. Another challenge in the treatment of HSR de-regulations is to only target cells showing a disease phenotype while minimizing deleterious effects on normal cells. To finally succeed in developing new pharmacological approaches, it will be essential to understand how the identified HSR modulators are organized and integrated at the organismal level.

6 References

Abravaya, K., M. P. Myers, S. P. Murphy and R. I. Morimoto (1992). "The human heat shock protein hsp70 interacts with HSF, the transcription factor that regulates heat shock gene expression." Genes Dev **6**(7): 1153-1164.

Abravaya, K., B. Phillips and R. I. Morimoto (1991). "Attenuation of the heat shock response in HeLa cells is mediated by the release of bound heat shock transcription factor and is modulated by changes in growth and in heat shock temperatures." Genes Dev **5**(11): 2117-2127.

Anckar, J. and L. Sistonen (2011). "Regulation of HSF1 function in the heat stress response: implications in aging and disease." Annu Rev Biochem **80**: 1089-1115.

Anfinsen, C. B. (1973). "Principles that govern the folding of protein chains." Science **181**(4096): 223-230.

Apetri, A. C. and A. L. Horwich (2008). "Chaperonin chamber accelerates protein folding through passive action of preventing aggregation." Proc Natl Acad Sci U S A **105**(45): 17351-17355.

Appenzeller-Herzog, C. and L. Ellgaard (2008). "The human PDI family: versatility packed into a single fold." Biochim Biophys Acta **1783**(4): 535-548.

Arndt, V., N. Dick, R. Tawo, M. Dreiseidler, D. Wenzel, M. Hesse, D. O. Furst, P. Saftig, R. Saint, B. K. Fleischmann, M. Hoch and J. Hohfeld (2010). "Chaperone-assisted selective autophagy is essential for muscle maintenance." Curr Biol **20**(2): 143-148.

Asher, G., N. Reuven and Y. Shaul (2006). "20S proteasomes and protein degradation "by default"." Bioessays **28**(8): 844-849.

Asher, G. and Y. Shaul (2005). "p53 proteasomal degradation: poly-ubiquitination is not the whole story." Cell Cycle **4**(8): 1015-1018.

Auluck, P. K., H. Y. Chan, J. Q. Trojanowski, V. M. Lee and N. M. Bonini (2002). "Chaperone suppression of alpha-synuclein toxicity in a Drosophila model for Parkinson's disease." Science **295**(5556): 865-868.

Baek, K., R. S. Brown, G. Birrane and J. A. Ladias (2007). "Crystal structure of human cyclin K, a positive regulator of cyclin-dependent kinase 9." J Mol Biol **366**(2): 563-573.

Baggett, B., R. Roy, S. Momen, S. Morgan, L. Tisi, D. Morse and R. J. Gillies (2004). "Thermostability of firefly luciferases affects efficiency of detection by in vivo bioluminescence." Mol Imaging **3**(4): 324-332.

Balch, W. E., R. I. Morimoto, A. Dillin and J. W. Kelly (2008). "Adapting proteostasis for disease intervention." Science **319**(5865): 916-919.

Ballinger, C. A., P. Connell, Y. Wu, Z. Hu, L. J. Thompson, L. Y. Yin and C. Patterson (1999). "Identification of CHIP, a novel tetratricopeptide repeat-containing protein that interacts with heat shock proteins and negatively regulates chaperone functions." Mol Cell Biol **19**(6): 4535-4545.

Balogh, G., I. Horvath, E. Nagy, Z. Hoyk, S. Benko, O. Bensaude and L. Vigh (2005). "The hyperfluidization of mammalian cell membranes acts as a signal to initiate the heat shock protein response." FEBS J **272**(23): 6077-6086.

Banerji, S. S., N. G. Theodorakis and R. I. Morimoto (1984). "Heat shock-induced translational control of HSP70 and globin synthesis in chicken reticulocytes." Mol Cell Biol **4**(11): 2437-2448.

Baram, D., E. Pyetan, A. Sittner, T. Auerbach-Nevo, A. Bashan and A. Yonath (2005). "Structure of trigger factor binding domain in biologically homologous complex with eubacterial ribosome reveals its chaperone action." Proc Natl Acad Sci U S A **102**(34): 12017-12022.

Barrett, M. J., V. Alones, K. X. Wang, L. Phan and R. H. Swerdlow (2004). "Mitochondria-derived oxidative stress induces a heat shock protein response." J Neurosci Res **78**(3): 420-429.

Bartlett, A. I. and S. E. Radford (2009). "An expanding arsenal of experimental methods yields an explosion of insights into protein folding mechanisms." Nat Struct Mol Biol **16**(6): 582-588.

Bedford, L., S. Paine, P. W. Sheppard, R. J. Mayer and J. Roelofs (2010). "Assembly, structure, and function of the 26S proteasome." Trends Cell Biol **20**(7): 391-401.

Ben-Zvi, A., E. A. Miller and R. I. Morimoto (2009). "Collapse of proteostasis represents an early molecular event in Caenorhabditis elegans aging." Proc Natl Acad Sci U S A **106**(35): 14914-14919.

Benbrook, D. M. and A. Long (2012). "Integration of autophagy, proteasomal degradation, unfolded protein response and apoptosis." Exp Oncol **34**(3): 286-297.

Bence, N. F., R. M. Sampat and R. R. Kopito (2001). "Impairment of the ubiquitin-proteasome system by protein aggregation." Science **292**(5521): 1552-1555.

Bettinger, B. T., D. M. Gilbert and D. C. Amberg (2004). "Actin up in the nucleus." Nat Rev Mol Cell Biol **5**(5): 410-415.

Bharadwaj, S., A. Ali and N. Ovsenek (1999). "Multiple components of the HSP90 chaperone complex function in regulation of heat shock factor 1 In vivo." Mol Cell Biol **19**(12): 8033-8041.

Biamonti, G. and J. F. Caceres (2009). "Cellular stress and RNA splicing." Trends Biochem Sci **34**(3): 146-153.

Biamonti, G. and C. Vourc'h (2010). "Nuclear stress bodies." Cold Spring Harb Perspect Biol **2**(6): a000695.

Boisvert, F. M., Y. W. Lam, D. Lamont and A. I. Lamond (2010). "A quantitative proteomics analysis of subcellular proteome localization and changes induced by DNA damage." Mol Cell Proteomics **9**(3): 457-470.

Bolognesi, B., J. R. Kumita, T. P. Barros, E. K. Esbjorner, L. M. Luheshi, D. C. Crowther, M. R. Wilson, C. M. Dobson, G. Favrin and J. J. Yerbury (2010). "ANS binding reveals common features of cytotoxic amyloid species." ACS Chem Biol **5**(8): 735-740.

Boulon, S., B. J. Westman, S. Hutten, F. M. Boisvert and A. I. Lamond (2010). "The nucleolus under stress." Mol Cell **40**(2): 216-227.

Boutros, M., A. A. Kiger, S. Armknecht, K. Kerr, M. Hild, B. Koch, S. A. Haas, R. Paro, N. Perrimon and C. Heidelberg Fly Array (2004). "Genome-wide RNAi analysis of growth and viability in Drosophila cells." Science **303**(5659): 832-835.

Bradford, M. M. (1976). "A rapid and sensitive method for the quantitation of microgram quantities of protein utilizing the principle of protein-dye binding." Anal Biochem **72**: 248-254.

Brinker, A., G. Pfeifer, M. J. Kerner, D. J. Naylor, F. U. Hartl and M. Hayer-Hartl (2001). "Dual function of protein confinement in chaperonin-assisted protein folding." Cell **107**(2): 223-233.

Brockwell, D. J. and S. E. Radford (2007). "Intermediates: ubiquitous species on folding energy landscapes?" Curr Opin Struct Biol **17**(1): 30-37.

Brownell, S. E., R. A. Becker and L. Steinman (2012). "The protective and therapeutic function of small heat shock proteins in neurological diseases." Front Immunol **3**: 74.

Brunet, A., L. B. Sweeney, J. F. Sturgill, K. F. Chua, P. L. Greer, Y. Lin, H. Tran, S. E. Ross, R. Mostoslavsky, H. Y. Cohen, L. S. Hu, H. L. Cheng, M. P. Jedrychowski, S. P. Gygi, D. A. Sinclair, F. W. Alt and M. E. Greenberg (2004). "Stress-dependent regulation of FOXO transcription factors by the SIRT1 deacetylase." Science **303**(5666): 2011-2015.

Bu, L., Y. Jin, Y. Shi, R. Chu, A. Ban, H. Eiberg, L. Andres, H. Jiang, G. Zheng, M. Qian, B. Cui, Y. Xia, J. Liu, L. Hu, G. Zhao, M. R. Hayden and X. Kong (2002). "Mutant DNA-binding domain of HSF4 is associated with autosomal dominant lamellar and Marner cataract." Nat Genet **31**(3): 276-278.

Buchan, J. R. and R. Parker (2009). "Eukaryotic stress granules: the ins and outs of translation." Mol Cell **36**(6): 932-941.

Buchberger, A., B. Bukau and T. Sommer (2010). "Protein quality control in the cytosol and the endoplasmic reticulum: brothers in arms." Mol Cell **40**(2): 238-252.

Bulteau, A. L., L. I. Szweda and B. Friguet (2002). "Age-dependent declines in proteasome activity in the heart." Arch Biochem Biophys **397**(2): 298-304.

Burnett, C., S. Valentini, F. Cabreiro, M. Goss, M. Somogyvari, M. D. Piper, M. Hoddinott, G. L. Sutphin, V. Leko, J. J. McElwee, R. P. Vazquez-Manrique, A. M. Orfila, D. Ackerman, C. Au, G. Vinti, M. Riesen, K. Howard, C. Neri, A. Bedalov, M. Kaeberlein, C. Soti, L. Partridge and D. Gems (2011). "Absence of effects of Sir2 overexpression on lifespan in C. elegans and Drosophila." Nature **477**(7365): 482-485.

Cabrita, L. D., S. T. Hsu, H. Launay, C. M. Dobson and J. Christodoulou (2009). "Probing ribosome-nascent chain complexes produced in vivo by NMR spectroscopy." Proc Natl Acad Sci U S A **106**(52): 22239-22244.

Cadwell, K. and L. Coscoy (2005). "Ubiquitination on nonlysine residues by a viral E3 ubiquitin ligase." Science **309**(5731): 127-130.

Calamini, B., M. C. Silva, F. Madoux, D. M. Hutt, S. Khanna, M. A. Chalfant, S. A. Saldanha, P. Hodder, B. D. Tait, D. Garza, W. E. Balch and R. I. Morimoto (2012). "Small-molecule proteostasis regulators for protein conformational diseases." Nat Chem Biol **8**(2): 185-196.

Caron, C., C. Boyault and S. Khochbin (2005). "Regulatory cross-talk between lysine acetylation and ubiquitination: role in the control of protein stability." Bioessays **27**(4): 408-415.

Carrard, G., A. L. Bulteau, I. Petropoulos and B. Friguet (2002). "Impairment of proteasome structure and function in aging." Int J Biochem Cell Biol **34**(11): 1461-1474.

Carter, S. D. and C. Sjogren (2012). "The SMC complexes, DNA and chromosome topology: right or knot?" Crit Rev Biochem Mol Biol **47**(1): 1-16.

Chachisvilis, M., Y. L. Zhang and J. A. Frangos (2006). "G protein-coupled receptors sense fluid shear stress in endothelial cells." Proc Natl Acad Sci U S A **103**(42): 15463-15468.

Chakraborty, K., M. Chatila, J. Sinha, Q. Shi, B. C. Poschner, M. Sikor, G. Jiang, D. C. Lamb, F. U. Hartl and M. Hayer-Hartl (2010). "Chaperonin-catalyzed rescue of kinetically trapped states in protein folding." Cell **142**(1): 112-122.

Chan, E. Y. (2009). "mTORC1 phosphorylates the ULK1-mAtg13-FIP200 autophagy regulatory complex." Sci Signal **2**(84): pe51.

Chang, H. C., Y. C. Tang, M. Hayer-Hartl and F. U. Hartl (2007). "SnapShot: molecular chaperones, Part I." Cell **128**(1): 212.

Chang, Y., P. Ostling, M. Akerfelt, D. Trouillet, M. Rallu, Y. Gitton, R. El Fatimy, V. Fardeau, S. Le Crom, M. Morange, L. Sistonen and V. Mezger (2006). "Role of heat-shock factor 2 in cerebral cortex formation and as a regulator of p35 expression." Genes Dev **20**(7): 836-847.

Chapman, H. A., R. J. Riese and G. P. Shi (1997). "Emerging roles for cysteine proteases in human biology." Annu Rev Physiol **59**: 63-88.

Chen, B., D. Zhong and A. Monteiro (2006). "Comparative genomics and evolution of the HSP90 family of genes across all kingdoms of organisms." BMC Genomics **7**: 156.

Chen, D., A. D. Steele, G. Hutter, J. Bruno, A. Govindarajan, E. Easlon, S. J. Lin, A. Aguzzi, S. Lindquist and L. Guarente (2008). "The role of calorie restriction and SIRT1 in prion-mediated neurodegeneration." Exp Gerontol **43**(12): 1086-1093.

Cheung, Z. H. and N. Y. Ip (2009). "The emerging role of autophagy in Parkinson's disease." Mol Brain **2**: 29.

Chiti, F. and C. M. Dobson (2006). "Protein misfolding, functional amyloid, and human disease." Annu Rev Biochem **75**: 333-366.

Chitra, S., G. Nalini and G. Rajasekhar (2012). "The ubiquitin proteasome system and efficacy of proteasome inhibitors in diseases." Int J Rheum Dis **15**(3): 249-260.

Cho, Y. W., T. Hong, S. Hong, H. Guo, H. Yu, D. Kim, T. Guszczynski, G. R. Dressler, T. D. Copeland, M. Kalkum and K. Ge (2007). "PTIP associates with MLL3- and MLL4-containing histone H3 lysine 4 methyltransferase complex." J Biol Chem **282**(28): 20395-20406.

Chou, S. D., T. Prince, J. Gong and S. K. Calderwood (2012). "mTOR is essential for the proteotoxic stress response, HSF1 activation and heat shock protein synthesis." PLoS One **7**(6): e39679.

Ciechanover, A. and P. Brundin (2003). "The ubiquitin proteasome system in neurodegenerative diseases: sometimes the chicken, sometimes the egg." Neuron **40**(2): 427-446.

Ciechanover, A., A. Orian and A. L. Schwartz (2000). "Ubiquitin-mediated proteolysis: biological regulation via destruction." Bioessays **22**(5): 442-451.

Ciocca, D. R., A. P. Arrigo and S. K. Calderwood (2013). "Heat shock proteins and heat shock factor 1 in carcinogenesis and tumor development: an update." Arch Toxicol **87**(1): 19-48.

Cohen, E., J. Bieschke, R. M. Perciavalle, J. W. Kelly and A. Dillin (2006). "Opposing activities protect against age-onset proteotoxicity." Science **313**(5793): 1604-1610.

Collier, N. C., M. P. Sheetz and M. J. Schlesinger (1993). "Concomitant changes in mitochondria and intermediate filaments during heat shock and recovery of chicken embryo fibroblasts." J Cell Biochem **52**(3): 297-307.

Conconi, M., L. I. Szweda, R. L. Levine, E. R. Stadtman and B. Friguet (1996). "Age-related decline of rat liver multicatalytic proteinase activity and protection from oxidative inactivation by heat-shock protein 90." Arch Biochem Biophys **331**(2): 232-240.

Daggett, V. and A. R. Fersht (2003). "Is there a unifying mechanism for protein folding?" Trends Biochem Sci **28**(1): 18-25.

Dai, C., L. Whitesell, A. B. Rogers and S. Lindquist (2007). "Heat shock factor 1 is a powerful multifaceted modifier of carcinogenesis." Cell **130**(6): 1005-1018.

Dang Do, A. N., S. R. Kimball, D. R. Cavener and L. S. Jefferson (2009). "eIF2alpha kinases GCN2 and PERK modulate transcription and translation of distinct sets of mRNAs in mouse liver." Physiol Genomics **38**(3): 328-341.

David, D. C., N. Ollikainen, J. C. Trinidad, M. P. Cary, A. L. Burlingame and C. Kenyon (2010). "Widespread protein aggregation as an inherent part of aging in C. elegans." PLoS Biol **8**(8): e1000450.

Demchenko, A. P. (2001). "Recognition between flexible protein molecules: induced and assisted folding." J Mol Recognit **14**(1): 42-61.

Denegri, M., I. Chiodi, M. Corioni, F. Cobianchi, S. Riva and G. Biamonti (2001). "Stress-induced nuclear bodies are sites of accumulation of pre-mRNA processing factors." Mol Biol Cell **12**(11): 3502-3514.

DePristo, M. A., D. M. Weinreich and D. L. Hartl (2005). "Missense meanderings in sequence space: a biophysical view of protein evolution." Nat Rev Genet **6**(9): 678-687.

Deshaies, R. J., B. D. Koch, M. Werner-Washburne, E. A. Craig and R. Schekman (1988). "A subfamily of stress proteins facilitates translocation of secretory and mitochondrial precursor polypeptides." Nature **332**(6167): 800-805.

Dick, T. P., A. K. Nussbaum, M. Deeg, W. Heinemeyer, M. Groll, M. Schirle, W. Keilholz, S. Stevanovic, D. H. Wolf, R. Huber, H. G. Rammensee and H. Schild (1998). "Contribution of proteasomal beta-subunits to the cleavage of peptide substrates analyzed with yeast mutants." J Biol Chem **273**(40): 25637-25646.

Dickson, R. C., E. E. Nagiec, M. Skrzypek, P. Tillman, G. B. Wells and R. L. Lester (1997). "Sphingolipids are potential heat stress signals in Saccharomyces." J Biol Chem **272**(48): 30196-30200.

Dill, K. A. and H. S. Chan (1997). "From Levinthal to pathways to funnels." Nat Struct Biol **4**(1): 10-19.

Dimauro, T. and G. David (2009). "Chromatin modifications: the driving force of senescence and aging?" Aging (Albany NY) **1**(2): 182-190.

Dobson, C. M. (2003). "Protein folding and misfolding." Nature **426**(6968): 884-890.

Dobson, C. M. (2004). "Principles of protein folding, misfolding and aggregation." Semin Cell Dev Biol **15**(1): 3-16.

Dokladny, K., M. N. Zuhl, M. Mandell, D. Bhattacharya, S. Schneider, V. Deretic and P. L. Moseley (2013). "Regulatory coordination between two major intracellular homeostatic systems: heat shock response and autophagy." J Biol Chem.

Dorman, J. B., B. Albinder, T. Shroyer and C. Kenyon (1995). "The age-1 and daf-2 genes function in a common pathway to control the lifespan of Caenorhabditis elegans." Genetics **141**(4): 1399-1406.

Douglas, P. M. and A. Dillin (2010). "Protein homeostasis and aging in neurodegeneration." J Cell Biol **190**(5): 719-729.

Dunker, A. K., I. Silman, V. N. Uversky and J. L. Sussman (2008). "Function and structure of inherently disordered proteins." Curr Opin Struct Biol **18**(6): 756-764.

Eichmann, C., S. Preissler, R. Riek and E. Deuerling (2010). "Cotranslational structure acquisition of nascent polypeptides monitored by NMR spectroscopy." Proc Natl Acad Sci U S A **107**(20): 9111-9116.

Eichner, T., A. P. Kalverda, G. S. Thompson, S. W. Homans and S. E. Radford (2011). "Conformational conversion during amyloid formation at atomic resolution." Mol Cell **41**(2): 161-172.

Ellis, R. J. (2001). "Macromolecular crowding: an important but neglected aspect of the intracellular environment." Curr Opin Struct Biol **11**(1): 114-119.

Ellis, R. J. and S. M. Hemmingsen (1989). "Molecular chaperones: proteins essential for the biogenesis of some macromolecular structures." Trends Biochem Sci **14**(8): 339-342.

Ellis, R. J. and A. P. Minton (2006). "Protein aggregation in crowded environments." Biol Chem **387**(5): 485-497.

Ferbitz, L., T. Maier, H. Patzelt, B. Bukau, E. Deuerling and N. Ban (2004). "Trigger factor in complex with the ribosome forms a molecular cradle for nascent proteins." Nature **431**(7008): 590-596.

Fersht, A. R. (2000). "Transition-state structure as a unifying basis in protein-folding mechanisms: contact order, chain topology, stability, and the extended nucleus mechanism." Proc Natl Acad Sci U S A **97**(4): 1525-1529.

Fischer, G. and H. Bang (1985). "The refolding of urea-denatured ribonuclease A is catalyzed by peptidyl-prolyl cis-trans isomerase." Biochim Biophys Acta **828**(1): 39-42.

Frydman, J. (2001). "Folding of newly translated proteins in vivo: the role of molecular chaperones." Annu Rev Biochem **70**: 603-647.

Frydman, J., E. Nimmesgern, K. Ohtsuka and F. U. Hartl (1994). "Folding of nascent polypeptide chains in a high molecular mass assembly with molecular chaperones." Nature **370**(6485): 111-117.

Fujimoto, M., N. Hayashida, T. Katoh, K. Oshima, T. Shinkawa, R. Prakasam, K. Tan, S. Inouye, R. Takii and A. Nakai (2010). "A novel mouse HSF3 has the potential to activate nonclassical heat-shock genes during heat shock." Mol Biol Cell **21**(1): 106-116.

Fujimoto, M., H. Izu, K. Seki, K. Fukuda, T. Nishida, S. Yamada, K. Kato, S. Yonemura, S. Inouye and A. Nakai (2004). "HSF4 is required for normal cell growth and differentiation during mouse lens development." EMBO J **23**(21): 4297-4306.

Fujimoto, M., E. Takaki, T. Hayashi, Y. Kitaura, Y. Tanaka, S. Inouye and A. Nakai (2005). "Active HSF1 significantly suppresses polyglutamine aggregate formation in cellular and mouse models." J Biol Chem **280**(41): 34908-34916.

Funk, R. H., F. Nagel, F. Wonka, H. E. Krinke, F. Golfert and A. Hofer (1999). "Effects of heat shock on the functional morphology of cell organelles observed by video-enhanced microscopy." Anat Rec **255**(4): 458-464.

Gamerdinger, M., P. Hajieva, A. M. Kaya, U. Wolfrum, F. U. Hartl and C. Behl (2009). "Protein quality control during aging involves recruitment of the macroautophagy pathway by BAG3." EMBO J **28**(7): 889-901.

Garrido, C., C. Paul, R. Seigneuric and H. H. Kampinga (2012). "The small heat shock proteins family: the long forgotten chaperones." Int J Biochem Cell Biol **44**(10): 1588-1592.

Gasch, A. P., P. T. Spellman, C. M. Kao, O. Carmel-Harel, M. B. Eisen, G. Storz, D. Botstein and P. O. Brown (2000). "Genomic expression programs in the response of yeast cells to environmental changes." Mol Biol Cell **11**(12): 4241-4257.

Geng, H., Q. Liu, C. Xue, L. L. David, T. M. Beer, G. V. Thomas, M. S. Dai and D. Z. Qian (2012). "HIF1alpha protein stability is increased by acetylation at lysine 709." J Biol Chem **287**(42): 35496-35505.

Gething, M. J. and J. Sambrook (1992). "Protein folding in the cell." Nature **355**(6355): 33-45.

Gidalevitz, T., V. Prahlad and R. I. Morimoto (2011). "The stress of protein misfolding: from single cells to multicellular organisms." Cold Spring Harb Perspect Biol **3**(6).

Gingras, A. C., B. Raught and N. Sonenberg (2004). "mTOR signaling to translation." Curr Top Microbiol Immunol **279**: 169-197.

Glickman, M. H. and A. Ciechanover (2002). "The ubiquitin-proteasome proteolytic pathway: destruction for the sake of construction." Physiol Rev **82**(2): 373-428.

Glickman, M. H., D. M. Rubin, O. Coux, I. Wefes, G. Pfeifer, Z. Cjeka, W. Baumeister, V. A. Fried and D. Finley (1998). "A subcomplex of the proteasome regulatory particle required for ubiquitin-conjugate degradation and related to the COP9-signalosome and eIF3." Cell **94**(5): 615-623.

Goodson, M. L. and K. D. Sarge (1995). "Heat-inducible DNA binding of purified heat shock transcription factor 1." J Biol Chem **270**(6): 2447-2450.

Groll, M., M. Bajorek, A. Kohler, L. Moroder, D. M. Rubin, R. Huber, M. H. Glickman and D. Finley (2000). "A gated channel into the proteasome core particle." Nat Struct Biol **7**(11): 1062-1067.

Gupta, R., P. Kasturi, A. Bracher, C. Loew, M. Zheng, A. Villella, D. Garza, F. U. Hartl and S. Raychaudhuri (2011). "Firefly luciferase mutants as sensors of proteome stress." Nat Methods **8**(10): 879-884.

Haass, C. and D. J. Selkoe (2007). "Soluble protein oligomers in neurodegeneration: lessons from the Alzheimer's amyloid beta-peptide." Nat Rev Mol Cell Biol **8**(2): 101-112.

Hahn, J. S., Z. Hu, D. J. Thiele and V. R. Iyer (2004). "Genome-wide analysis of the biology of stress responses through heat shock transcription factor." Mol Cell Biol **24**(12): 5249-5256.

Hanahan, D. (1983). "Studies on transformation of Escherichia coli with plasmids." J Mol Biol **166**(4): 557-580.

Harding, H. P., Y. Zhang and D. Ron (1999). "Protein translation and folding are coupled by an endoplasmic-reticulum-resident kinase." Nature **397**(6716): 271-274.

Hartl, F. U., A. Bracher and M. Hayer-Hartl (2011). "Molecular chaperones in protein folding and proteostasis." Nature **475**(7356): 324-332.

Hartl, F. U. and M. Hayer-Hartl (2002). "Molecular chaperones in the cytosol: from nascent chain to folded protein." Science **295**(5561): 1852-1858.

Hartl, F. U. and M. Hayer-Hartl (2009). "Converging concepts of protein folding in vitro and in vivo." Nat Struct Mol Biol **16**(6): 574-581.

Haslbeck, M. (2002). "sHsps and their role in the chaperone network." Cell Mol Life Sci **59**(10): 1649-1657.

Haslberger, T., A. Zdanowicz, I. Brand, J. Kirstein, K. Turgay, A. Mogk and B. Bukau (2008). "Protein disaggregation by the AAA+ chaperone ClpB involves partial threading of looped polypeptide segments." Nat Struct Mol Biol **15**(6): 641-650.

Hatakeyama, S., M. Matsumoto, M. Yada and K. I. Nakayama (2004). "Interaction of U-box-type ubiquitin-protein ligases (E3s) with molecular chaperones." Genes Cells **9**(6): 533-548.

Hatakeyama, S., M. Yada, M. Matsumoto, N. Ishida and K. I. Nakayama (2001). "U box proteins as a new family of ubiquitin-protein ligases." J Biol Chem **276**(35): 33111-33120.

Haynes, C. M. and D. Ron (2010). "The mitochondrial UPR - protecting organelle protein homeostasis." J Cell Sci **123**(Pt 22): 3849-3855.

Haze, K., H. Yoshida, H. Yanagi, T. Yura and K. Mori (1999). "Mammalian transcription factor ATF6 is synthesized as a transmembrane protein and activated by proteolysis in response to endoplasmic reticulum stress." Mol Biol Cell **10**(11): 3787-3799.

Helling, R. B., H. M. Goodman and H. W. Boyer (1974). "Analysis of endonuclease R-EcoRI fragments of DNA from lambdoid bacteriophages and other viruses by agarose-gel electrophoresis." J Virol **14**(5): 1235-1244.

Hershko, A. and A. Ciechanover (1998). "The ubiquitin system." Annu Rev Biochem **67**: 425-479.

Hershko, A., H. Heller, S. Elias and A. Ciechanover (1983). "Components of ubiquitin-protein ligase system. Resolution, affinity purification, and role in protein breakdown." J Biol Chem **258**(13): 8206-8214.

Hershko, A., H. Heller, E. Eytan, G. Kaklij and I. A. Rose (1984). "Role of the alpha-amino group of protein in ubiquitin-mediated protein breakdown." Proc Natl Acad Sci U S A **81**(22): 7021-7025.

Hesterkamp, T., S. Hauser, H. Lutcke and B. Bukau (1996). "Escherichia coli trigger factor is a prolyl isomerase that associates with nascent polypeptide chains." Proc Natl Acad Sci U S A **93**(9): 4437-4441.

Heydari, A. R., S. You, R. Takahashi, A. Gutsmann-Conrad, K. D. Sarge and A. Richardson (2000). "Age-related alterations in the activation of heat shock transcription factor 1 in rat hepatocytes." Exp Cell Res **256**(1): 83-93.

Hietakangas, V., J. K. Ahlskog, A. M. Jakobsson, M. Hellesuo, N. M. Sahlberg, C. I. Holmberg, A. Mikhailov, J. J. Palvimo, L. Pirkkala and L. Sistonen (2003). "Phosphorylation of serine 303 is a prerequisite for the stress-inducible SUMO modification of heat shock factor 1." Mol Cell Biol **23**(8): 2953-2968.

Hipp, M. S., B. Kalveram, S. Raasi, M. Groettrup and G. Schmidtke (2005). "FAT10, a ubiquitin-independent signal for proteasomal degradation." Mol Cell Biol **25**(9): 3483-3491.

Hocine, S., R. H. Singer and D. Grunwald (2010). "RNA processing and export." Cold Spring Harb Perspect Biol **2**(12): a000752.

Hollien, J. and J. S. Weissman (2006). "Decay of endoplasmic reticulum-localized mRNAs during the unfolded protein response." Science **313**(5783): 104-107.

Holmberg, C. I., V. Hietakangas, A. Mikhailov, J. O. Rantanen, M. Kallio, A. Meinander, J. Hellman, N. Morrice, C. MacKintosh, R. I. Morimoto, J. E. Eriksson and L. Sistonen (2001). "Phosphorylation of serine 230 promotes inducible transcriptional activity of heat shock factor 1." EMBO J **20**(14): 3800-3810.

Homma, S., X. Jin, G. Wang, N. Tu, J. Min, N. Yanasak and N. F. Mivechi (2007). "Demyelination, astrogliosis, and accumulation of ubiquitinated proteins, hallmarks of CNS disease in hsf1-deficient mice." J Neurosci **27**(30): 7974-7986.

Horton, P., K. J. Park, T. Obayashi, N. Fujita, H. Harada, C. J. Adams-Collier and K. Nakai (2007). "WoLF PSORT: protein localization predictor." Nucleic Acids Res **35**(Web Server issue): W585-587.

Horwich, A. L. and W. A. Fenton (2009). "Chaperonin-mediated protein folding: using a central cavity to kinetically assist polypeptide chain folding." Q Rev Biophys **42**(2): 83-116.

Hsu, A. L., C. T. Murphy and C. Kenyon (2003). "Regulation of aging and age-related disease by DAF-16 and heat-shock factor." Science **300**(5622): 1142-1145.

Hulkko, S. M., H. Wakui and J. Zilliacus (2000). "The pro-apoptotic protein death-associated protein 3 (DAP3) interacts with the glucocorticoid receptor and affects the receptor function." Biochem J **349 Pt 3**: 885-893.

Hundley, H. A., W. Walter, S. Bairstow and E. A. Craig (2005). "Human Mpp11 J protein: ribosome-tethered molecular chaperones are ubiquitous." Science **308**(5724): 1032-1034.

Ibata, K., M. Fukuda, T. Hamada, H. Kabayama and K. Mikoshiba (2000). "Synaptotagmin IV is present at the Golgi and distal parts of neurites." J Neurochem **74**(2): 518-526.

Iwata, A., B. E. Riley, J. A. Johnston and R. R. Kopito (2005). "HDAC6 and microtubules are required for autophagic degradation of aggregated huntingtin." J Biol Chem **280**(48): 40282-40292.

Jackson, S. E. (1998). "How do small single-domain proteins fold?" Fold Des **3**(4): R81-91.

Jackson, S. E. (2013). "Hsp90: structure and function." Top Curr Chem **328**: 155-240.

Jahn, T. R. and S. E. Radford (2005). "The Yin and Yang of protein folding." FEBS J **272**(23): 5962-5970.

Jahn, T. R. and S. E. Radford (2008). "Folding versus aggregation: polypeptide conformations on competing pathways." Arch Biochem Biophys **469**(1): 100-117.

Jakob, U., M. Gaestel, K. Engel and J. Buchner (1993). "Small heat shock proteins are molecular chaperones." J Biol Chem **268**(3): 1517-1520.

Johnston, H., J. Kneer, I. Chackalaparampil, P. Yaciuk and J. Chrivia (1999). "Identification of a novel SNF2/SWI2 protein family member, SRCAP, which interacts with CREB-binding protein." J Biol Chem **274**(23): 16370-16376.

Johnston, J. A., C. L. Ward and R. R. Kopito (1998). "Aggresomes: a cellular response to misfolded proteins." J Cell Biol **143**(7): 1883-1898.

Jolly, C. and S. C. Lakhotia (2006). "Human sat III and Drosophila hsr omega transcripts: a common paradigm for regulation of nuclear RNA processing in stressed cells." Nucleic Acids Res **34**(19): 5508-5514.

Jolly, C., R. Morimoto, M. Robert-Nicoud and C. Vourc'h (1997). "HSF1 transcription factor concentrates in nuclear foci during heat shock: relationship with transcription sites." J Cell Sci **110 (Pt 23)**: 2935-2941.

Kaeberlein, M., M. McVey and L. Guarente (1999). "The SIR2/3/4 complex and SIR2 alone promote longevity in Saccharomyces cerevisiae by two different mechanisms." Genes Dev **13**(19): 2570-2580.

Kaileh, M., W. Vanden Berghe, A. Heyerick, J. Horion, J. Piette, C. Libert, D. De Keukeleire, T. Essawi and G. Haegeman (2007). "Withaferin a strongly elicits IkappaB kinase beta hyperphosphorylation concomitant with potent inhibition of its kinase activity." J Biol Chem **282**(7): 4253-4264.

Kaiser, C. M., H. C. Chang, V. R. Agashe, S. K. Lakshmipathy, S. A. Etchells, M. Hayer-Hartl, F. U. Hartl and J. M. Barral (2006). "Real-time observation of trigger factor function on translating ribosomes." Nature **444**(7118): 455-460.

Kallio, M., Y. Chang, M. Manuel, T. P. Alastalo, M. Rallu, Y. Gitton, L. Pirkkala, M. T. Loones, L. Paslaru, S. Larney, S. Hiard, M. Morange, L. Sistonen and V. Mezger (2002). "Brain abnormalities, defective meiotic chromosome synapsis and female subfertility in HSF2 null mice." EMBO J **21**(11): 2591-2601.

Kampinga, H. H. and E. A. Craig (2010). "The HSP70 chaperone machinery: J proteins as drivers of functional specificity." Nat Rev Mol Cell Biol **11**(8): 579-592.

Kang, R., H. J. Zeh, M. T. Lotze and D. Tang (2011). "The Beclin 1 network regulates autophagy and apoptosis." Cell Death Differ **18**(4): 571-580.

Kanu, N. and A. Behrens (2007). "ATMIN defines an NBS1-independent pathway of ATM signalling." EMBO J **26**(12): 2933-2941.

Kanu, N., K. Penicud, M. Hristova, B. Wong, E. Irvine, F. Plattner, G. Raivich and A. Behrens (2010). "The ATM cofactor ATMIN protects against oxidative stress and accumulation of DNA damage in the aging brain." J Biol Chem **285**(49): 38534-38542.

Katahira, J. (2009). "[Regulation of nuclear export and cytoplasmic localization of mRNAs by NXF family proteins]." Tanpakushitsu Kakusan Koso **54**(16 Suppl): 2109-2113.

Kawaguchi, T., K. Miyazawa, S. Moriya, T. Ohtomo, X. F. Che, M. Naito, M. Itoh and A. Tomoda (2011). "Combined treatment with bortezomib plus bafilomycin A1 enhances the cytocidal effect and induces endoplasmic reticulum stress in U266 myeloma cells: crosstalk among proteasome, autophagy-lysosome and ER stress." Int J Oncol **38**(3): 643-654.

Kenyon, C., J. Chang, E. Gensch, A. Rudner and R. Tabtiang (1993). "A C. elegans mutant that lives twice as long as wild type." Nature **366**(6454): 461-464.

Kerner, M. J., D. J. Naylor, Y. Ishihama, T. Maier, H. C. Chang, A. P. Stines, C. Georgopoulos, D. Frishman, M. Hayer-Hartl, M. Mann and F. U. Hartl (2005). "Proteome-wide analysis of chaperonin-dependent protein folding in Escherichia coli." Cell **122**(2): 209-220.

Kim, J. Y., K. B. Kim, G. H. Eom, N. Choe, H. J. Kee, H. J. Son, S. T. Oh, D. W. Kim, J. H. Pak, H. J. Baek, H. Kook, Y. Hahn, H. Kook, D. Chakravarti and S. B. Seo (2012). "KDM3B is the H3K9 demethylase involved in transcriptional activation of lmo2 in leukemia." Mol Cell Biol **32**(14): 2917-2933.

Kim, P. S. and R. L. Baldwin (1982). "Specific intermediates in the folding reactions of small proteins and the mechanism of protein folding." Annu Rev Biochem **51**: 459-489.

Kimura, Y. and K. Tanaka (2010). "Regulatory mechanisms involved in the control of ubiquitin homeostasis." J Biochem **147**(6): 793-798.

Kirkin, V., T. Lamark, Y. S. Sou, G. Bjorkoy, J. L. Nunn, J. A. Bruun, E. Shvets, D. G. McEwan, T. H. Clausen, P. Wild, I. Bilusic, J. P. Theurillat, A. Overvatn, T. Ishii, Z.

Elazar, M. Komatsu, I. Dikic and T. Johansen (2009). "A role for NBR1 in autophagosomal degradation of ubiquitinated substrates." Mol Cell **33**(4): 505-516.

Kisselev, A. F., T. N. Akopian, K. M. Woo and A. L. Goldberg (1999). "The sizes of peptides generated from protein by mammalian 26 and 20 S proteasomes. Implications for understanding the degradative mechanism and antigen presentation." J Biol Chem **274**(6): 3363-3371.

Kisselev, A. F. and A. L. Goldberg (2001). "Proteasome inhibitors: from research tools to drug candidates." Chem Biol **8**(8): 739-758.

Kittler, R., A. K. Heninger, K. Franke, B. Habermann and F. Buchholz (2005). "Production of endoribonuclease-prepared short interfering RNAs for gene silencing in mammalian cells." Nat Methods **2**(10): 779-784.

Kittler, R., L. Pelletier, A. K. Heninger, M. Slabicki, M. Theis, L. Miroslaw, I. Poser, S. Lawo, H. Grabner, K. Kozak, J. Wagner, V. Surendranath, C. Richter, W. Bowen, A. L. Jackson, B. Habermann, A. A. Hyman and F. Buchholz (2007). "Genome-scale RNAi profiling of cell division in human tissue culture cells." Nat Cell Biol **9**(12): 1401-1412.

Klomsiri, C., P. A. Karplus and L. B. Poole (2011). "Cysteine-based redox switches in enzymes." Antioxid Redox Signal **14**(6): 1065-1077.

Knauf, U., E. M. Newton, J. Kyriakis and R. E. Kingston (1996). "Repression of human heat shock factor 1 activity at control temperature by phosphorylation." Genes Dev **10**(21): 2782-2793.

Koegl, M., T. Hoppe, S. Schlenker, H. D. Ulrich, T. U. Mayer and S. Jentsch (1999). "A novel ubiquitination factor, E4, is involved in multiubiquitin chain assembly." Cell **96**(5): 635-644.

Komander, D. (2009). "The emerging complexity of protein ubiquitination." Biochem Soc Trans **37**(Pt 5): 937-953.

Kong, X., Z. Lin, D. Liang, D. Fath, N. Sang and J. Caro (2006). "Histone deacetylase inhibitors induce VHL and ubiquitin-independent proteasomal degradation of hypoxia-inducible factor 1alpha." Mol Cell Biol **26**(6): 2019-2028.

Korolchuk, V. I., A. Mansilla, F. M. Menzies and D. C. Rubinsztein (2009). "Autophagy inhibition compromises degradation of ubiquitin-proteasome pathway substrates." Mol Cell **33**(4): 517-527.

Kourtis, N. and N. Tavernarakis (2011). "Cellular stress response pathways and ageing: intricate molecular relationships." EMBO J **30**(13): 2520-2531.

Kramer, D. L., B. D. Chang, Y. Chen, P. Diegelman, K. Alm, A. R. Black, I. B. Roninson and C. W. Porter (2001). "Polyamine depletion in human melanoma cells leads to G1 arrest associated with induction of p21WAF1/CIP1/SDI1, changes in the expression of p21-regulated genes, and a senescence-like phenotype." Cancer Res **61**(21): 7754-7762.

Kramer, G., T. Rauch, W. Rist, S. Vorderwulbecke, H. Patzelt, A. Schulze-Specking, N. Ban, E. Deuerling and B. Bukau (2002). "L23 protein functions as a chaperone docking site on the ribosome." Nature **419**(6903): 171-174.

Krogh, A., B. Larsson, G. von Heijne and E. L. Sonnhammer (2001). "Predicting transmembrane protein topology with a hidden Markov model: application to complete genomes." J Mol Biol **305**(3): 567-580.

Kruuv, J., D. Glofcheski, K. H. Cheng, S. D. Campbell, H. M. Al-Qysi, W. T. Nolan and J. R. Lepock (1983). "Factors influencing survival and growth of mammalian cells exposed to hypothermia. I. Effects of temperature and membrane lipid perturbers." J Cell Physiol **115**(2): 179-185.

Kuzmin, E. V., O. V. Karpova, T. E. Elthon and K. J. Newton (2004). "Mitochondrial respiratory deficiencies signal up-regulation of genes for heat shock proteins." J Biol Chem **279**(20): 20672-20677.

Laemmle, A., A. Lechleiter, V. Roh, C. Schwarz, S. Portmann, C. Furer, A. Keogh, M. P. Tschan, D. Candinas, S. A. Vorburger and D. Stroka (2012). "Inhibition of SIRT1 impairs the accumulation and transcriptional activity of HIF-1alpha protein under hypoxic conditions." PLoS One **7**(3): e33433.

Laemmli, U. K. (1970). "Cleavage of structural proteins during the assembly of the head of bacteriophage T4." Nature **227**(5259): 680-685.

Lakshmipathy, S. K., S. Tomic, C. M. Kaiser, H. C. Chang, P. Genevaux, C. Georgopoulos, J. M. Barral, A. E. Johnson, F. U. Hartl and S. A. Etchells (2007). "Identification of nascent chain interaction sites on trigger factor." J Biol Chem **282**(16): 12186-12193.

Langer, T., C. Lu, H. Echols, J. Flanagan, M. K. Hayer and F. U. Hartl (1992). "Successive action of DnaK, DnaJ and GroEL along the pathway of chaperone-mediated protein folding." Nature **356**(6371): 683-689.

Lee, A. H., N. N. Iwakoshi and L. H. Glimcher (2003). "XBP-1 regulates a subset of endoplasmic reticulum resident chaperone genes in the unfolded protein response." Mol Cell Biol **23**(21): 7448-7459.

Lee, I. H., L. Cao, R. Mostoslavsky, D. B. Lombard, J. Liu, N. E. Bruns, M. Tsokos, F. W. Alt and T. Finkel (2008). "A role for the NAD-dependent deacetylase Sirt1 in the regulation of autophagy." Proc Natl Acad Sci U S A **105**(9): 3374-3379.

Levinthal, C. J. (1968). "Are there pathways for protein folding?" J Chim Phys **65**: 44-45.

Lewis, M., P. J. Helmsing and M. Ashburner (1975). "Parallel changes in puffing activity and patterns of protein synthesis in salivary glands of Drosophila." Proc Natl Acad Sci U S A **72**(9): 3604-3608.

Li, Q., H. Xiao and K. Isobe (2002). "Histone acetyltransferase activities of cAMP-regulated enhancer-binding protein and p300 in tissues of fetal, young, and old mice." J Gerontol A Biol Sci Med Sci **57**(3): B93-98.

Li, X. (2013). "SIRT1 and energy metabolism." Acta Biochim Biophys Sin (Shanghai) **45**(1): 51-60.

Liberek, K., A. Lewandowska and S. Zietkiewicz (2008). "Chaperones in control of protein disaggregation." EMBO J **27**(2): 328-335.

Lin, K., J. B. Dorman, A. Rodan and C. Kenyon (1997). "daf-16: An HNF-3/forkhead family member that can function to double the life-span of Caenorhabditis elegans." Science **278**(5341): 1319-1322.

Lin, Z., D. Madan and H. S. Rye (2008). "GroEL stimulates protein folding through forced unfolding." Nat Struct Mol Biol **15**(3): 303-311.

Lindberg, M. O. and M. Oliveberg (2007). "Malleability of protein folding pathways: a simple reason for complex behaviour." Curr Opin Struct Biol **17**(1): 21-29.

Lindquist, S. (1986). "The heat-shock response." Annu Rev Biochem **55**: 1151-1191.

Littlefield, O. and H. C. Nelson (1999). "A new use for the 'wing' of the 'winged' helix-turn-helix motif in the HSF-DNA cocrystal." Nat Struct Biol **6**(5): 464-470.

Liu, J., D. J. O'Kane and A. Escher (1997). "Secretion of functional Renilla reniformis luciferase by mammalian cells." Gene **203**(2): 141-148.

Loison, F., L. Debure, P. Nizard, P. le Goff, D. Michel and Y. le Drean (2006). "Up-regulation of the clusterin gene after proteotoxic stress: implication of HSF1-HSF2 heterocomplexes." Biochem J **395**(1): 223-231.

Lorbeck, M. T., N. Singh, A. Zervos, M. Dhatta, M. Lapchenko, C. Yang and F. Elefant (2010). "The histone demethylase Dmel\Kdm4A controls genes required for life span and male-specific sex determination in Drosophila." Gene **450**(1-2): 8-17.

Lu, J. and C. Deutsch (2005). "Folding zones inside the ribosomal exit tunnel." Nat Struct Mol Biol **12**(12): 1123-1129.

Luders, J., J. Demand and J. Hohfeld (2000). "The ubiquitin-related BAG-1 provides a link between the molecular chaperones Hsc70/Hsp70 and the proteasome." J Biol Chem **275**(7): 4613-4617.

Lupas, A., W. Baumeister and K. Hofmann (1997). "A repetitive sequence in subunits of the 26S proteasome and 20S cyclosome (anaphase-promoting complex)." Trends Biochem Sci **22**(6): 195-196.

Malo, N., J. A. Hanley, S. Cerquozzi, J. Pelletier and R. Nadon (2006). "Statistical practice in high-throughput screening data analysis." Nat Biotechnol **24**(2): 167-175.

Marambaud, P., H. Zhao and P. Davies (2005). "Resveratrol promotes clearance of Alzheimer's disease amyloid-beta peptides." J Biol Chem **280**(45): 37377-37382.

Marone, M., S. Mozzetti, D. De Ritis, L. Pierelli and G. Scambia (2001). "Semiquantitative RT-PCR analysis to assess the expression levels of multiple transcripts from the same sample." Biol Proced Online **3**: 19-25.

Massey, A. C., C. Zhang and A. M. Cuervo (2006). "Chaperone-mediated autophagy in aging and disease." Curr Top Dev Biol **73**: 205-235.

Mathew, A., S. K. Mathur and R. I. Morimoto (1998). "Heat shock response and protein degradation: regulation of HSF2 by the ubiquitin-proteasome pathway." Mol Cell Biol **18**(9): 5091-5098.

Maupin-Furlow, J. A., H. L. Wilson, S. J. Kaczowka and M. S. Ou (2000). "Proteasomes in the archaea: from structure to function." Front Biosci **5**: D837-865.

Mayer, C. and I. Grummt (2006). "Ribosome biogenesis and cell growth: mTOR coordinates transcription by all three classes of nuclear RNA polymerases." Oncogene **25**(48): 6384-6391.

Mayer, M. P. and B. Bukau (2005). "Hsp70 chaperones: cellular functions and molecular mechanism." Cell Mol Life Sci **62**(6): 670-684.

Mazur, P. (1984). "Freezing of living cells: mechanisms and implications." Am J Physiol **247**(3 Pt 1): C125-142.

McClellan, A. J., S. Tam, D. Kaganovich and J. Frydman (2005). "Protein quality control: chaperones culling corrupt conformations." Nat Cell Biol **7**(8): 736-741.

McMillan, D. R., X. Xiao, L. Shao, K. Graves and I. J. Benjamin (1998). "Targeted disruption of heat shock transcription factor 1 abolishes thermotolerance and protection against heat-inducible apoptosis." J Biol Chem **273**(13): 7523-7528.

Medicherla, B. and A. L. Goldberg (2008). "Heat shock and oxygen radicals stimulate ubiquitin-dependent degradation mainly of newly synthesized proteins." J Cell Biol **182**(4): 663-673.

Mehta, R., K. A. Steinkraus, G. L. Sutphin, F. J. Ramos, L. S. Shamieh, A. Huh, C. Davis, D. Chandler-Brown and M. Kaeberlein (2009). "Proteasomal regulation of the hypoxic response modulates aging in C. elegans." Science **324**(5931): 1196-1198.

Mendillo, M. L., S. Santagata, M. Koeva, G. W. Bell, R. Hu, R. M. Tamimi, E. Fraenkel, T. A. Ince, L. Whitesell and S. Lindquist (2012). "HSF1 drives a transcriptional program distinct from heat shock to support highly malignant human cancers." Cell **150**(3): 549-562.

Mercier, P. A., N. A. Winegarden and J. T. Westwood (1999). "Human heat shock factor 1 is predominantly a nuclear protein before and after heat stress." J Cell Sci **112 (Pt 16)**: 2765-2774.

Merz, F., A. Hoffmann, A. Rutkowska, B. Zachmann-Brand, B. Bukau and E. Deuerling (2006). "The C-terminal domain of Escherichia coli trigger factor represents the central module of its chaperone activity." J Biol Chem **281**(42): 31963-31971.

Metz, A., J. Soret, C. Vourc'h, J. Tazi and C. Jolly (2004). "A key role for stress-induced satellite III transcripts in the relocalization of splicing factors into nuclear stress granules." J Cell Sci **117**(Pt 19): 4551-4558.

Mizushima, N., Y. Ohsumi and T. Yoshimori (2002). "Autophagosome formation in mammalian cells." Cell Struct Funct **27**(6): 421-429.

Mizushima, N., T. Yoshimori and Y. Ohsumi (2011). "The role of Atg proteins in autophagosome formation." Annu Rev Cell Dev Biol **27**: 107-132.

Mogk, A., T. Haslberger, P. Tessarz and B. Bukau (2008). "Common and specific mechanisms of AAA+ proteins involved in protein quality control." Biochem Soc Trans **36**(Pt 1): 120-125.

Mori, T., Y. Anazawa, K. Matsui, S. Fukuda, Y. Nakamura and H. Arakawa (2002). "Cyclin K as a direct transcriptional target of the p53 tumor suppressor." Neoplasia **4**(3): 268-274.

Morimoto, R. I. (1998). "Regulation of the heat shock transcriptional response: cross talk between a family of heat shock factors, molecular chaperones, and negative regulators." Genes Dev **12**(24): 3788-3796.

Morimoto, R. I. (2008). "Proteotoxic stress and inducible chaperone networks in neurodegenerative disease and aging." Genes Dev **22**(11): 1427-1438.

Morley, J. F., H. R. Brignull, J. J. Weyers and R. I. Morimoto (2002). "The threshold for polyglutamine-expansion protein aggregation and cellular toxicity is dynamic and influenced by aging in Caenorhabditis elegans." Proc Natl Acad Sci U S A **99**(16): 10417-10422.

Morris, C. B. (1995). "Cryopreservation of animal and human cell lines." Methods Mol Biol **38**: 179-187.

Mortimore, G. E. and A. R. Poso (1987). "Intracellular protein catabolism and its control during nutrient deprivation and supply." Annu Rev Nutr **7**: 539-564.

Morton, E. A. and T. Lamitina (2013). "Caenorhabditis elegans HSF-1 is an essential nuclear protein that forms stress granule-like structures following heat shock." Aging Cell **12**(1): 112-120.

Mosmann, T. (1983). "Rapid colorimetric assay for cellular growth and survival: application to proliferation and cytotoxicity assays." J Immunol Methods **65**(1-2): 55-63.

Mosser, D. D., P. T. Kotzbauer, K. D. Sarge and R. I. Morimoto (1990). "In vitro activation of heat shock transcription factor DNA-binding by calcium and biochemical conditions that affect protein conformation." Proc Natl Acad Sci U S A **87**(10): 3748-3752.

Mukhopadhyay, D. and H. Riezman (2007). "Proteasome-independent functions of ubiquitin in endocytosis and signaling." Science **315**(5809): 201-205.

Mullis, K., F. Faloona, S. Scharf, R. Saiki, G. Horn and H. Erlich (1986). "Specific enzymatic amplification of DNA in vitro: the polymerase chain reaction." Cold Spring Harb Symp Quant Biol **51 Pt 1**: 263-273.

Murray, J. I., M. L. Whitfield, N. D. Trinklein, R. M. Myers, P. O. Brown and D. Botstein (2004). "Diverse and specific gene expression responses to stresses in cultured human cells." Mol Biol Cell **15**(5): 2361-2374.

Nawaz, Z. and B. W. O'Malley (2004). "Urban renewal in the nucleus: is protein turnover by proteasomes absolutely required for nuclear receptor-regulated transcription?" Mol Endocrinol **18**(3): 493-499.

Neef, D. W., A. M. Jaeger and D. J. Thiele (2011). "Heat shock transcription factor 1 as a therapeutic target in neurodegenerative diseases." Nat Rev Drug Discov **10**(12): 930-944.

Netzer, W. J. and F. U. Hartl (1997). "Recombination of protein domains facilitated by co-translational folding in eukaryotes." Nature **388**(6640): 343-349.

Nickells, R. W., M. J. Cavey and L. W. Browder (1988). "The effects of heat shock on the morphology and protein synthesis of the epidermis of Xenopus laevis larvae." J Cell Biol **106**(3): 905-914.

Ninomiya, K., N. Kataoka and M. Hagiwara (2011). "Stress-responsive maturation of Clk1/4 pre-mRNAs promotes phosphorylation of SR splicing factor." J Cell Biol **195**(1): 27-40.

Nover, L., K. D. Scharf and D. Neumann (1989). "Cytoplasmic heat shock granules are formed from precursor particles and are associated with a specific set of mRNAs." Mol Cell Biol **9**(3): 1298-1308.

Novoa, I., H. Zeng, H. P. Harding and D. Ron (2001). "Feedback inhibition of the unfolded protein response by GADD34-mediated dephosphorylation of eIF2alpha." J Cell Biol **153**(5): 1011-1022.

Ogiso, Y., A. Tomida and T. Tsuruo (2002). "Nuclear localization of proteasomes participates in stress-inducible resistance of solid tumor cells to topoisomerase II-directed drugs." Cancer Res **62**(17): 5008-5012.

Ogryzko, V. V., R. L. Schiltz, V. Russanova, B. H. Howard and Y. Nakatani (1996). "The transcriptional coactivators p300 and CBP are histone acetyltransferases." Cell **87**(5): 953-959.

Ohta, T. and M. Fukuda (2004). "Ubiquitin and breast cancer." Oncogene **23**(11): 2079-2088.

Olzmann, J. A., L. Li, M. V. Chudaev, J. Chen, F. A. Perez, R. D. Palmiter and L. S. Chin (2007). "Parkin-mediated K63-linked polyubiquitination targets misfolded DJ-1 to aggresomes via binding to HDAC6." J Cell Biol **178**(6): 1025-1038.

Olzscha, H., S. M. Schermann, A. C. Woerner, S. Pinkert, M. H. Hecht, G. G. Tartaglia, M. Vendruscolo, M. Hayer-Hartl, F. U. Hartl and R. M. Vabulas (2011). "Amyloid-like aggregates sequester numerous metastable proteins with essential cellular functions." Cell **144**(1): 67-78.

Ong, S. E. and M. Mann (2006). "A practical recipe for stable isotope labeling by amino acids in cell culture (SILAC)." Nat Protoc **1**(6): 2650-2660.

Onuchic, J. N. and P. G. Wolynes (2004). "Theory of protein folding." Curr Opin Struct Biol **14**(1): 70-75.

Orlowski, M. and S. Wilk (2000). "Catalytic activities of the 20 S proteasome, a multicatalytic proteinase complex." Arch Biochem Biophys **383**(1): 1-16.

Ostling, P., J. K. Bjork, P. Roos-Mattjus, V. Mezger and L. Sistonen (2007). "Heat shock factor 2 (HSF2) contributes to inducible expression of hsp genes through interplay with HSF1." J Biol Chem **282**(10): 7077-7086.

Otto, H., C. Conz, P. Maier, T. Wolfle, C. K. Suzuki, P. Jeno, P. Rucknagel, J. Stahl and S. Rospert (2005). "The chaperones MPP11 and Hsp70L1 form the mammalian ribosome-associated complex." Proc Natl Acad Sci U S A **102**(29): 10064-10069.

Pace, C. N., L. M. Fisher and J. F. Cupo (1981). "Globular protein stability: aspects of interest in protein turnover." Acta Biol Med Ger **40**(10-11): 1385-1392.

Pallos, J., L. Bodai, T. Lukacsovich, J. M. Purcell, J. S. Steffan, L. M. Thompson and J. L. Marsh (2008). "Inhibition of specific HDACs and sirtuins suppresses pathogenesis in a Drosophila model of Huntington's disease." Hum Mol Genet **17**(23): 3767-3775.

Pandey, U. B., Z. Nie, Y. Batlevi, B. A. McCray, G. P. Ritson, N. B. Nedelsky, S. L. Schwartz, N. A. DiProspero, M. A. Knight, O. Schuldiner, R. Padmanabhan, M. Hild, D. L. Berry, D. Garza, C. C. Hubbert, T. P. Yao, E. H. Baehrecke and J. P. Taylor (2007). "HDAC6 rescues neurodegeneration and provides an essential link between autophagy and the UPS." Nature **447**(7146): 859-863.

Pankiv, S., T. H. Clausen, T. Lamark, A. Brech, J. A. Bruun, H. Outzen, A. Overvatn, G. Bjorkoy and T. Johansen (2007). "p62/SQSTM1 binds directly to Atg8/LC3 to

facilitate degradation of ubiquitinated protein aggregates by autophagy." J Biol Chem **282**(33): 24131-24145.

Park, C. and S. Marqusee (2005). "Pulse proteolysis: a simple method for quantitative determination of protein stability and ligand binding." Nat Methods **2**(3): 207-212.

Park, S. H., Y. Kukushkin, R. Gupta, T. Chen, A. Konagai, M. S. Hipp, M. Hayer-Hartl and F. U. Hartl (2013). "PolyQ Proteins Interfere with Nuclear Degradation of Cytosolic Proteins by Sequestering the Sis1p Chaperone." Cell **154**(1): 134-145.

Parsell, D. A., A. S. Kowal, M. A. Singer and S. Lindquist (1994). "Protein disaggregation mediated by heat-shock protein Hsp104." Nature **372**(6505): 475-478.

Patriarca, E. J. and B. Maresca (1990). "Acquired thermotolerance following heat shock protein synthesis prevents impairment of mitochondrial ATPase activity at elevated temperatures in Saccharomyces cerevisiae." Exp Cell Res **190**(1): 57-64.

Pearl, L. H. and C. Prodromou (2006). "Structure and mechanism of the Hsp90 molecular chaperone machinery." Annu Rev Biochem **75**: 271-294.

Pech, M., T. Spreter, R. Beckmann and B. Beatrix (2010). "Dual binding mode of the nascent polypeptide-associated complex reveals a novel universal adapter site on the ribosome." J Biol Chem **285**(25): 19679-19687.

Pelham, H. R. (1982). "A regulatory upstream promoter element in the Drosophila hsp 70 heat-shock gene." Cell **30**(2): 517-528.

Pelham, H. R. (1984). "Hsp70 accelerates the recovery of nucleolar morphology after heat shock." EMBO J **3**(13): 3095-3100.

Peteranderl, R. and H. C. Nelson (1992). "Trimerization of the heat shock transcription factor by a triple-stranded alpha-helical coiled-coil." Biochemistry **31**(48): 12272-12276.

Peteranderl, R., M. Rabenstein, Y. K. Shin, C. W. Liu, D. E. Wemmer, D. S. King and H. C. Nelson (1999). "Biochemical and biophysical characterization of the trimerization domain from the heat shock transcription factor." Biochemistry **38**(12): 3559-3569.

Petesch, S. J. and J. T. Lis (2008). "Rapid, transcription-independent loss of nucleosomes over a large chromatin domain at Hsp70 loci." Cell **134**(1): 74-84.

Petrucelli, L., D. Dickson, K. Kehoe, J. Taylor, H. Snyder, A. Grover, M. De Lucia, E. McGowan, J. Lewis, G. Prihar, J. Kim, W. H. Dillmann, S. E. Browne, A. Hall, R. Voellmy, Y. Tsuboi, T. M. Dawson, B. Wolozin, J. Hardy and M. Hutton (2004). "CHIP and Hsp70 regulate tau ubiquitination, degradation and aggregation." Hum Mol Genet **13**(7): 703-714.

Pirkkala, L., T. P. Alastalo, X. Zuo, I. J. Benjamin and L. Sistonen (2000). "Disruption of heat shock factor 1 reveals an essential role in the ubiquitin proteolytic pathway." Mol Cell Biol **20**(8): 2670-2675.

Pirkkala, L., P. Nykanen and L. Sistonen (2001). "Roles of the heat shock transcription factors in regulation of the heat shock response and beyond." FASEB J **15**(7): 1118-1131.

Ponnappan, U., M. Zhong and G. U. Trebilcock (1999). "Decreased proteasome-mediated degradation in T cells from the elderly: A role in immune senescence." Cell Immunol **192**(2): 167-174.

Poon, E., E. V. Howman, S. E. Newey and K. E. Davies (2002). "Association of syncoilin and desmin: linking intermediate filament proteins to the dystrophin-associated protein complex." J Biol Chem **277**(5): 3433-3439.

Powers, E. T., R. I. Morimoto, A. Dillin, J. W. Kelly and W. E. Balch (2009). "Biological and chemical approaches to diseases of proteostasis deficiency." Annu Rev Biochem **78**: 959-991.

Prahlad, V., T. Cornelius and R. I. Morimoto (2008). "Regulation of the cellular heat shock response in Caenorhabditis elegans by thermosensory neurons." Science **320**(5877): 811-814.

Prasad, T. S., K. Kandasamy and A. Pandey (2009). "Human Protein Reference Database and Human Proteinpedia as discovery tools for systems biology." Methods Mol Biol **577**: 67-79.

Preissler, S. and E. Deuerling (2012). "Ribosome-associated chaperones as key players in proteostasis." Trends Biochem Sci **37**(7): 274-283.

Ptitsyn, O. B. (1998). "Protein folding: nucleation and compact intermediates." Biochemistry (Mosc) **63**(4): 367-373.

Ptitsyn, O. B., R. H. Pain, G. V. Semisotnov, E. Zerovnik and O. I. Razgulyaev (1990). "Evidence for a molten globule state as a general intermediate in protein folding." FEBS Lett **262**(1): 20-24.

Qian, S. B., X. Zhang, J. Sun, J. R. Bennink, J. W. Yewdell and C. Patterson (2010). "mTORC1 links protein quality and quantity control by sensing chaperone availability." J Biol Chem **285**(35): 27385-27395.

Rape, M. and S. Jentsch (2002). "Taking a bite: proteasomal protein processing." Nat Cell Biol **4**(5): E113-116.

Rappsilber, J., Y. Ishihama and M. Mann (2003). "Stop and go extraction tips for matrix-assisted laser desorption/ionization, nanoelectrospray, and LC/MS sample pretreatment in proteomics." Anal Chem **75**(3): 663-670.

Ravikumar, B., C. Vacher, Z. Berger, J. E. Davies, S. Luo, L. G. Oroz, F. Scaravilli, D. F. Easton, R. Duden, C. J. O'Kane and D. C. Rubinsztein (2004). "Inhibition of mTOR induces autophagy and reduces toxicity of polyglutamine expansions in fly and mouse models of Huntington disease." Nat Genet **36**(6): 585-595.

Raynes, R., K. M. Pombier, K. Nguyen, J. Brunquell, J. E. Mendez and S. D. Westerheide (2013). "The SIRT1 modulators AROS and DBC1 regulate HSF1 activity and the heat shock response." PLoS One **8**(1): e54364.

Richter, K., M. Haslbeck and J. Buchner (2010). "The heat shock response: life on the verge of death." Mol Cell **40**(2): 253-266.

Rikhvanov, E. G., N. N. Varakina, T. M. Rusaleva, E. I. Rachenko, D. A. Knorre and V. K. Voinikov (2005). "Do mitochondria regulate the heat-shock response in Saccharomyces cerevisiae?" Curr Genet **48**(1): 44-59.

Rincon, M., E. Rudin and N. Barzilai (2005). "The insulin/IGF-1 signaling in mammals and its relevance to human longevity." Exp Gerontol **40**(11): 873-877.

Rine, J. and I. Herskowitz (1987). "Four genes responsible for a position effect on expression from HML and HMR in Saccharomyces cerevisiae." Genetics **116**(1): 9-22.

Ritossa, F. (1962). "A new puffing pattern induced by temperature shock and DNP in Drosophila." Experientia **18**: 571-573.

Rivera, R. M., K. L. Kelley, G. W. Erdos and P. J. Hansen (2004). "Reorganization of microfilaments and microtubules by thermal stress in two-cell bovine embryos." Biol Reprod **70**(6): 1852-1862.

Rogina, B. and S. L. Helfand (2004). "Sir2 mediates longevity in the fly through a pathway related to calorie restriction." Proc Natl Acad Sci U S A **101**(45): 15998-16003.

Ron, D. and P. Walter (2007). "Signal integration in the endoplasmic reticulum unfolded protein response." Nat Rev Mol Cell Biol **8**(7): 519-529.

Rubinsztein, D. C. (2006). "The roles of intracellular protein-degradation pathways in neurodegeneration." Nature **443**(7113): 780-786.

Ruden, D. M. and X. Lu (2008). "Hsp90 affecting chromatin remodeling might explain transgenerational epigenetic inheritance in Drosophila." Curr Genomics **9**(7): 500-508.

Rudiger, S., A. Buchberger and B. Bukau (1997). "Interaction of Hsp70 chaperones with substrates." Nat Struct Biol **4**(5): 342-349.

Rutherford, S. L. and S. Lindquist (1998). "Hsp90 as a capacitor for morphological evolution." Nature **396**(6709): 336-342.

Ryan, M. T. and N. J. Hoogenraad (2007). "Mitochondrial-nuclear communications." Annu Rev Biochem **76**: 701-722.

Saad, A. H. and G. M. Hahn (1992). "Activation of potassium channels: relationship to the heat shock response." Proc Natl Acad Sci U S A **89**(20): 9396-9399.

Sakata, E., S. Bohn, O. Mihalache, P. Kiss, F. Beck, I. Nagy, S. Nickell, K. Tanaka, Y. Saeki, F. Forster and W. Baumeister (2012). "Localization of the proteasomal ubiquitin receptors Rpn10 and Rpn13 by electron cryomicroscopy." Proc Natl Acad Sci U S A **109**(5): 1479-1484.

Salomons, F. A., V. Menendez-Benito, C. Bottcher, B. A. McCray, J. P. Taylor and N. P. Dantuma (2009). "Selective accumulation of aggregation-prone proteasome substrates in response to proteotoxic stress." Mol Cell Biol **29**(7): 1774-1785.

Sandqvist, A., J. K. Bjork, M. Akerfelt, Z. Chitikova, A. Grichine, C. Vourc'h, C. Jolly, T. A. Salminen, Y. Nymalm and L. Sistonen (2009). "Heterotrimerization of heat-shock factors 1 and 2 provides a transcriptional switch in response to distinct stimuli." Mol Biol Cell **20**(5): 1340-1347.

Santagata, S., M. L. Mendillo, Y. C. Tang, A. Subramanian, C. C. Perley, S. P. Roche, B. Wong, R. Narayan, H. Kwon, M. Koeva, A. Amon, T. R. Golub, J. A. Porco, Jr., L. Whitesell and S. Lindquist (2013). "Tight coordination of protein translation and HSF1 activation supports the anabolic malignant state." Science **341**(6143): 1238303.

Santos, S. D. and M. J. Saraiva (2004). "Enlarged ventricles, astrogliosis and neurodegeneration in heat shock factor 1 null mouse brain." Neuroscience **126**(3): 657-663.

Sarge, K. D., S. P. Murphy and R. I. Morimoto (1993). "Activation of heat shock gene transcription by heat shock factor 1 involves oligomerization, acquisition of DNA-binding activity, and nuclear localization and can occur in the absence of stress." Mol Cell Biol **13**(3): 1392-1407.

Schiene, C. and G. Fischer (2000). "Enzymes that catalyse the restructuring of proteins." Curr Opin Struct Biol **10**(1): 40-45.

Schlunzen, F., D. N. Wilson, P. Tian, J. M. Harms, S. J. McInnes, H. A. Hansen, R. Albrecht, J. Buerger, S. M. Wilbanks and P. Fucini (2005). "The binding mode of the trigger factor on the ribosome: implications for protein folding and SRP interaction." Structure **13**(11): 1685-1694.

Schnell, J. D. and L. Hicke (2003). "Non-traditional functions of ubiquitin and ubiquitin-binding proteins." J Biol Chem **278**(38): 35857-35860.

Schroder, H., T. Langer, F. U. Hartl and B. Bukau (1993). "DnaK, DnaJ and GrpE form a cellular chaperone machinery capable of repairing heat-induced protein damage." EMBO J **12**(11): 4137-4144.

Shaid, S., C. H. Brandts, H. Serve and I. Dikic (2013). "Ubiquitination and selective autophagy." Cell Death Differ **20**(1): 21-30.

Shamovsky, I., M. Ivannikov, E. S. Kandel, D. Gershon and E. Nudler (2006). "RNA-mediated response to heat shock in mammalian cells." Nature **440**(7083): 556-560.

Shamovsky, I. and E. Nudler (2008). "New insights into the mechanism of heat shock response activation." Cell Mol Life Sci **65**(6): 855-861.

Sharma, S., K. Chakraborty, B. K. Muller, N. Astola, Y. C. Tang, D. C. Lamb, M. Hayer-Hartl and F. U. Hartl (2008). "Monitoring protein conformation along the pathway of chaperonin-assisted folding." Cell **133**(1): 142-153.

Sharma, S. K., P. De los Rios, P. Christen, A. Lustig and P. Goloubinoff (2010). "The kinetic parameters and energy cost of the Hsp70 chaperone as a polypeptide unfoldase." Nat Chem Biol **6**(12): 914-920.

Shevchenko, A., M. Wilm, O. Vorm and M. Mann (1996). "Mass spectrometric sequencing of proteins silver-stained polyacrylamide gels." Anal Chem **68**(5): 850-858.

Shi, Y., D. D. Mosser and R. I. Morimoto (1998). "Molecular chaperones as HSF1-specific transcriptional repressors." Genes Dev **12**(5): 654-666.

Shibatani, T., M. Nazir and W. F. Ward (1996). "Alteration of rat liver 20S proteasome activities by age and food restriction." J Gerontol A Biol Sci Med Sci **51**(5): B316-322.

Shinjyo, N. and K. Kita (2007). "Relationship between reactive oxygen species and heme metabolism during the differentiation of Neuro2a cells." Biochem Biophys Res Commun **358**(1): 130-135.

Smith, D. M., S. C. Chang, S. Park, D. Finley, Y. Cheng and A. L. Goldberg (2007). "Docking of the proteasomal ATPases' carboxyl termini in the 20S proteasome's alpha ring opens the gate for substrate entry." Mol Cell **27**(5): 731-744.

Spradling, A., M. L. Pardue and S. Penman (1977). "Messenger RNA in heat-shocked Drosophila cells." J Mol Biol **109**(4): 559-587.

Stark, C., B. J. Breitkreutz, A. Chatr-Aryamontri, L. Boucher, R. Oughtred, M. S. Livstone, J. Nixon, K. Van Auken, X. Wang, X. Shi, T. Reguly, J. M. Rust, A. Winter, K. Dolinski and M. Tyers (2011). "The BioGRID Interaction Database: 2011 update." Nucleic Acids Res **39**(Database issue): D698-704.

Sullivan, E. K., C. S. Weirich, J. R. Guyon, S. Sif and R. E. Kingston (2001). "Transcriptional activation domains of human heat shock factor 1 recruit human SWI/SNF." Mol Cell Biol **21**(17): 5826-5837.

Sun, M., T. Nishino and J. F. Marko (2013). "The SMC1-SMC3 cohesin heterodimer structures DNA through supercoiling-dependent loop formation." Nucleic Acids Res.

Sunde, M. and C. Blake (1997). "The structure of amyloid fibrils by electron microscopy and X-ray diffraction." Adv Protein Chem **50**: 123-159.

Taipale, M., D. F. Jarosz and S. Lindquist (2010). "HSP90 at the hub of protein homeostasis: emerging mechanistic insights." Nat Rev Mol Cell Biol **11**(7): 515-528.

Takahashi, Y. H., G. H. Westfield, A. N. Oleskie, R. C. Trievel, A. Shilatifard and G. Skiniotis (2011). "Structural analysis of the core COMPASS family of histone H3K4 methylases from yeast to human." Proc Natl Acad Sci U S A **108**(51): 20526-20531.

Tan, J. M., E. S. Wong, D. S. Kirkpatrick, O. Pletnikova, H. S. Ko, S. P. Tay, M. W. Ho, J. Troncoso, S. P. Gygi, M. K. Lee, V. L. Dawson, T. M. Dawson and K. L. Lim (2008). "Lysine 63-linked ubiquitination promotes the formation and autophagic clearance of protein inclusions associated with neurodegenerative diseases." Hum Mol Genet **17**(3): 431-439.

Tanaka, K., T. Namba, Y. Arai, M. Fujimoto, H. Adachi, G. Sobue, K. Takeuchi, A. Nakai and T. Mizushima (2007). "Genetic evidence for a protective role for heat shock factor 1 and heat shock protein 70 against colitis." J Biol Chem **282**(32): 23240-23252.

Tang, Y. C., H. C. Chang, A. Roeben, D. Wischnewski, N. Wischnewski, M. J. Kerner, F. U. Hartl and M. Hayer-Hartl (2006). "Structural features of the GroEL-GroES nano-cage required for rapid folding of encapsulated protein." Cell **125**(5): 903-914.

Theodorakis, N. G. and R. I. Morimoto (1987). "Posttranscriptional regulation of hsp70 expression in human cells: effects of heat shock, inhibition of protein synthesis, and adenovirus infection on translation and mRNA stability." Mol Cell Biol **7**(12): 4357-4368.

Thrower, J. S., L. Hoffman, M. Rechsteiner and C. M. Pickart (2000). "Recognition of the polyubiquitin proteolytic signal." EMBO J **19**(1): 94-102.

Tissieres, A., H. K. Mitchell and U. M. Tracy (1974). "Protein synthesis in salivary glands of Drosophila melanogaster: relation to chromosome puffs." J Mol Biol **84**(3): 389-398.

Tooze, S. A. and T. Yoshimori (2010). "The origin of the autophagosomal membrane." Nat Cell Biol **12**(9): 831-835.

Towbin, H., T. Staehelin and J. Gordon (1979). "Electrophoretic transfer of proteins from polyacrylamide gels to nitrocellulose sheets: procedure and some applications." Proc Natl Acad Sci U S A **76**(9): 4350-4354.

Trinklein, N. D., J. I. Murray, S. J. Hartman, D. Botstein and R. M. Myers (2004). "The role of heat shock transcription factor 1 in the genome-wide regulation of the mammalian heat shock response." Mol Biol Cell **15**(3): 1254-1261.

Trott, A., J. D. West, L. Klaic, S. D. Westerheide, R. B. Silverman, R. I. Morimoto and K. A. Morano (2008). "Activation of heat shock and antioxidant responses by the natural product celastrol: transcriptional signatures of a thiol-targeted molecule." Mol Biol Cell **19**(3): 1104-1112.

Tycko, R. (2004). "Progress towards a molecular-level structural understanding of amyloid fibrils." Curr Opin Struct Biol **14**(1): 96-103.

Vabulas, R. M., S. Raychaudhuri, M. Hayer-Hartl and F. U. Hartl (2010). "Protein folding in the cytoplasm and the heat shock response." Cold Spring Harb Perspect Biol **2**(12): a004390.

Valas, R. E. and P. E. Bourne (2008). "Rethinking proteasome evolution: two novel bacterial proteasomes." J Mol Evol **66**(5): 494-504.

van der Veen, A. G. and H. L. Ploegh (2012). "Ubiquitin-like proteins." Annu Rev Biochem **81**: 323-357.

van Ham, T. J., K. L. Thijssen, R. Breitling, R. M. Hofstra, R. H. Plasterk and E. A. Nollen (2008). "C. elegans model identifies genetic modifiers of alpha-synuclein inclusion formation during aging." PLoS Genet **4**(3): e1000027.

van Oosten-Hawle, P., R. S. Porter and R. I. Morimoto (2013). "Regulation of organismal proteostasis by transcellular chaperone signaling." Cell **153**(6): 1366-1378.

Varshavsky, A. (1997). "The N-end rule pathway of protein degradation." Genes Cells **2**(1): 13-28.

Verma, R., L. Aravind, R. Oania, W. H. McDonald, J. R. Yates, 3rd, E. V. Koonin and R. J. Deshaies (2002). "Role of Rpn11 metalloprotease in deubiquitination and degradation by the 26S proteasome." Science **298**(5593): 611-615.

Vigh, L., H. Nakamoto, J. Landry, A. Gomez-Munoz, J. L. Harwood and I. Horvath (2007). "Membrane regulation of the stress response from prokaryotic models to mammalian cells." Ann N Y Acad Sci **1113**: 40-51.

Vilar, M., M. Murillo-Carretero, H. Mira, K. Magnusson, V. Besset and C. F. Ibanez (2006). "Bex1, a novel interactor of the p75 neurotrophin receptor, links neurotrophin signaling to the cell cycle." EMBO J **25**(6): 1219-1230.

Vujanac, M., A. Fenaroli and V. Zimarino (2005). "Constitutive nuclear import and stress-regulated nucleocytoplasmic shuttling of mammalian heat-shock factor 1." Traffic **6**(3): 214-229.

Walter, P. and D. Ron (2011). "The unfolded protein response: from stress pathway to homeostatic regulation." Science **334**(6059): 1081-1086.

Wandinger, S. K., K. Richter and J. Buchner (2008). "The Hsp90 chaperone machinery." J Biol Chem **283**(27): 18473-18477.

Wang, G., Z. Ying, X. Jin, N. Tu, Y. Zhang, M. Phillips, D. Moskophidis and N. F. Mivechi (2004). "Essential requirement for both hsf1 and hsf2 transcriptional activity in spermatogenesis and male fertility." Genesis **38**(2): 66-80.

Wang, X., R. A. Herr, W. J. Chua, L. Lybarger, E. J. Wiertz and T. H. Hansen (2007). "Ubiquitination of serine, threonine, or lysine residues on the cytoplasmic tail can induce ERAD of MHC-I by viral E3 ligase mK3." J Cell Biol **177**(4): 613-624.

Wang, Y., M. M. Pearce, D. A. Sliter, J. A. Olzmann, J. C. Christianson, R. R. Kopito, S. Boeckmann, C. Gagen, G. S. Leichner, J. Roitelman and R. J. Wojcikiewicz (2009). "SPFH1 and SPFH2 mediate the ubiquitination and degradation of inositol 1,4,5-

trisphosphate receptors in muscarinic receptor-expressing HeLa cells." Biochim Biophys Acta **1793**(11): 1710-1718.

Weber, F. E., K. T. Vaughan, F. C. Reinach and D. A. Fischman (1993). "Complete sequence of human fast-type and slow-type muscle myosin-binding-protein C (MyBP-C). Differential expression, conserved domain structure and chromosome assignment." Eur J Biochem **216**(2): 661-669.

Wei, D. and Y. Sun (2010). "Small RING Finger Proteins RBX1 and RBX2 of SCF E3 Ubiquitin Ligases: The Role in Cancer and as Cancer Targets." Genes Cancer **1**(7): 700-707.

Welch, W. J. and J. P. Suhan (1985). "Morphological study of the mammalian stress response: characterization of changes in cytoplasmic organelles, cytoskeleton, and nucleoli, and appearance of intranuclear actin filaments in rat fibroblasts after heat-shock treatment." J Cell Biol **101**(4): 1198-1211.

Welch, W. J. and J. P. Suhan (1986). "Cellular and biochemical events in mammalian cells during and after recovery from physiological stress." J Cell Biol **103**(5): 2035-2052.

Welchman, R. L., C. Gordon and R. J. Mayer (2005). "Ubiquitin and ubiquitin-like proteins as multifunctional signals." Nat Rev Mol Cell Biol **6**(8): 599-609.

Westerheide, S. D., J. Anckar, S. M. Stevens, Jr., L. Sistonen and R. I. Morimoto (2009). "Stress-inducible regulation of heat shock factor 1 by the deacetylase SIRT1." Science **323**(5917): 1063-1066.

Westerheide, S. D., J. D. Bosman, B. N. Mbadugha, T. L. Kawahara, G. Matsumoto, S. Kim, W. Gu, J. P. Devlin, R. B. Silverman and R. I. Morimoto (2004). "Celastrols as inducers of the heat shock response and cytoprotection." J Biol Chem **279**(53): 56053-56060.

Westerheide, S. D. and R. I. Morimoto (2005). "Heat shock response modulators as therapeutic tools for diseases of protein conformation." J Biol Chem **280**(39): 33097-33100.

Wilkinson, B. and H. F. Gilbert (2004). "Protein disulfide isomerase." Biochim Biophys Acta **1699**(1-2): 35-44.

Wilkinson, K. D. (1997). "Regulation of ubiquitin-dependent processes by deubiquitinating enzymes." FASEB J **11**(14): 1245-1256.

Williams, G. T., T. K. McClanahan and R. I. Morimoto (1989). "E1a transactivation of the human HSP70 promoter is mediated through the basal transcriptional complex." Mol Cell Biol **9**(6): 2574-2587.

Woelk, T., S. Sigismund, L. Penengo and S. Polo (2007). "The ubiquitination code: a signalling problem." Cell Div **2**: 11.

Wolynes, P. G., J. N. Onuchic and D. Thirumalai (1995). "Navigating the folding routes." Science **267**(5204): 1619-1620.

Woolhead, C. A., P. J. McCormick and A. E. Johnson (2004). "Nascent membrane and secretory proteins differ in FRET-detected folding far inside the ribosome and in their exposure to ribosomal proteins." Cell **116**(5): 725-736.

Wright, C. F., S. A. Teichmann, J. Clarke and C. M. Dobson (2005). "The importance of sequence diversity in the aggregation and evolution of proteins." Nature **438**(7069): 878-881.

Wu, C. (1995). "Heat shock transcription factors: structure and regulation." Annu Rev Cell Dev Biol **11**: 441-469.

Wullschleger, S., R. Loewith and M. N. Hall (2006). "TOR signaling in growth and metabolism." Cell **124**(3): 471-484.

Xu, W., M. Marcu, X. Yuan, E. Mimnaugh, C. Patterson and L. Neckers (2002). "Chaperone-dependent E3 ubiquitin ligase CHIP mediates a degradative pathway for c-ErbB2/Neu." Proc Natl Acad Sci U S A **99**(20): 12847-12852.

Xu, Z., A. L. Horwich and P. B. Sigler (1997). "The crystal structure of the asymmetric GroEL-GroES-(ADP)7 chaperonin complex." Nature **388**(6644): 741-750.

Ye, J., R. B. Rawson, R. Komuro, X. Chen, U. P. Dave, R. Prywes, M. S. Brown and J. L. Goldstein (2000). "ER stress induces cleavage of membrane-bound ATF6 by the same proteases that process SREBPs." Mol Cell **6**(6): 1355-1364.

Yorimitsu, T. and D. J. Klionsky (2005). "Autophagy: molecular machinery for self-eating." Cell Death Differ **12 Suppl 2**: 1542-1552.

Yoshida, H., K. Haze, H. Yanagi, T. Yura and K. Mori (1998). "Identification of the cis-acting endoplasmic reticulum stress response element responsible for transcriptional induction of mammalian glucose-regulated proteins. Involvement of basic leucine zipper transcription factors." J Biol Chem **273**(50): 33741-33749.

Yoshida, H., T. Matsui, A. Yamamoto, T. Okada and K. Mori (2001). "XBP1 mRNA is induced by ATF6 and spliced by IRE1 in response to ER stress to produce a highly active transcription factor." Cell **107**(7): 881-891.

Young, J. A., D. Sermwittayawong, H. J. Kim, S. Nandu, N. An, H. Erdjument-Bromage, P. Tempst, L. Coscoy and A. Winoto (2011). "Fas-associated death domain (FADD) and the E3 ubiquitin-protein ligase TRIM21 interact to negatively regulate virus-induced interferon production." J Biol Chem **286**(8): 6521-6531.

Young, J. C., V. R. Agashe, K. Siegers and F. U. Hartl (2004). "Pathways of chaperone-mediated protein folding in the cytosol." Nat Rev Mol Cell Biol **5**(10): 781-791.

Zhang, K. and R. J. Kaufman (2006). "Protein folding in the endoplasmic reticulum and the unfolded protein response." Handb Exp Pharmacol(172): 69-91.

Zhang, M., C. M. Pickart and P. Coffino (2003). "Determinants of proteasome recognition of ornithine decarboxylase, a ubiquitin-independent substrate." EMBO J **22**(7): 1488-1496.

Zhang, M., M. Poplawski, K. Yen, H. Cheng, E. Bloss, X. Zhu, H. Patel and C. V. Mobbs (2009). "Role of CBP and SATB-1 in aging, dietary restriction, and insulin-like signaling." PLoS Biol **7**(11): e1000245.

Zhang, M., M. Windheim, S. M. Roe, M. Peggie, P. Cohen, C. Prodromou and L. H. Pearl (2005). "Chaperoned ubiquitylation--crystal structures of the CHIP U box E3 ubiquitin ligase and a CHIP-Ubc13-Uev1a complex." Mol Cell **20**(4): 525-538.

Zhao, Q., J. Wang, I. V. Levichkin, S. Stasinopoulos, M. T. Ryan and N. J. Hoogenraad (2002). "A mitochondrial specific stress response in mammalian cells." EMBO J **21**(17): 4411-4419.

Zhong, M., A. Orosz and C. Wu (1998). "Direct sensing of heat and oxidation by Drosophila heat shock transcription factor." Mol Cell **2**(1): 101-108.

Zhou, B. B. and S. J. Elledge (2000). "The DNA damage response: putting checkpoints in perspective." Nature **408**(6811): 433-439.

Zhu, X., X. Zhao, W. F. Burkholder, A. Gragerov, C. M. Ogata, M. E. Gottesman and W. A. Hendrickson (1996). "Structural analysis of substrate binding by the molecular chaperone DnaK." Science **272**(5268): 1606-1614.

Zimmerman, S. B. and S. O. Trach (1991). "Estimation of macromolecule concentrations and excluded volume effects for the cytoplasm of Escherichia coli." J Mol Biol **222**(3): 599-620.

Zolkiewski, M., T. Zhang and M. Nagy (2012). "Aggregate reactivation mediated by the Hsp100 chaperones." Arch Biochem Biophys **520**(1): 1-6.

Zou, J., Y. Guo, T. Guettouche, D. F. Smith and R. Voellmy (1998). "Repression of heat shock transcription factor HSF1 activation by HSP90 (HSP90 complex) that forms a stress-sensitive complex with HSF1." Cell **94**(4): 471-480.

7 Appendices

7.1 Tables

Table 7-1: Positive HSR modulators

Ensembl ID	Gene Symbol	Full Name	Hsp70 mRNA level (% of control)
ENSG00000005339	CREBBP	CREB binding protein	11±8
ENSG00000064115	TM7SF3	transmembrane 7 superfamily member 3	not tested
ENSG00000066135	KDM4A	lysine (K)-specific demethylase 4A	not tested
ENSG00000080603	SRCAP	Snf2-related CREBBP activator protein	13±9
ENSG00000085224	ATRX	alpha thalassemia/mental retardation syndrome X-linked	8
ENSG00000086967	MYBPC2	myosin binding protein C, fast type	not tested
ENSG00000100393	EP300	E1A binding protein p300	8±5
ENSG00000102057	KCND1	potassium voltage-gated channel, Shal-related subfamily, member 1	6
ENSG00000108055	SMC3	structural maintenance of chromosomes 3	not tested
ENSG00000115524	SF3B1	splicing factor 3b, subunit 1, 155kDa	50±29
ENSG00000115760	BIRC6	baculoviral IAP repeat containing 6	not tested
ENSG00000117222	RBBP5	retinoblastoma binding protein 5	23
ENSG00000118181	RPS25	ribosomal protein S25	no reduction
ENSG00000118990	GLRXP3	glutaredoxin (thioltransferase) pseudogene 3	not tested
ENSG00000119041	GTF3C3	general transcription factor IIIC, polypeptide 3, 102kDa	7
ENSG00000120656	TAF12	TAF12 RNA polymerase II, TATA box binding protein (TBP)-associated factor, 20kDa	not tested
ENSG00000120733	KDM3B	lysine (K)-specific demethylase 3B	15
ENSG00000122692	SMU1	smu-1 suppressor of mec-8 and unc-52 homolog (C. elegans)	58±20
ENSG00000124143	C20orf95 (ARHGAP40)	Rho GTPase activating protein 40	not tested
ENSG00000126945	HNRNPH2	heterogeneous nuclear ribonucleoprotein H2 (H')	14
ENSG00000131009	AC007379.2 (TTTY9A)	testis-specific transcript, Y-linked 9A (non-protein coding)	not tested
ENSG00000132661	NXT1	NTF2-like export factor 1	7
ENSG00000132872	SYT4	synaptotagmin IV	not tested
ENSG00000133169	BEX1	brain expressed, X-linked 1	not tested
ENSG00000135801	TAF5L	TAF5-like RNA polymerase II, p300/CBP-associated factor (PCAF)-associated factor, 65kDa	not tested
ENSG00000136250	AOAH	acyloxyacyl hydrolase (neutrophil)	50
ENSG00000137801	THBS1	thrombospondin 1	not tested
ENSG00000137819	PAQR5	progestin and adipoQ receptor family member V	not tested
ENSG00000139343	SNRPF	small nuclear ribonucleoprotein polypeptide F	77±22
ENSG00000139874	SSTR1	somatostatin receptor 1	29

Ensembl ID	Gene Symbol	Full Name	Hsp70 mRNA level (% of control)
ENSG00000143224	PPOX	protoporphyrinogen oxidase	not tested
ENSG00000146731	CCT6A	chaperonin containing TCP1, subunit 6A (zeta 1)	no reduction
ENSG00000155096	AZIN1	antizyme inhibitor 1	49
ENSG00000156261	CCT8	chaperonin containing TCP1, subunit 8 (theta)	no reduction
ENSG00000162520	SYNC	syncoilin, intermediate filament protein	not tested
ENSG00000162961	DPY30	dpy-30 homolog (C. elegans)	not tested
ENSG00000163029	SMC6	structural maintenance of chromosomes 6	not tested
ENSG00000163468	CCT3	chaperonin containing TCP1, subunit 3 (gamma)	no reduction
ENSG00000163749	CCDC158	coiled-coil domain containing 158	not tested
ENSG00000166454	ATMIN	ATM interactor	70
ENSG00000167279	AP001267.4-2	Not known	7
ENSG00000167380	ZNF226	zinc finger protein 226	not tested
ENSG00000168002	POLR2G	polymerase (RNA) II (DNA directed) polypeptide G	not tested
ENSG00000168439	AP005668.2 (STIP1)	stress-induced-phosphoprotein 1	no reduction
ENSG00000170500	LONRF2	LON peptidase N-terminal domain and ring finger 2	88
ENSG00000172264	C20orf133 (MACROD2)	MACRO domain containing 2	not tested
ENSG00000172269	DPAGT1	dolichyl-phosphate (UDP-N-acetylglucosamine) N-acetylglucosaminephosphotransferase 1 (GlcNAc-1-P transferase)	not tested
ENSG00000173705	SUSD5	sushi domain containing 5	36
ENSG00000174677	VN1R4	vomeronasal 1 receptor 4	not tested
ENSG00000184374	COLEC10	collectin sub-family member 10 (C-type lectin)	57
ENSG00000185122	HSF1	heat-shock transcription factor 1	16±4
ENSG00000187715	KLHDC6 (KBTBD12)	kelch repeat and BTB (POZ) domain containing 12	not tested
ENSG00000196290	NIF3L1	NIF3 NGG1 interacting factor 3-like 1 (S. pombe)	not tested
ENSG00000197865		Not known	not tested
ENSG00000198326	C20orf141 (TMEM239)	transmembrane protein 239	not tested

Table 7-2: Negative HSR modulators

Ensembl ID	Gene Symbol	Full Name	Hsp70 mRNA level (% of control)
ENSG00000090061	CCNK	cyclin K	not tested
ENSG00000100387	RBX1	ring-box 1, E3 ubiquitin protein ligase	397±268
ENSG00000100804	PSMB5	proteasome (prosome, macropain) subunit, beta type, 5	not tested
ENSG00000101182	PSMA7	proteasome (prosome, macropain) subunit, alpha type, 7	230

Ensembl ID	Gene Symbol	Full Name	Hsp70 mRNA level (% of control)
ENSG00000107882	SUFU	suppressor of fused homolog (Drosophila)	not tested
ENSG00000108294	PSMB3	proteasome (prosome, macropain) subunit, beta type, 3	328±119
ENSG00000108671	PSMD11	proteasome (prosome, macropain) 26S subunit, non-ATPase, 11	240
ENSG00000129084	PSMA1	proteasome (prosome, macropain) subunit, alpha type, 1	not tested
ENSG00000132676	DAP3	death associated protein 3	not tested
ENSG00000142507	PSMB6	proteasome (prosome, macropain) subunit, beta type, 6	671±245
ENSG00000143106	PSMA5	proteasome (prosome, macropain) subunit, alpha type, 5	not tested
ENSG00000182446	NPLOC4	nuclear protein localization 4 homolog (S. cerevisiae)	not tested
ENSG00000184624	ZNF72P	zinc finger protein 72, pseudogene	not tested
ENSG00000198951	NAGA	N-acetylgalactosaminidase, alpha	not tested

Table 7-3: Components of largest connected interaction network of HSR modulators are listed. Positive and negative HSR modulators are highlighted in grey and red, respectively. Proteins forming network nodes interacting with 5 or more HSR modulators are highlighted in blue.

Uniprot	Gene symbol	Group	Number of interactions
Q00613	HSF1	pos_mod_HSR	35
Q09472	EP300	pos_mod_HSR	191
Q92793	CREBBP	pos_mod_HSR	164
O75533	SF3B1	pos_mod_HSR	51
Q9UQE7	SMC3	pos_mod_HSR	31
P55795	HNRNPH2	pos_mod_HSR	30
Q15291	RBBP5	pos_mod_HSR	30
P62306	SNRPF	pos_mod_HSR	28
Q9GZT8	NIF3L1	pos_mod_HSR	24
Q2TAY7	SMU1	pos_mod_HSR	20
Q9Y5Q9	GTF3C3	pos_mod_HSR	15
Q16514	TAF12	pos_mod_HSR	13
O75529	TAF5L	pos_mod_HSR	12
P46100	ATRX	pos_mod_HSR	12
O75164	KDM4A	pos_mod_HSR	11

Uniprot	Gene symbol	Group	Number of interactions
Q9C005	DPY30	pos_mod_HSR	11
Q6ZRS2	SRCAP	pos_mod_HSR	9
P62487	POLR2G	pos_mod_HSR	7
Q7LBC6	KDM3B	pos_mod_HSR	6
P07996	THBS1	pos_mod_HSR	5
Q9NR09	BIRC6	pos_mod_HSR	4
O14977	AZIN1	pos_mod_HSR	3
P50336	PPOX	pos_mod_HSR	3
A1Z1Q3	MACROD2	pos_mod_HSR	2
Q9NYT6	ZNF226	pos_mod_HSR	2
Q96SB8	SMC6	pos_mod_HSR	2
Q9NS93	TM7SF3	pos_mod_HSR	1
Q9HBH7	BEX1	pos_mod_HSR	1
Q9H3H5	DPAGT1	pos_mod_HSR	1
Q14324	MYBPC2	pos_mod_HSR	1
P28066	PSMA5	neg_mod_HSR	78
P25786	PSMA1	neg_mod_HSR	73
O14818	PSMA7	neg_mod_HSR	72
O00231	PSMD11	neg_mod_HSR	65
P28074	PSMB5	neg_mod_HSR	61
P49720	PSMB3	neg_mod_HSR	60
P62877	RBX1	neg_mod_HSR	51
P28072	PSMB6	neg_mod_HSR	50
Q8TAT6	NPLOC4	neg_mod_HSR	20
P51398	DAP3	neg_mod_HSR	11
O75909	CCNK	neg_mod_HSR	9
P17050	NAGA	neg_mod_HSR	2
Q9UMX1	SUFU	neg_mod_HSR	2
Q15004	KIAA0101	node	12
Q15717	ELAVL1	node	12
P01106	MYC	node	11
Q13616	CUL1	node	10
P53350	PLK1	node	9
P25788	PSMA3	node	9
Q13618	CUL3	node	9
P02751	FN1	node	8
P61956	SUMO2	node	8
P03372	ESR1	node	8
P25787	PSMA2	node	8
P62195	PSMC5	node	8
P55036	PSMD4	node	8
P60900	PSMA6	node	8
P54725	RAD23A	node	8
P20618	PSMB1	node	7
O43242	PSMD3	node	7
Q99460	PSMD1	node	7
P48556	PSMD8	node	7

Uniprot	Gene symbol	Group	Number of interactions
Q13200	PSMD2	node	7
P25789	PSMA4	node	7
P62191	PSMC1	node	7
O00232	PSMD12	node	7
P35998	PSMC2	node	7
Q9UNM6	PSMD13	node	7
Q15008	PSMD6	node	7
P17980	PSMC3	node	7
Q99436	PSMB7	node	7
P62333	PSMC6	node	7
P49721	PSMB2	node	7
Q15051	IQCB1	node	7
Q92905	COPS5	node	7
Q9Y5K5	UCHL5	node	7
P51665	PSMD7	node	7
P28070	PSMB4	node	7
P43686	PSMC4	node	7
P05067	APP	node	6
Q9UQL6	HDAC5	node	6
Q8TAA3	PSMA8	node	6
Q9Y244	POMP	node	6
Q14318	FKBP8	node	6
P09661	SNRPA1	node	6
O00487	PSMD14	node	6
Q15843	NEDD8	node	6
P24941	CDK2	node	6
Q9BQ83	SLX1A	node	6
P28062	PSMB8	node	6
P55072	VCP	node	6
P63165	SUMO1	node	6
P10275	AR	node	5
P04637	TP53	node	5
P40337	VHL	node	5
Q6ZW49	PAXIP1	node	5
Q9UL46	PSME2	node	5
P24928	POLR2A	node	5
P20226	TBP	node	5
Q14686	NCOA6	node	5
Q16695	HIST3H3	node	5
Q7L5N1	COPS6	node	5
Q13620	CUL4B	node	5
Q86VP6	CAND1	node	5
P61289	PSME3	node	5
Q16665	HIF1A	node	5
P62805	HIST1H4A	other	4
Q92831	KAT2B	other	4
Q00987	MDM2	other	4

Uniprot	Gene symbol	Group	Number of interactions
P40306	PSMB10	other	4
Q9Y2T2	AP3M1	other	4
P68431	HIST1H3A	other	4
O75376	NCOR1	other	4
P38398	BRCA1	other	4
P84022	SMAD3	other	4
P33176	KIF5B	other	4
Q9NRC8	SIRT7	other	4
O15379	HDAC3	other	4
Q99814	EPAS1	other	4
Q15797	SMAD1	other	4
Q13547	HDAC1	other	4
P13612	ITGA4	other	4
P35228	NOS2	other	4
Q13617	CUL2	other	4
Q06323	PSME1	other	4
Q92769	HDAC2	other	4
P19320	VCAM1	other	4
O15205	UBD	other	4
P28065	PSMB9	other	4
P10242	MYB	other	4
Q12834	CDC20	other	3
Q00403	GTF2B	other	3
P78345	RPP38	other	3
P24864	CCNE1	other	3
Q71DI3	HIST2H3A	other	3
P17844	DDX5	other	3
O75368	SH3BGRL	other	3
P40763	STAT3	other	3
P25208	NFYB	other	3
P10646	TFPI	other	3
Q15834	CCDC85B	other	3
Q9Y297	BTRC	other	3
Q93009	USP7	other	3
Q9H4G0	EPB41L1	other	3
P06454	PTMA	other	3
Q8TCJ0	FBXO25	other	3
P68400	CSNK2A1	other	3
Q9NRD1	FBXO6	other	3
P61964	WDR5	other	3
Q13363	CTBP1	other	3
Q92993	KAT5	other	3
P17676	CEBPB	other	3
O15350	TP73	other	3
P67809	YBX1	other	3
Q16401	PSMD5	other	3
Q9BT73	PSMG3	other	3

Uniprot	Gene symbol	Group	Number of interactions
Q14498	RBM39	other	3
P20810	CAST	other	3
Q86X55	CARM1	other	3
P63104	YWHAZ	other	3
P42224	STAT1	other	3
P18848	ATF4	other	3
P08670	VIM	other	3
P04150	NR3C1	other	3
P38936	CDKN1A	other	3
Q15796	SMAD2	other	3
Q9Y3Q8	TSC22D4	other	3
P12956	XRCC6	other	3
Q9Y5U4	INSIG2	other	3
Q9UHV2	SERTAD1	other	3
P38919	EIF4A3	other	3
Q16594	TAF9	other	3
Q92731	ESR2	other	3
Q14997	PSME4	other	3
Q8TAD8	SNIP1	other	3
Q9UER7	DAXX	other	3
Q15459	SF3A1	other	3
Q92466	DDB2	other	3
Q8IYB3	SRRM1	other	3
P07900	HSP90AA1	other	3
Q6P2Q9	PRPF8	other	3
P54274	TERF1	other	3
P06400	RB1	other	3
Q53H96	PYCRL	other	3
Q9Y3D8	TAF9	other	3
Q9Y6Q9	NCOA3	other	3
Q99717	SMAD5	other	3
P84243	H3F3A	other	3
O15265	ATXN7	other	3
P15172	MYOD1	other	3
Q16531	DDB1	other	3
Q13243	SRSF5	other	3
P31749	AKT1	other	2
Q8N3Y1	FBXW8	other	2
P10276	RARA	other	2
P41182	BCL6	other	2
Q99081	TCF12	other	2
Q14566	MCM6	other	2
Q13123	IK	other	2
O60381	HBP1	other	2
P10914	IRF1	other	2
P60896	SHFM1	other	2
P37231	PPARG	other	2

Uniprot	Gene symbol	Group	Number of interactions
Q9UBL3	ASH2L	other	2
Q9Y618	NCOR2	other	2
Q9BXP5	SRRT	other	2
Q01094	E2F1	other	2
P10071	GLI3	other	2
P35659	DEK	other	2
Q05086	UBE3A	other	2
Q13131	PRKAA1	other	2
P52272	HNRNPM	other	2
O95400	CD2BP2	other	2
O75177	SS18L1	other	2
P20823	HNF1A	other	2
Q8WUA4	GTF3C2	other	2
Q96MF7	NSMCE2	other	2
P21246	PTN	other	2
Q12772	SREBF2	other	2
Q13216	ERCC8	other	2
P23511	NFYA	other	2
P51610	HCFC1	other	2
P14618	PKM	other	2
P28482	MAPK1	other	2
P51858	HDGF	other	2
Q93034	CUL5	other	2
O43918	AIRE	other	2
P08047	SP1	other	2
P62736	ACTA2	other	2
P01100	FOS	other	2
P42768	WAS	other	2
P15407	FOSL1	other	2
P17483	HOXB4	other	2
Q14653	IRF3	other	2
Q99683	MAP3K5	other	2
Q96PK6	RBM14	other	2
Q9Y5Q8	GTF3C5	other	2
Q96RS0	TGS1	other	2
Q9UHX1	PUF60	other	2
Q16891	IMMT	other	2
Q15527	SURF2	other	2
Q7L2J0	MEPCE	other	2
P22415	USF1	other	2
P50402	EMD	other	2
P14921	ETS1	other	2
Q07666	KHDRBS1	other	2
Q13950	RUNX2	other	2
Q92995	USP13	other	2
Q9UQ35	SRRM2	other	2
P53992	SEC24C	other	2

Uniprot	Gene symbol	Group	Number of interactions
Q07869	PPARA	other	2
P16871	IL7R	other	2
P42574	CASP3	other	2
Q02447	SP3	other	2
P68363	TUBA1B	other	2
P54578	USP14	other	2
P35520	CBS	other	2
P49336	CDK8	other	2
Q9Y3R0	GRIP1	other	2
O94953	KDM4B	other	2
P17275	JUNB	other	2
O95600	KLF8	other	2
Q9HCE7	SMURF1	other	2
P11142	HSPA8	other	2
Q8N5Z5	KCTD17	other	2
Q13568	IRF5	other	2
Q13569	TDG	other	2
Q9BUJ2	HNRNPUL1	other	2
P13569	CFTR	other	2
Q01844	EWSR1	other	2
Q92985	IRF7	other	2
Q9Y620	RAD54B	other	2
Q9BRP4	PAAF1	other	2
Q12962	TAF10	other	2
O15360	FANCA	other	2
P43364	MAGEA11	other	2
P62993	GRB2	other	2
O43809	NUDT21	other	2
P18146	EGR1	other	2
P46531	NOTCH1	other	2
Q13309	SKP2	other	2
Q14676	MDC1	other	2
O60216	RAD21	other	2
Q99961	SH3GL1	other	2
Q96KM6	ZNF512B	other	2
Q16236	NFE2L2	other	2
Q12789	GTF3C1	other	2
P04406	GAPDH	other	2
P20962	PTMS	other	2
Q14814	MEF2D	other	2
Q15788	NCOA1	other	2
Q9UMX0	UBQLN1	other	2
P49841	GSK3B	other	2
Q9BRQ0	PYGO2	other	2
P78406	RAE1	other	2
O95359	TACC2	other	2
Q10570	CPSF1	other	2

Uniprot	Gene symbol	Group	Number of interactions
Q9Y6X2	PIAS3	other	2
Q15020	SART3	other	2
Q99966	CITED1	other	2
Q99967	CITED2	other	2
P42226	STAT6	other	2
Q92794	KAT6A	other	2
P25490	YY1	other	2
Q96PN7	TRERF1	other	2
Q05516	ZBTB16	other	2
Q14683	SMC1A	other	2
Q9UL17	TBX21	other	2
Q86UW6	N4BP2	other	2
Q8TAF3	WDR48	other	2
Q9UM63	PLAGL1	other	2
Q9Y265	RUVBL1	other	2
Q9UKT8	FBXW2	other	2
O75528	TADA3	other	2
Q86TI2	DPP9	other	2
Q9H7U1	CCSER2	other	2
Q9Y3C4	TPRKB	other	2
P05412	JUN	other	2
Q01196	RUNX1	other	2
Q9UK99	FBXO3	other	2
P12830	CDH1	other	2
O43390	HNRNPR	other	2
Q8IXW5	RPAP2	other	2
P09874	PARP1	other	2
Q00839	HNRNPU	other	2
Q15650	TRIP4	other	2
Q14872	MTF1	other	2
Q9UBP6	METTL1	other	2
Q9UJX3	ANAPC7	other	2
Q13887	KLF5	other	2
Q03164	MLL	other	2
Q12933	TRAF2	other	2
O00762	UBE2C	other	2
Q92841	DDX17	other	2
P68036	UBE2L3	other	2
Q15910	EZH2	other	2
Q13330	MTA1	other	2
Q9Y5V3	MAGED1	other	2
Q99743	NPAS2	other	2
O60260	PARK2	other	2
P62316	SNRPD2	other	2
O60318	MCM3AP	other	2
Q96GG9	DCUN1D1	other	2
Q13526	PIN1	other	2

Uniprot	Gene symbol	Group	Number of interactions
Q16778	HIST2H2BE	other	2
P15336	ATF2	other	2
P52948	NUP98	other	2
Q8WWY3	PRPF31	other	2
P29590	PML	other	2
P28358	HOXD10	other	2
Q92922	SMARCC1	other	2
P35222	CTNNB1	other	2
P35558	PCK1	other	2
Q7Z6G3	NECAB2	other	2
P54252	ATXN3	other	2
P54257	HAP1	other	2
P52630	STAT2	other	2
P23443	RPS6KB1	other	2
P00747	PLG	other	2
P12931	SRC	other	2
P61326	MAGOH	other	2
Q96GF1	RNF185	other	2
P54105	CLNS1A	other	2
P16220	CREB1	other	2
P15036	ETS2	other	2
P25054	APC	other	2
Q9NQG5	RPRD1B	other	2
O43852	CALU	other	2
O75486	SUPT3H	other	2
P15923	TCF3	other	2
O60664	PLIN3	other	2
Q99929	ASCL2	other	2
O43524	FOXO3	other	2
Q99728	BARD1	other	2
O94888	UBXN7	other	2
P16104	H2AFX	other	2
Q15596	NCOA2	other	2
Q15287	RNPS1	other	2
P61244	MAX	other	2
Q13619	CUL4A	other	2
Q12906	ILF3	other	2
Q93052	LPP	other	2
Q9UK53	ING1	other	2
O75582	RPS6KA5	other	2
Q96P16	RPRD1A	other	2
Q92585	MAML1	other	2
Q9H4L7	SMARCAD1	other	2
P10827	THRA	other	2
P54727	RAD23B	other	2
O95456	PSMG1	other	2
O95073	FSBP	other	2

Uniprot	Gene symbol	Group	Number of interactions
P06401	PGR	other	2
P34947	GRK5	other	2
Q6NZY4	ZCCHC8	other	2
P38432	COIL	other	2
Q96EB6	SIRT1	other	2
Q07955	SRSF1	other	2
Q04206	RELA	other	2
O15111	CHUK	other	2
Q00653	NFKB2	other	2
Q9H2X6	HIPK2	other	2
P07437	TUBB	other	2
Q01658	DR1	other	2
P24385	CCND1	other	2
P08107	HSPA1A	other	2
Q9Y3D3	MRPS16	other	2
P25963	NFKBIA	other	2
Q13042	CDC16	other	2
P04004	VTN	other	2
O96006	ZBED1	other	2
Q13469	NFATC2	other	2
O43474	KLF4	other	2
P11473	VDR	other	2
P36956	SREBF1	other	2
Q15428	SF3A2	other	2
P49588	AARS	other	2
Q15554	TERF2	other	2
Q9UBK2	PPARGC1A	other	2
Q9Y2Y9	KLF13	other	2
P35869	AHR	other	2
P52292	KPNA2	other	2
O00422	SAP18	other	2
P23246	SFPQ	other	2
P52701	MSH6	other	2
P26447	S100A4	other	2
Q04864	REL	other	2
P49366	DHPS	other	2
P19012	KRT15	other	2
P11441	UBL4A	other	2
P61457	PCBD1	other	2
P51531	SMARCA2	other	2
P51532	SMARCA4	other	2
P50750	CDK9	other	2
O15047	SETD1A	other	2
P51668	UBE2D1	other	2
Q9UKA1	FBXL5	other	2
Q12824	SMARCB1	other	2
Q15393	SF3B3	other	2

Uniprot	Gene symbol	Group	Number of interactions
P10244	MYBL2	other	2
O75444	MAF	other	2
P09016	HOXD4	other	2
Q02246	CNTN2	other	2
Q8IZL8	PELP1	other	2
Q13485	SMAD4	other	2
P32121	ARRB2	other	2
P53539	FOSB	other	2
Q9UJX4	ANAPC5	other	2
Q9UJX6	ANAPC2	other	2
P62158	CALM1	other	2

Table 7-4: Proteins enriched >1.66 fold in the nuclear fraction of HeLa cells upon HS at 43°C for 2 h.

Uniprot	Median log2 change	Gene	Protein
Q8N584	4,1213	TTC39C	Tetratricopeptide repeat protein 39C
Q00613	2,533	HSF1	Heat shock factor protein 1
P50135	2,0166	HNMT	Histamine N-methyltransferase
P25685	1,818	DNAJB1	DnaJ homolog subfamily B member 1
Q99615	1,815	DNAJC7	DnaJ homolog subfamily C member 7
Q9UL15	1,5455	BAG5	BAG family molecular chaperone regulator 5
Q9UNZ2	1,1642	NSFL1C	NSFL1 cofactor p47
Q8WW22	1,1519	DNAJA4	DnaJ homolog subfamily A member 4
Q5VT25	1,1304	CDC42BPA	Serine/threonine-protein kinase MRCK alpha
Q7Z4L5	1,1132	TTC21B	Tetratricopeptide repeat protein 21B
P08107	1,0532	HSPA1A	Heat shock 70 kDa protein 1A/1B
P17066	1,0464	HSPA6	Heat shock 70 kDa protein 6
Q9UDY4	1,0386	DNAJB4	DnaJ homolog subfamily B member 4
P31689	0,9847	DNAJA1	DnaJ homolog subfamily A member 1
P11142	0,965	HSPA8	Heat shock cognate 71 kDa protein
Q9UNN5	0,9437	FAF1	FAS-associated factor 1
P50502	0,9143	ST13	Hsc70-interacting protein
P62979	0,907	RPS27A	Ubiquitin-40S ribosomal protein S27a
P28074	0,8755	PSMB5	Proteasome subunit beta type-5
Q02535	0,8609	ID3	DNA-binding protein inhibitor ID-3
P25786	0,8565	PSMA1	Proteasome subunit alpha type-1
P31948	0,8535	STIP1	Stress-induced-phosphoprotein 1
O43396	0,8498	TXNL1	Thioredoxin-like protein 1
P49720	0,8488	PSMB3	Proteasome subunit beta type-3
P25788	0,8486	PSMA3	Proteasome subunit alpha type-3
P28070	0,8419	PSMB4	Proteasome subunit beta type-4
P28072	0,8408	PSMB6	Proteasome subunit beta type-6
Q8NEF9	0,8041	SRFBP1	Serum response factor-binding protein 1

Uniprot	Median log2 change	Gene	Protein
P20618	0,8009	PSMB1	Proteasome subunit beta type-1
P25787	0,7813	PSMA2	Proteasome subunit alpha type-2
Q99436	0,7735	PSMB7	Proteasome subunit beta type-7
P60900	0,7659	PSMA6	Proteasome subunit alpha type-6

Table 7-5: Proteins enriched (>1.66 fold) in nucleus with heat shock at 43°C for 2 h followed by a recovery at 37°C for 2 h.

Uniprot	Median log2 change	Gene	Protein
Q86UN6	5,3723	AKAP14	A-kinase anchor protein 14
Q86X83	4,297	COMMD2	COMM domain-containing protein 2
P05412	2,6584	JUN	Transcription factor AP-1
P25685	2,6125	DNAJB1	DnaJ homolog subfamily B member 1
O14974	1,7233	PPP1R12A	Protein phosphatase 1 regulatory subunit 12A
Q8N584	1,7142	TTC39C	Tetratricopeptide repeat protein 39C
Q9UDY4	1,5774	DNAJB4	DnaJ homolog subfamily B member 4
Q8IXM6	1,5232	NRM	Nurim
O43829	1,3988	ZFP161	Zinc finger protein 161 homolog
P08107	1,2987	HSPA1A	Heat shock 70 kDa protein 1A/1B
P17066	1,2782	HSPA6	Heat shock 70 kDa protein 6
P15408	1,1808	FOSL2	Fos-related antigen 2
Q03252	1,0116	LMNB2	Lamin-B2
Q9UKK6	0,9761	NXT1	NTF2-related export protein 1
Q8N8S7	0,9545	ENAH	Protein enabled homolog
Q02040	0,9522	AKAP17A	A-kinase anchor protein 17A
P24844	0,9291	MYL9	Myosin regulatory light polypeptide 9
Q8WW22	0,8597	DNAJA4	DnaJ homolog subfamily A member 4
P46782	0,8502	RPS5	40S ribosomal protein S5
Q7Z460	0,841	CLASP1	CLIP-associating protein 1
Q5JTV8	0,8358	TOR1AIP1	Torsin-1A-interacting protein 1
Q5VT25	0,8251	CDC42BPA	Serine/threonine-protein kinase MRCK alpha
P11233	0,8141	RALA	Ras-related protein Ral-A
P16220	0,8047	CREB1	Cyclic AMP-responsive element-binding protein 1
P38432	0,799	COIL	Coilin
Q9UKA9	0,7915	PTBP2	Polypyrimidine tract-binding protein 2
Q9BR76	0,7725	CORO1B	Coronin-1B
Q8IVT2	0,7715	C19orf21	Uncharacterized protein C19orf21
Q96NC0	0,7529	ZMAT2	Zinc finger matrin-type protein 2
O43707	0,7487	ACTN4	Alpha-actinin-4
P14678	0,7421	SNRPB	Small nuclear ribonucleoprotein-associated proteins B and B'
Q96C19	0,7333	EFHD2	EF-hand domain-containing protein D2
Q99615	0,7303	DNAJC7	DnaJ homolog subfamily C member 7
O14979	0,7302	HNRPDL	Heterogeneous nuclear ribonucleoprotein D-like

Table 7-6: Proteins depleted (< 0.63 fold) in nucleus with heat shock at 43°C for 2 h.

Uniprot	Median log2 change	Gene	Protein
Q4L235	-7,3267	AASDH	Acyl-CoA synthetase family member 4
Q8IW75	-7,0581	SERPINA12	Serpin A12
P31146	-6,91	CORO1A	Coronin-1A
Q9NWX6	-6,1421	THG1L	Probable tRNA(His) guanylyltransferase
Q9Y520	-5,9581	PRRC2C	Protein PRRC2C
Q5VZL5	-5,7475	ZMYM4	Zinc finger MYM-type protein 4
P35030	-5,713	PRSS3	Trypsin-3
Q6TDU7	-5,6626	CASC1	Cancer susceptibility candidate protein 1
Q8WVJ2	-5,4294	NUDCD2	NudC domain-containing protein 2
O95376	-4,3924	ARIH2	E3 ubiquitin-protein ligase ARIH2
Q8NHM4	-4,0748	TRY6	Putative trypsin-6
P06746	-3,9379	POLB	DNA polymerase beta
O75152	-3,6159	ZC3H11A	Zinc finger CCCH domain-containing protein 11A
Q08378	-3,565	GOLGA3	Golgin subfamily A member 3
Q9C0B1	-3,5483	FTO	Alpha-ketoglutarate-dependent dioxygenase FTO
P11532	-3,3472	DMD	Dystrophin
Q5VWI1	-3,2705	TCERG1L	Transcription elongation regulator 1-like protein
A2RRP1	-2,9821	NBAS	Neuroblastoma-amplified sequence
Q8NEV9	-2,8801	IL27	Interleukin-27 subunit alpha
P05109	-2,7637	S100A8	Protein S100-A8
P49761	-2,7016	CLK3	Dual specificity protein kinase CLK3
Q9BVK6	-2,6393	TMED9	Transmembrane emp24 domain-containing protein 9
P81605	-2,6331	DCD	Dermcidin
Q8N3E9	-2,3998	PLCD3	1-phosphatidylinositol 4,5-bisphosphate phosphodiesterase delta-3
Q8NFT6	-2,3342	DBF4B	Protein DBF4 homolog B
Q15397	-2,2165	KIAA0020	Pumilio domain-containing protein KIAA0020
Q9NWY4	-2,2079	C4orf27	UPF0609 protein C4orf27
P55795	-2,2028	HNRNPH2	Heterogeneous nuclear ribonucleoprotein H2
P38432	-2,1675	COIL	Coilin
Q13309	-2,1137	SKP2	S-phase kinase-associated protein 2
Q14690	-2,056	PDCD11	Protein RRP5 homolog
O60942	-2,0387	RNGTT	mRNA-capping enzyme
Q13085	-2,0232	ACACA	Acetyl-CoA carboxylase 1
Q9BWT3	-1,9982	PAPOLG	Poly(A) polymerase gamma
Q86T24	-1,9486	ZBTB33	Transcriptional regulator Kaiso
P61626	-1,9425	LYZ	Lysozyme C
O43829	-1,8952	ZFP161	Zinc finger protein 161 homolog
Q9BZE4	-1,8471	GTPBP4	Nucleolar GTP-binding protein 1
Q5T4S7	-1,7935	UBR4	E3 ubiquitin-protein ligase UBR4
Q8N137	-1,7615	CNTROB	Centrobin
P54277	-1,7566	PMS1	PMS1 protein homolog 1
Q5T9A4	-1,7551	ATAD3B	ATPase family AAA domain-containing protein 3B
Q13148	-1,7278	TARDBP	TAR DNA-binding protein 43
P58107	-1,683	EPPK1	Epiplakin

Uniprot	Median log2 change	Gene	Protein
P30154	-1,6517	PPP2R1B	Serine/threonine-protein phosphatase 2A 65 kDa regulatory subunit A beta isoform
P46939	-1,6207	UTRN	Utrophin
Q96PK6	-1,6201	RBM14	RNA-binding protein 14
Q13601	-1,6145	KRR1	KRR1 small subunit processome component homolog
Q9Y5Q9	-1,6122	GTF3C3	General transcription factor 3C polypeptide 3
Q9BVP2	-1,6104	GNL3	Guanine nucleotide-binding protein-like 3
P10412	-1,6041	HIST1H1E	Histone H1.4
Q9HAZ1	-1,5868	CLK4	Dual specificity protein kinase CLK4
Q9HCF4	-1,5739	RNF213	E3 ubiquitin-protein ligase RNF213
Q8IXT5	-1,5684	RBM12B	RNA-binding protein 12B
Q16270	-1,5638	IGFBP7	Insulin-like growth factor-binding protein 7
Q8IWR0	-1,5466	ZC3H7A	Zinc finger CCCH domain-containing protein 7A
Q14865	-1,5369	ARID5B	AT-rich interactive domain-containing protein 5B
Q9NP50	-1,4897	FAM60A	Protein FAM60A
Q14191	-1,476	WRN	Werner syndrome ATP-dependent helicase
Q13322	-1,4695	GRB10	Growth factor receptor-bound protein 10
Q5T5X7	-1,466	BEND3	BEN domain-containing protein 3
Q9Y5T4	-1,4476	DNAJC15	DnaJ homolog subfamily C member 15
Q9Y5Q8	-1,4441	GTF3C5	General transcription factor 3C polypeptide 5
Q9NRZ9	-1,4196	HELLS	Lymphoid-specific helicase
Q96SZ6	-1,412	CDK5RAP1	CDK5 regulatory subunit-associated protein 1
Q8WUU5	-1,3914	GATAD1	GATA zinc finger domain-containing protein 1
Q9Y5J1	-1,3615	UTP18	U3 small nucleolar RNA-associated protein 18 homolog
O43427	-1,354	FIBP	Acidic fibroblast growth factor intracellular-binding protein
Q5C9Z4	-1,3512	NOM1	Nucleolar MIF4G domain-containing protein 1
Q8NEJ9	-1,3443	NGDN	Neuroguidin
P15924	-1,3435	DSP	Desmoplakin
O94906	-1,3267	PRPF6	Pre-mRNA-processing factor 6
P40692	-1,3219	MLH1	DNA mismatch repair protein Mlh1
Q08380	-1,3214	LGALS3BP	Galectin-3-binding protein
Q9NRR4	-1,3179	DROSHA	Ribonuclease 3
P00374	-1,3033	DHFR	Dihydrofolate reductase
Q8N9N5	-1,3032	BANP	Protein BANP
Q9NVN8	-1,2815	GNL3L	Guanine nucleotide-binding protein-like 3-like protein
Q9UHL9	-1,2785	GTF2IRD1	General transcription factor II-I repeat domain-containing protein 1
P46100	-1,2523	ATRX	Transcriptional regulator ATRX
Q08043	-1,2415	ACTN3	Alpha-actinin-3
P07093	-1,2408	SERPINE2	Glia-derived nexin
Q9NV31	-1,2357	IMP3	U3 small nucleolar ribonucleoprotein protein IMP3
P80723	-1,2285	BASP1	Brain acid soluble protein 1
Q3L8U1	-1,2244	CHD9	Chromodomain-helicase-DNA-binding protein 9
P51692	-1,2149	STAT5B	Signal transducer and activator of transcription 5B
Q7Z6Z7	-1,2105	HUWE1	E3 ubiquitin-protein ligase HUWE1
Q12802	-1,2043	AKAP13	A-kinase anchor protein 13
Q6DKI1	-1,2015	RPL7L1	60S ribosomal protein L7-like 1

Uniprot	Median log2 change	Gene	Protein
O43159	-1,201	RRP8	Ribosomal RNA-processing protein 8
Q9HCK8	-1,1974	CHD8	Chromodomain-helicase-DNA-binding protein 8
Q9P0W2	-1,1936	HMG20B	SWI/SNF-related matrix-associated actin-dependent regulator of chromatin subfamily E member 1-related
Q13506	-1,1874	NAB1	NGFI-A-binding protein 1
Q12789	-1,1863	GTF3C1	General transcription factor 3C polypeptide 1
Q8IVF2	-1,1833	AHNAK2	Protein AHNAK2
P56182	-1,1818	RRP1	Ribosomal RNA processing protein 1 homolog A
Q9Y2R4	-1,1634	DDX52	Probable ATP-dependent RNA helicase DDX52
Q86U38	-1,1598	C14orf21	Nucleolar protein 9
P17480	-1,1349	UBTF	Nucleolar transcription factor 1
Q6ZRQ5	-1,1324	MMS22L	Protein MMS22-like
Q9BSC4	-1,1279	NOL10	Nucleolar protein 10
Q9H6W3	-1,1258	NO66	Bifunctional lysine-specific demethylase and histidyl-hydroxylase NO66
P52895	-1,1224	AKR1C2	Aldo-keto reductase family 1 member C2
Q9H8M2	-1,1161	BRD9	Bromodomain-containing protein 9
Q96HA7	-1,1123	TONSL	Tonsoku-like protein
Q9HBL8	-1,0933	NMRAL1	NmrA-like family domain-containing protein 1
Q8N5A5	-1,0928	ZGPAT	Zinc finger CCCH-type with G patch domain-containing protein
Q99519	-1,0922	NEU1	Sialidase-1
Q99986	-1,0919	VRK1	Serine/threonine-protein kinase VRK1
Q8N6T7	-1,0872	SIRT6	NAD-dependent protein deacetylase sirtuin-6
Q14149	-1,0862	MORC3	MORC family CW-type zinc finger protein 3
Q63HN8	-1,0796	RNF213	E3 ubiquitin-protein ligase RNF213
Q9UJZ1	-1,0791	STOML2	Protein AATF
Q9NY61	-1,0791	AATF	Stomatin-like protein 2
P43243	-1,0772	MATR3	Matrin-3
Q9H981	-1,0763	ACTR8	Actin-related protein 8
O00257	-1,0739	CBX4	E3 SUMO-protein ligase CBX4
Q9Y4X0	-1,0738	AMMECR1	AMME syndrome candidate gene 1 protein
Q9BQG0	-1,0733	MYBBP1A	Myb-binding protein 1A
O95239	-1,0675	KIF4A	Chromosome-associated kinesin KIF4A
Q969X6	-1,0633	CIRH1A	Cirhin
Q9BWF3	-1,0566	RBM4	RNA-binding protein 4
Q9BXW9	-1,0519	FANCD2	Fanconi anemia group D2 protein
O95900	-1,0512	TRUB2	Probable tRNA pseudouridine synthase 2
Q96EK9	-1,0503	KTI12	Protein KTI12 homolog
Q9H8H2	-1,0433	DDX31	Probable ATP-dependent RNA helicase DDX31
Q9HCD6	-1,0433	TANC2	Protein TANC2
Q5EBL8	-1,0427	PDZD11	PDZ domain-containing protein 11
Q13421	-1,0423	MSLN	Mesothelin
O00541	-1,0381	PES1	Pescadillo homolog
Q5T0N5	-1,0188	FNBP1L	Formin-binding protein 1-like
Q7Z2E3	-1,008	APTX	Aprataxin
P06858	-1,0054	LPL	Lipoprotein lipase
Q2KHR3	-1,0051	QSER1	Glutamine and serine-rich protein 1
Q9UNX4	-0,9993	WDR3	WD repeat-containing protein 3

Uniprot	Median log2 change	Gene	Protein
Q8IUH3	-0,9902	RBM45	RNA-binding protein 45
Q9H0U9	-0,9882	TSPYL1	Testis-specific Y-encoded-like protein 1
Q9NZM5	-0,9882	GLTSCR2	Glioma tumor suppressor candidate region gene 2 protein
Q9Y4C2	-0,9881	FAM115A	Protein FAM115A
O15270	-0,9856	SPTLC2	Serine palmitoyltransferase 2
Q8IY37	-0,9852	DHX37	Probable ATP-dependent RNA helicase DHX37
P31269	-0,9757	HOXA9	Homeobox protein Hox-A9
Q9H6R4	-0,9748	NOL6	Nucleolar protein 6
P21127	-0,9739	CDK11B	Cyclin-dependent kinase 11B
Q8WUA4	-0,9692	GTF3C2	General transcription factor 3C polypeptide 2
Q9Y3A4	-0,9632	RRP7A	Ribosomal RNA-processing protein 7 homolog A
P47914	-0,9616	RPL29	60S ribosomal protein L29
P04062	-0,9593	GBA	Glucosylceramidase
O75592	-0,9481	MYCBP2	Probable E3 ubiquitin-protein ligase MYCBP2
P52945	-0,9481	PDX1	Pancreas/duodenum homeobox protein 1
Q14807	-0,9442	KIF22	Kinesin-like protein KIF22
Q9BQ39	-0,9327	DDX50	ATP-dependent RNA helicase DDX50
Q9H4L4	-0,9295	SENP3	Sentrin-specific protease 3
Q16850	-0,9281	CYP51A1	Lanosterol 14-alpha demethylase
Q15269	-0,9277	PWP2	Periodic tryptophan protein 2 homolog
Q96T88	-0,9249	UHRF1	E3 ubiquitin-protein ligase UHRF1
Q5SY16	-0,9225	NOL9	Polynucleotide 5'-hydroxyl-kinase NOL9
Q9UBW7	-0,9223	ZMYM2	Zinc finger MYM-type protein 2
Q9Y613	-0,9216	FHOD1	FH1/FH2 domain-containing protein 1
Q9UNF1	-0,9206	MAGED2	Melanoma-associated antigen D2
Q9UL42	-0,9162	PNMA2	Paraneoplastic antigen Ma2
Q8N2U0	-0,9144	C17orf61	Transmembrane protein 256
Q7LBC6	-0,9117	KDM3B	Lysine-specific demethylase 3B
Q8N726	-0,9108	CDKN2A	Cyclin-dependent kinase inhibitor 2A, isoform 4
Q5JTH9	-0,9103	RRP12	RRP12-like protein
Q9UH99	-0,9086	SUN2	SUN domain-containing protein 2
Q86UV5	-0,9045	USP48	Ubiquitin carboxyl-terminal hydrolase 48
Q15061	-0,8996	WDR43	WD repeat-containing protein 43
Q5VZF2	-0,8961	MBNL2	Muscleblind-like protein 2
P98160	-0,896	HSPG2	Basement membrane-specific heparan sulfate proteoglycan core protein
O75367	-0,8955	H2AFY	Core histone macro-H2A.1
P16989	-0,8934	CSDA	DNA-binding protein A
P78347	-0,8925	GTF2I	General transcription factor II-I
Q14257	-0,8879	RCN2	Reticulocalbin-2
Q9UM00	-0,8866	TMCO1	Transmembrane and coiled-coil domain-containing protein 1
O15379	-0,88	HDAC3	Histone deacetylase 3
Q27J81	-0,875	INF2	Inverted formin-2
P98179	-0,8724	RBM3	Putative RNA-binding protein 3
P25490	-0,8621	YY1	Transcriptional repressor protein YY1
O43663	-0,8614	PRC1	Protein regulator of cytokinesis 1
P27816	-0,8598	MAP4	Microtubule-associated protein 4
Q9NR09	-0,8563	BIRC6	Baculoviral IAP repeat-containing protein 6

Uniprot	Median log2 change	Gene	Protein
Q6P6C2	-0,853	ALKBH5	RNA demethylase ALKBH5
Q12788	-0,8521	TBL3	Transducin beta-like protein 3
P18887	-0,8511	XRCC1	DNA repair protein XRCC1
Q96T37	-0,8503	RBM15	Putative RNA-binding protein 15
Q9H0D6	-0,8452	XRN2	5'-3' exoribonuclease 2
Q96T60	-0,8446	PNKP	Bifunctional polynucleotide phosphatase/kinase
Q9NQ55	-0,8388	PPAN	Suppressor of SWI4 1 homolog
P52272	-0,8339	HNRNPM	Heterogeneous nuclear ribonucleoprotein M
O60287	-0,8338	URB1	Nucleolar pre-ribosomal-associated protein 1
Q9Y314	-0,8317	NOSIP	Nitric oxide synthase-interacting protein
Q69YL0	-0,827		Uncharacterized protein DKFZp762I1415
Q9Y4P3	-0,8198	TBL2	Transducin beta-like protein 2
Q13242	-0,8179	SRSF9	Serine/arginine-rich splicing factor 9
Q9BTE7	-0,8177	DCUN1D5	DCN1-like protein 5
Q4VC44	-0,8152	FLYWCH1	FLYWCH-type zinc finger-containing protein 1
P49005	-0,8112	POLD2	DNA polymerase delta subunit 2
Q08945	-0,8096	SSRP1	FACT complex subunit SSRP1
Q9H019	-0,8035	FAM54B	Protein FAM54B
Q9C0C2	-0,7991	TNKS1BP1	182 kDa tankyrase-1-binding protein
Q99996	-0,7984	AKAP9	A-kinase anchor protein 9
Q9H3P2	-0,7972	WHSC2	Negative elongation factor A
O43286	-0,7933	B4GALT5	Beta-1,4-galactosyltransferase 5
Q15582	-0,7894	TGFBI	Transforming growth factor-beta-induced protein ig-h3
Q8NFJ5	-0,7894	GPRC5A	Retinoic acid-induced protein 3
Q15014	-0,7893	MORF4L2	Mortality factor 4-like protein 2
O95229	-0,786	ZWINT	ZW10 interactor
P42677	-0,7854	RPS27	40S ribosomal protein S27
Q13356	-0,7845	PPIL2	Peptidyl-prolyl cis-trans isomerase-like 2
Q9Y6X9	-0,7831	MORC2	MORC family CW-type zinc finger protein 2
P50750	-0,7823	CDK9	Cyclin-dependent kinase 9
Q92989	-0,782	CLP1	Polyribonucleotide 5'-hydroxyl-kinase Clp1
P33552	-0,7806	CKS2	Cyclin-dependent kinases regulatory subunit 2
Q8NI36	-0,7788	WDR36	WD repeat-containing protein 36
P78563	-0,7783	ADARB1	Double-stranded RNA-specific editase 1
O95453	-0,7752	PARN	Poly(A)-specific ribonuclease PARN
Q9UBU8	-0,7736	MORF4L1	Mortality factor 4-like protein 1
Q71UM5	-0,7721	RPS27L	40S ribosomal protein S27-like
Q15125	-0,7718	EBP	3-beta-hydroxysteroid-Delta(8),Delta(7)-isomerase
Q13895	-0,7658	BYSL	Bystin
Q6RFH5	-0,7627	WDR74	WD repeat-containing protein 74
Q9Y2H6	-0,7618	FNDC3A	Fibronectin type-III domain-containing protein 3A
Q9BZK7	-0,7585	TBL1XR1	F-box-like/WD repeat-containing protein TBL1XR1
Q9NY93	-0,7533	DDX56	Probable ATP-dependent RNA helicase DDX56
Q9Y4W2	-0,7514	LAS1L	Ribosomal biogenesis protein LAS1L
Q9BRJ6	-0,7504	C7orf50	Uncharacterized protein C7orf50
Q9NX40	-0,7472	OCIAD1	OCIA domain-containing protein 1
Q02818	-0,7459	NUCB1	Nucleobindin-1
Q8WV22	-0,7434	NSMCE1	Non-structural maintenance of chromosomes element 1 homolog

Uniprot	Median log2 change	Gene	Protein
Q08J23	-0,7426	NSUN2	tRNA (cytosine(34)-C(5))-methyltransferase
O95714	-0,7392	HERC2	E3 ubiquitin-protein ligase HERC2
O75695	-0,7368	RP2	Protein XRP2
Q9UJV9	-0,7367	DDX41	Probable ATP-dependent RNA helicase DDX41
Q9NRP0	-0,7352	OSTC	Oligosaccharyltransferase complex subunit OSTC
Q9NZJ4	-0,7327	SACS	Sacsin
Q9BZL1	-0,7319	UBL5	Ubiquitin-like protein 5

Table 7-7: Proteins depleted (< 0.63 fold) in nucleus with heat shock at 43°C for 2 h followed by a recovery at 37°C for 2 h.

Uniprot	Median log2 change	Gene	Protein
Q8IW75	-7.2876	SERPINA12	Serpin A12
Q4L235	-6.9119	AASDH	Acyl-CoA synthetase family member 4
P31146	-6.51	CORO1A	Coronin-1A
P35030	-6.3101	PRSS3	Trypsin-3
Q5VZL5	-5.8957	ZMYM4	Zinc finger MYM-type protein 4
O95376	-5.1743	ARIH2	E3 ubiquitin-protein ligase ARIH2
Q6TDU7	-4.9749	CASC1	Cancer susceptibility candidate protein 1
Q9Y520	-4.8937	PRRC2C	Protein PRRC2C
Q8WVJ2	-4.5038	NUDCD2	NudC domain-containing protein 2
P11532	-4.4455	DMD	Dystrophin
Q9C0B1	-4.2165	FTO	Alpha-ketoglutarate-dependent dioxygenase FTO
Q5VWI1	-4.0508	TCERG1L	Transcription elongation regulator 1-like protein
Q8NHM4	-3.9354	TRY6	Putative trypsin-6
P61626	-3.6849	LYZ	Lysozyme C
Q08378	-3.5313	GOLGA3	Golgin subfamily A member 3
Q8N3E9	-3.4169	PLCD3	1-phosphatidylinositol-4,5-bisphosphate phosphodiesterase delta-3
A2RRP1	-3.0119	NBAS	Neuroblastoma-amplified sequence
Q8NEV9	-2.9763	IL27	Interleukin-27 subunit alpha
P05109	-2.9679	S100A8	Protein S100-A8
Q08554	-2.8217	DSC1	Desmocollin-1
Q8NFT6	-2.7278	DBF4B	Protein DBF4 homolog B
P81605	-2.6421	DCD	Dermcidin
O75152	-2.5318	ZC3H11A	Zinc finger CCCH domain-containing protein 11A
P06746	-2.4882	POLB	DNA polymerase beta
Q02413	-2.3504	DSG1	Desmoglein-1
Q9BVK6	-2.316	TMED9	Transmembrane emp24 domain-containing protein 9
Q8N137	-2.264	CNTROB	Centrobin
P58107	-2.0673	EPPK1	Epiplakin
Q6P4H8	-1.981	FAM173B	Protein FAM173B
Q86TJ2	-1.9137	TADA2B	Transcriptional adapter 2-beta
P52895	-1.8703	AKR1C2	Aldo-keto reductase family 1 member C2
Q14149	-1.8629	MORC3	MORC family CW-type zinc finger protein 3
Q08499	-1.8068	PDE4D	cAMP-specific 3',5'-cyclic phosphodiesterase 4D

Uniprot	Median log2 change	Gene	Protein
Q12802	-1.8052	AKAP13	A-kinase anchor protein 13
Q99590	-1.7637	SCAF11	Protein SCAF11
Q8IWE2	-1.7223	FAM114A1	Protein NOXP20
P19971	-1.718	TYMP	Thymidine phosphorylase
O60343	-1.7051	TBC1D4	TBC1 domain family member 4
Q96SZ6	-1.6742	CDK5RAP1	CDK5 regulatory subunit-associated protein 1
Q27J81	-1.6226	INF2	Inverted formin-2
Q12904	-1.6187	AIMP1	Aminoacyl tRNA synthase complex-interacting multifunctional protein 1
Q9H0D6	-1.6045	XRN2	5'-3' exoribonuclease 2
Q9UHL9	-1.5909	GTF2IRD1	General transcription factor II-I repeat domain-containing protein 1
Q8IY21	-1.578	DDX60	Probable ATP-dependent RNA helicase DDX60
Q9Y2G8	-1.5582	DNAJC16	DnaJ homolog subfamily C member 16
Q5SW96	-1.5569	LDLRAP1	Low density lipoprotein receptor adapter protein 1
A0FGR8	-1.5563	ESYT2	Extended synaptotagmin-2
Q92616	-1.528	GCN1L1	Translational activator GCN1
Q14191	-1.523	WRN	Werner syndrome ATP-dependent helicase
Q6IA86	-1.5218	ELP2	Elongator complex protein 2
Q86T24	-1.4698	ZBTB33	Transcriptional regulator Kaiso
O60942	-1.4532	RNGTT	mRNA-capping enzyme
Q8TF05	-1.4501	PPP4R1	Serine/threonine-protein phosphatase 4 regulatory subunit 1
Q96C90	-1.4477	PPP1R14B	Protein phosphatase 1 regulatory subunit 14B
O94906	-1.4276	PRPF6	Pre-mRNA-processing factor 6
Q6Y7W6	-1.4272	GIGYF2	PERQ amino acid-rich with GYF domain-containing protein 2
Q14C86	-1.4064	GAPVD1	GTPase-activating protein and VPS9 domain-containing protein 1
Q96M27	-1.4061	PRRC1	Protein PRRC1
P08195	-1.3974	SLC3A2	4F2 cell-surface antigen heavy chain
O75153	-1.3952	KIAA0664	Protein KIAA0664
Q9P260	-1.3943	KIAA1468	LisH domain and HEAT repeat-containing protein KIAA1468
P51692	-1.3671	STAT5B	Signal transducer and activator of transcription 5B
O43852	-1.3549	CALU	Calumenin
P80723	-1.3521	BASP1	Brain acid soluble protein 1
Q9HAU0	-1.3401	PLEKHA5	Pleckstrin homology domain-containing family A member 5
Q5T9A4	-1.3362	ATAD3B	ATPase family AAA domain-containing protein 3B
O14578	-1.336	CIT	Citron Rho-interacting kinase
P04114	-1.3358	APOB	Apolipoprotein B-100
Q9NSV4	-1.3273	DIAPH3	Protein diaphanous homolog 3
Q9H2M9	-1.3264	RAB3GAP2	Rab3 GTPase-activating protein non-catalytic subunit
O15357	-1.3246	INPPL1	Phosphatidylinositol-3,4,5-trisphosphate 5-phosphatase 2
Q9NRZ9	-1.3201	HELLS	Lymphoid-specific helicase
P30154	-1.3193	PPP2R1B	Serine/threonine-protein phosphatase 2A 65 kDa regulatory subunit A beta isoform
Q6KC79	-1.3146	NIPBL	Nipped-B-like protein
Q8IWR0	-1.3047	ZC3H7A	Zinc finger CCCH domain-containing protein 7A

Uniprot	Median log2 change	Gene	Protein
O00443	-1.2934	PIK3C2A	Phosphatidylinositol-4-phosphate 3-kinase C2 domain-containing subunit alpha
P46939	-1.287	UTRN	Utrophin
Q9NWY4	-1.2852	C4orf27	UPF0609 protein C4orf27
Q13309	-1.2636	SKP2	S-phase kinase-associated protein 2
Q96TA1	-1.2524	FAM129B	Niban-like protein 1
Q9NT62	-1.2515	ATG3	Ubiquitin-like-conjugating enzyme ATG3
Q8IWZ3	-1.2507	ANKHD1	Ankyrin repeat and KH domain-containing protein 1
Q9HCF4	-1.244	KIAA1618	Protein ALO17
Q07960	-1.2428	ARHGAP1	Rho GTPase-activating protein 1
Q8TEX9	-1.2427	IPO4	Importin-4
P63313	-1.2372	TMSB10	Thymosin beta-10
Q13144	-1.237	EIF2B5	Translation initiation factor eIF-2B subunit epsilon
Q63HN8	-1.236	RNF213	RING finger protein 213
A0MZ66	-1.2335	KIAA1598	Shootin-1
P40692	-1.2297	MLH1	DNA mismatch repair protein Mlh1
Q8IX01	-1.2295	SUGP2	SURP and G-patch domain-containing protein 2
Q96RT1	-1.2263	ERBB2IP	Protein LAP2
Q15418	-1.2247	RPS6KA1	Ribosomal protein S6 kinase alpha-1
P16949	-1.2216	STMN1	Stathmin
Q9NR09	-1.2174	BIRC6	Baculoviral IAP repeat-containing protein 6
P27708	-1.215	CAD	CAD protein
Q9NP79	-1.212	VTA1	Vacuolar protein sorting-associated protein VTA1 homolog
P06454	-1.2088	PTMA	Prothymosin alpha
P17858	-1.2081	PFKL	6-phosphofructokinase, liver type
Q6NUM9	-1.2079	RETSAT	All-trans-retinol 13,14-reductase
O94979	-1.1991	SEC31A	Protein transport protein Sec31A
Q9H173	-1.1975	SIL1	Nucleotide exchange factor SIL1
Q02818	-1.1921	NUCB1	Nucleobindin-1
Q8N5G0	-1.1911	C4orf52	Uncharacterized protein C4orf52
Q69YL0	-1.19		Uncharacterized protein DKFZp762I1415
Q5T5X7	-1.1861	BEND3	BEN domain-containing protein 3
Q15293	-1.1826	RCN1	Reticulocalbin-1
O75592	-1.18	MYCBP2	Probable E3 ubiquitin-protein ligase MYCBP2
Q99735	-1.1772	MGST2	Microsomal glutathione S-transferase 2
Q9Y678	-1.1725	COPG	Coatomer subunit gamma
O76094	-1.1694	SRP72	Signal recognition particle 72 kDa protein
Q9H981	-1.1691	ACTR8	Actin-related protein 8
Q07864	-1.1671	POLE	DNA polymerase epsilon catalytic subunit A
O94905	-1.1663	ERLIN2	Erlin-2
Q6XQN6	-1.1661	NAPRT1	Nicotinate phosphoribosyltransferase
Q14254	-1.166	FLOT2	Flotillin-2
Q08J23	-1.1576	NSUN2	tRNA (cytosine(34)-C(5))-methyltransferase
Q8IZ83	-1.1548	ALDH16A1	Aldehyde dehydrogenase family 16 member A1
P47712	-1.1542	PLA2G4A	Cytosolic phospholipase A2
Q3L8U1	-1.1537	CHD9	Chromodomain-helicase-DNA-binding protein 9
Q9BXB4	-1.1514	OSBPL11	Oxysterol-binding protein-related protein 11
Q13177	-1.1482	PAK2	Serine/threonine-protein kinase PAK 2
O75477	-1.1462	ERLIN1	Erlin-1

Uniprot	Median log2 change	Gene	Protein
Q9NV35	-1.1421	NUDT15	Probable 8-oxo-dGTP diphosphatase NUDT15
Q9NZM1	-1.137	MYOF	Myoferlin
Q9C0C9	-1.1309	UBE2O	Ubiquitin-conjugating enzyme E2 O
O75787	-1.13	ATP6AP2	Renin receptor
Q9UBW7	-1.1298	ZMYM2	Zinc finger MYM-type protein 2
Q6UW78	-1.1242	C11orf83	UPF0723 protein C11orf83
Q12789	-1.1232	GTF3C1	General transcription factor 3C polypeptide 1
Q13322	-1.1232	GRB10	Growth factor receptor-bound protein 10
Q96IR7	-1.1227	HPDL	4-hydroxyphenylpyruvate dioxygenase-like protein
Q99519	-1.1227	NEU1	Sialidase-1
P49321	-1.1107	NASP	Nuclear autoantigenic sperm protein
Q9H6W3	-1.1107	NO66	Lysine-specific demethylase NO66
Q5T447	-1.1104	HECTD3	E3 ubiquitin-protein ligase HECTD3
Q14186	-1.1038	TFDP1	Transcription factor Dp-1
Q6P2E9	-1.0931	EDC4	Enhancer of mRNA-decapping protein 4
Q9BYN0	-1.0904	SRXN1	Sulfiredoxin-1
P29034	-1.0869	S100A2	Protein S100-A2
Q9BSL1	-1.0868	UBAC1	Ubiquitin-associated domain-containing protein 1
O75717	-1.0867	WDHD1	WD repeat and HMG-box DNA-binding protein 1
Q13395	-1.0866	TARBP1	Probable methyltransferase TARBP1
P00533	-1.0862	EGFR	Epidermal growth factor receptor
Q9UNF1	-1.0846	MAGED2	Melanoma-associated antigen D2
Q9UMX0	-1.0829	UBQLN1	Ubiquilin-1
Q9HCD6	-1.0808	TANC2	Protein TANC2
Q13310	-1.0794	PABPC4	Polyadenylate-binding protein 4
Q5VYK3	-1.0755	ECM29	Proteasome-associated protein ECM29 homolog
A8MW06	-1.0751	TMSL3	Thymosin beta-4-like protein 3
Q9NPI6	-1.0731	DCP1A	mRNA-decapping enzyme 1A
Q00577	-1.0709	PURA	Transcriptional activator protein Pur-alpha
Q14195	-1.0704	DPYSL3	Dihydropyrimidinase-related protein 3
O60287	-1.0628	URB1	Nucleolar pre-ribosomal-associated protein 1
Q93008	-1.0599	USP9X	Probable ubiquitin carboxyl-terminal hydrolase FAF-X
P42224	-1.0565	STAT1	Signal transducer and activator of transcription 1-alpha/beta
Q15058	-1.0534	KIF14	Kinesin-like protein KIF14
P16989	-1.0525	CSDA	DNA-binding protein A
Q14166	-1.051	TTLL12	Tubulin--tyrosine ligase-like protein 12
P61421	-1.0505	ATP6V0D1	V-type proton ATPase subunit d 1
Q96SU4	-1.0498	OSBPL9	Oxysterol-binding protein-related protein 9
Q9H019	-1.0482	FAM54B	Protein FAM54B
Q5T1M5	-1.0462	FKBP15	FK506-binding protein 15
O96006	-1.0425	ZBED1	Zinc finger BED domain-containing protein 1
O94915	-1.0387	FRYL	Protein furry homolog-like
A5YKK6	-1.036	CNOT1	CCR4-NOT transcription complex subunit 1
Q9H8Y8	-1.0335	GORASP2	Golgi reassembly-stacking protein 2
Q15021	-1.0216	NCAPD2	Condensin complex subunit 1
Q13043	-1.0068	STK4	Serine/threonine-protein kinase 4
O60664	-1.0065	PLIN3	Perilipin-3
P10588	-1.0055	NR2F6	Nuclear receptor subfamily 2 group F member 6

Uniprot	Median log2 change	Gene	Protein
Q9ULX3	-1.004	NOB1	RNA-binding protein NOB1
P20585	-1.0028	MSH3	DNA mismatch repair protein Msh3
Q99614	-1.0011	TTC1	Tetratricopeptide repeat protein 1
P52735	-0.9973	VAV2	Guanine nucleotide exchange factor VAV2
O15031	-0.9937	PLXNB2	Plexin-B2
P54132	-0.9933	BLM	Bloom syndrome protein
P46459	-0.9929	NSF	Vesicle-fusing ATPase
Q6PJG6	-0.9929	BRAT1	BRCA1-associated ATM activator 1
Q99575	-0.9906	POP1	Ribonucleases P/MRP protein subunit POP1
P27816	-0.987	MAP4	Microtubule-associated protein 4
Q14573	-0.9842	ITPR3	Inositol 1,4,5-trisphosphate receptor type 3
Q8WTV0	-0.9827	SCARB1	Scavenger receptor class B member 1
Q5T0N5	-0.9797	FNBP1L	Formin-binding protein 1-like
Q9BXW9	-0.9776	FANCD2	Fanconi anemia group D2 protein
O95466	-0.9771	FMNL1	Formin-like protein 1
O95239	-0.9765	KIF4A	Chromosome-associated kinesin KIF4A
Q5VZK9	-0.9755	LRRC16A	Leucine-rich repeat-containing protein 16A
Q8IY37	-0.9723	DHX37	Probable ATP-dependent RNA helicase DHX37
Q9NRR4	-0.9721	DROSHA	Ribonuclease 3
P49366	-0.9709	DHPS	Deoxyhypusine synthase
Q96PU4	-0.9698	UHRF2	E3 ubiquitin-protein ligase UHRF2
O14920	-0.9691	IKBKB	Inhibitor of nuclear factor kappa-B kinase subunit beta
P22059	-0.9688	OSBP	Oxysterol-binding protein 1
Q8IWB7	-0.9669	WDFY1	WD repeat and FYVE domain-containing protein 1
Q9H4I3	-0.9658	TRABD	TraB domain-containing protein
Q6NW34	-0.9619	C3orf17	Uncharacterized protein C3orf17
P53384	-0.9603	NUBP1	Cytosolic Fe-S cluster assembly factor NUBP1
Q9Y2H6	-0.9596	FNDC3A	Fibronectin type-III domain-containing protein 3A
O43681	-0.9595	ASNA1	ATPase ASNA1
Q8N5A5	-0.9592	ZGPAT	Zinc finger CCCH-type with G patch domain-containing protein
Q14376	-0.9582	GALE	UDP-glucose 4-epimerase
Q9H6T3	-0.9558	RPAP3	RNA polymerase II-associated protein 3
Q5VT79	-0.955	ANXA8L2	Annexin A8-like protein 2
Q04637	-0.953	EIF4G1	Eukaryotic translation initiation factor 4 gamma 1
Q9NUQ8	-0.9503	ABCF3	ATP-binding cassette sub-family F member 3
P21127	-0.9486	CDK11B	Cyclin-dependent kinase 11B
Q9UHB4	-0.9448	NDOR1	NADPH-dependent diflavin oxidoreductase 1
P06858	-0.944	LPL	Lipoprotein lipase
Q9UGJ1	-0.9434	TUBGCP4	Gamma-tubulin complex component 4
O43264	-0.9361	ZW10	Centromere/kinetochore protein zw10 homolog
Q9C0C2	-0.9359	TNKS1BP1	182 kDa tankyrase-1-binding protein
Q9UPU5	-0.9354	USP24	Ubiquitin carboxyl-terminal hydrolase 24
Q9HCK8	-0.9348	CHD8	Chromodomain-helicase-DNA-binding protein 8
O75376	-0.9335	NCOR1	Nuclear receptor corepressor 1
Q4G0J3	-0.9299	LARP7	La-related protein 7
P10114	-0.9292	RAP2A	Ras-related protein Rap-2a
Q9UI12	-0.9268	ATP6V1H	V-type proton ATPase subunit H
Q9H8Y5	-0.9259	ANKZF1	Ankyrin repeat and zinc finger domain-containing

Uniprot	Median log2 change	Gene	Protein
			protein 1
Q9UKK3	-0.9242	PARP4	Poly [ADP-ribose] polymerase 4
P51812	-0.9232	RPS6KA3	Ribosomal protein S6 kinase alpha-3
Q06210	-0.9223	GFPT1	Glucosamine--fructose-6-phosphate aminotransferase [isomerizing] 1
P42356	-0.9217	PI4KA	Phosphatidylinositol 4-kinase alpha
P35221	-0.9208	CTNNA1	Catenin alpha-1
P49005	-0.9205	POLD2	DNA polymerase delta subunit 2
P40121	-0.9193	CAPG	Macrophage-capping protein
Q12765	-0.9191	SCRN1	Secernin-1
O75955	-0.9189	FLOT1	Flotillin-1
Q6FI81	-0.9188	CIAPIN1	Anamorsin
Q9BQE3	-0.9116	TUBA1C	Tubulin alpha-1C chain
Q9NRP0	-0.9112	OSTC	Oligosaccharyltransferase complex subunit OSTC
Q14558	-0.9103	PRPSAP1	Phosphoribosyl pyrophosphate synthase-associated protein 1
Q9Y5Q9	-0.9102	GTF3C3	General transcription factor 3C polypeptide 3
O14981	-0.91	BTAF1	TATA-binding protein-associated factor 172
Q8N3C0	-0.9074	ASCC3	Activating signal cointegrator 1 complex subunit 3
Q06323	-0.9071	PSME1	Proteasome activator complex subunit 1
Q9Y5Q8	-0.9028	GTF3C5	General transcription factor 3C polypeptide 5
Q7Z6Z7	-0.9026	HUWE1	E3 ubiquitin-protein ligase HUWE1
Q99536	-0.9024	VAT1	Synaptic vesicle membrane protein VAT-1 homolog
P17174	-0.8956	GOT1	Aspartate aminotransferase, cytoplasmic
P16083	-0.8928	NQO2	Ribosyldihydronicotinamide dehydrogenase [quinone]
Q5T6F2	-0.8927	UBAP2	Ubiquitin-associated protein 2
P05161	-0.8926	ISG15	Ubiquitin-like protein ISG15
Q13576	-0.8925	IQGAP2	Ras GTPase-activating-like protein IQGAP2
P55786	-0.8915	NPEPPS	Puromycin-sensitive aminopeptidase
Q13601	-0.8899	KRR1	KRR1 small subunit processome component homolog
P35520	-0.8895	CBS	Cystathionine beta-synthase
P29373	-0.8888	CRABP2	Cellular retinoic acid-binding protein 2
Q8IVD9	-0.8862	NUDCD3	NudC domain-containing protein 3
O43399	-0.8859	TPD52L2	Tumor protein D54
Q96SB8	-0.8829	SMC6	Structural maintenance of chromosomes protein 6
P47914	-0.8807	RPL29	60S ribosomal protein L29
Q16850	-0.8779	CYP51A1	Lanosterol 14-alpha demethylase
P20645	-0.8772	M6PR	Cation-dependent mannose-6-phosphate receptor
O95373	-0.8763	IPO7	Importin-7
Q9UBB9	-0.8755	TFIP11	Tuftelin-interacting protein 11
Q13228	-0.873	SELENBP1	Selenium-binding protein 1
Q9H832	-0.8721	UBE2Z	Ubiquitin-conjugating enzyme E2 Z
Q96PZ0	-0.868	PUS7	Pseudouridylate synthase 7 homolog
Q8NFF5	-0.8678	FLAD1	FAD synthase
P62891	-0.8675	RPL39	60S ribosomal protein L39
Q08380	-0.866	LGALS3BP	Galectin-3-binding protein
P50995	-0.8659	ANXA11	Annexin A11
Q15654	-0.8658	TRIP6	Thyroid receptor-interacting protein 6
A1X283	-0.8653	SH3PXD2B	SH3 and PX domain-containing protein 2B

Uniprot	Median log2 change	Gene	Protein
O14972	-0.8636	DSCR3	Down syndrome critical region protein 3
O75925	-0.8623	PIAS1	E3 SUMO-protein ligase PIAS1
Q8N543	-0.8621	OGFOD1	2-oxoglutarate and iron-dependent oxygenase domain-containing protein 1
O95336	-0.8607	PGLS	6-phosphogluconolactonase
Q96CT7	-0.858	CCDC124	Coiled-coil domain-containing protein 124
Q8IYD1	-0.8557	GSPT2	Eukaryotic peptide chain release factor GTP-binding subunit ERF3B
A6NDU8	-0.8536	C5orf51	UPF0600 protein C5orf51
P62861	-0.8473	FAU	40S ribosomal protein S30
Q9P003	-0.8467	CNIH4	Protein cornichon homolog 4
Q5T2E6	-0.8458	C10orf76	UPF0668 protein C10orf76
Q9NR46	-0.8449	SH3GLB2	Endophilin-B2
O14880	-0.8432	MGST3	Microsomal glutathione S-transferase 3
P49915	-0.8431	GMPS	GMP synthase [glutamine-hydrolyzing]
Q96EK9	-0.8427	KTI12	Protein KTI12 homolog
P52756	-0.8422	RBM5	RNA-binding protein 5
Q9BZX2	-0.8413	UCK2	Uridine-cytidine kinase 2
P46926	-0.8409	GNPDA1	Glucosamine-6-phosphate isomerase 1
P08237	-0.8407	PFKM	6-phosphofructokinase, muscle type
Q12797	-0.8391	ASPH	Aspartyl/asparaginyl beta-hydroxylase
Q9BWT3	-0.8387	PAPOLG	Poly(A) polymerase gamma
P07093	-0.8384	SERPINE2	Glia-derived nexin
Q8TCE6	-0.8377	FAM45A	Protein FAM45A
Q6ZMR3	-0.837	LDHAL6A	L-lactate dehydrogenase A-like 6A
P07741	-0.835	APRT	Adenine phosphoribosyltransferase
P53634	-0.8334	CTSC	Dipeptidyl peptidase 1
P42330	-0.8249	AKR1C3	Aldo-keto reductase family 1 member C3
Q9H0W9	-0.8231	C11orf54	Ester hydrolase C11orf54
Q5VW32	-0.8201	BROX	BRO1 domain-containing protein BROX
Q9UBF2	-0.8193	COPG2	Coatomer subunit gamma-2
Q9NXG2	-0.8191	THUMPD1	THUMP domain-containing protein 1
Q96AY3	-0.8182	FKBP10	Peptidyl-prolyl cis-trans isomerase FKBP10
P30508	-0.8144	HLA-C	HLA class I histocompatibility antigen, Cw-12 alpha chain
Q8N6L1	-0.8132	KRTCAP2	Keratinocyte-associated protein 2
Q96FW1	-0.8124	OTUB1	Ubiquitin thioesterase OTUB1
Q9H4A4	-0.8115	RNPEP	Aminopeptidase B
P49770	-0.8112	EIF2B2	Translation initiation factor eIF-2B subunit beta
P31153	-0.8074	MAT2A	S-adenosylmethionine synthase isoform type-2
P21266	-0.8066	GSTM3	Glutathione S-transferase Mu 3
Q7Z4G4	-0.8058	TRMT11	tRNA (guanine(10)-N2)-methyltransferase homolog
Q53EL6	-0.8057	PDCD4	Programmed cell death protein 4
Q15126	-0.8056	PMVK	Phosphomevalonate kinase
Q86TG7	-0.8055	PEG10	Retrotransposon-derived protein PEG10
Q13885	-0.8029	TUBB2A	Tubulin beta-2A chain
Q14315	-0.8028	FLNC	Filamin-C
Q5K651	-0.8006	SAMD9	Sterile alpha motif domain-containing protein 9
P01891	-0.7996	HLA-A	HLA class I histocompatibility antigen, A-68 alpha chain
P32004	-0.7977	L1CAM	Neural cell adhesion molecule L1

Uniprot	Median log2 change	Gene	Protein
Q8IY67	-0.7976	RAVER1	Ribonucleoprotein PTB-binding 1
O60256	-0.7974	PRPSAP2	Phosphoribosyl pyrophosphate synthase-associated protein 2
Q86Y56	-0.7927	HEATR2	HEAT repeat-containing protein 2
Q9Y3A4	-0.7915	RRP7A	Ribosomal RNA-processing protein 7 homolog A
P55795	-0.7901	HNRNPH2	Heterogeneous nuclear ribonucleoprotein H2
P08243	-0.7899	ASNS	Asparagine synthetase [glutamine-hydrolyzing]
P13798	-0.7886	APEH	Acylamino-acid-releasing enzyme
Q9Y4R8	-0.7882	TELO2	Telomere length regulation protein TEL2 homolog
P30740	-0.7872	SERPINB1	Leukocyte elastase inhibitor
P46109	-0.7869	CRKL	Crk-like protein
Q08379	-0.7852	GOLGA2	Golgin subfamily A member 2
Q9NR45	-0.7847	NANS	Sialic acid synthase
P12955	-0.7814	PEPD	Xaa-Pro dipeptidase
Q99733	-0.7812	NAP1L4	Nucleosome assembly protein 1-like 4
P30520	-0.7806	ADSS	Adenylosuccinate synthetase isozyme 2
P23526	-0.7748	AHCY	Adenosylhomocysteinase
Q7LBC6	-0.7747	KDM3B	Lysine-specific demethylase 3B
Q9Y490	-0.7728	TLN1	Talin-1
P22102	-0.7677	GART	Trifunctional purine biosynthetic protein adenosine-
Q9H0B6	-0.7669	KLC2	Kinesin light chain 2
O75165	-0.763	DNAJC13	DnaJ homolog subfamily C member 13
Q96IJ6	-0.7623	GMPPA	Mannose-1-phosphate guanyltransferase alpha
Q5PRF9	-0.7622	SAMD4B	Protein Smaug homolog 2
Q7Z417	-0.7619	NUFIP2	Nuclear fragile X mental retardation-interacting protein 2
Q9NQW7	-0.7593	XPNPEP1	Xaa-Pro aminopeptidase 1
O00425	-0.7571	IGF2BP3	Insulin-like growth factor 2 mRNA-binding protein
P61960	-0.7546	UFM1	Ubiquitin-fold modifier 1
Q99829	-0.7545	CPNE1	Copine-1
Q96PK6	-0.7533	RBM14	RNA-binding protein 14
Q99538	-0.7524	LGMN	Legumain
P42694	-0.7522	HELZ	Probable helicase with zinc finger domain
P98160	-0.7519	HSPG2	Basement membrane-specific heparan sulfate proteoglycan core protein
O75962	-0.7513	TRIO	Triple functional domain protein
Q14643	-0.7485	ITPR1	Inositol 1,4,5-trisphosphate receptor type 1
Q15386	-0.7481	UBE3C	Ubiquitin-protein ligase E3C
P68366	-0.7476	TUBA4A	Tubulin alpha-4A chain
Q9BTT0	-0.7436	ANP32E	Acidic leucine-rich nuclear phosphoprotein 32 family member E
Q9Y5Y2	-0.7413	NUBP2	Cytosolic Fe-S cluster assembly factor NUBP2
Q01628	-0.7404	IFITM3	Interferon-induced transmembrane protein 3
O60826	-0.7401	CCDC22	Coiled-coil domain-containing protein 22
Q9NRL2	-0.7391	BAZ1A	Bromodomain adjacent to zinc finger domain protein 1A
P52701	-0.7353	MSH6	DNA mismatch repair protein Msh6
Q13630	-0.7345	TSTA3	GDP-L-fucose synthase
P07814	-0.7339	EPRS	Bifunctional glutamate/proline--tRNA ligase

Uniprot	Median log2 change	Gene	Protein
P14174	-0.7317	MIF	Macrophage migration inhibitory factor
P08133	-0.7312	ANXA6	Annexin A6

Table 7-8: HSR induction upon down-regulation of positive HSR modulators after thermal stress, proteasome inhibition, and celastrol treatment.

Ensembl ID	Gene symbol	2 h 37°C, 4 h 37°C			8 h 5 µM MG132			8 h 5 µM celastrol		
		z score			z score			z score		
		A	B	C	A	B	C	A	B	C
ENSG00000005339	CREBBP	-4,7	-2,7	-1,3	-1,5	-5,8	-5,8	-3,6	-0,5	-0,6
ENSG00000064115	TM7SF3	-4,2	-4,3	-2,9	-4,3	-3,8	-1,5	18,4	3,0	3,5
ENSG00000066135	KDM4A	-3,4	-3,8	-4,1	-5,7	-5,6	-4,8	-3,4	13,8	15,7
ENSG00000080603	SRCAP	-4,8	-3,3	-3,5	-5,7	-4,1	-4,0	-5,3	-6,0	-6,4
ENSG00000085224	ATRX	-4,2	-4,9	-4,6	-6,0	-8,7	-6,2	-7,4	-10,2	-11,6
ENSG00000086967	MYBPC2	-1,7	-2,4	-2,0	-2,4	-0,1	-0,4	4,5	2,9	4,0
ENSG00000100393	EP300	-6,7	-6,9	-7,4	-5,7	-3,2	-1,5	-1,1	-4,4	-1,4
ENSG00000102057	KCND1	-2,3	-2,8	-3,0	-4,6	-7,1	-1,9	-2,6	-2,5	-2,9
ENSG00000108055	SMC3	-2,7	-2,8	-1,9	-5,6	-6,3	-5,1	-1,4	-8,8	-10,0
ENSG00000115524	SF3B1	-4,1	-4,9	-5,6	-5,8	-6,3	-5,5	5,8	22,4	25,6
ENSG00000115760	BIRC6	-4,9	-4,7	-3,7	-2,6	-5,5	0,1	1,4	-3,5	-4,0
ENSG00000117222	RBBP5	-5,2	-4,5	-4,8	-6,1	-7,2	-6,1	-7,2	-14,4	-16,4
ENSG00000118990	GLRXP3	-4,4	-4,6	-4,4	-5,8	-2,7	-5,7	15,5	28,2	32,2
ENSG00000119041	GTF3C3	-3,1	-2,5	-1,1	-5,0	-5,3	-3,4	2,6	-0,5	-0,6
ENSG00000120656	TAF12	-5,8	-5,7	-4,7	-3,6	-3,4	-5,2	3,8	-3,9	-4,4
ENSG00000120733	KDM3B	-5,8	-5,7	-5,4	-3,0	-1,4	-2,1	-0,6	30,6	34,9
ENSG00000122692	SMU1	-4,8	-4,2	-2,7	-4,3	-4,4	-4,4	6,2	14,5	16,5
ENSG00000124143	ARHGAP40	-5,6	-3,4	-3,7	-4,8	-3,3	-0,7	-4,8	-3,5	-4,0
ENSG00000126945	HNRNPH2	-4,9	-3,3	-3,8	-4,9	-3,0	0,0	-1,4	-3,4	-3,8
ENSG00000131009	TTTY9A	-4,0	-2,1	0,5	-5,0	-4,5	-2,0	13,8	-6,1	-7,0
ENSG00000132661	NXT1	-4,8	-5,6	-4,2	-5,0	-4,7	-4,1	-4,8	7,6	8,6
ENSG00000132872	SYT4	-2,7	-3,1	-2,7	1,3	-6,5	-1,5	-7,1	-8,5	-9,7
ENSG00000133169	BEX1	-2,4	-2,0	-1,3	-2,9	0,0	0,1	-11,1	-2,2	-0,9
ENSG00000135801	TAF5L	-4,6	-4,7	-3,0	-5,0	-5,0	-3,8	4,0	4,2	4,8
ENSG00000136250	AOAH	-3,3	-3,2	-3,0	-4,7	-6,4	-2,8	-5,9	-7,0	-8,0
ENSG00000137801	THBS1	-2,0	-3,4	-2,0	-4,0	-7,4	-4,2	-1,0	-3,0	-3,5
ENSG00000137819	PAQR5	-4,9	14,3	-3,4	-1,6	-6,2	-2,3	7,2	-1,6	-1,9
ENSG00000139343	SNRPF	-7,5	-7,0	-6,0	-6,3	-6,4	-5,4	0,8	3,3	3,8
ENSG00000139874	SSTR1	-4,0	-2,6	-3,2	-2,9	-7,5	-3,8	-0,7	-1,6	-1,8
ENSG00000143224	PPOX	-4,3	-4,9	-2,5	-4,4	-5,1	0,3	-1,6	2,9	3,3
ENSG00000155096	AZIN1	-3,7	-3,1	-3,0	-2,5	-5,0	-2,8	0,3	-4,8	-5,4
ENSG00000162520	SYNC	-4,7	-3,6	-2,6	-4,9	-3,4	-0,8	-5,5	13,8	15,7
ENSG00000162961	DPY30	-3,3	-1,6	-2,3	-5,8	-6,1	-3,8	9,3	0,9	1,0
ENSG00000163029	SMC6	-3,3	-3,0	-3,7	-2,3	-6,0	0,9	-4,1	-5,6	-6,4

Ensembl ID	Gene symbol	2 h 37°C, 4 h 37°C			8 h 5 µM MG132			8 h 5 µM celastrol		
		z score			z score			z score		
		A	B	C	A	B	C	A	B	C
ENSG00000163749	CCDC158	-4,4	-4,7	-4,6	-0,2	-7,1	-2,6	-5,1	-7,0	-8,0
ENSG00000166454	ATMIN	-3,6	-3,4	-2,3	-5,1	-6,4	-1,6	-7,5	-12,0	-13,6
ENSG00000167279		-3,1	-3,4	-1,6	-3,9	-3,2	-0,9	-12,6	-3,1	-2,0
ENSG00000167380	ZNF226	-3,0	-3,0	-1,9	-4,9	-6,0	-1,4	-2,7	-2,9	-3,3
ENSG00000168002	POLR2G	-4,9	-2,5	-4,1	-5,1	-2,4	-0,8	19,5	5,3	6,1
ENSG00000170500	LONRF2	-4,1	-1,8	-2,9	-4,7	-6,3	-2,9	-8,9	-12,8	-14,6
ENSG00000172264	MACROD2	-4,2	-4,0	-3,1	-4,0	-6,5	-1,5	2,8	9,4	10,7
ENSG00000172269	DPAGT1	-2,7	-2,5	-1,2	-4,4	-5,2	-2,2	-5,1	-4,8	-5,5
ENSG00000173705	SUSD5	-4,4	-3,4	-2,4	-4,7	-4,4	-2,8	8,0	-0,6	-0,7
ENSG00000174677	VN1R4	-0,5	-3,2	-2,1	3,4	1,1	-0,2	12,8	5,6	1,7
ENSG00000184374	COLEC10	-3,4	-4,0	-1,1	-4,6	-3,6	-3,1	27,8	38,5	43,9
ENSG00000185122	HSF1	-6,3	-5,3	-5,3	-4,8	-7,1	-2,6	-6,0	-6,2	-7,1
ENSG00000187715	KBTBD12	-2,1	-3,5	-3,4	-4,9	-6,3	-1,9	20,6	-1,9	-2,1
ENSG00000196290	NIF3L1	-1,9	-2,5	-2,5	-3,2	-2,8	-4,4	-0,4	-0,5	-0,6
ENSG00000197865		-4,7	-4,4	-4,9	-2,2	-1,2	-1,3	-0,4	-1,7	0,8
ENSG00000198326	TMEM239	-2,4	-1,9	-2,6	2,1	6,7	5,4	-2,1	2,7	2,4

7.2 List of abbreviations

°C	degree Centigrade
µl	microliter
µM	micromolar
µm	micrometer
17-AAG	17-(Allylamino)-17-desmethoxygeldanamycin
17-DMAG	17-[2-(Dimethylamino)ethyl]amino-17-desmethoxygeldanamycin
3-MA	3-methyladenine
AAA	ATPases associated with various cellular activities
ADP	adenosine 5'-diphosphat
AMP	adenosine 5'-monophosphat
APS	ammonium persulfate
ATF6	activating transcription factor 6
ATG	autophagy-related gene
ATP	adenosine 5'-triphosphat
Bag	BCL-2-associated athanogene
BiP/GRP78	Ig-binding protein/glucose-regulated protein 78
Bis-Tris	bis(2-hydroxyethyl)-amino-tris(hydroxymethyl)-methane
bp	base pairs
BSA	bovine serum albumin
C. elegans	*Caenorhnbditis elegans*
$CaCl_2$	calcium chloride
CCT	chaperonin-containing t-complex polypeptide 1
CD	C-terminal domain
cDNA	complementary DNA
CHIP	carboxyl-terminus of heat-shock cognate70 interacting protein

CHX	cycloheximide
CIP	calf intestinal alkaline phosphatase
Clp	caseinolytic protease
CMA	chaperone-mediated autophagy
CMV	cytomegalovirus
CP	core particle
CREB	cAMP-responsive element binding protein
CREBBP	CREB binding protein
Cy3	cyanine 3
Da	Dalton
DAPI	4',6-diamidino-2-phenyl-indole, dihydrochloride
DBD	DNA binding domain
DCIC	3,4-dichloroisocoumarin
DMEM	Dulbecco's Modified Eagle's medium
DMSO	dimethyl sulfoxide
DNA	desoxyribonucleic acid
DnaJ	bacterial Hsp40 chaperone
DnaJ	bacterial Hsp40 chaperone
DnaK	bacterial Hsp70 chaperone
dNTPs	desoxyribonucleotides
E.coli	*Escherichia coli*
ECL	enhanced chemiluminescence
EDTA	Ethylenediaminetetraacetic acid
EGFP	enhanced green fluorescent protein
EGS	Ethylene-glycol-bis(succinimidyl succinate)
eIF	eukaryotic initiation factor
EP300	E1A binding protein p300
ER	endoplasmic reticulum
ERAD	ER-associated degradation
esiRNA	endoribonuclease-prepared siRNA
EtOH	ethanol
FAT	antigen-F associated transcript
FBS	fetal bovine serum
FCS	fetal calf serum
Fluc	firefly luciferase
FOXO	forkhead transcription factor
g	gram, earth's gravitational force
G418	Geneticin 418
GAPDH	glyceraldehyde 3-phosphate dehydrogenase
GPCR	G-protein coupled receptor
GroEL	large *growthE* gene product
GroES	small *growthE* gene product
Grp	glucose-regulated protein
GrpE	Growth P-like protein
h	hour
HCl	hydrochloride
HDAC	histone deacetylase
HEK293T	human embryonic kidney 293T cells
HeLa	cervical cancer cell line derived from Henrietta Lacks
HEPES	4-(2-hydroxyethyl)-1-piperazineethanesulfonic acid
HIP	Hsp70 interacting protein

HOP	Hsp organizing protein
HR	heptad repeat
HRP	horseradish peroxidase
HRPD	Human Resorce Reference Database
HS	heat-shock
Hsc	heat-shock cognate
HSE	heat-shock element
HSF	heat-shock transcription factor
HSF1	heat-shock transcription factor 1
Hsp	heat-shock protein
HSR	heat-shock response
HSR-1	heat-shock RNA-1
IGF-1	insulin-like growth factor 1
IgG	immunoglobulin G
IP	immunoprecipitation
IRE1	inositol requiring enzyme 1
IRES	internal ribosome entry site
k	kilo
K	lysine
KAc	potassium acetate
KCl	potassium chloride
kDa	kilo Dalton
KH_2PO_4	potassium phosphate monobasic
l	liter
LAMP2A	lysosome-associated membrane protein 2A
LB	Luria Bertani
LC3	microtubule-associated protein1 light chain 3
LC-MS	liquid chromatography-mass spectrometry
M	molar
m	meter, milli
MD	middle domain
MeOH	methanol
$MgCl_2$	magnesium chloride
$MgSO_4$	magnesium sulfate
min	minute
ml	milliliter
mM	millimolar
$MnCl_2$	Manganese(II) chloride
MOPS	3-(N-morpholino)propanesulfonic acid
mRAC	mammalian ribosome-associated complex
MS	mass spectrometry
mTOR	mammalian target of rapamycin
mTORC1	mammalian target of rapamycin complex 1
MTT	thaizolyl blue tetrazolium bromide
MTT	3-(4,5-dimethylthiazol-2-yl)-2,5-diphenyltetrazolium bromide
MW	molecular weight
n	nano
Na_2HPO_4	sodium phosphate, dibasic
NAC	nascent chain-associated complex
NaCl	sodium chloride

NBD	nucleotide binding domain
NBR	neighbor of breast cancer
ND	N-terminal domain
NEDD	neuronal-precursor-cell-expressed developmentally downregulated protein
NEF	nucleotide exchange factor
NLS	nuclear localization signal
nM	nanomolar
NP40	Nonidet P40
nSB	nuclear stress body
OD	optical density
ODC	ornithine decarboxylase
PAGE	polyacrylamide gel electrophoresis
PBS	phosphate buffered saline
PCR	polymerase chain reation
PERK	PKR-like ER kinase
PFD	prefoldin
Pfu	*Pyrococcus furiosus*
pH	potentia hydrogenii
pmol	picomol
PPI	peptidyl-prolyl cis-trans isomerase
PTM	post-translational modification
RAC	ribosome-associated complex
$RbCl_2$	rubidium chloride
RD	regulatory domain
RIDD	regulated IRE1-dependent decay
Rluc	*Renilla* luciferase
RNA	ribonucleic acid
RNAi	ribonucleic acid interference
ROS	reactive oxygen species
RP	regulatory particle
rpm	revolutions per minute
Rpn	regulatory particle non-ATPase
Rpt	regulatory particle ATPase
RT	room temperature
RT-PCR	reverse transcription polymerase chain reaction
s	second
S	Svedberg
SDS	sodium dodecylsulfate
sHsp	small heat-shock protein
SILAC	stable isotope labeling by amino acids in cell culture
Sir	sirtuin
SIRT1	sirtuin 1
SRCAP	Snf2-related CREBBP activator protein
SUMO	small ubiquitin-like modifier
TAD	trans-activation domain
TBE	Tris-borate-EDTA
TBS	Tris buffered saline
TEMED	N,N,N',N'-tetramethylethylenediamine
TF	trigger factor
TOR	target of rapamycin
TPR	tetratricopeptide repeat

TriC	tailless complex peptide 1 (TCP1) ring complex
Tris	tris(hydroxymethyl)aminomethane
UBC	ubiquitin-conjugation enzyme
UBL	ubiquitin-like protein
uORF	upstream open reading frame
UPR	unfolded protein response
UPS	ubiquitin-proteasome system
UTR	untranslated region
UV	ultraviolet
v/v	volume per volume
VHL	von Hippel-Lindau
w/v	weight per volume